Lecture Series in Physical Oceanography

By Prof.A.S.N.Murty

Lecture Series of Berhampur University in Physical Oceanography

By Prof.A.S.N.Murty

Chapter – 1

General Introduction

While about 75% of the earth's surface is occupied by oceans, only 25% of land remains for the life on the earth. Ocean studies are essential for human life, in general, as they can be used for transportation, food and exploitation of oil, natural gas and other mineral and fisheries resources which also controls the general climate of earth as a whole. It is particularly more important for the climate scientist as air-sea interaction and general circulation will keep the mean temperature of the earth as constant. Studies of ocean currents play a vital role in our present day understanding of dynamics of the ocean. Ocean dynamics deals with different types of motions in the oceans like ocean currents, waves, tides and other vertical motions like upwelling and downwelling.

Among all these dynamics first and foremost item is currents. Ocean currents at the sea surface are generated by two ways, one is due to difference in density and the other is wind force. The density difference is caused due to differential heating at the earth's surface. As Lower latitudes receive more heat than the higher latitudes, Ocean surface is subjected to change in density and so change in sea level. The other one is due to change in wind pattern over the globe. The prevailing wind pattern in lower latitudes is easterlies (trade winds), westerlies in subtropical latitudes and again easterlies in polar latitudes at the surface and meridional circulation in the upper air as shown in Fig.1(left). These respective wind patterns in respective latitudinal zones cause different ocean circulations Fig.1(right). Apart from surface circulation there is circulation in sea bottom (average depth of the ocean is 4000meters). This bottom circulation (Fig.2) is called abyssal circulation. This abyssal circulation is caused due to thermo-haline (temperature and salinity effect together) circulation.

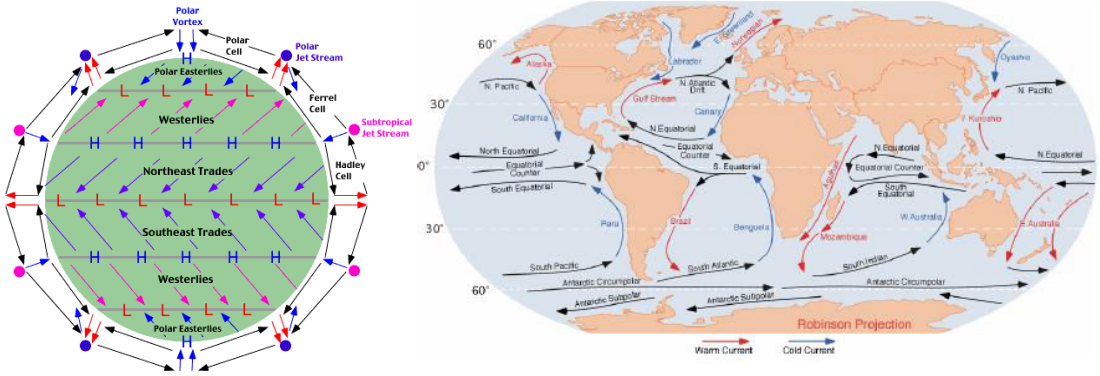

Fig.1.Surface and upper air wind pattern & ocean surface circulation on the earth

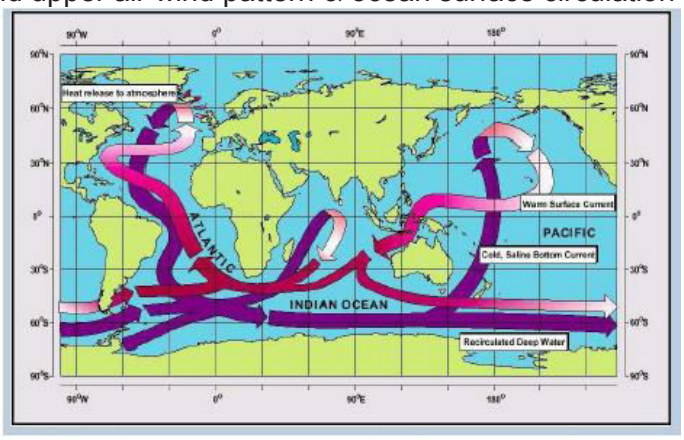

Fig.2. Ocean circulation at sea bottom (abyssal circulation)

Equation of motion

To understand the movement of a ocean particle, we have to consider different forces. The forces that are working are pressure gradient force, coriolis force, acceleration due to gravity and friction. The summation of all these forces is balanced by total force. As we consider a unit mass, the force is equal to acceleration. The total equation is called equation of motion.

Total acceleration = pressure gradient + coriolis + acceleration due to gravity + friction

$$\frac{dV}{dt} = -\alpha \nabla P + 2\Omega K \times V + g + F \quad \text{.....(1)}$$

Where V = $iu + jv + kw$, P = $ip_x + jp_y + kp_z$, F = $iF_x + jF_y + kF_z$

Derivation and explanation of each of the terms of the equation of motion:

2.2.1. **Equations in a rotating Coordinate System: Coriolis acceleration**

Let us consider a coordinate system with the coordinates x',y' and z' as shown in Fig.2.1. Let the coordinate system rotated by an angle Ωt and the new coordinates are x,y and z respectively. From the rotational coordinate system we can write

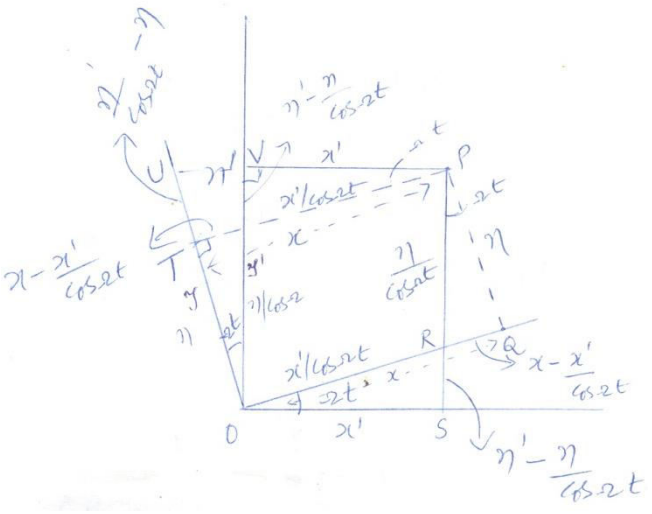

Fig.2.1 Rotating coordinates

From triangle ORS, OR = $\frac{X'}{Cos\Omega t}$,

From triangle PQR, QR = OQ-OR = $X - \frac{X'}{Cos\Omega t}$; PR = $\frac{\eta}{\cos \Omega t}$

From triangle PQR, $Sin\Omega t = \frac{QR}{PR} = \frac{X - \frac{X'}{Cos\Omega t}}{\frac{\eta}{\cos \Omega t}} \Rightarrow X' = XCos\Omega t - \eta Sin\Omega t$

Similarly from triangle PTU, PT = X, From triangle OUV, TU = $\frac{\eta'}{\cos \Omega t} - \eta \left(\because OT = \eta, OU = \frac{\eta'}{\cos \Omega t} \right)$

From triangle PTU, $Tan\Omega t = \frac{TU}{PT} = \frac{\frac{\eta'}{\cos \Omega t} - \eta}{X}$ = $\frac{Sin\Omega t}{Cos\Omega t}$

$\therefore$ η' = X Sin Ωt + η Cos Ωt

It may be noted that the letter 'Y' may be read in place of η then the we get the following equations.

$X^{/}$ = X Cos Ωt - Y Sin Ωt

$Y^{/}$ = X Sin Ωt + Y Cos Ωt (2.1)

$Z^{/}$ = Z

Similarly in place of X, Y, and Z if forces F_x, F_y, and F_z are considered we can write

$F_x^{/}$ = F_x Cos Ωt – F_y SinΩt

$F_y^{/}$ = F_x Sin Ωt + F_y Cos Ωt (2.2)

$F_z^{/}$ = F_z

If we differentiate equation 2.1 twice with respect to time we get

$\ddot{X}' = Cos\Omega t(X\ \ddot{X} - 2y\Omega - X\Omega^2$ - Sin $\Omega t(\dot{y} + 2\dot{x}\ \Omega - y\Omega^2)$.....(2.3)

According to Newton's law, a = F/m = $\ddot{X}$ .....(2.4)

So equation 2.2 and 2.4 combining we write

$$F'_x/m = \left[F_x/m\right]\cos\Omega t - \left[F_y/m\right]\sin\Omega t \quad \text{.....2.5}$$

since $\ddot{X}' = F'_x/m$ Equations 2.3 and 2.5 can be equated. After equating and comparing the coefficients of CosΩt and SinΩt we get as below:

$\ddot{X} - 2\dot{Y}X - X\Omega^2 = F_x/m$ or $\ddot{X} = X\Omega^2 + 2\dot{Y}X + F_x/m$

$\ddot{Y} + 2\dot{X}\Omega - Y\Omega^2 = F_y/m$ $\quad \ddot{Y} = Y\Omega^2 - 2\dot{X}\Omega + F_y/m$ ..... (2.6)

Similarly can be written $\ddot{Z} - \frac{F_z}{m} = 0$

Equations (2.6) are Newton's second law transformed to a rotating coordinate system.

The first of the terms on the right hand side ($X\Omega^2$, $Y\Omega^2$) denote the centrifugal accelerations pointing radially outward. The second terms on the right hand side ($2\dot{Y}X, 2\dot{X}\Omega$) represent accelerations owing to the combined effects of rotation of the coordinate axes and motion of

the particle, relative to the rotating coordinate system. These are called Coriolis accelerations. The action of this Coriolis acceleration is:

1. It acts only perpendicular to the plane of the moving particle.
2. It acts right hand side in the N.H and left hand side in the S.H of the moving particle.
3. It comes into being only for a moving particle but not for a fixed particle.
4. It does not change the magnitude of the velocity but changes only the direction of the moving particle as it acts perpendicular to the plane of moving particle.

Thus the centrifugal and Coriolis accelerations are extra terms obtained due to non inertial (non Newtonian) frame of reference.

2.3. Spherical coordinate system:

We shall now apply these results on a rotating spherical earth, in which x is tangent eastward, y meridionally northward and z radially upward into the atmosphere as shown in Fig.2.2. Let 'P' be a point on the earth's surface which is rotating with the angular velocity Ω, at a distance of 'acosϕ' from the axis of rotation where 'a' is the radius of the earth and 'ϕ' is the latitude. From fig.2.2, Ω_x = Ω Cos 90 = 0, Ω_y = Ω Sin (90-ϕ) = Ω Cos ϕ, Ω_z = Ω Sinϕ.

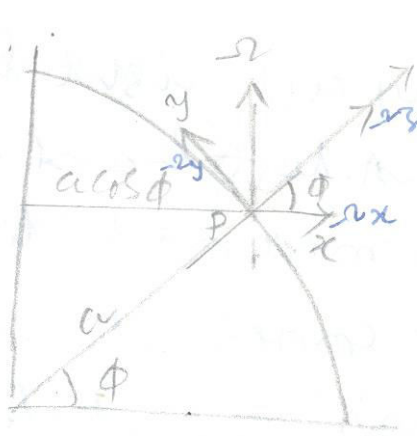

Fig.2.2

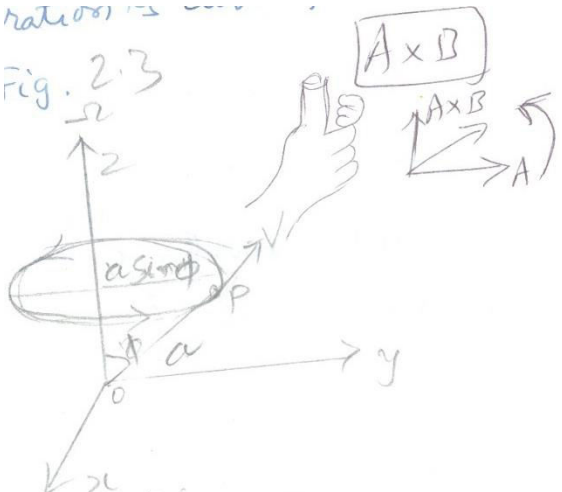

Fig.2.3

If the velocity of the particle is V= iu +jv+kw then the Coriolis acceleration is curl of the vector as shown in fig.2.3. The direction of the vector Ω is such that when the fingers of the right hand

bend(curl) about the axis of rotation in the same sense as the motion, the thumb points in the direction of Ω.

In fig. 2.3 let 'a' is the position vector of the moving particle'P' as measured from the origin of coordinates (centre of the earth). So the vector Ω×a has the magnitude 'Ω a sinϕ', which is just the linear speed of the particle (V). Therefore V = Ω×a. Similarly if the magnitude of velocity (V) is considered as the position vector, then the acceleration is Ω×V. Thus we got the Coriolis accelerations in equation 2.3 as $-2\dot{X}\Omega and -2\dot{Y}\Omega$, where $\dot{X} and \dot{Y}$ are the velocities ($\frac{dx}{dt}, \frac{dy}{dt}$). Which means the Coriolis accelerations on the surface of the earth can be written as -2Ω×V.

$$C = -2\Omega \times V = -2\Omega \begin{vmatrix} i & j & k \\ 0 & \cos\phi & \sin\phi \\ u & v & w \end{vmatrix} = -2\Omega \begin{vmatrix} i & j & k \\ \Omega_x & \Omega_y & \Omega_z \\ u & v & w \end{vmatrix}$$

where u,v,w are the x,y,z components of the velocity. Expanding the determinant and separating the different components we get,

$C_x = -2\Omega w \cos\phi + 2\Omega v \sin\phi$

$C_y = -2\Omega u \sin\phi$ ……(2.7)

$C_z = 2\Omega u \cos\phi$

The Newton's second law of motion on a rotating coordinate system becomes from equation 2.6 as

$$\ddot{X} - \frac{F_x}{m} = 2\Omega v Sin\phi - 2\Omega w Cos\phi$$
$$\ddot{Y} - \frac{F_y}{m} = -2\Omega u Sin\phi \qquad \text{…….(2.8)}$$
$$\ddot{Z} - \frac{F_z}{m} = 2\Omega u Cos\phi$$

2.4. Other forces or accelerations:

2.4.1. Gravitation and Gravity:

The term gravitation solely means the attractive force between bodies which is described by Newton's law of gravitation. This force of attraction is proportional to the product of the masses and inversely related to the square of the distance between them.

$$g_a = -(GM/r^2)r$$

Where G= 6.658×10^{-8}, M = 5.988×10^{27} grams is the mass of the earth, r = the position vector of the unit mass of the air molecule measured from the centre of the earth.

As the particle on the surface of the earth is rotating along with the earth, it has centrifugal acceleration and the net effect appears as acceleration due to gravity as shown in Fig.2.4.

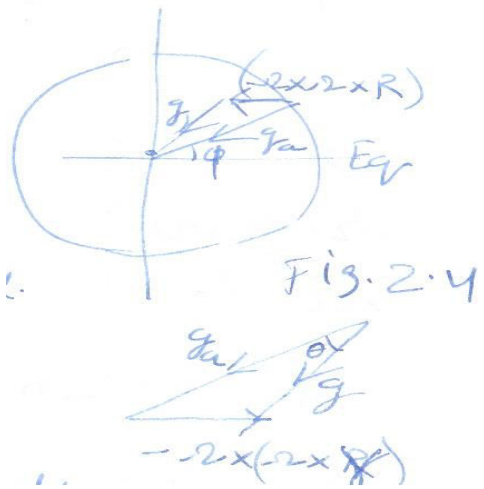

Fig.2.4. Generation of centrifugal force due to resultant action of gravity and gravitation

$g = g_a - \Omega\times(\Omega\times r)$ which is equal to acceleration due to gravity = gravitation – centrifugal acceleration.

At the surface of the earth acceleration due to gravity(g) depends on the latitude. At poles it is maximum and minimum at the equator.

2.4.2. The Pressure gradient force

Consider a rectangular volume having the sides $\delta_x, \delta_y and \delta_z$ fixed in a coordinate system relative to the solid earth as shown in Fig.2.5. Then the force in the x-direction due to the atmospheric pressure is, p $\delta_y\delta_z$ where 'p' is the atmospheric pressure and $\delta_y\delta_z$ is the area of the face it is acting.

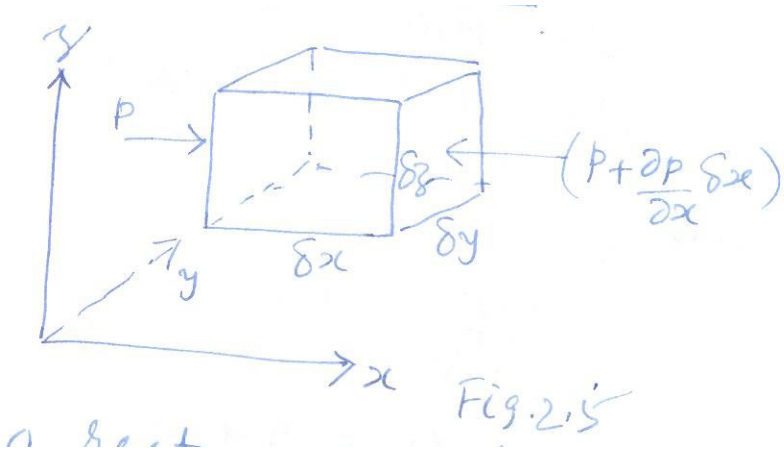

Fig. 2.5

Similarly the pressure force acting on the opposite face would be - $\left(p+\frac{\partial \mathrm{P}}{\partial x}\delta x\right)\delta y\delta z$

The net force acting in the x direction (i) would be $\left(ip\delta y\delta z\right)+\left\{-i(p+\frac{\partial p}{\partial x}\delta x)\delta y\delta z\right\}=-i\frac{\partial p}{\partial x}\delta x\delta y\delta z$

, pressure force per unit volume= -i∂p/∂x because the volume of the cube is δxδyδz.

Similarly considering in other directions the total pressure force would be

$$-\left\{i\frac{\partial p}{\partial x}+j\frac{\partial p}{\partial y}+k\frac{\partial p}{\partial z}\right\}$$

The force per unit mass = $-\frac{1}{\rho}\left\{i\frac{\partial p}{\partial x}+j\frac{\partial p}{\partial y}+k\frac{\partial p}{\partial z}\right\}$ = -α∇p .....(2.9)

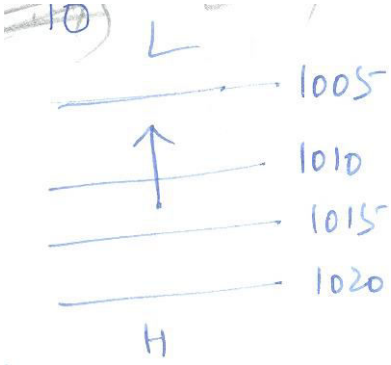

The minus sign indicates that as the pressure increases in one direction, the pressure force acts in opposite direction. Because of the presence of gradient (del,∇) operator, it is called as the pressure gradient force.

2.5. FINAL EQUATION OF MOTION:

Finally including all the forces, the vector equation of motion can be written as (from equations 2.7): Table 2.11

Total acceleration	Coriolis acceleration	Pressure gradient	Acceleration due to gravity	Friction
$\ddot{X} = \frac{d^2x}{dt^2} = \frac{du}{dt}$	f.v- 2Ωwcosϕ	$-\alpha\frac{\partial p}{\partial x}$	0	F_x/m
$\ddot{Y} = \frac{d^2y}{dt^2} = \frac{dv}{dt}$	-f.u	$-\alpha\frac{\partial p}{\partial y}$	0	F_y/m
$\ddot{Z} = \frac{d^2z}{dt^2} = \frac{dw}{dt}$	+2Ωucosϕ	$-\alpha\frac{\partial p}{\partial z}$	-g	F_z/m

4.1. THE EQUATION OF CONTINUITY:

An important restriction upon the velocity of a fluid may be obtained by kinematic methods applied to the law of conservation of mass.

Consider an infinitesimal rectangular volume fixed in space with sides of lengths δx, δy,δz in a moving fluid having velocities u,v,w respectively. Consider first the flow parallel to the x-axis. As 'u' is x- component of velocity and ρ is density of the fluid the mass flow through the left face is ρ u.

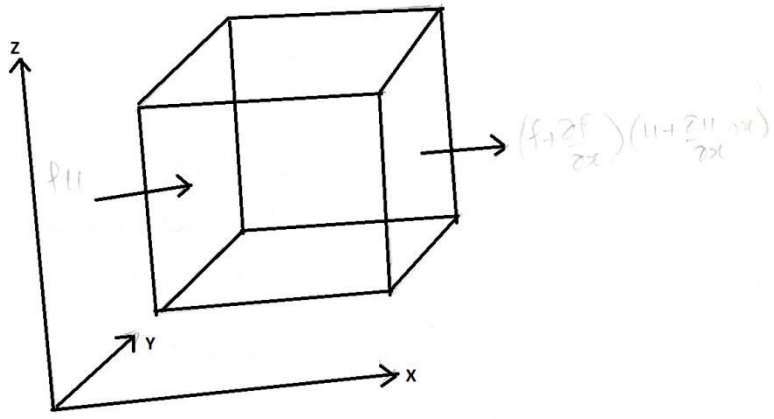

The mass flow into the volume per unit time is (ρ u)δyδz

The mass flow out of the volume per unit time on the right face is

$$(\rho + \frac{\partial \rho}{\partial x}\delta x)(u + \frac{\partial u}{\partial x}\delta x)\delta y \delta z$$

So the net flow out of the volume in the x-direction is

$$(\rho u \delta y \delta z) - \left[(\rho + \frac{\partial \rho}{\partial x}\delta x)(u + \frac{\partial u}{\partial x}\delta x) \right]\delta y \delta z$$
$$-\left[\frac{\partial}{\partial x}(\rho u) + \frac{\partial \rho}{\partial x}\frac{\partial u}{\partial x}\delta x \right]$$

As the volume of the rectangular element considered is infinitesimal, δx is very small and so higher order term (second term) is negligible.

Therefore, the net flow in the x-direction is $= -\left[\frac{\partial}{\partial x}(\rho u) \right]\delta x \delta y \delta z$

Taking the mass flow in all the three component directions, the total flow out would be $\left[\frac{\partial}{\partial x}(\rho u) + \frac{\partial}{\partial y}(\rho v) + \frac{\partial}{\partial z}(\rho w) \right]\delta x \delta y \delta z$

where 'v' and 'w' are the velocity components in the y and z directions respectively.

We shall compute the rate at which mass enters the box as a result of fluid motion and, since mass must be conserved, we shall equate this to the rate of change with time of the mass contained within the cube.

In other words, if mass is neither created nor destroyed and if the sum is not zero, it must be balanced by a change of density (rate of change of density $\frac{\partial \rho}{\partial t}$)

$$\therefore \left(\frac{\partial \rho}{\partial T} \right)\delta X \delta Y \delta Z = -\left[\frac{\partial}{\partial X}(\rho U) + \frac{\partial}{\partial y}(\rho V) + \frac{\partial}{\partial z}(\rho W) \right]\delta x \delta y \delta z$$
$$-\frac{\partial \rho}{\partial t} = \frac{\partial}{\partial x}(\rho U) + \frac{\partial}{\partial y}(\rho V) + \frac{\partial}{\partial z}(\rho W) = \nabla . \rho \bar{V} \ldots\ldots\ldots\ldots (4.1)$$

$$\frac{1}{\rho}\frac{d\rho}{dt} + \left[\frac{\partial U}{\partial X} + \frac{\partial V}{\partial Y} + \frac{\partial W}{\partial Z} \right] = 0 \ldots\ldots (4.2)$$

This is called the equation of continuity. The first term is the fractional rate of change of density and the second term is the fractional rate of change of volume.

If the fluid is incompressible, the density is uniform(constant), then $\frac{d\rho}{dt}=0$

$\therefore \frac{1}{\rho}\frac{d\rho}{dt}=0$ Then the equation of continuity is $\frac{\partial u}{\partial x}+\frac{\partial v}{\partial y}+\frac{\partial w}{\partial z}=\nabla.\bar{V}=0$.....(4.3)

$where \bar{V}=iu+jv+kw$

Equation (4.3) is frequently considered convenient as it is nothing but horizontal three dimensional divergence.

2.6: SCALING THE EQUATION OF MOTION:

In order to avoid the complicated and non significant terms in the equations of 2,3 and 4, scaling is useful. Scaling means the weight or amount of each parameter will be calculated from each force and the unimportant terms will be neglected basing on the weight. These weights are obtained from general measurements on an average in the oceans which are given in the table as below:

Thus scaling is useful to know which term weighs more than the other terms in the equation of motion and so the terms that weigh more can be retained and the others can be neglected or ignored for different calculations. The procedure is to take approximate rounded off values (order of magnitude) of each term and substitute as per the dimensional value of the each term as given in the table below:

The equations of the three components of x,y and z from table 2.11 such that in the ocean x is east, y is meridional and z is vertically down in the oceans, we can write:

$$\frac{du}{dt}=-\alpha\frac{\partial p}{\partial x}+2\Omega v\sin\phi+2\Omega w\cos\phi+F_x \quad \text{.....(2)}$$

$$\frac{dv}{dt}=-\alpha\frac{\partial p}{\partial y}-2\Omega u\sin\phi+F_y \quad \text{.....(3)}$$

$$\frac{dw}{dt}=-\alpha\frac{\partial p}{\partial z}+2\Omega u\cos\phi+g+F_z \quad \text{.....(4)}$$

Item	Order of magnitude
1. horizontal velocity u ,v	10 m/s = 10^3 cm/s
2. vertical velocity	1 cm/s

3.horizontal length of a synoptic system,Δx,Δy	1000 km, $=10^8$ cm
Vertical depth of the system, Δz	10 km, = 10^6 cm
5. pressure fluctuation, Δp	10 mb = 10^4 dynes/cm^2
6.time dimension	10^5 seconds

2.6.1. Scaling the different terms:

1. Acceleration: $du/dt = 10^3/10^5 = 10^{-2}$

2. Coriolis terms:

a) $2\Omega v \sin\phi = 2\times7.292\times10^{-5}\times\text{Sin}90^o\times v = 10\times10^{-5}\times1\times10^3 = 10^{-1.}$ So 2Ω v sinϕ is valid.

b) $2\Omega w \cos\phi = 2\times7.292\times10^{-5}\times\text{Cos}(0)\times w = 10\times10^{-5}\times1\times1 = 10^{-4}$.

Which means $2\Omega w \text{Cos}\phi$ is negligibly smaller than $2\Omega v\text{Sin}\phi$. So $2\Omega w\text{Cos}\phi$ can be neglected.

c) $2\Omega u\text{Sin}\phi = 2\times7.292\times10^{-5}\times\text{Sin}90\times u = 10\times10^{-5}\times1\times10^3 = 10^{-1}$, valid.

d) $2\Omega u \text{ Cos } \phi = 2^* 7.292^*10^{-5}{}^*\text{Sin}90^*u = 10^*10^{-5}{}^*1^*10^3 = 10^{-1}$

3. Gravity term: $g = 9.8 = 10\text{m/s}^2 = 10^3$ cm.

4. Pressure gradient terms:

$\alpha\partial p/\partial x$, $\alpha\partial p/\partial y = (1/\rho)\partial p/\partial n = 10^4/(10^{-3} * 10^8) = 10^{-1}$

$\alpha\partial p/\partial z = (1/\rho)\partial p/\partial z = 10^4/(10^{-3}*10^6) = 10^1$

i) Scaling x equation: (frictionless flow):

$\frac{du}{dt} = -\alpha\frac{\partial p}{\partial x} + 2\Omega v\sin\Phi - 2\Omega w\cos\Phi$ $= 10^{-2} = 10^{-1} + 10^{-1} - 10^{-4}$ The last term is negligibly small compared to the other two terms in the right hand side and so can be neglected.

$\therefore \frac{du}{dt} = -\alpha\frac{\partial p}{\partial x} + 2\Omega v\sin\Phi$

ii) Scaling y-equation:

$\frac{dv}{dt} = -\alpha \frac{\partial p}{\partial y} - 2\Omega u Sin\Phi \rightarrow 10^{-2} = 10^{-1} - 10^{-1}$, both terms in the right hand side are equal and so all are important.

iii) Scaling z- equation:

$\frac{dw}{dt} = -\alpha \frac{\partial p}{\partial z} + 2\Omega u \cos\Phi - g \rightarrow 10^{-5} = 10^{1} + 10^{-1} - 10^{3}$, when compared to pressure gradient and gravity, 2Ωu cosϕ is negligibly small.

$$\frac{dw}{dt} = -\alpha \frac{\partial p}{\partial z} - g$$

Lecture Series of Berhampur University in Physical Oceanography

By Prof.A.S.N.Murty

CHAPTER-2

Frictionless ocean currents

2.1. EQUATION OF MOTION IN THE OCEANS:

The fundamental law of motion states that the acceleration of a body is equal to the sum of all forces per unit mass acting on the body. Depending on the forces that act upon a water particle, the motions will be different. If the forces exactly balance each other, the motion will be non-accelerated. In Ocean dynamics frictionless and frictional motion is separately considered due to the complicated effect of friction on the water particle.

The equation of motion in the atmosphere and oceans are same with slight difference in the action of acceleration due to gravity such that 'g' is taken as positive in the ocean and 'g' is taken negative in the atmosphere. The different forces taken are same in both the cases. They are pressure gradient force, Coriolis and frictional forces. So the equations are written as

$$\frac{du}{dt} = -\alpha \frac{\partial p}{\partial x} + fv + F_x \quad \text{.....(1)}$$

$$\frac{dv}{dt} = -\alpha \frac{\partial p}{\partial y} - fu + F_y \quad \text{.....(2)}$$

$$\frac{dw}{dt} = -\alpha \frac{\partial p}{\partial z} + g + F_z \quad \text{.....(3)}$$

If friction is neglected, the vertical component of equation of motion under non-accelerated motion turns out to be hydrostatic equation.

$$\frac{dw}{dt} = -\alpha \frac{\partial p}{\partial z} + g + 0 = 0$$

$$\therefore \frac{\partial p}{\partial z} = \rho g \quad \text{.....(4)}$$

This is called the hydrostatic equation. This can be written as

$$\alpha dp = gdz \quad \text{or} \quad \phi = \int d\phi = \int \alpha dp = \int gdz \quad \text{.....(5)}$$

This ϕ is called the geopotential and has the dimensions L^2T^{-2}. The constant geopotential lines are called equi-geopotential lines. The unit of geopotential is dynamic meter which is numerically 2% smaller than the geometric meter because while the work needed to lift a unit mass through one geometric metre is about 0.98 dynamic meters, which is close to 1.0 geopotential meter. The value gdz is the potential energy between the thicknesses of two levels. Constant geopotential lines are called equi-geopotential lines which are also level surfaces. To move along an equi-geopotential line no extra energy is required as the acceleration due to gravity is constant on the equi-potential lines. Fig.2.6 shows all the equi-geopotential surfaces are oblate spheroidal like that of the earth as equatorial radius is larger than polar radius.

These equigeopotential lines are also called level surfaces and on these surfaces potential energy (gz) is conserved. So if the isobaric surfaces and isopycnic surfaces (level surfaces) are parallel, it is called barotropic mode and if they are inclined at each other it is called baroclinic mode where the motion is maximum as shown in figure 2.1 below.

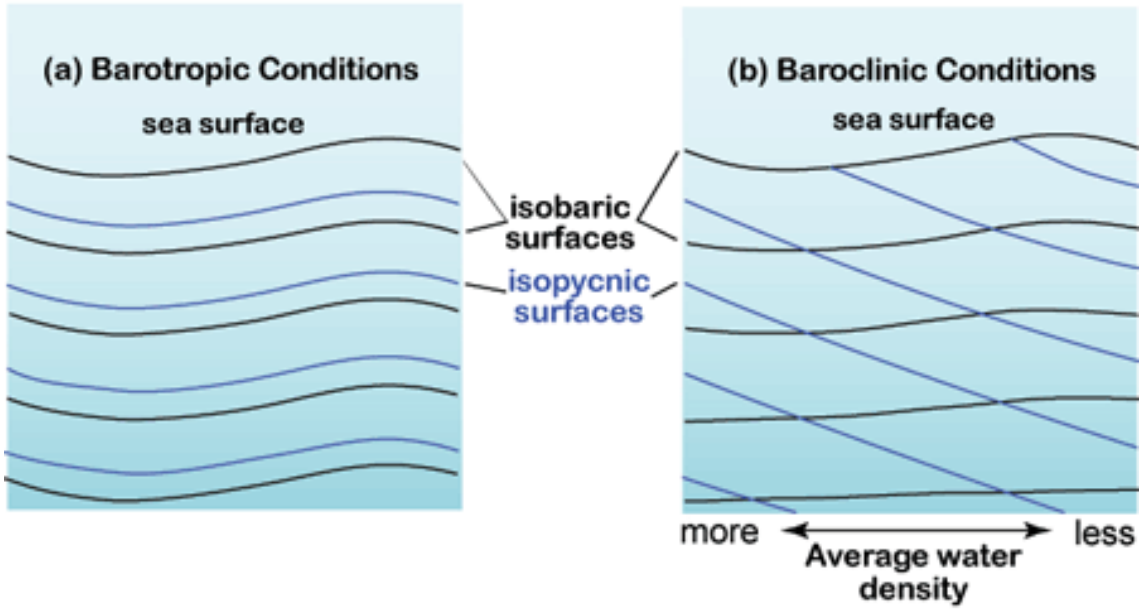

Fig.2.1. Barotropic and baroclinic conditions in the sea

2.1.2. HORIZONTAL FRICTIONLESS MOTION:

Under this category we have mainly two types of motion. One is accelerated (inertial) motion and the other is non accelerated (geostrophic) motion.

Inertial Motion

Inertial motion is typically excited when the surface currents are impulsively excited by wind forcing. If the wind were to remain steady, then the currents would eventually reach equilibrium and the time-dependent term would go to zero. But suppose the winds blew for a few hours and then turned off, the current would be in motion, but once the winds turned off there would be no forcing. If we are far from boundaries we can neglect pressure gradients and friction (bottom is also far away). This is a simple case of accelerated currents without friction.

The main assumption here is that the isobaric surfaces are horizontal and so pressure is constant in the horizontal. Hence the pressure gradient vanishes.

$$\therefore \frac{du}{dt} = fv \quad \text{.....(6)}$$

$$\frac{dv}{dt} = -fu \quad \text{.....(7)}$$

Multiply (6) by u and (7) by v and add then we get

$$u\frac{du}{dt} + v\frac{dv}{dt} = 0 \qquad \text{i.e. } \frac{1}{2}\frac{d}{dt}\left(u^2 + v^2\right) = 0 \text{ or } \frac{1}{2}\frac{d}{dt}\left(V_H{}^2\right) = 0$$

where $V_H = iu+jv$

This means V_H is constant implies that water particle moves with constant speed.

$$\frac{\mathbf{1}}{\mathbf{2}}\left(\frac{\partial \mathbf{u}^2}{\partial \mathbf{t}} + \frac{\partial \mathbf{v}^2}{\partial \mathbf{t}}\right) = \frac{\partial(\mathbf{ke})}{\partial \mathbf{t}} = \mathbf{0} \text{.....(8)}$$

This Equation states that in inertial motion, the kinetic energy remains constant . Even though the flow is accelerating (du/dt and dv/dt are not zero). What happens is that current speed remains constant but changes directions and a particle embedded in this would simply go around in a circle called inertial circle.

Then according to Newton, acceleration will result from change of direction under constant velocity. This can be easily seen by multiplying the equation (6) by v and (7) by u and subtract one from the other

$$v\frac{du}{dt} - u\frac{dv}{dt} = f\left(v^2 + u^2\right) = fV_H{}^2$$

$$v^2\frac{d}{dt}\left(\frac{u}{v}\right) = fV_H^2 \quad \text{.....(9)}$$

If α is the angle between the x-axis and the direction of current (u) then the velocities are $u = V_H \cos\alpha$ and $v = V_H \sin\alpha$ as shown in Fig. 2.7.

$\therefore \frac{u}{v} = \cot\alpha$, substituting this in equation (8) and simplifying we get

$\frac{d}{dt}\cot\alpha = \frac{f}{\sin^2\alpha}$ on differentiating we get $\frac{d\alpha}{dt} = -f$ .....(10)

$\therefore \alpha = -ft$

$\therefore u = V_H \cos\alpha$ = $V_H \cos(ft)$

$\therefore v = V_H \sin\alpha$ = $-V_H \sin(ft)$

These are the velocities of particles in the northern hemisphere oceans traveling clock wise. They are called gyres.

Equation (9) states that the water particle moves in a clockwise circulation in Northern Hemisphere while changing its direction at a constant rate of latitude (θ). These are called inertial currents and the circle is called inertial circle.

If the radius of inertial circle is say B (=V_H/f) with center (B/f,-A/f), then the balance of forces at point 'P' are centrifugal force $\left(\frac{V_H^2}{B}\right)$ and coriolis force (f.V_H) such that the particle velocity (V_H) is along the tangent at the point 'P' as shown in Fig.2.2.

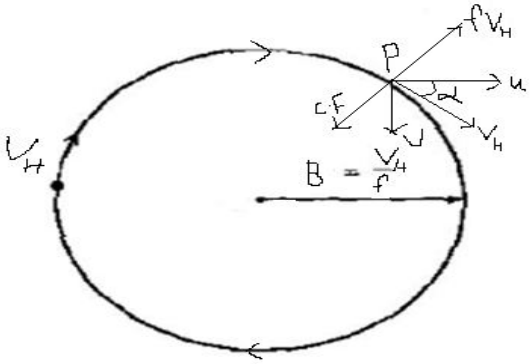

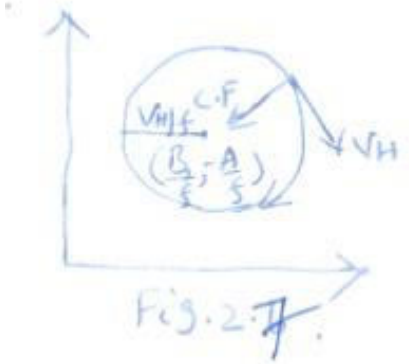

Fig.2.2. Inertial circle and the action of forces

$\therefore \left(\frac{V_H^2}{B}\right)$ = (f.V_H), $\therefore B = \frac{V_H}{f}$

And the center of the inertial circle is (B/f, -A/f). This 'B' is the radius of inertial circle.

The time period of the inertial circle (T) is the circumference of the inertial circle divided by its velocity

$$\therefore T = \frac{2\pi B}{V_H} = \frac{2\pi}{f} = \frac{\pi}{\Omega \sin\theta} \quad \text{.....(11)}$$

This can also be found by taking the time derivative of equation 6 and substituting in equation 7 for the right hand side to yield

$$\frac{\partial^2 \mathbf{u}}{\partial \mathbf{t}^2} = -\mathbf{f}^2 \mathbf{u} \quad \text{.....(12)}$$

Similarly taking the time derivative of equation 7 and substituting in equation 6 for the right hand yields

$$\frac{\partial^2 \mathbf{v}}{\partial \mathbf{t}^2} = \mathbf{f}^2 \mathbf{v} \quad \text{.....(13)}$$

Equations 12 and 13 are wave equations—and have solutions that can use either the sin or cosine functions. Let's use the sin function, then

$u(t)=U\sin(\omega t)$ .....(14)

where U is the amplitude of the wave and ω is the wave's frequency

So substituting 14 into 12 we find

$\omega^2=f^2$ (15)

This reveals that the frequency of the wave is the Coriolis frequency, f.

From equation 11 we know, $f = 2\pi/T$ where T is the local inertial period or the time it takes a particle to complete a single loop.

So we can write

$u(t)=U \sin(ft)$

By inspection of 6 and 7 we can see that if u varies with the sin(ft) then v (which is the derivative of u) must vary with –cos(ft).

Thus u = U sin (ft) and v = -Ucos(ft).

This can be written in complex notation, where u=u*iv, this yields

$u=U\ e^{ift}$, Where $e^{ift} = \cos(ft)+i*\sin(ft)$ which traces out a circle over period $T=2\pi/f$.

Note that in the southern Hemisphere f is negative. So the rotation is in the opposite sense (counterclockwise).

In reality a storm that excites inertial oscillations has a finite length scale. This leads to spatial variability in the strength of inertial oscillations. This variability leads to horizontal flow divergences (and convergences) which then excites internal waves at or near the inertial frequency. The propagation of these waves away from the generation site will have a downward component and this can increase vertical shears in the main oceanic thermocline and reduce the Richardson number to a point where mixing may occur. Downward propagating inertial waves is an important mechanism that transmits the surface wind forcing to the main oceanic thermocline. Furthermore, these inertial waves interact with the mean flow fields that can focus there energy in regions of negative vorticity.

The period of inertial circle at different latitudes is

At poles = 11.97 hours

At 30^o = 24 hours

At 45^o = 16.93 hours

At 0^o = infinity

Thus it decreases with increase of latitude (θ)

SIZE OF THE INERTIAL CIRCLE:

Since the radius of curvature of the path varies inversely as f ($B = V_H/f$), the path in middle and high latitudes has a smaller radius on its pole ward side than its equator side (Fig.2.3). Thus the path will not really be closed but the particle will move westward while describing almost circular paths. This effect becomes of great importance in low latitudes where 'f' varies rapidly with 'θ', and where inertia trajectories differ greatly from circles.

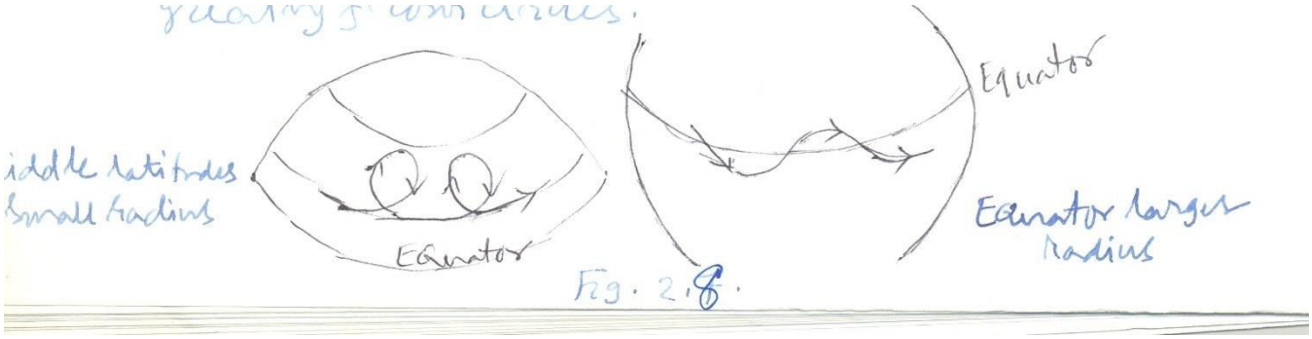

Fig.2.3. inertical circle size at middle latitudes and equatorial radius.

2.1.4. GEOSTROPHIC MOTION:

It is a nonaccelerated frictionless horizontal motion where pressure gradient balances Coriolis acceleration as shown in Fig.2.4i.

From equations (1) and (2) we can write

$\alpha \frac{\partial p}{\partial x} = fv$ and $\alpha \frac{\partial p}{\partial y} = -fu$ squaring these two and adding we get

$$\alpha \sqrt{\left(\frac{\partial p}{\partial x}\right)^2 + \left(\frac{\partial p}{\partial y}\right)^2} = f\sqrt{u^2 + v^2}$$

$$\alpha \frac{\partial p}{\partial n} = fV_H \quad \text{or} \quad V_H = \frac{\alpha}{f}\frac{\partial p}{\partial n} \qquad \text{.....(11)}$$

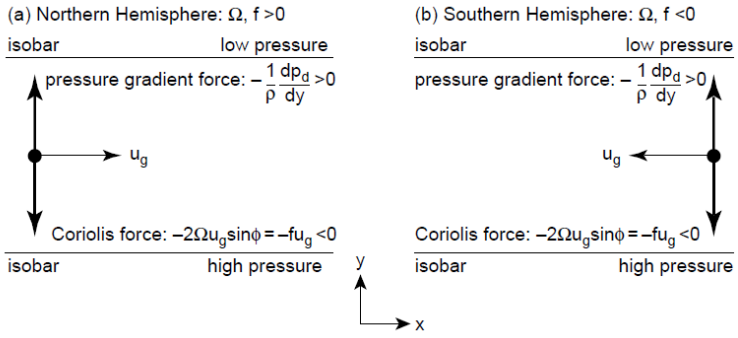

Fig. 2.4i. Balance of forces under Geostrophic motion. Note coriolis force acts right hand side of the current (u_g) in N.H (a) and left hand side in S.H (b).

2.2. HELLAND-HANSEN'S COMPUTATION OF SLOPE AND CURRENTS:

The theoretical geostrophic equation (11) is not practicable to measure the slope of the sea surface. So the distribution of density is used as the density variation in the oceans is related to the slope of the sea surface.

2.2.1. SLOPE OF THE ISOBARIC SURFACE:

Under barotropic conditions the slope of the isobaric surface is constant ($\theta_1 = \theta_2 = \theta$) with the level surface or geopotential surface where as under baroclinic conditions this slope is different at different depths ($\theta_1 \neq \theta_2$).

The geostrophic currents can be calculated from fig.2.4

If the balance of forces at 'B' is taken

$$\alpha \frac{\partial p}{\partial n} \cos\theta = g$$

$$\alpha \frac{\partial p}{\partial n} \sin\theta = fu$$

$$\therefore u = \frac{g}{f} \tan\theta \quad \text{.....(12)}$$

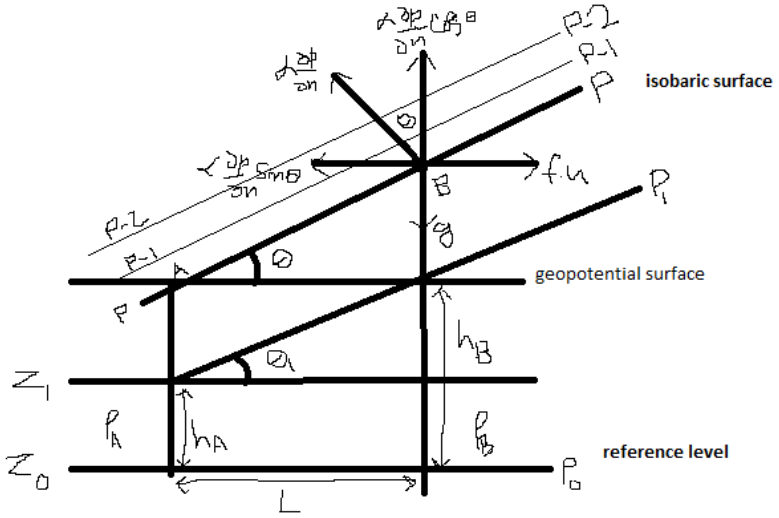

Fig.2.4. Helland-Hansen's computation of slope currents

If the subsurface layer Z_1 to Z_o is considered, we can write the slope. Let θ_1 is the inclination of the isobaric surface P_1 at Z_1 depth and let Z_o is the reference level which coincides with the geopotential

surface. So this will be considered as the level of no motion as shown in Fig.2.4. Let the height of this isobaric surface from the reference level is h_A and h_B and the densities be ρ_A and ρ_B respectively at stations A and B. Let 'L' is the horizontal distance between the two stations A and B.

$$\therefore \tan\theta_1 = \frac{h_B - h_A}{L}$$

Using equation (12) we can write

$$u_1 = \frac{g}{f}\left[\frac{h_B - h_A}{L}\right] \quad \text{.....} \quad (13)$$

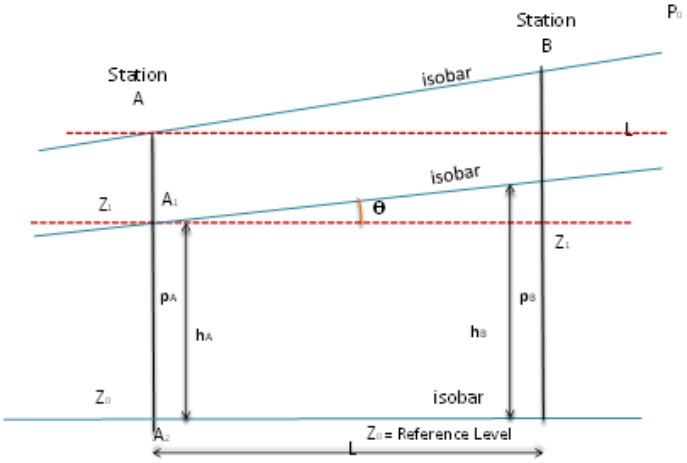

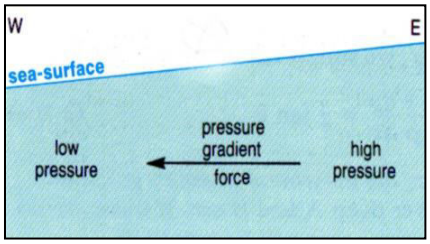

The difference in hydrostatic pressure between P_1 and P_o at station A and B is same because at both the same stations same isobaric surfaces.

$\therefore$ *pressure* difference at 'A' = pressure difference at 'B'

$\therefore (P_{1A} - P_o) = (P_{1B} - P_o)$

since $P_{1A} = P_{1B}$ and $P = \rho gh$,

$$\rho_A g h_A = \rho_B g h_B$$

$$\therefore \quad h_A = h_B . \frac{\rho_B}{\rho_A} \quad \text{.....} \quad (14)$$

Substituting (14) in (13) we get

$$u_1 = \frac{g}{fL} h_B \left[1 - \frac{\rho_B}{\rho_A}\right] \quad \text{.....} \quad (15)$$

This is called Helland-Hansen's equation. This shows that the geostrophic current depends on the density distribution. The direction of current is taken as denser water (low topography) to the left in the Northern hemisphere and to the right hand side in the southern hemisphere.

2.3. PRACTICAL METHOD OF COMPUTATION OF RELATIVE CURRENTS:

To compute currents at successive depths in a series of manner a little modified formula of Helland-Hansen is used. It works out in the same lines but uses dynamic depths which can be conveniently computed from the temperature salinity data that is regularly collected in the oceans.

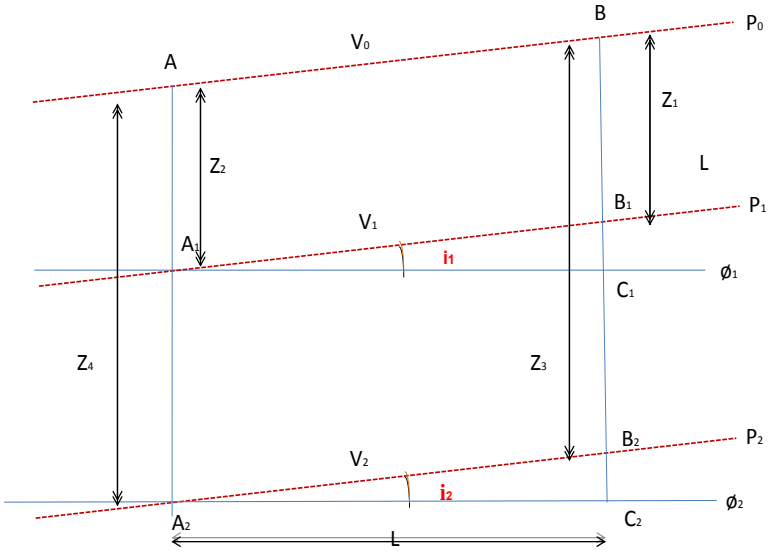

Fig.2.7

As per the figure 2.7 let the two stations A and B are at a distance of L on the sea surface AB. Let the isobaric surfaces P_1 and P_2 are inclined at angles θ_1 and θ_2 with respect to equigeopotential surfaces ϕ_1 and ϕ_2 respectively and let v_1 and v_2 are the currents at these surfaces. Let the depths Z_1, Z_2, Z_3 and Z_4 of the respective points as indicated in the figure 2.7.

We know from equation (12)

$$fv_1 = g\tan\theta_1 \quad \text{and} \quad fv_2 = g\tan\theta_2$$

$$\therefore f(v_1 - v_2) = g(\tan\theta_1 - \tan\theta_2) = g\left[\frac{B_1C_1}{A_1C_1} - \frac{B_2C_2}{A_2C_2}\right]$$

We know $B_1C_1 = B_1C_2 - C_1C_2$ and $B_2C_2 = B_1C_2 - B_1B_2$

$\therefore$ B_1C_1 - B_2C_2 = B_1B_2 - C_1C_2 we also know A_1C_1 = A_2C_2 = L

$$\therefore f(v_1 - v_2) = \frac{g}{L}\left[B_1B_2 - A_1A_2\right] \quad (\because C_1C_2 = A_1A_2)$$

We can write $B_1B_2 = BB_2 - BB_1 = Z_3 - Z_1$

And $A_1A_2 = AA_2 - AA_1 = Z_4 - Z_2$

$$\therefore f(v_1 - v_2) = \frac{g}{L}\left[(Z_3 - Z_1) - (Z_4 - Z_2)\right]$$

Now from hydrostatic equation and geopotential we know

$$\int_{Z_1}^{Z_3} g\,dz = \int_{P_1}^{P_2} \alpha\,dp = \int_{P_1}^{P_2} (\alpha_{35,0,P} + \delta_A)\,dp$$

Similarly for station B we can write $\int_{Z_2}^{Z_4} g\,dz = \int_{P_1}^{P_2} \alpha\,dp = \int_{P_1}^{P_2} (\alpha_{35,0,P} + \delta_B)\,dp$

Substituting all the above we get

$$\frac{g}{L}\left[(Z_3 - Z_1) - (Z_4 - Z_2)\right] = \frac{1}{L}\left[\int_{P_1}^{P_2} \delta_A\,dp - \int_{P_1}^{P_2} \delta_B\,dp - \right]$$

$$\therefore f(v_1 - v_2) = \frac{1}{fL}\left[(\Delta\phi_A) - (\Delta\phi_B)\right]$$

Where $(\Delta\phi_A and \Delta\phi_B)$ are called geopotential anomalies at A and B

$$\therefore (v_1 - v_2) = \frac{10}{fL}\left[(\Delta\phi_A) - (\Delta\phi_B)\right] \quad \text{.....(16)}$$

The conversion factor 10 is used to convert the geometric meter (dz) to dynamic meter (D) since d ϕ = gdz = 10dz as geopotential is measured in dynamic meters. So these depths are called dynamic depths.

If L is in meters, δ in cm^3g^{-1} and P in decibars the current will be in ms^{-1}.

2.3.1. ABSOLUTE CURRENTS & LEVEL OF NO MOTION:

The relative currents are calculated using the equation (16). As the equation says, actually these are the differences between the currents of one layer to the other subsurface layer. So to know the

actual or absolute current at any depth we must know any one current at any other level. So that on cumulative addition we can get currents at other upper levels.

As we do not know the current at any depth a 'level of no motion' which exists somewhere in the deep layers say around 2000 to 3000 m in general. If the level of no motion has zero current from that level, the relative current ($v_1 - v_2$) can be added serially above to get the absolute current at the desired level. There are different methods available to estimate the layer of no motion. One such well known method is Defant's method. It uses the relative dynamic topography $(\Delta\phi_A - \Delta\phi_B)$. When this is plotted against the depth, at some depth below, this curve goes parallel to the ordinate (depth). This indicates that at this depth the current is zero because $(\Delta\phi_A - \Delta\phi_B)$ is zero.

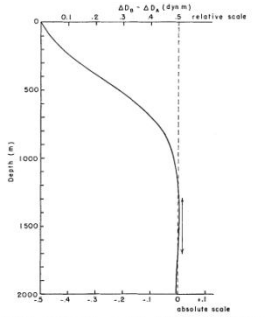

Fig.38. Dynamic depth differences, $\Delta D_A - \Delta D_B$, of isobaric surfaces for Atlantis station numbers 5298 and 5299 as a function of depth. The relative scale is shown at the top, the most probable absolute scale at the bottom of the graph.

2.3.2. DIRECTION OF RELATIVE CURRENT AND DYNAMIC TOPOGRAPHY:

As we have seen earlier in figure 2.7 the current flows at right angles to the slope of the isobaric surface and so flows along the contours of dynamic height. The direction of flow will be such that the isobaric surface slopes up towards right in N.H and left in the S.H.

So the faster the current, the steeper is the dynamic topography. In other words the closer the spacing of the lines of topography the faster is the current as shown in Fig.2.8.

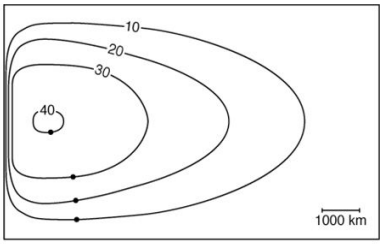

Fig.2.8. Left hand side the lines are closer than right hand side implies the topography is steeper in left and so currents are faster in left than in the right.

2.8.3. GRADIENT MOTION:

While the geostrophic current flows parallel to the straight isobars, the gradient motion is parallel to the curved isobars. So apart from pressure gradient force and Coriolis force, centrifugal force also comes into being in the case of gradient motion.

The balance of forces for gradient motion is

$$-\alpha \frac{\partial p}{\partial n} = f.C \pm \frac{C^2}{r} \quad \text{.....(2.20)}$$

where C^2/r is the centrifugal acceleration, $\pm$ sign is because, the centrifugal acceleration may add either to Coriolis or pressure gradient.

If the flow is cyclonic, it is positive and so centrifugal force will be added to Coriolis and vice versa. Here the positive sign is taken for cyclonic flow and negative sign for anticyclonic flow for both the hemispheres as shown in Figures 43 & 2.10.

So the balance of forces for gradient motion around a cyclonic flow (Low pressure) is :

$$-\alpha \frac{\partial p}{\partial n} = f.C + \frac{C^2}{r} \quad \text{.....(2.21)}$$

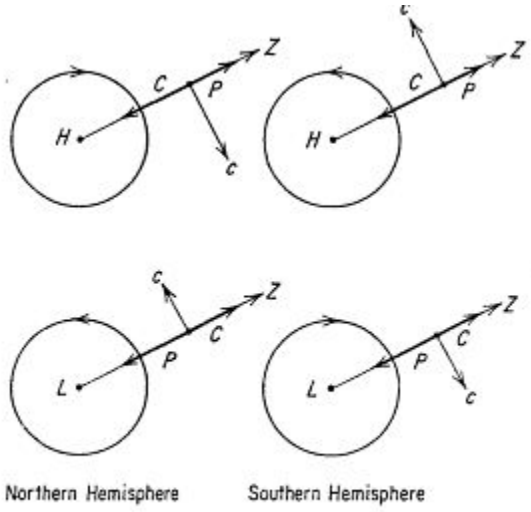

Fig.43. Balance of forces in a gradient current. P denotes the pressure gradient, C the Coriolis force, and Z the centrifugal force.

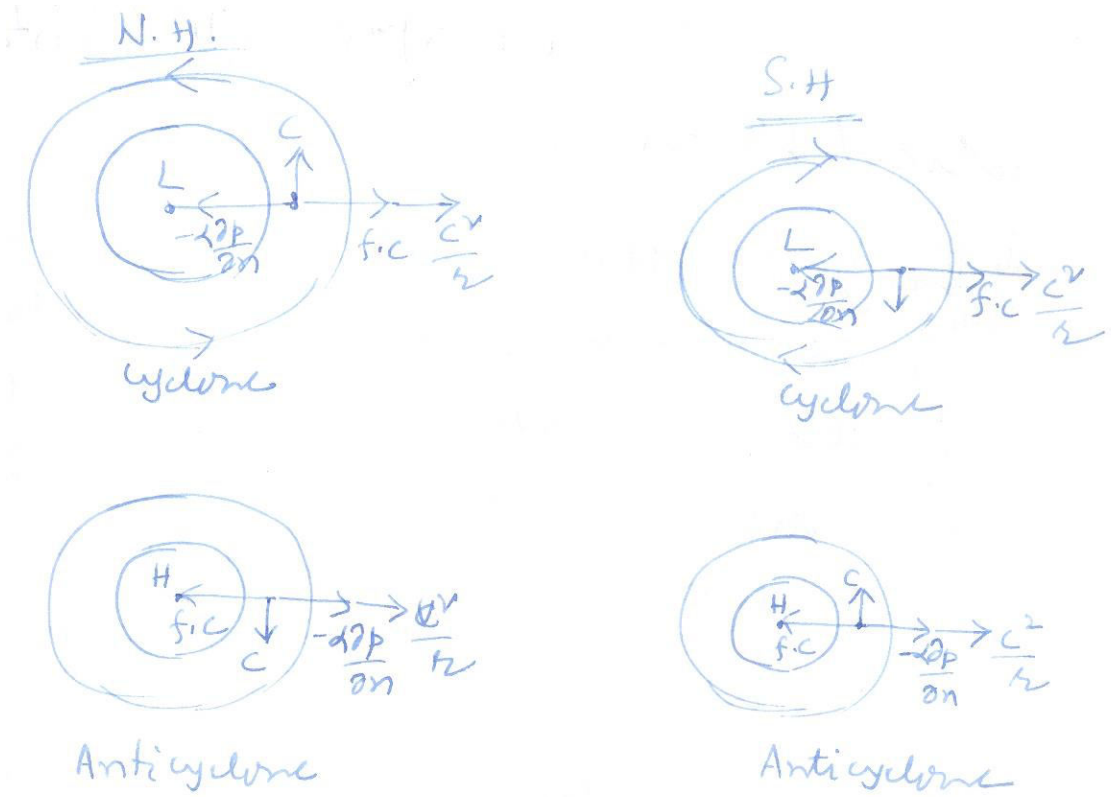

Fig.2.10 shows the balance of forces in a cyclone and anticyclone in N.H and S.H respectively. Which clearly shows that pressure gradient is more than the Coriolis for cyclonic motion (Low) and Coriolis is more than the pressure gradient for anticyclonic motion (High).

Balance of forces under an anticyclone is:

$$f.C = -\alpha \frac{\partial p}{\partial n} + \frac{C^2}{r} \quad \text{.....(2.22)}$$

From the observation of equations 2.17 and 2.18 it is clear that in the case of cyclonic flow, the centrifugal force augments the Coriolis force and for anticyclonic flow it augments the pressure gradient force.

In the absence of a pressure gradient, equations 2.17 and 2.18 reduces to the balance between Coriolis and centrifugal forces as

$$f.C = \pm \frac{C^2}{r}$$

Which is nothing but the inertial motion and ‘r’ is the inertial radius.

Considering the equation for cyclone (equation 2.21):

$$-r\alpha\frac{\partial p}{\partial n} = rfC + C^2$$

$$C^2 + rfc + r\alpha\frac{\partial p}{\partial n} = 0$$

This is a quadratic equation in C and its roots are

$$C = \frac{-rf \pm \sqrt{r^2 f^2 - 4r\alpha\frac{\partial p}{\partial n}}}{2} = \frac{-rf}{2} \pm \frac{1}{2}\sqrt{r(rf^2 - 4\alpha\frac{\partial p}{\partial n})} \quad .....(2.23)$$

Out of the two roots of the equation 2.23, which root is valid is known when we put $\alpha\partial p/\partial n=0$,C=0 taking the positive sign for the radical. Therefore, the valid equation for the cyclone is:

$$C = \frac{-rf}{2} + \sqrt{\frac{f^2 r^2}{4} - r\alpha\frac{\partial p}{\partial n}} \quad .....(2.24)$$

And the corresponding flow for anticyclone is (equation 2.22).

$C^2 - rfc - r\alpha\frac{\partial p}{\partial n} = 0$ solving this quadratic equation, we get two roots again, taking the condition when $\alpha\partial p/\partial n = 0$, C=0when the radical is taken as negative. So the valid root for anticyclone is:

$$C = \frac{rf}{2} - \sqrt{\frac{f^2 r^2}{4} + r\alpha\frac{\partial p}{\partial n}} \quad .....(2.25)$$

Thus out of the four roots of equations (2.21) and (2.22), only two are valid such that the radical for the cyclonic flow is positive and negative for anticyclonic flow.

From the equation 2.26, it is obvious that if $r\alpha\frac{\partial p}{\partial n} \geq \frac{f^2 r^2}{4}$ the roots will be imaginary. Therefore the pressure gradient in an anticyclone theoretically can not exceed the Coriolis force. Thus in order to maintain a real value of 'C' for a current around a high pressure, it is necessary that

$$r\alpha\frac{\partial p}{\partial n} \leq \frac{f^2 r^2}{4}$$

$$or \left|\frac{\partial p}{\partial n}\right| \leq \frac{rf^2}{4\alpha}$$

$$or$$

$$\left\|\frac{\partial p}{\partial n}\right\| \leq \left\|\frac{r}{\alpha}\Omega^2 \sin^2\Phi\right\|$$

That is, in a high the magnitude of the pressure gradient may not exceed a certain value determined largely by the latitude ϕ and distance from the centre (r). Which means as r becomes small; the pressure gradient also becomes small. This is the reason for the small pressure gradient and light currents over a high pressure (anticyclone). In a cyclone (low) there is no such restriction and the pressure gradient and currents can be very large near the centre.

2.7.5. COMPARISON OF GEOSTROPHIC AND GRADIENT MOTIONS:

We know the equation of geostrophic current from equation 2.15 as

$$-\alpha \frac{\partial p}{\partial n} = f.v_g$$
$$or V_g = -\frac{1}{f\rho}\frac{\partial p}{\partial n}$$

we know the gradient motion equation for cyclone as (from equation 2.24)

$$C = -\frac{rf}{2} + \sqrt{\frac{f^2 r^2}{4} - r(-f.V_g)}$$
$$\left[C + \frac{fr}{2}\right]^2 = \frac{f^2 r^2}{4} + frV_g$$
$$V_g = \frac{C^2}{fr} + C = C(1 + \frac{C}{fr}).....(2.27)$$

In normal flow around a low, c is cyclonic and therefore positive. Both 'r' and 'f'' are also positive in N.H. Thus in a 'low' V_g is greater than 'C' and the geostrophic value is an over estimate of the gradient motion.

And around a high pressure both c and V_g are negative. So taking the modulus

$$\left|V_g\right| = |C| - \left|\frac{C^2}{fr}\right|.....(2.28)$$

Hence in a 'High', $V_g <$ C, or the geostrophic value is an under estimate of the gradient motion.

Lecture Series of Berhampur University in Physical Oceanography
By Prof.A.S.N.Murty

Chapter – 3

Two Layer approximation-Margule's equation

The general distribution of density in the oceans is like a two layer ocean as shown below.

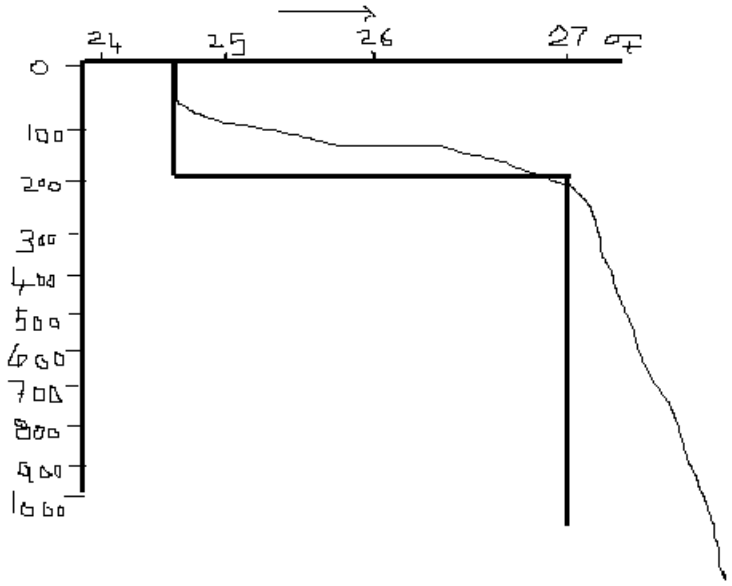

A layer of more or less uniform density near the surface and a deeper layer of higher density below with sharp increase of density between is called pycnocline. The approximation of distinctly showing the stratification of two Layer Ocean is shown by the thick solid line. Here the pycnocline acts as a discontinuity or front between the two different water masses above and below.

A general derivation of the relationship between the inclination of a discontinuity between layers of differing density and velocity are given below:

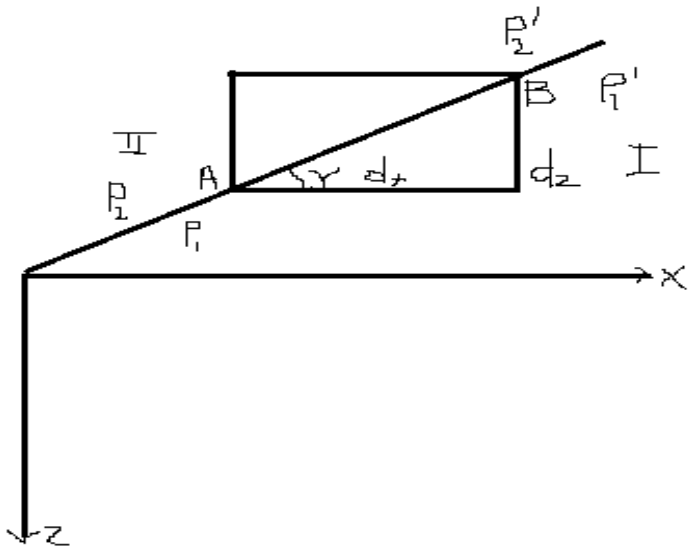

In the above figure the y-axis is oriented along the isobaric surface (P = constant) which is the discontinuity surface(S) such that AB is a small length element 'ds' and 'z' is pointing downward along depth of the ocean.

At the points A and B as pressure is uniform we can write taking $p_1' = p_2'$ and using Taylor's expansion we can write:

$$p_1 + \left(\frac{\partial p}{\partial x}\right)_1 dx + \left(\frac{\partial p}{\partial z}\right)_1 dz = p_1' \quad \text{.....(1)}$$

$$p_2 + \left(\frac{\partial p}{\partial x}\right)_2 dx + \left(\frac{\partial p}{\partial z}\right)_2 dz = p_2' \quad \text{.....(2)}$$

After subtracting the equation (2) from equation (1) we get as:

$$\left[\left(\frac{\partial p}{\partial x}\right)_1 - \left(\frac{\partial p}{\partial x}\right)_2\right] dx + \left[\left(\frac{\partial p}{\partial z}\right)_1 - \left(\frac{\partial p}{\partial z}\right)_2\right] dz = 0$$

Let the slope $\frac{dz}{dx} = \gamma$ and can be written as

$$\tan\gamma = \frac{dz}{dx} = -\frac{\left[\left(\frac{\partial p}{\partial x}\right)_1 - \left(\frac{\partial p}{\partial x}\right)_2\right]}{\left[\left(\frac{\partial p}{\partial z}\right)_1 - \left(\frac{\partial p}{\partial z}\right)_2\right]} \quad \text{.....(3)}$$

To express this slope in terms of densities and velocities we have to use the equation of motion.

$$\frac{du}{dt} = -\alpha\frac{\partial p}{\partial x} + fv \quad \text{.....(4)}$$

$$\frac{dw}{dt} = -\alpha\frac{\partial p}{\partial z} + g \quad \text{.....(5)}$$

Let $\frac{du}{dt} = b_x$ and $\frac{dw}{dt} = b_z$ and we know $\alpha = \frac{1}{\rho}$. Substituting rewriting

$$b_x = -\frac{1}{\rho}\frac{\partial p}{\partial x} + fv \quad \text{.....(6)}$$

$$b_z = -\frac{1}{\rho}\frac{\partial p}{\partial z} + g \quad \text{.....(7)}$$

From equation (6) we can write as:

$$\frac{\partial p}{\partial x} = f\rho v - \rho b_x$$

For the two layers the equations can be written as

$$\left(\frac{\partial p}{\partial x}\right)_1 = f(\rho v)_1 - (\rho b_x)_1$$

$$\left(\frac{\partial p}{\partial x}\right)_2 = f(\rho v)_2 - (\rho b_x)_2$$

Subtracting one from the other we get

$$\left(\frac{\partial p}{\partial x}\right)_1 - \left(\frac{\partial p}{\partial x}\right)_2 = f\left[(\rho v)_1 - (\rho v)_2\right] - \left[(\rho b_x)_1 - (\rho b_x)_2\right] \quad \text{.....(8)}$$

Similarly we can write for b_z using equation (7) as

$$\left(\frac{\partial p}{\partial z}\right)_1 - \left(\frac{\partial p}{\partial z}\right)_2 = g\left[(\rho)_1 - (\rho)_2\right] - \left[(\rho b_z)_1 - (\rho b_z)_2\right] \quad \text{.....(9)}$$

Hence from equation (3) and equations (8) and (9), it follows:

$$\tan\gamma = \frac{dz}{dx} = -\frac{f\left[(\rho v)_1 - (\rho v)_2\right] - \left[(\rho b_x)_1 - (\rho b_x)_2\right]}{g\left[(\rho)_1 - (\rho)_2\right] - \left[(\rho b_z)_1 - (\rho b_z)_2\right]}$$

Under non accelerated frictionless uniform motion we know $b_x = \frac{du}{dt} = b_z = \frac{dw}{dt} = 0$

$$\therefore \tan\gamma = -\frac{f}{g}\left[\frac{\rho_1 v_1 - \rho_2 v_2}{\rho_1 - \rho_2}\right]$$

Figure below shows schematically for Northern Hemisphere, isobaric surfaces and the inclination of density discontinuity between two different water bodies.

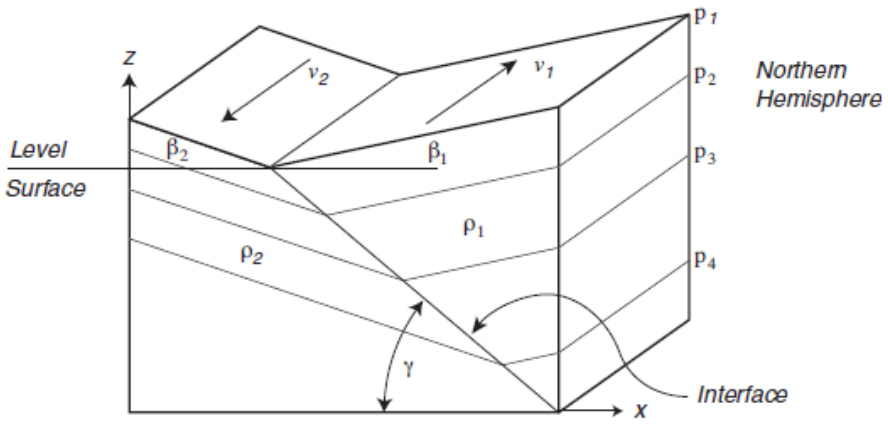

Fig. Slopes β_1 and β_2 of the sea surface and the slope of the interface between two homogeneous, moving layers, with densities ρ_1 and ρ_2 in the northern hemisphere.

The above figure shows the isobaric surfaces and currents in a two layer ocean where a less dense water mass ρ_1 is separated from a denser water mass ρ_2 such that γ is the angle or slope of discontinuity with the level surface. The angles β_1 and β_2 are the angles of the sea surfaces with the level surface in the rarer and denser waters respectively corresponding to the geostrophic velocities v_1 and v_2.

Lecture Series of Berhampur University in Physical Oceanography
By Prof.A.S.N.Murty

Chapter – 4

CURRENTS WITH FRICTION

Earlier people were under the impression that if wind blows on a body in a fluid on the earth's surface, the body will move in the direction of the wind. But this concept was proved wrong by Nansen (1902) while studying the drift of ice berg due to wind during Fram expedition (1893-96). He found that the drift of ice with respect to the wind did not follow the wind direction, but deviated from it by about 20 to 40^o to the right. He explained that this deviation may be due to earth's rotation.

Later his student Ekman investigated this problem and explained mathematically. This finally laid the foundation for one of the most remarkable theoretical developments in dynamic oceanography.

Pure drift currents are produced by the drag of the wind passing over homogeneous ocean. So Ekman considered the velocity into two parts. One is geostrophic velocity (v_g) and the other is velocity due to friction (it is called Ekman velocity, v_E).

$\therefore\ f.v \ = \ f\,(v_g + v_E)$

we know the equation of motion with friction as

$$\frac{du}{dt} = -\alpha\frac{\partial p}{\partial x} + f.v + \frac{A_z}{\rho}.\frac{\partial^2 u}{\partial z^2}$$

for non-accelerated uniform motion

$$f.v = \alpha\frac{\partial p}{\partial x} - \frac{A_z}{\rho}.\frac{\partial^2 u}{\partial z^2} \quad \text{or} \quad f.(v_g + v_E) = \alpha\frac{\partial p}{\partial x} - \frac{A_z}{\rho}.\frac{\partial^2 u}{\partial z^2}$$

We know the geostrophic balance $f.v_g = \alpha\frac{\partial p}{\partial x}$

$$\therefore\ f.(v_E) = -\frac{A_z}{\rho}.\frac{\partial^2 u}{\partial z^2} \quad \ldots\ldots\ldots\ldots\ldots\ldots\ldots\ldots\ldots\ldots(17)$$

Similarly x component of equation can be written as

$$f.(u_E) = \frac{A_z}{\rho}.\frac{\partial^2 v}{\partial z^2} \quad \ldots\ldots\ldots\ldots\ldots\ldots\ldots\ldots\ldots\ldots(18)$$

2.4.1. ASSUMPTIONS OF EKMAN:

To solve the frictional equation (17) of motion, Ekman made some assumptions. They are:

i) They are no boundaries to oceans (no lateral friction)
ii) Infinitely deep water (so u = v = 0 at bottom)
iii) Homogeneous water (ρ = constant)
iv) No slope at the surface ($\frac{\partial p}{\partial x} = 0$)
v) A steady wind blowing over the sea surface for a long time in the direction of y component (i.e. wind stress in x direction , $\tau_x = 0$)

vi) Eddy viscosity coefficient (A_z) is constant.

vii) The flow is nonaccelerated (i.e. $\frac{du}{dt} = \frac{dv}{dt} = 0$) and horizontal.

2.4.2. EKMAN'S DERIVATION:

The equations (17) and (18) can be written after omitting the suffixes as:

$$\frac{\partial^2 u}{\partial z^2} = -\frac{f\rho}{A} v \quad \text{and} \quad \frac{\partial^2 v}{\partial z^2} = \frac{f\rho}{A} u, \qquad \text{Let } \frac{f\rho}{A} = a^2$$

Substituting i^2 for –ve for former and multiplying both sides by i to the later we can write as:

$$\frac{\partial^2 u}{\partial z^2} + i\frac{\partial^2 v}{\partial z^2} = ia^2(u+iv) \text{ or } \frac{\partial^2}{\partial z^2}(u+iv) = ia^2(u+iv)$$

Let $(u+iv) = W$

$$\therefore \frac{\partial^2}{\partial z^2}(W) = ia^2(W).$$

This is a second order differential equation and the solution is:

$\therefore W = Ae^{az\sqrt{i}} + Be^{-az\sqrt{i}}$ where $A = C_1 e^{ip}$ and $B = C_2 e^{-iq}$ are complex constants and p and q are also constants in the hyperbolic function and C_1 and C_2 are linear constants. So substituting them

$$\therefore W = C_1 e^{ip} e^{az\sqrt{i}} + C_2 e^{-iq} e^{-az\sqrt{i}}$$

we know $e^{ip} = \cos p + i \sin p$ and $e^{-iq} = \cos q - i \sin q$ substituting and simplifying using the relation $\sqrt{i} = \frac{1+i}{\sqrt{2}}$ we get

$$W = u + iv = (C_1 \cos p + iC_1 \sin p) e^{\frac{az}{\sqrt{2}}} . e^{i\frac{az}{\sqrt{2}}} + (C_2 \cos q - iC_2 \sin q) e^{-\frac{az}{\sqrt{2}}} . e^{-i\frac{az}{\sqrt{2}}}$$

On expanding and separating the real and imaginary parts we get

$$u = C_1 e^{\frac{az}{\sqrt{2}}} \cos\left(\frac{az}{\sqrt{2}} + p\right) + C_2 e^{-\frac{az}{\sqrt{2}}} \cos\left(\frac{az}{\sqrt{2}} + q\right)$$

similarly

$$v = C_1 e^{\frac{az}{\sqrt{2}}} \sin\left(\frac{az}{\sqrt{2}} + p\right) - C_2 e^{-\frac{az}{\sqrt{2}}} \sin\left(\frac{az}{\sqrt{2}} + q\right)$$

The four constants C_1, p, C_2 and q have to be determined from the boundary conditions.

i) the lower boundary condition is that the velocity becomes zero (u = v = 0) for infinitely deep water (z = ∞). It is obvious that $C_1 = 0$ in order to satisfy this condition. Then the equations reduces to

$$u = C_2 e^{-\frac{az}{\sqrt{2}}} \cos\left(\frac{az}{\sqrt{2}} + q\right) \quad \ldots\ldots\ldots\ldots\ldots(18)$$

$$v = C_2 e^{-\frac{az}{\sqrt{2}}} \sin\left(\frac{az}{\sqrt{2}} + q\right) \quad \ldots\ldots\ldots\ldots\ldots(19)$$

ii) At the upper boundary a constant wind stress is applied to the sea surface (z =0) along y direction. So the wind stress along x direction

$$\tau_x = -A\left(\frac{du}{dz}\right)_{z=0} = 0 \quad \text{and} \quad \tau_y = -A\left(\frac{dv}{dz}\right)_{z=0}$$

Differentiating equations (18) with respect to z and applying the boundary condition of τ_x on z = 0 we get

$$\left(\frac{du}{dz}\right)_{z=0} = -\frac{a}{\sqrt{2}} C_2 (\sin q + \cos q) = 0$$

which means $(\sin q + \cos q) = 0$, $\sin q = -\cos q$ or $\tan q = -1$ or $q = -\frac{\pi}{4}$

Similarly differentiating equation (19) and applying the boundary condition of τ_y on z = 0 we get

$$\left(\frac{dv}{dz}\right)_{z=0} = -\frac{a}{\sqrt{2}} C_2 (\cos q - \sin q) = -\frac{\tau_y}{A}$$

or

$$\frac{a}{\sqrt{2}} C_2 \left[\cos\left(-\frac{\pi}{4}\right) - \sin\left(-\frac{\pi}{4}\right)\right] = -\frac{\tau_y}{A}$$

on simplifying we get $C_2 = \frac{\tau_y}{Aa}$ where we put $a = \frac{f\rho}{A}$

Substituting all the known constants and rewriting finally we can write

$$u = V_0 e^{-\frac{\pi z}{D}} \cos\left(45 - \frac{\pi z}{D}\right) \quad \ldots\ldots\ldots\ldots\ldots(20)$$

$$v = V_0 e^{-\frac{\pi z}{D}} \sin\left(45 - \frac{\pi z}{D}\right) \quad \ldots\ldots\ldots\ldots\ldots(21)$$

Here $V_0 = \frac{\tau_y}{Aa} = \frac{\pi\tau_y\sqrt{2}}{Df\rho}$ and $D = \pi\sqrt{\frac{2A}{f\rho}} = \pi\sqrt{\frac{A}{\rho\Omega\sin\phi}}$ ….(22)

These are called Ekman equations. These indicate that the surface current is deflected 45^o right hand side to the direction of wind and the current vector decreases continuously with depth. This decrease continues up to a depth of frictional influence where the current speed will be $e^{-\pi}\left(\frac{1}{23}\right)$ times of the current and it is just opposite to the surface current. This is shown through a hodograph in Fig.2.9. The arrows show the velocity and direction of current vectors at depths of equal intervals. When projected on a horizontal plane the end points of the current vectors form a logarithmic spiral called 'Ekman Spiral' indicated by the dashed curve in the figure 2.9.

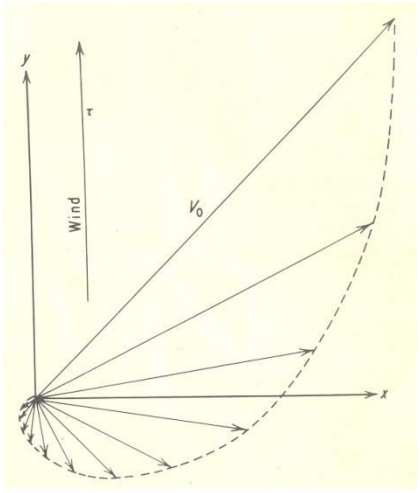

Fig.2.9. Hodograph (dashed line) derived from Ekaman spiral

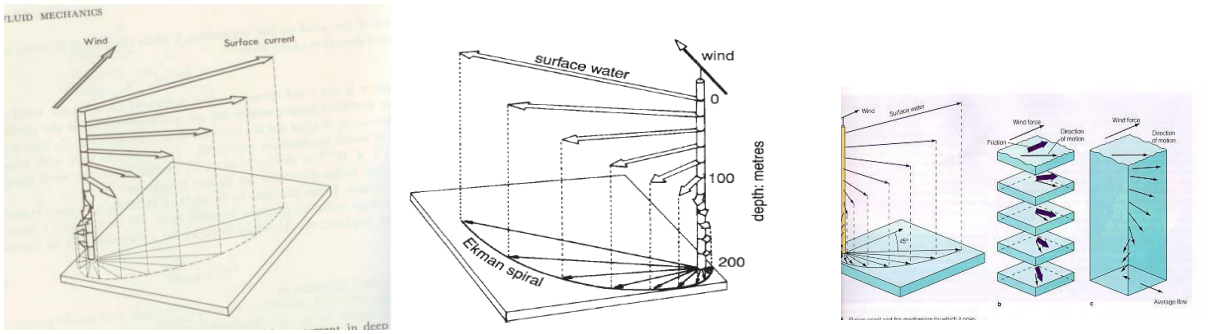

Fig.2.9i. Ekman spiral in N.H(a) and S.H (b), Ekman currents in different depths (c)

2.4.3. EKMAN NET TRANSPORT AND EKMAN PUMPING

The net Ekman mass transport is 90^o to the direction of wind such that right hand side in the N.H and left hand side in the S.H as shown in Fig.2.10. As a result of this horizontal motion vertical motions develop to fill the hollow space. These vertical motions are due to Ekman Pumping.

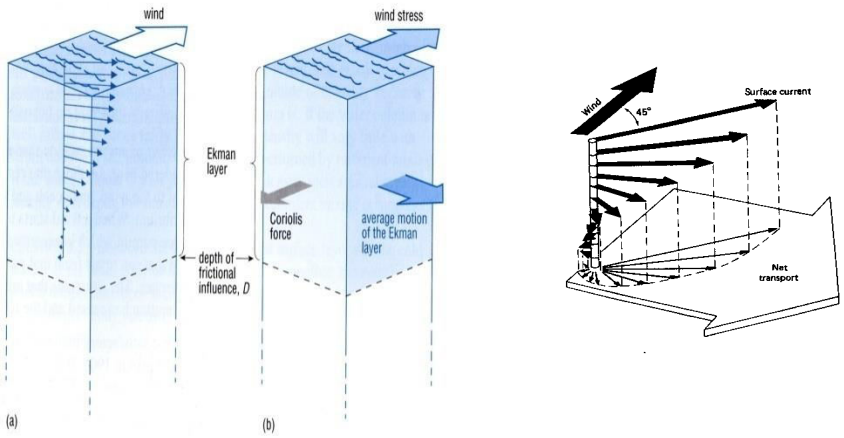

Fig.2.10. a)The Ekman spiral current pattern which under ideal conditions would result from the action of wind (broad white arrow) on surfact waters. The lengths and directions of the thin blue arrows below represent the speed and direction of the wind driven currents. b) For the Ekman layer as a whole, the force resulting from the wind is balanced by the Coriolis force, which in the Northern Hemisphere is 90^0 to the right of the average motion of the layer (broad blue arrow). The depth of frictional influence (or resistance)'D' is indicated by the horizontal dotted lines. From sea surface to Depth of frictional influence is called Ekman layer.

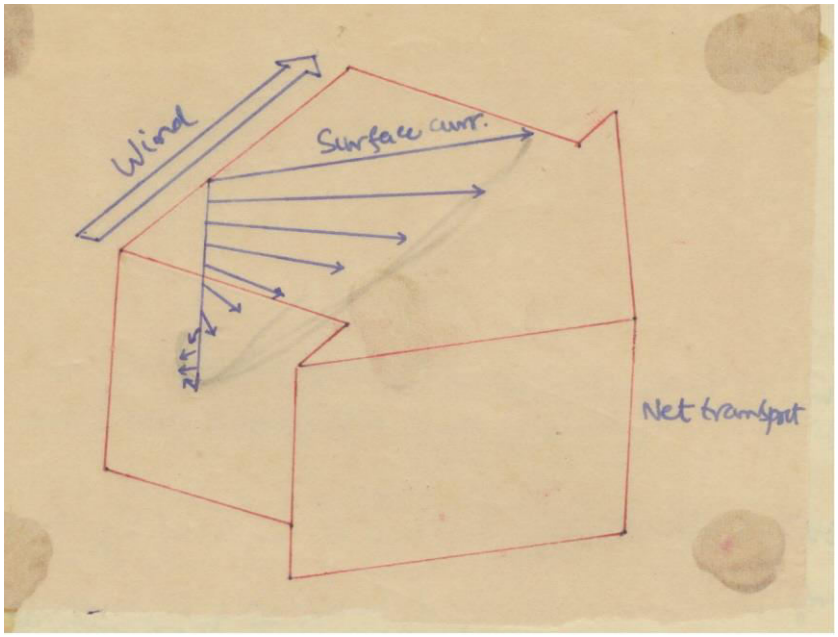

Fig.2.10. Ekman net transport is perpendicular to the wind direction

2.4.4. Interpretation of Ekman's results:

i) At the sea surface (where z = 0) the solutions of equations 20 and 21 become:
$u = \pm V_0 Cos45^0$, $v = V_0 Sin45^0$ …….(23)

which means that the surface current flows at an angle of 45^0 to the direction of wind speed such that right hand side of it in Northern Hemisphere(N.H) and left hand side of it in Southern Hemisphere (S.H

ii) Below the surface, where z is no longer zero, the total current speed would be:

$$V_z = \sqrt{u^2 + v^2} = V_0 e^{-\frac{\pi z}{D}} \left[\sin^2\left(\frac{\pi z}{D} + \frac{\pi}{4}\right) + \cos^2\left(\frac{\pi z}{D} + \frac{\pi}{4}\right) \right] = \pm V_0 e^{-\pi z / D} \quad ..(24)$$

here +ve sign used for N.H and negative sign for S.H.). This also implies as z increases current speed decreases as z is in exponential function. That is, as z increases more in the negative z direction while the direction of velocity changes clockwise in the N.H and anticlockwise in the S.H.

iii) The direction of flow becomes opposite to that of the surface current at a depth z = -D where the speed falls as: $V_D = V_0 . \exp\left(\pi \frac{-D}{D}\right) = V_0 . \exp(-\pi) = 0.04 . V_0$ .....(25)

such that V_0 is surface current. This implies that the current at the depth of frictional resistance is $e^{-\pi}$ (0.04) times of the surface current and it is just opposite to the surface current.

The depth D_E is usually arbitrarily taken as the effective depth of the wind driven current or the Ekman layer. When viewed in a plane, the tips of the arrows of the current vector form a decreasing spiral called Ekman spiral as shown in fig.

2.4.5. Computation of Eddy coefficient of viscosity from Ekman solution:

We know from equation 22, $D = \pi \sqrt{\frac{2A}{f\rho}}$, $\therefore \frac{D^2}{\pi^2} = \frac{2A}{f\rho}$

or $A = \frac{D^2 f\rho}{2\pi^2}$ kg $m^{-1}S^{-1}$.....(26)

Taking $D = 10^2$ meters, $f = 10^{-4}$ and $\rho = 1025$ kg/m^3=10^3,

$A = 50$ kg $m^{-1}S^{-1}$

2.4.6. Estimation of wind factor and Depth of frictional resistance:

The ratio between the surface wind drift current and wind speed is known as 'wind factor' $\left(\frac{V_0}{W}\right)$. In order to obtain numerical relations between the surface current V_0, wind speed W and depth of frictional resistance D, Ekman used some experimental observations.

We know the surface current equation from equation (22) : $V_0 = \frac{\tau_y}{Aa} = \frac{\pi \tau_y \sqrt{2}}{Df\rho}$

We also know $\tau_y = \rho_a C_d W^2$ where ρ_a = density of air = 1.3 kg m^{-3}, C_d = drag coefficient = 1.4×10^{-3} for wind speeds less than 4 m/s and 2.4×10^{-3} for wind speeds more than 4 m/s., W = wind speed in m/s. using these values for W < 4 m/s, $\tau_y = 1.8\times10^{-3}W^2$.

Substituting these values, we can write $V_0 = \frac{0.79\times10^{-5}W^2}{D.f}$ m/s, here ρ = density of water taken as 1025 kg m^{-3}

According to Ekman the wind factor was $\frac{V_0}{W} = \frac{0.0127}{\sqrt{\sin\varphi}}$. This is applicable $\pm10^0$ latitude from the equator. Substituting the value of V_0 in the wind factor comes to

$$\frac{V_0}{W} = \frac{0.79\times10^{-5}W}{D.f} = \frac{0.0127}{\sqrt{\sin\varphi}}$$

$$\therefore D = \frac{4.3W}{\sqrt{\sin\varphi}} \quad \text{.....(27)}$$

Therefore if we know 'W' at latitude φ we can calculate V_0 from equation (22) and the velocity at any depth below the surface from equation (24) and D from equation (27).
The variation of depth of frictional resistance with latitude and wind is as follows:

	φ	10^0	45^0	80^0	A(m^2/s)
	$\frac{V_0}{W}$	0.03	0.05	0.013	
W=10m/s	D (m)	100	50	45	0.014
W=20m/s	D(m)	200	100	90	0.055

2.5. UPWELLING AND DOWNWELLING:

Wind stress at the sea surface not only causes horizontal movement of water (Ekman Net transport), but also leads to vertical motion (Ekman Pumping). This horizontal movement of water leads to a divergence of surface water and so deeper water rises up. Conversely when there is a convergence of the surface water, sinking occurs. This rising and sinking of water are called upwelling and down welling.

Upwelling and down welling occur throughout the oceans both at coastal boundaries as well as in the open ocean. While coastal upwelling occurs due to Ekman pumping, open ocean upwelling causes due to divergences caused due to currents or cyclonic motions in the oceans (Fig.2.11).

Of the several processes occurring in the sea, vertical motions have special significance because of their significant effects on biological productivity on the oceanic environment, though their speeds are much less compared to the horizontal currents.

According to Smith (1964), upwelling is defined as 'an ascending motion of some minimum duration and extent, by which water from subsurface layers is brought to the surface layer and is removed from that area by horizontal flow.

Though upwelling can occur anywhere in the oceans, but it is maximum and significant in the eastern shores (west coasts of continents) of the oceans.

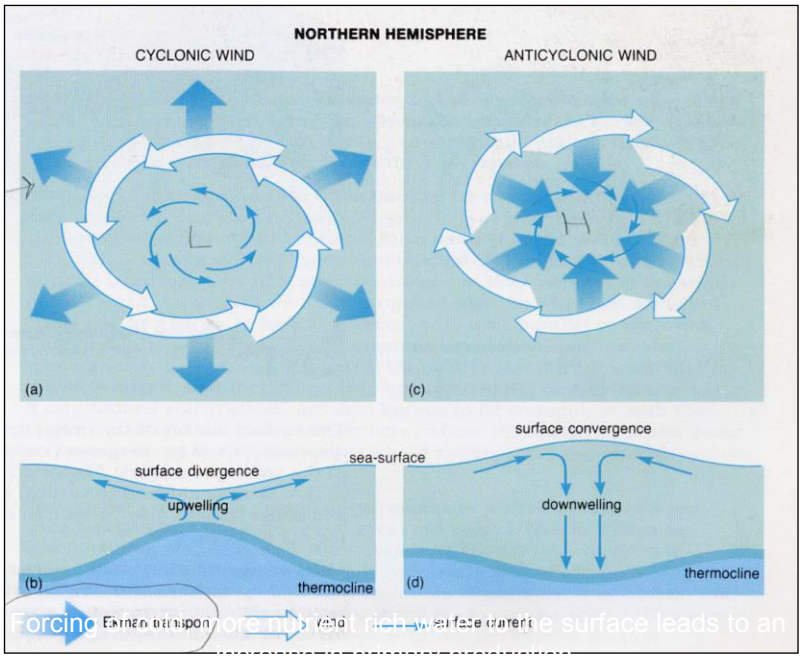

Fig.2.11. a) A Low (L=cyclone) generates upwelling and (c) High (H= anticyclone) generates downwelling. b)decrease of MLD and rising of thermocline in upwelling zone and (d) increase of MLD and depression of thermocline in downwelling.

2.5.1. COASTAL UPWELLING:

Upwelling occurs along the coasts where the prevailing winds carry the surface waters away from the coast. Due to earth's rotation and frictional forces the Ekman net transport due to the wind stress is directed 90^{o} to the right of the wind in the N.H and to the left in the S.H.

So a northerly wind along the west coast of the continent in the N.H carries the surface waters away from the coast resulting in upwelling. Similarly a southerly wind carries the surface waters towards the coast and results in down welling. A southerly wind along the east coast induces upwelling and a northerly wind along the east coast induces down welling in the N.H as shown in Fig.2.12(a).

For the southern hemisphere a southerly wind along the west coast and a northerly wind along the east coast produces upwelling, while a northerly wind along the west coast and a southerly wind along the east coast generates down welling as shown in Fig.2.12(b).

Apart from the wind the ocean currents also produce upwelling and down welling in a similar way.

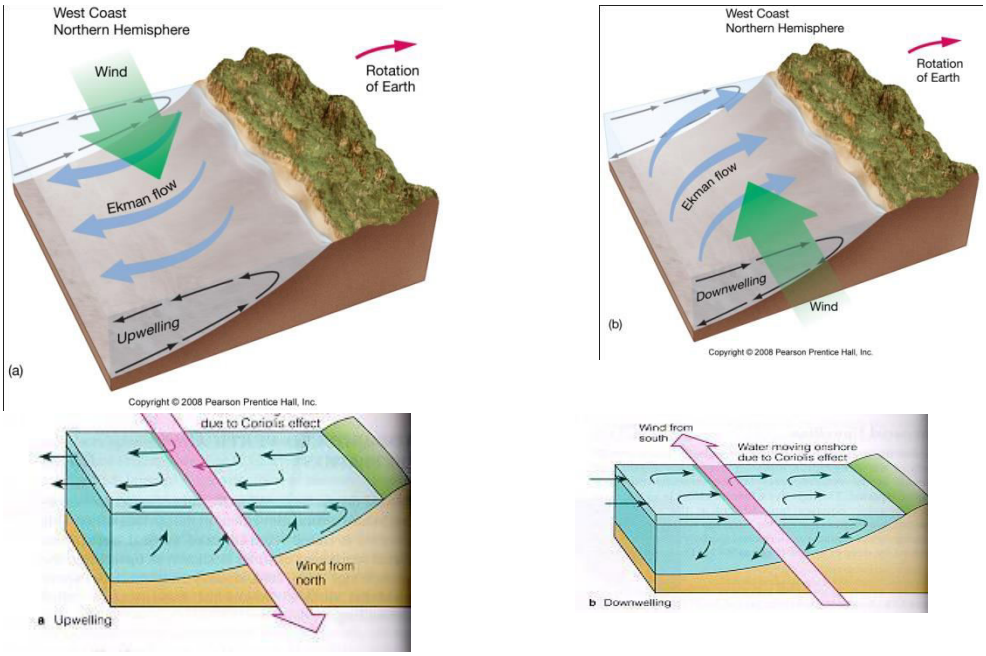

Fig.2.12. (a) generation of upwelling by north wind along a west coast and (b) generation of downwelling by a southwind along a west coast.

2.5.2. OPEN OCEAN UPWELLING AND DOWN WELLING:

Open ocean upwelling causes due to diverging currents or cyclonic motions in the N.H. Similarly down welling results due to converging currents anticyclones as shown in Fig 2.13.

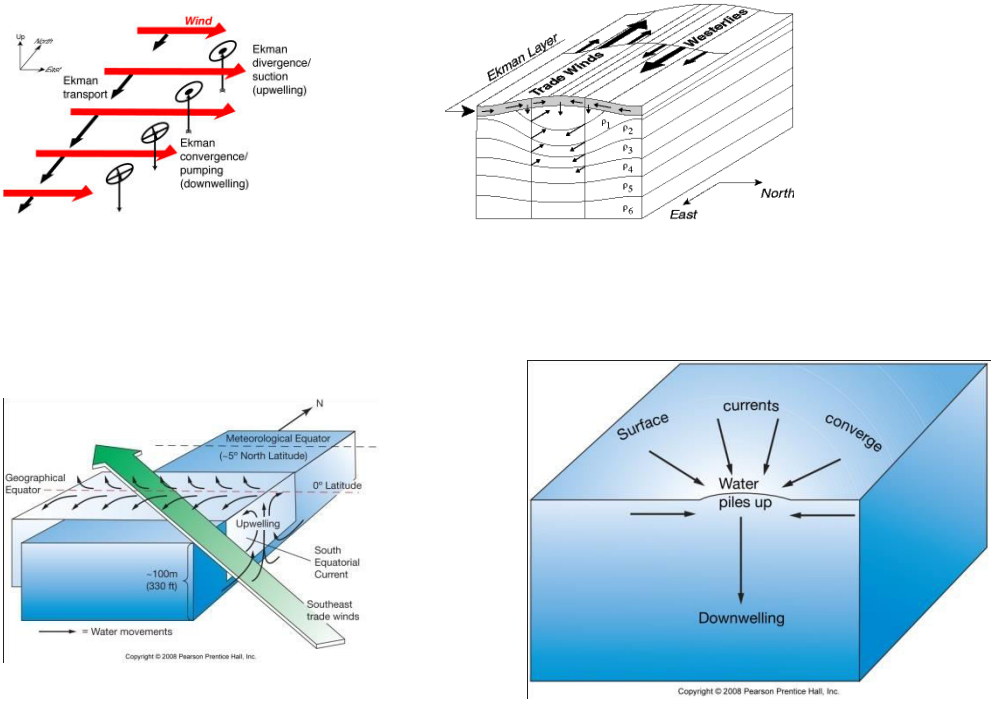

Fig.2.13. Method of occurrence of Open ocean upwelling and downwelling

2.5.3. REGIONS OF UPWELLING:

The most intense upwelling occurs in the coastal regions off the west coasts of the continents where a one sided divergence of the surface layer is caused due to the wind stress parallel to the coasts. Positive numbers (blue, red & yellow) indicate upwelling and negative (green) values downwelling in Fig.2.14 .

The most extensive upwelling regions are associated with the eastern boundary currents as they are the weak zones of surface circulations. So the major upwelling regions in the world which are associated with the eastern boundary currents are the Peru, the Benguela, the Canary and the California current system (fig.2.14). Some areas of western boundary currents in some seasons also develop upwelling as off the coast of Somali, Arabia and east and west coast of India and Gulf of Guinea. The famous equatorial upwelling is associated with the equatorial under current in association with the divergence of equatorial counter current.

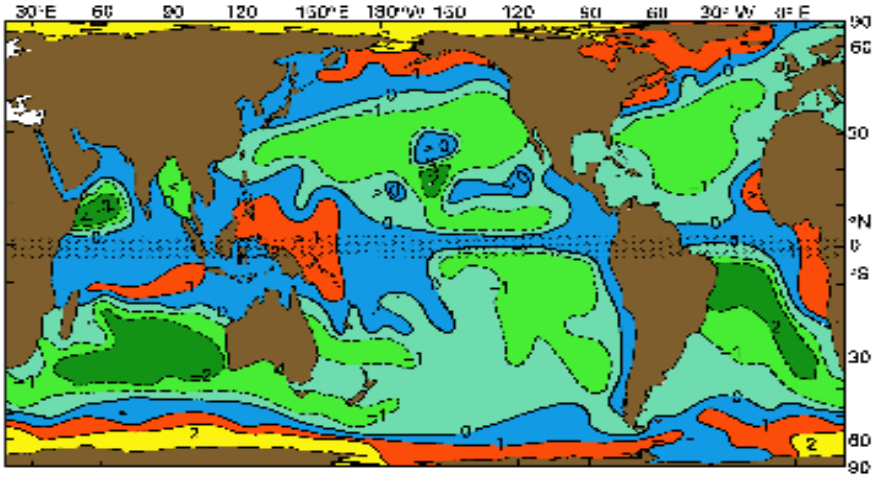

Fig.2.14. Annual mean distribution of Ekman pumping calculated from the mean wind stress (10^{-3} kg $m^2 s^{-1}$). Positive numbers indicate upwelling and negative values sinking. Equatorial region (2^0N to 2^0S) hatched by straight dotted lines is not defined and is to be inferred from dynamical arguments as coriolis is zero here.

2.5.5. EFFECTS OF UPWELLING:

i) The temperature decreases as the cooler subsurface water rises to the sea surface.
ii) As the subsurface water is denser than the surface water, increase of density results.
iii) Increase in the concentration of nutrients like phosphates, nitrates and silicates as subsurface water is not utilized due to less population.
iv) Decrease in the concentration dissolved oxygen
v) Decrease of the thickness of the mixed layer or in other words cropping up of thermocline to naviface as shown in Fig.2.11b.
vi) The mean sea level is lowered as cold subsurface water occupies lesser volume than the warm surface water

2.5.6. IMPORTANCE OF UPWELLING:

Everyone is more interested on upwelling rather than downwelling because upwelling brings lot of changes in the ecosystem of the region whereas downwelling doesn't have any such impact.

As upwelling brings the nutrient rich subsurface water to the sea surface, productivity in this region suddenly increases. So phytoplankton and zooplankton population increases which attracts the fish population and increases their productivity. So if we can identify the regions of upwelling and inform the fishermen community, fish catches will increase and so economy of the country will increase like that of Peru during LaNina period.

Many countries are using remote sensing methods to quickly identify the zones of upwelling in the offshore regions and communicating through radio, television and news papers for enhancing the fish catches. India is a pioneer in this field and giving this technology to at least all the countries bordering the Indian Ocean region.

2.5.7. DYNAMICS OF UPWELLING:

We know the equations motion with friction as:

$$\frac{du}{dt} = -\alpha \frac{\partial p}{\partial x} + fv + \alpha \frac{\partial \tau_x}{\partial z} \ , \ \frac{dv}{dt} = -\alpha \frac{\partial p}{\partial y} - fu + \alpha \frac{\partial \tau_y}{\partial z} \quad \text{....(28a)}$$

these can be written as

$$-fv = -g \frac{\partial \zeta}{\partial x} + A_x \frac{\partial^2 u}{\partial x^2} + A_z \frac{\partial^2 u}{\partial z^2} \qquad (28b)$$

$$fu = -g \frac{\partial \zeta}{\partial y} + A_x \frac{\partial^2 v}{\partial x^2} + A_z \frac{\partial^2 v}{\partial z^2}$$

The equation of continuity is $\frac{\partial u}{\partial x} + \frac{\partial w}{\partial z} = 0$ (29)

On scaling we know the depth of frictional resistance from equation (22) can be written as

$$\therefore D_x = \left[\frac{A_x}{f}\right]^{\frac{1}{2}} \ , \qquad D_y = \left[\frac{A_y}{f}\right]^{\frac{1}{2}} \quad \text{.....(30)}$$

Where D_x is horizontal mixing length and D_y is the Ekman layer depth

Hidaka(1954) assumed for upwelling current as;

i) water surface has no slope parallel to the coast so that $-g \frac{\partial \zeta}{\partial y} = 0$ .....(31)

ii) infinitely deep water

iii) constant wind stress acting over the areas extending from the coast to a distance $2\pi D_x$

The most significant features of the solution are

a) the offshore mass transport takes place in a surface layer of thickness D_y
b) upwelling takes place within a zone adjacent to the coast of width D_x
c) the ratio of vertical horizontal velocity to that of D_y to D_x is

$$\frac{w}{u} = \frac{D_y}{D_x} = \left[\frac{A_y}{A_x}\right]^{1/2} \quad \text{……(32)}$$

If $\frac{A_y}{A_x}$ is taken as 10^{-6} and u = 1 cm/sec then w = 10^{-3} cm/sec, then $\frac{D_x}{D_y} = 10^3$ which means if D_y is taken as 20 m then D_x = 20 km.

2.5.8. Steady state homogeneous water model (Garvine model):

Garvine (1971) retained the term $\frac{\partial \zeta}{\partial y}$ and considered water of uniform depth H which was large compared to D_y. he also included a finite $\frac{\partial \zeta}{\partial y}$ term which lead to the following arguments;

i) beyond a narrow coastal boundary layer, the frictional terms on the right hand side of equation (23) can be neglected, then

$$fu = -g\frac{\partial \zeta}{\partial y} \quad \text{……(33)}$$

ii) Out side the coastal boundary layer the net transport offshore across any vertical section parallel to the coat is zero so that $M_x = \int_{-H}^{0} \rho u dz = 0$ ……(34)

iii) In the surface layer the offshore Ekman transport is $M_x = \frac{\tau_{sy}}{f}$ ……..(35)

iv) The transport due to geostrophic flow thoughout the depth is from equation (33) & (34)can be written as

$$M_x = \frac{\tau_{sy}}{f} = \int_{-H}^{0} \rho \frac{g}{f}\frac{\partial \zeta}{\partial y} dz = -\frac{\rho g H}{f}\frac{\partial \zeta}{\partial y} \quad \text{…….(36)}$$

$$\therefore \frac{\partial \zeta}{\partial y} = \frac{\tau_{sy}}{\rho g H} \quad \text{……(37)}$$

v) Further analysis of Garvine showed $M_y = \int_{-H}^{0} \rho v dz = 0$ ….(38)

This means that below the surface current parallel to the coast in the direction of wind, there must be a compensating under current flowing in the opposite direction.

Example:

i) if $\tau_{sy} = 0.2\ Nm^{-2}$, H = 100m, $g = 9.8\ m\ s^{-2}$, $\rho = 1025\ kg\ m^{-3}$ then the longshore slope from equation (31), $\frac{\partial \zeta}{\partial y} = 2 \times 10^{-7} \Rightarrow$ 2 cm in 100 km

ii) At latitude 30^0 from equation (28), $u = -\frac{g}{f}\frac{\partial \zeta}{\partial y} = -\frac{10}{7.29 \times 10^{-5}} \times 2 \times 10^{-7}$ = 2.7 cm/s

iii) If the offshore Ekman transport is confined to the upper 20m, the average offshore velocity in the layer would be about 11 cm/s

Lecture Series of Berhampur University in Physical Oceanography

By Prof.A.S.N.Murty

Chapter – 5

Sverdrup, Stommel, Fofonoff & Munk contributions on wind currents

5.1. Sverdrup's Contribution:

The problem the oceanographer's could not understand for long is if wind is to generate the currents and circulation how some strong currents like equatorial counter currents and western boundary currents developed? Why such strong eastern boundary currents could not be developed like that of the west?

Ekman's initial work (1905) on wind driven currents, intended to explain current flow at an angle to the wind direction. Sverdrup (1947) demonstrated another surprising relationship between wind stress and ocean circulation as shown in Fig, below.

Sverdrup's aim was to determine current flow in response to wind stress and horizontal pressure gradients. Unlike Ekman, Sverdrup was not interested in determining how flow varied with depth; instead, he derived an equation for the net flow resulting from wind stress.

To derive the relation ship, Sverdrup assumed that the flow is stationary, the lateral friction and molecular viscosity are small, the non linear terms such as $u\frac{\partial u}{\partial x}$ are small and that turbulence near the sea surface can be described using a vertical eddy viscosity. He also assumed that wind driven circulation vanishes at the depth of frictional resistance (-D). With these assumptions the horizontal components of equations of motion (23a) become:

$$\alpha\frac{\partial p}{\partial x} = f.v + \alpha\frac{\partial \tau_x}{\partial z} \quad \text{and} \quad \alpha\frac{\partial p}{\partial y} = -f.u + \alpha\frac{\partial \tau_y}{\partial z} \quad \text{.....(32)}$$

One may note that while Ekman ignored the horizontal pressure gradient terms, Sverdrup included them but he ignored horizontal friction terms. Sverdrup wanted to see the total net transport in the entire layer upto the depth of frictional resistance. So he integrated the equations (32)for the whole column between the limits –D to zero(surface).

$$\int_{-D}^{0} \frac{\partial p}{\partial x} dz = \int_{-D}^{0} f.\rho.v + \int_{\tau_D}^{\tau_0} d\tau_x \,, \;\rightarrow\; \int_{-D}^{0} \frac{\partial p}{\partial x} dz = f.M_y + \tau_{x0}$$

$$\int_{-D}^{0} \frac{\partial p}{\partial y} dz = -\int_{-D}^{0} f.\rho.u.dz + \int_{\tau_0}^{\tau_0} d\tau_y \;\rightarrow\; \int_{-D}^{0} \frac{\partial p}{\partial y} dz = -f.M_x + \tau_{y0} \text{.....(33)}$$

To solve these two equations (33), differentiate the first one with respect to y and the second one with respect to x and equate as both on the left hand side are equal.

$$\int_{-D}^{0} \frac{\partial}{\partial y}\frac{\partial p}{\partial x} dz = \int_{-D}^{0} \frac{\partial}{\partial y} f.M_y + \int_{-D}^{0} \frac{\partial}{\partial y}\tau_{x0} \,, \quad \int_{-D}^{0} \frac{\partial}{\partial x}\frac{\partial p}{\partial y} dz = -\int_{-D}^{0} \frac{\partial}{\partial x}(f.M_x) + \int_{\tau_0}^{\tau_0} \frac{\partial}{\partial x}(\tau_{y0})$$

Further these equations can be written as;

$$\int_{-D}^{0} \frac{\partial^2 p}{\partial x \partial y} dz = f.\frac{\partial M_y}{\partial y} + M_y \frac{\partial f}{\partial y} + \frac{\partial \tau_{x0}}{\partial y} \,, \quad \text{.....(34)}$$

$$\int_{-D}^{0} \frac{\partial^2 p}{\partial x \partial y} dz = -f.\frac{\partial M_x}{\partial x} - M_x \frac{\partial f}{\partial x} + \frac{\partial \tau_{y0}}{\partial x} \text{.....(35)}$$

As equation (34) is equal to (35), we can re arrange and write

$$f\left[\frac{\partial M_x}{\partial x} + \frac{\partial M_y}{\partial y}\right] + M_x \frac{\partial f}{\partial x} + M_y \frac{\partial f}{\partial y} = \left[\frac{\partial \tau_{y0}}{\partial x} - \frac{\partial \tau_{x0}}{\partial y}\right] \text{.....(36)}$$

In equation (36)The first term on the left hand side is equation of continuity which is zero and the second term $\frac{\partial f}{\partial x}$ is variation of coriolis parameter along x direction (zonal) is zero. Let $\frac{\partial f}{\partial y} = \beta$. Then we can write equation (36) as

$$\beta M_y = \left[\frac{\partial \tau_{y0}}{\partial x} - \frac{\partial \tau_{x0}}{\partial y} \right] \quad \text{.....(37)}$$

We know $\nabla = \left[i\frac{\partial}{\partial x} + j\frac{\partial}{\partial y} \right]$ and $\tau_0 = i\tau_{x0} + j\tau_{y0}$

$$\therefore \beta M_y = \nabla_z \times \tau_0 \quad \text{.....(38)}$$

This is called Sverdrup's equation. The most interesting aspect of this equation is that the net meridional transport depends not on the absolute value of the wind stress but on the curl (shear), $(\nabla_z \times \tau_0)$, of the wind stress. That is the tendency of the wind to cause rotation or its ability to supply relative vorticity to the ocean. Thus Sverdrup showed that the net amount of water transported meridionally is directly proportional to the shear of the wind stress.

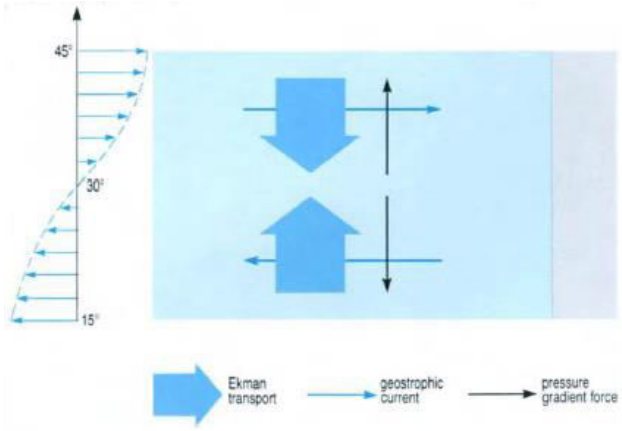

Fig.5.1.(Left) : A hypothetical wind field in which the wind is purely zonal (i.e. easterly or westerly) and varies in strength with latitude sinusoidally. (Right): Plan view of a rectangular ocean in the Northern Hemisphere, showing the direction of the Ekman transports, horizontal pressure gradients and geostrophic currents that result from the wind field shown in left.

Thus as per the figures 5.1 & 5.2, the Ekman wind drift in the northern half-basin is southward whereas that of the southern half-basin it is northward. Water piles up at middle latitudes (STH) develop a high pressure ridge due to rising of free surface level. The induced eastward geostrophic flow in the northern half-basin requires a low pressure.

The pattern of flow suggested by Sverdrup shown in the right side of fig 5.3 comes due to the geostrophic velocity (u_g) generated due to the balance of pressure gradient ($\alpha \frac{\partial p}{\partial n}$) and coriolis ($fu_g$) forces. Also it is clear that at 30^0 latitude the shear is greatest and at 15^0 and 45^0 it is least. The areas where the shear is least, the flow is zonal. The pattern of flow shown by Sverdrup in Fig. is the 'gyre'. The gyre is incomplete because he considered only the eastern boundary of the ocean. Thus the right

side of figure 5.2 indicates the interpretation of Sverdrup by joining geostrophic velocities (u_g) in the left figure of 5.2.

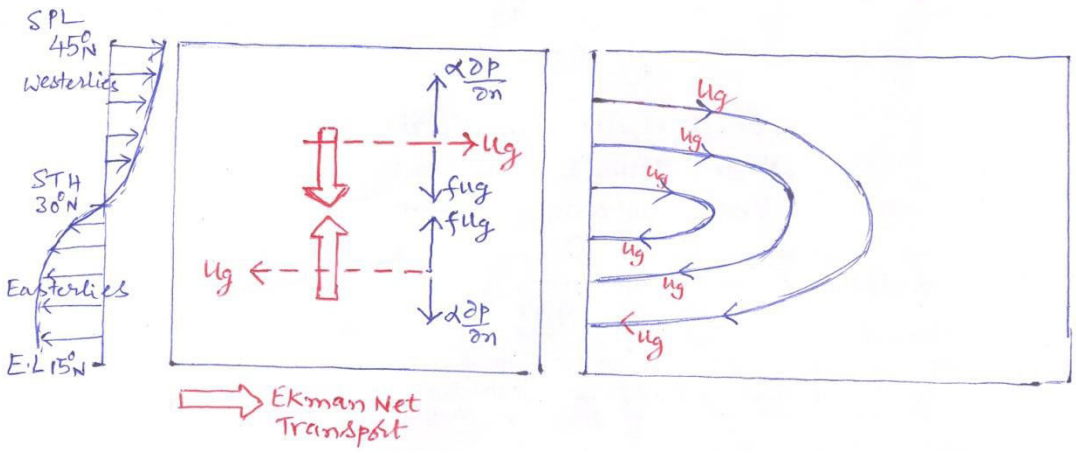

Fig.5.2. Left: Ekman net transport & geostrophic velocity (u_g) generated by balance of forces as per the wind. Right: Sverdrup's interpretation of geostrophic (u_g) transport generated in the left figure.

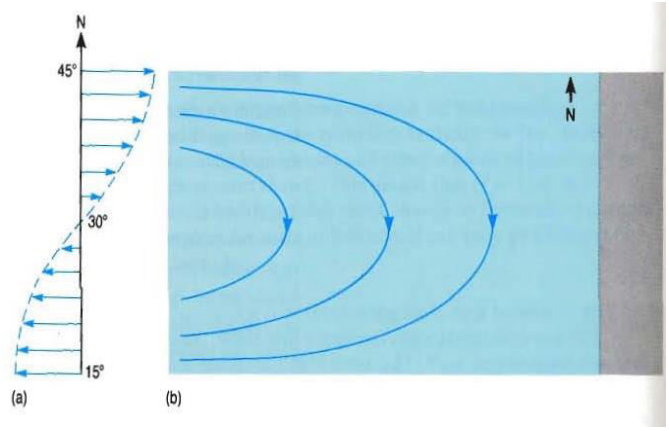

Fig.5.3. Pattern of ocean circulation suggested by Sverdrup due to presence of lower latitude easterlies and middle latitude westerlies in the northern oceans.

Since the general circulation is very large scale and not filled with ever-increasing vortices, the response is to move with latitude rather than to spin up locally. This response to Ekman pumping or suction is called the "Sverdrup transport". Sverdrup transport is equatorward in subtropical regions of Ekman pumping and poleward in subpolar regions of Ekman suction (Fig.5.4).

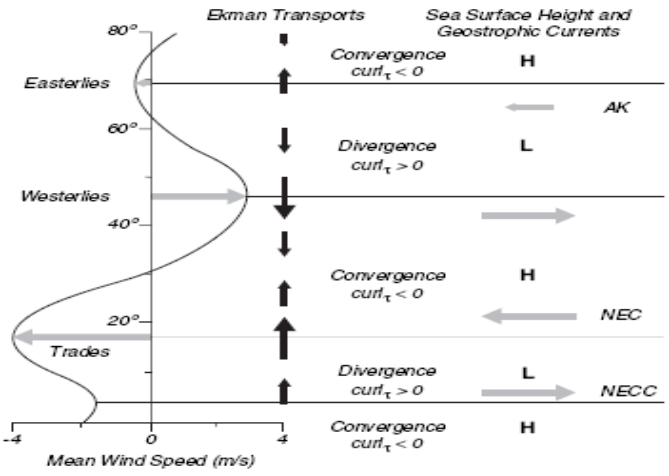

Fig.5.4. Winds, Ekman transport, geostrophic velocities and the NEC, NECC sea surface heights

5.2. Application of Sverdrup equation to trade wind region:

Sverdrup applied these equations to the trade wind region in lower latitudes where τ_y and $\frac{\partial}{\partial x}(\tau_y)$ are negligibly small and τ_x variations with x are averaged out taking f = 2Ωsinϕ and dy = Rdϕ where R is radius of the earth, then

We can write $$\beta = \frac{\partial f}{\partial y} = \frac{d}{dy}(2\Omega \sin\varphi) = \frac{d(2\Omega \sin\varphi)}{Rd\varphi} = \frac{2\Omega}{R}\frac{d}{d\varphi}(\sin\varphi) = \frac{2\Omega\cos\varphi}{R} \quad \text{....(39)}$$

Taking Sverdrup's equation (38): $M_y = \dfrac{\left(\dfrac{\partial \tau_y}{\partial x} - \dfrac{\partial \tau_x}{\partial y}\right)}{\dfrac{\partial f}{\partial y}}$ .....(40)

we also know $\left[\dfrac{\partial M_x}{\partial x} + \dfrac{\partial M_y}{\partial y}\right] = 0$ .....(40a)

$\therefore \left[\dfrac{\partial M_x}{\partial x} = -\dfrac{\partial M_y}{\partial y}\right]$

So differentiating equation (40) with respect to 'y' and then equate it to $\left[\dfrac{\partial M_x}{\partial x}\right]$

So $\left[\dfrac{\partial M_x}{\partial x}\right] = -\dfrac{\partial}{\partial y}\dfrac{\left(\dfrac{\partial \tau_y}{\partial x} - \dfrac{\partial \tau_x}{\partial y}\right)}{\dfrac{\partial f}{\partial y}} = -\dfrac{\dfrac{\partial f}{\partial y}\left(-\dfrac{\partial^2 \tau_x}{\partial y^2}\right) - \left(\dfrac{\partial \tau_y}{\partial x} - \dfrac{\partial \tau_x}{\partial y}\right)\dfrac{\partial^2 f}{\partial y^2}}{\left(\dfrac{\partial f}{\partial y}\right)^2}$ ...(41)

Over much of the open ocean, especially in the tropics, the wind is zonal and $\dfrac{\partial \tau_y}{\partial x}$ is negligibly small and from equation (39) we can write $\dfrac{\partial^2 f}{\partial y^2} = \dfrac{\partial}{\partial y}\left(\dfrac{\partial f}{\partial y}\right) = \dfrac{d}{R d\varphi}\left(\dfrac{2\Omega \cos\varphi}{R}\right) = \dfrac{2\Omega}{R^2}(-\sin\varphi) = -\dfrac{2\Omega \sin\varphi}{R^2}$

...(42)

Substituting all these values in equation (41) and simplifying we get

$$\frac{\partial M_x}{\partial x} = -\frac{\left[-\left\{\dfrac{2\Omega\cos\varphi}{R}\left(-\dfrac{\partial^2 \tau_x}{\partial y^2}\right) + \left(\dfrac{\partial \tau_x}{\partial y}\right)\dfrac{2\Omega \sin\varphi}{R^2}\right\}\right]}{\left(\dfrac{2\Omega\cos\varphi}{R}\right)^2}$$

$$\frac{\partial M_x}{\partial x} = \frac{1}{2\Omega\cos\varphi}\left[R\left(\frac{\partial^2\tau_x}{\partial y^2}\right)+\frac{\partial\tau_x}{\partial y}\tan\varphi\right] = \text{K (say)}$$

Then $dM_x = Kdx$ or $M_x = \int Kdx = K.x$

Sverdrup integrated this equation from a north-south eastern boundary at x = 0, assuming no flow into the boundary. This requires $M_x = 0$ at x = 0. Then

$$M_x = \frac{x}{2\Omega\cos\varphi}\left[R\left(\frac{\partial^2\tau_x}{\partial y^2}\right)+\frac{\partial\tau_x}{\partial y}\tan\varphi\right] \quad \text{.....(42)}$$

Where x is the distance from the eastern boundary of the ocean basin as shown in Fig.

Similarly M_y can be obtained taking

$$\frac{\partial M_y}{\partial y} = -\frac{\partial M_x}{\partial x} = -\mu\frac{1}{2\Omega\cos\varphi}\left[R\left(\frac{\partial^2\tau_x}{\partial y^2}\right)+\frac{\partial\tau_x}{\partial y}\tan\varphi\right]$$

$$\therefore \int dM_y = -\int\frac{1}{2\Omega\cos\varphi}\left[R\left(\frac{\partial^2\tau_x}{\partial y^2}\right)+\frac{\partial\tau_x}{\partial y}\tan\varphi\right]dy$$

$$\therefore M_y = -\frac{1}{2\Omega\cos\varphi}\left[R\frac{\partial\tau_x}{\partial y}+0\right] = -\frac{R}{2\Omega\cos\varphi}\left[\frac{\partial\tau_x}{\partial y}\right] \text{.....(43)}$$

Here 'x' is the distance from a north south coast line in the eastern boundary of the ocean (i.e coast is east side and ocean is west side as shown in the figure 5.5). So from the coast west side into the ocean to a point 'P' is in the negative x-direction.

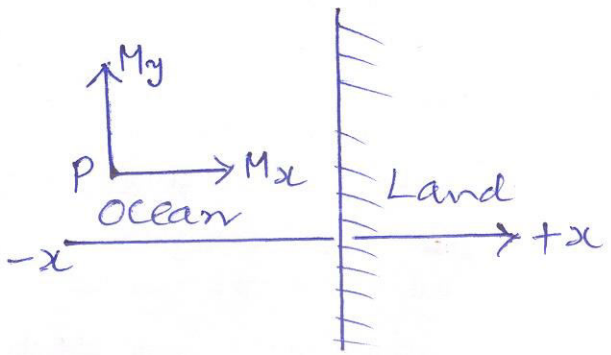

Fig. 5.5. Eastern boundary of the ocean according to Sverdrup

From the above equation of M_x in (42), it is apparent that in trade wind and equatorial zones of the ocean the important term is $\frac{\partial^2 \tau_x}{\partial y^2}$. The fig 5.6 below shows the variation of wind speed and stress($\frac{\partial^2 \tau_x}{\partial y^2}$) with latitude in eastern Pacific. North of about 15^0N and south of about 2^0N, the value of $\frac{\partial^2 \tau_x}{\partial y^2}$ is positive and so x is negative and so the flow (M_x) is negative which is westward flowing north & south equatorial currents. Between 15^0N and 2^0N the value of $\frac{\partial^2 \tau_x}{\partial y^2}$ is negative and so x is positive so the flow (M_x) is positive which is eastward flowing Equatorial counter current.

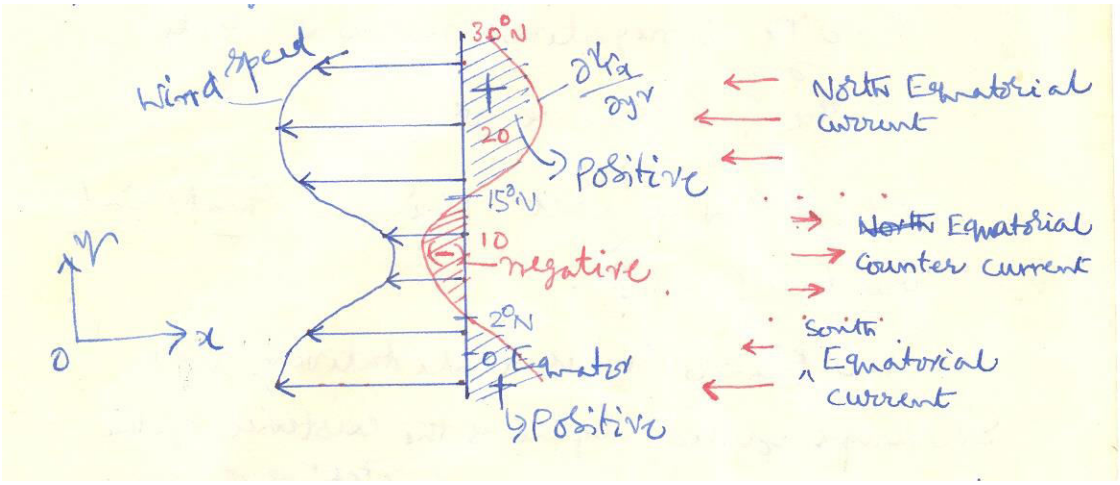

Fig.5.6. The variation of wind speed and stress($\frac{\partial^2 \tau_x}{\partial y^2}$) with latitude in the Eastern Pacific.

Thus the above figure 5.6 shows qualitatively how Sverdrup's solution of equation (42) explains the existence of the equatorial current system. Comparing the solutions of Ekman and Sverdrup while Ekman concentrated in the current variation with depth, Sverdrup studied the effect of coastal boundary in the east which is more realistic than Ekman as Ekman considered horizontally infinite boundary less ocean.

To test the theory of Sverdrup, Reid (1948) compared transports calculated from known winds in the eastern tropical Pacific with transports calculated from hydrographic data collected by the Carnegie and Bushnell in October and November 1928, 1929 and 1939 between 34^0N and 10^0S and between 80^0W and 160^0W is as shown in the Fig.5.7.

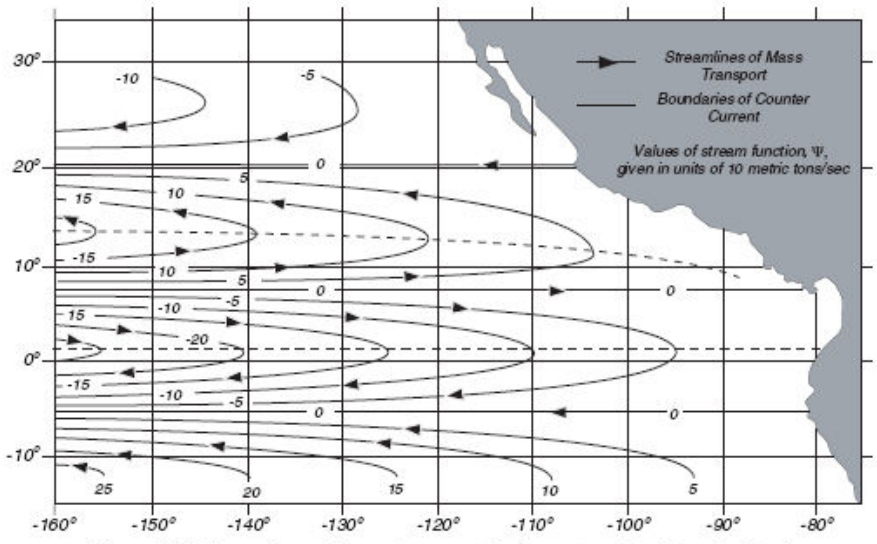

Fig.5.7. Stream lines of mass transport in the eastern pacific calculated from Sverdrup's theory using mean annual wind stress (After Reid 1948)

5.3.Fofonoff's analysis of interior transport:

In order to analyze the vertically integrated equations of motion start with the non accelerated equations of motion with vertical friction terms as considered by Sverdrup in equations (32):

$$-f\rho v = -\frac{\partial p}{\partial x} + \frac{\partial \tau_x}{\partial z}$$

$$f\rho u = -\frac{\partial p}{\partial y} + \frac{\partial \tau_y}{\partial z}$$

Expressing in terms of mass transports and On integrating these equations from ocean bottom (D) to the sea surface(η), we get:

$$-\int_D^\eta f\rho v dz = -\int_D^\eta \frac{\partial p}{\partial x} dz + \int_D^\eta \partial \tau_x$$
$$\int_D^\eta f\rho u dz = -\int_D^\eta \frac{\partial p}{\partial y} dz + \int_D^\eta \partial \tau_y \quad \text{.....(44)}$$

The whole exercise of these equations to understand the transport in the subsurface layer due to the effect of wind stress at the surface lies on the evaluation of the first term on the right hand side. Fofonoff (1962) did extensive analysis. His analysis is as below:

Evaluation of $\int_D^\eta \frac{\partial p}{\partial x} dz$:

Put $E_p = \int_D^\eta p dz$ .....(45)

where E_P is the potential energy of a column of water of unit horizontal area, relative the bottom of the ocean. Then we can write:

$$E_p = \int_D^\eta \frac{p\alpha}{g\alpha} g dz = \frac{1}{g}\int_D^\eta (p\alpha)\rho g dz = \frac{1}{g}\int_D^\eta (p\alpha)(-dp) = -\frac{1}{g}\int_D^\eta (p\alpha)(dp) = \frac{1}{g}\int_\eta^D (p\alpha)(dp)$$

$$E_P = \frac{1}{g}\int_\eta^D (p\alpha)(dp) = \frac{1}{g}\int_\eta^D (p\alpha_{35,0,p})(dp) + \frac{1}{g}\int_\eta^D (p\delta)(dp) = E_p^0 + \chi \quad \text{.....(46)}$$

Here χ is anomaly of potential energy and E_p^0 is the potential energy which is a function of bottom pressure P_D only.

$$\therefore \frac{\partial E_p}{\partial x} = \frac{\partial E_P^0}{\partial x} + \frac{\partial \chi}{\partial x} \quad \text{.....(47)}$$

From equation (45) we can write:

$$\frac{\partial}{\partial x}\left(E_p\right) = \frac{\partial}{\partial x}\int_D^\eta p dz = \int_D^\eta \frac{\partial p}{\partial x} dz + p_\eta \frac{\partial \eta}{\partial x} - p_D \frac{\partial D}{\partial x} \quad \text{.....(48)}$$

As η and D vary with x the last two terms in equation (48) appear. But it may be noted that P_η is pressure at sea surface is zero. So the second term in the right hand side of equation(48) vanishes. Hence equation (48)can be written as:

$$\int_D^\eta \frac{\partial p}{\partial x} dz = \frac{\partial}{\partial x}\left(E_p\right) + p_D \frac{\partial D}{\partial x} \quad \text{.....(49)}$$

Substituting (47) in (49) we can get

$$\int_D^\eta \frac{\partial p}{\partial x} dz = \frac{\partial E_P^0}{\partial x} + \frac{\partial \chi}{\partial x} + p_D \frac{\partial D}{\partial x} \text{.....(50)}$$

Fofonoff (1962) combined these two terms ($\frac{\partial E_P^0}{\partial x} + p_D \frac{\partial D}{\partial x}$) and expressed as

$$\int_D^\eta \frac{\partial p}{\partial x} dz = \frac{\partial \chi}{\partial x} + \frac{p_D \alpha_D}{g} \frac{\partial P_D}{\partial x} \quad \text{.....(51)}$$

Where $\frac{\partial P_D}{\partial x}$ is a component of pressure gradient along a level surface at the bottom and $\alpha_{35,0,p} P_D$ is assumed to be equal to the specific volume at the bottom, α_D.

Substituting equation (51) in equations (44) we get:

$$-\int_D^\eta f\rho v dz = -\frac{\partial \chi}{\partial x} - \frac{p_D \alpha_D}{g}\frac{\partial P_D}{\partial x} + \tau_{x\eta} - \tau_{xD}$$

$$\int_D^\eta f\rho u dz = -\frac{\partial \chi}{\partial y} - \frac{p_D \alpha_D}{g}\frac{\partial P_D}{\partial y} + \tau_{y\eta} - \tau_{yD} \quad \text{.....(52)}$$

i) First terms on the right hand side of the equations (52):

The first terms on the R.H.S are associated with variations in density and so these can be interpreted as the baroclinic part of the geostrophic velocity. So this is like balance between pressure gradient of mass transport to the coriolis part of the transport $\therefore -fM_{yc} = -\frac{\partial \chi}{\partial x}$ and

$$fM_{xc} = -\frac{\partial \chi}{\partial y} \quad \text{.....(53)}$$

ii) Second terms on the right hand side of the equations (52):

The mass transports near the bottom are assumed as geostrophic as velocities near the bottom are small and tangential stresses near the bottom are neglected. So the pressure gradient at the bottom is equal to the coriolis at bottom. $\therefore fu_D = -\alpha_D \frac{\partial P_D}{\partial y}$ and $fv_D = -\alpha_D \frac{\partial P_D}{\partial x}$

....(54)

So the term $-\frac{p_D \alpha_D}{g}\frac{\partial P_D}{\partial x}$ can be written, substituting eqn (54) as

$$\frac{fp_D v_D}{g} \quad \text{.....(55)}$$

This equation (55) can be related to fM_{yD} because $M_{yD} = \int_D^\eta \rho v_D dz = v_D \int_D^\eta \rho dz$ as v_D does not vary with depth. Taking ρdz = -dp/g, this becomes

$$v_D \int_D^\eta \rho dz = -v_D \int_D^\eta \frac{dp}{g} dz = -\frac{v_D}{g}\left(p_\eta - p_D\right) = \frac{v_D p_D}{g} \left(\because p_\eta = 0\right) \text{.....(56)}$$

So from 55 & 56 we can write $fM_{yD} = \frac{fp_D v_D}{g}$ .....(57)

Similarly y component of the second term can be written as

$$fM_{xD} = \frac{fp_D u_D}{g} \quad \text{.....(58)}$$

iii) Third terms on the right hand side of the equations (52):

According to Ekman these terms can be written from equation (29a) as: $M_{xDE} = \frac{\tau_{yD}}{f}$ and

$$M_{yDE} = -\frac{\tau_{xD}}{f} \quad \text{.....(59)}$$

So finally equations (52) for total transport can be written using equations (53), (57) and (59) as:

$$-fM_y = -fM_{yc} - fM_{yD} - fM_{yDE}$$

$$fM_x = fM_{xc} + fM_{xD} + fM_{xDE}$$

Which means

$$M_y = M_{yc} + M_{yD} + M_{yDE} \quad \text{.....(60)}$$

$$M_x = M_{xc} + M_{xD} + M_{xDE}$$

Thus the total transport in the interior of the ocean can be considered to be made up of three types of transports (baroclinic, barotropic and Ekman types). While both the baroclinic (M_{yc}) and barotropic (M_{yD}) transports are geostrophic, the Ekman transport (M_{yDE}) is non geostrophic slope current due to the influence of wind stresses at the sea surface.

Though the mass continuity equation (40a) requires that the divergence of sum of the three types of transports in equation (60) is zero (or equal to rate at which water is added at the surface), this need not hold good for each type of transport separately. So Fofonoff (1962) interprets the equation (52) following the approach of Sverdrup by cross differentiation and adding both the equations as :

$$f\left[\frac{\partial M_{xg}}{\partial x} + \frac{\partial M_{yg}}{\partial y}\right] + \beta M_{yg} = 0 \quad \text{.....(61)}$$

$$f\left[\frac{\partial M_{xE}}{\partial x}+\frac{\partial M_{yE}}{\partial y}\right]+\beta M_{yE}=\frac{\partial \tau_{My}}{\partial x}-\frac{\partial \tau_{Mx}}{\partial y}\ \text{.....(62)}$$

$$f\left[\frac{\partial M_{xD}}{\partial x}+\frac{\partial M_{yD}}{\partial y}\right]+\beta M_{yD}=-\rho' f\left[u_D\frac{\partial D}{\partial x}+v_D\frac{\partial D}{\partial y}\right]\text{.....(63)}$$

Where $\rho'=\rho_D\left[1+\frac{p_D}{\alpha_D}\left(\frac{\partial \alpha}{\partial p}\right)_D\right]$

Combining all these equations of (61) to (63) we can write

$$\beta M_y=\nabla\times\tau_\eta-\nabla\times\tau_D-\rho' f\left[u_D\frac{\partial D}{\partial x}+v_D\frac{\partial D}{\partial y}\right]\text{.....(64)}$$

Here χ terms cancel each other while cross differentiating both the equations of (52). If the barotropic deep flow is assumed as zero and Tangential stresses near the bottom are also assumed as zero, equation (64) reduces to the Sverdrup's equation (38).

5.4. VORTICITY EQUATION:

To obtain a quantitative understanding of the rotating fluids with a change of ω, express the motion in Cartesian coordinates of x and y. The rotation is considered for two infinitesimal lines dx and dy in 'x' and 'y' directions. Let 'u' and 'v' are the linear velocity components in y and x directions respectively. As the angular velocity is different on the two axes

$v = \omega_1 x$ and $-u = -\omega_2 y$ or $\frac{\partial v}{\partial x}=\omega_1$, $-\frac{\partial u}{\partial y}=\omega_2$ The average of the two angular velocities say 'ω' is

$$\omega=(\omega_1+\omega_2)/2=\frac{1}{2}\left(\frac{\partial v}{\partial x}-\frac{\partial u}{\partial y}\right)=\frac{1}{2}\zeta=\omega \text{ or } \zeta = 2\omega \quad \text{.....(65)}$$

where 'ζ' is called the vorticity which is twice the local average angular velocity.

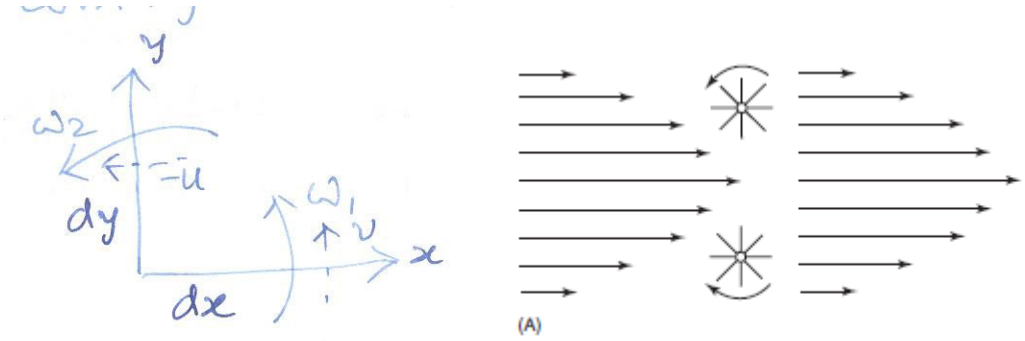

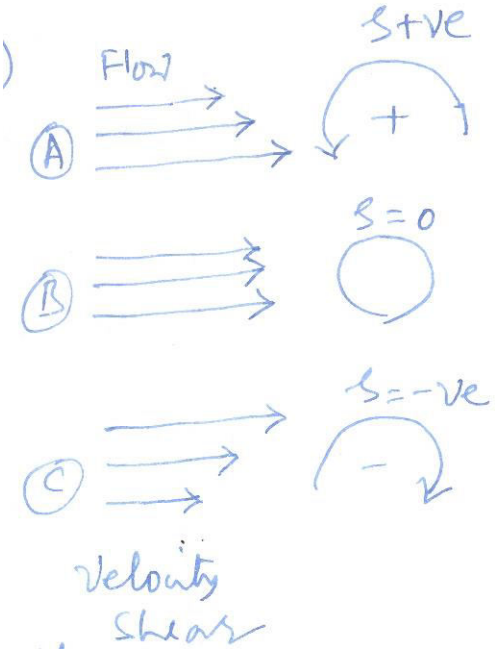

5.4.1. PLANETARY VORTICITY:

In the case of earth rotation this is considered as vertical component. We know that the rotation of the earth about its axis results in the deflection of winds by Coriolis force. These deflections are explained in terms of the poleward decrease in the eastward velocity of the surface of the earth. In addition to the linear eastward velocity, the surface of the earth has an angular velocity. Like the linear eastward velocity, this angular velocity depends on latitude. At the poles, the angular velocity, of the surface of the earth is simply Ω (= 7.292×10^{-5} rad sec^{-1}). At lower latitudes, it is a proportion of Ω. The larger the angle between the earth's axis of rotation and the local vertical, the smaller is the angular velocity of the surface of the earth. At the equator, where a vertical axis is at right angles to the axis of rotation of the earth, the angular velocity of the

surface is zero. Thus the angular velocity of the surface of the earth about a vertical axis at latitude Φ is given by Ω sin Φ. As the vorticity is twice the local average angular velocity (as given by equation 65), the planetary vorticity is equal to 2(Ω sin Φ) (= f). The planetary vorticity at the poles and the equator respectively are '2Ω' and zero.

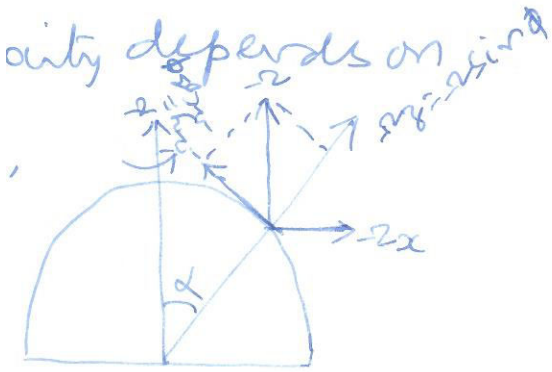

5.4.2. ABSOLUTE VORTICITY:

We then define the absolute vorticity as the sum of the two vortices ,(ζ + f). The vorticity 'ζ' is measured rotation of the particle relative to the surface of the earth and so it is called relative vorticity.

Considering the frictionless horizontal equation of motion:

$$\frac{du}{dt} = -\alpha \frac{\partial p}{\partial x} + fv$$
$$\frac{dv}{dt} = -\alpha \frac{\partial p}{\partial y} - fu$$

if these are cross differentiated and subtracted one from the other, to eliminate pressure gradient terms, we get: $\frac{d}{dt}(\zeta + f) = -(\zeta + f)\left[\frac{\partial u}{\partial x} + \frac{\partial v}{\partial y}\right]$

Since we know the equation of continuity $\frac{\partial u}{\partial x} + \frac{\partial v}{\partial y} = 0$, $\frac{d}{dt}(\zeta + f) = 0$

upto the column of thickness 'D' in the atmosphere called gradient wind level is considered, then $\frac{d}{dt}(\frac{\zeta + f}{D}) = 0$. The term $\frac{\zeta + f}{D}$ is called the potential vorticity.

5.4.3. VORTICITY THEOREM:

While circulation is a measure of tendency of fluid rotation, vorticity is the same property of fluid for an infinitely small area.

To obtain the vorticity theorem, the horizontal equations of motion are

$$\frac{\partial u}{\partial t}+u\frac{\partial u}{\partial x}+v\frac{\partial u}{\partial y}+w\frac{\partial u}{\partial z}=fv-\alpha\frac{\partial p}{\partial x}+F_x \ldots\ldots\ldots\ldots\ldots 66$$

$$\frac{\partial v}{\partial t}+u\frac{\partial v}{\partial x}+v\frac{\partial v}{\partial y}+w\frac{\partial v}{\partial z}=-fu-\alpha\frac{\partial p}{\partial y}+F_y \ldots\ldots\ldots\ldots\ldots 67$$

and we know $\zeta=\frac{\partial v}{\partial x}-\frac{\partial u}{\partial y}$ ……68

Take partial derivative with respect to (w.r.t) y to equation 66 and differentiate w.r.t x to equation 67 and subtract 66 from 67 and re arrange, then we get

$$\frac{\partial}{\partial t}\left[\frac{\partial v}{\partial x}-\frac{\partial u}{\partial y}\right]+u\frac{\partial}{\partial x}\left[\frac{\partial v}{\partial x}-\frac{\partial u}{\partial y}\right]+v\frac{\partial}{\partial y}\left[\frac{\partial v}{\partial x}-\frac{\partial u}{\partial y}\right]+w\frac{\partial}{\partial z}$$
$$\left[\frac{\partial v}{\partial x}-\frac{\partial u}{\partial y}\right]+\frac{\partial u}{\partial x}\left[\frac{\partial v}{\partial x}-\frac{\partial u}{\partial y}\right]+\frac{\partial v}{\partial y}\left[\frac{\partial v}{\partial x}-\frac{\partial u}{\partial y}\right]+\left[\frac{\partial v}{\partial z}.\frac{\partial w}{\partial x}-\frac{\partial u}{\partial z}.\frac{\partial w}{\partial y}\right]$$

$$=-f\left[\frac{\partial u}{\partial x}+\frac{\partial v}{\partial y}\right]-\left[u\frac{\partial f}{\partial x}+v\frac{\partial f}{\partial y}\right]-\alpha[0]-\left[\frac{\partial p}{\partial y}\frac{\partial \alpha}{\partial x}-\frac{\partial p}{\partial x}\frac{\partial \alpha}{\partial y}\right]+\left[\frac{\partial F_y}{\partial x}-\frac{\partial F_x}{\partial y}\right] \ldots\ldots..69$$

$$\frac{\partial}{\partial t}(\zeta)+u\frac{\partial \zeta}{\partial x}+v\frac{\partial \zeta}{\partial y}+w\frac{\partial \zeta}{\partial z}+\zeta(D)+\left[\frac{\partial v}{\partial z}\frac{\partial w}{\partial x}-\frac{\partial u}{\partial z}\frac{\partial w}{\partial y}\right]=-f.D-v\frac{\partial f}{\partial y}-\left[\frac{\partial p}{\partial y}\frac{\partial \alpha}{\partial x}-\frac{\partial p}{\partial x}\frac{\partial \alpha}{\partial y}\right]+\left[\frac{\partial F_y}{\partial x}-\frac{\partial F_x}{\partial y}\right]$$
……70

since $\frac{\partial f}{\partial x}=0$ and $v\frac{\partial f}{\partial y}=\frac{dy}{dt}.\frac{df}{dy}=\frac{df}{dt}$

It can be further written as

$$\frac{d}{dt}(\zeta)+\frac{d}{dt}(f)=-D(f+\zeta)-\left[\frac{\partial v}{\partial z}\frac{\partial w}{\partial x}-\frac{\partial u}{\partial z}\frac{\partial w}{\partial y}\right]-\left[\frac{\partial p}{\partial y}\frac{\partial \alpha}{\partial x}-\frac{\partial p}{\partial x}\frac{\partial \alpha}{\partial y}\right]+\left[\frac{\partial F_y}{\partial x}-\frac{\partial F_x}{\partial y}\right]$$

$$\frac{d}{dt}(\zeta+f)=-D(f+\zeta)-\left[\frac{\partial v}{\partial z}\frac{\partial w}{\partial x}-\frac{\partial u}{\partial z}\frac{\partial w}{\partial y}\right]-\left[\frac{\partial p}{\partial y}\frac{\partial \alpha}{\partial x}-\frac{\partial p}{\partial x}\frac{\partial \alpha}{\partial y}\right]+\left[\frac{\partial F_y}{\partial x}-\frac{\partial F_x}{\partial y}\right] \quad \ldots\ldots..(71)$$

I II III IV

The term on the right hand side (r.h.s) is called the rate of change of absolute vorticity. This equation says that the absolute vorticity of a parcel of water can change only through the contribution of four terms on the right hand side.

Show that the equation for the time evolution of ζ is

$$\frac{d\zeta}{dt} = -(f+\zeta)\left(\frac{\partial u}{\partial x}+\frac{\partial v}{\partial y}\right) - \left(\frac{\partial w}{\partial x}\frac{\partial v}{\partial z} - \frac{\partial w}{\partial y}\frac{\partial u}{\partial z}\right) + \left(\frac{\partial \rho}{\partial x}\frac{\partial p}{\partial y} - \frac{\partial \rho}{\partial y}\frac{\partial p}{\partial x}\right) - v\frac{df}{dy}$$

convergence tilting Baroclinic term "beta"-term

5.4.4. PHYSICAL INTERPRETATION OF THE TERMS OF VORTICITY EQUATION:

The first term (I) on the r.h.s of equation (71) is called the divergence (or convergence) term. Positive divergence increases the radius of rotation. As the term is negative, it decreases the magnitude of absolute vorticity.

The second term (II) of equation (71) on the r.h.s is known as the tripping (or tilting) term. When the vertical shear ($\frac{\partial w}{\partial x}$) of the first half of this term decreases, horizontal shear ($\frac{\partial v}{\partial z}$) increases upward. As it has minus sign, its contribution to (f+ ζ) is positive. Which means (f+ ζ) will increase with time. A corresponding analogy can easily be made for the second half of this term ($\frac{\partial w}{\partial y}\frac{\partial u}{\partial z}$).

The third term on the r.h.s of equation (71) is known as solenoid (or baroclinic) term of the circulation applied to an infinitely small horizontal circuit.

The last term on the r.h.s of equation (71) is the frictional term (or also beta term) that arises due to turbulence in the atmosphere.

Calculation from synoptic data indicates that the contribution of divergence term [(f+ ζ)D] is more than the other terms in large scale systems.

5.4.5. POTENTIAL VORTICITY THEOREM:

For the case of incompressible barotropic fluid, the potential vorticity equation can be derived using the continuity equation:

$$\therefore \left(\frac{\partial u}{\partial x}+\frac{\partial v}{\partial y}+\frac{\partial w}{\partial z}\right)=0 \text{ which means } \therefore \left(\frac{\partial u}{\partial x}+\frac{\partial v}{\partial y}\right)=-\frac{\partial w}{\partial z} \text{ ……..(72)}$$

The vorticity equation (72) can be written with the help of equation (73) as

$$\frac{d}{dt}(\zeta+f)=(f+\zeta)\frac{\partial w}{\partial z} \text{ ……(73)}$$

In the case of barotropic condition, the thermal wind vanishes and so the geostrophic velocity is independent of depth. Then integrating vertically from z=D_1 to D_2 equation (73) can be written as

$\frac{d}{dt}(\zeta+f)dz=(f+\zeta)dw$ on integration gives rise to

$$\frac{d}{dt}(\zeta+f)_g[Z]_{D_1}^{D_2}=(f+\zeta)_g W_{wD_1}^{wD_2}$$

$$\frac{d}{dt}(\zeta+f)_g[D_2-D_1]=(f+\zeta)_g[W_{D2}-W_{D1}] \text{ ……..(74)}$$

The suffix ‘g’ denotes under geostrophic condition. But since W = $\frac{dz}{dt}$ we can further write

$W_{D2}=\frac{dD_2}{dt}$ and $W_{D1}=\frac{dD_1}{dt}$ and let H =D_2 –D_1 is the depth of the column we can write (74) as

$$\frac{d}{dt}(\zeta+f)_g[D_2-D_1]=(f+\zeta)_g\left[\frac{dD_2}{dt}-\frac{dD_1}{dt}\right] = (f+\zeta)\frac{d}{dt}(D_2-D_1)$$

D. $\frac{d}{dt}(\zeta+f) = (f+\zeta)\frac{d}{dt}(D)$ re arranging the terms

$$(\frac{1}{\zeta+f})\ \frac{d}{dt}(\zeta+f) = \frac{1}{D}\frac{d}{dt}(D) \text{ which gives rise to}$$

$$\frac{d}{dt}[\ln\left(\frac{\zeta+f}{D}\right)] = 0$$

or $\frac{d}{dt}\left(\frac{\zeta+f}{D}\right) = 0$ ……..75

This is the potential vorticity equation.

If the flow is purely horizontal (w = o), equation (75) reduces to

$$\frac{d}{dt}(\zeta + f) = 0.$$

This is called the barotropic vorticity equation, which states that the absolute vorticity $(\zeta + f)$is conserved .This means $(\zeta + f)$ = constant.

That is in the case of a ring of water parcel revolving round the earth, the absolute vorticity is constant. Which means as 'f' increases, the relative vorticity (ζ) should decrease and vice versa in order that $(f + \zeta)$ to be constant. So if water moves pole ward, 'f' increases and so ζ decreases. Which means pole ward moving water must gain momentum and so swifter. The converse is true for the water moving equator ward. Thus the trajectory of a water parcel in the meridional direction can be drawn using the constant absolute vorticity (CAV) values as shown in Figure below.

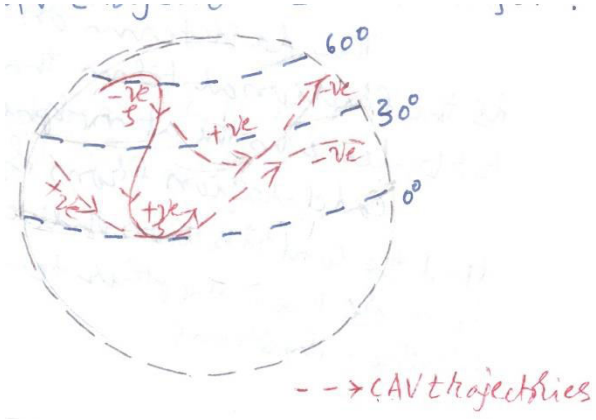

So if the depth of the column of the water parcel 'D' is considered, the vorticity theorem will change to the equation as given in equation (75), the potential vorticity which is to be conserved instead of simply absolute vorticity. The concept of conservation of potential vorticity has far reaching consequences, and its application to fluid flow in the ocean gives a deeper understanding of ocean currents.

5.5. Stommel's contribution:

Sverdrup's contribution could not take into account of the western boundary and so could not explain about the circulation what happened along the west coast of the ocean. Thus his circulation as shown in Fig.5.3 is incomplete. This problem was solved by American Oceanographer, Henry Stommel in 1948. Stommel considered the effect of a symmetrical gyral wind field on a rectangular ocean and calculated in three different situations: a) non rotating earth b) the earth is rotating but the coriolis

parameter is constant and c) the earth is rotating and coriolis parameter varies with latitude taking the following assumptions.

1. Earth is flat and ocean is rectangular with constant depth
2. All the ocean is one side of the equator
3. Taken β-plane approximation such that $f = f_0 + \beta y$ where f_0 is the value of f at some point where the ocean's plane intersects the earth's surface and β is variation of coriolis parameter with latitude.
4. He assumed simple wind stress which varied with latitude such that it is to the west at the south and east at the north.
5. While he included simple friction term basically he used Sverdrup's equation.

Figure5.8 below summarizes the results of Stommel's calculations.

Stommel elucidated why currents are fast and narrow in the west and broad and relatively slow in the east. Stommel used Sverdrup's equation and included bottom friction. He calculated vertically integrated flow patterns over an idealized ocean with a prescribed wind forcing, which was a function of latitude, under a variety of conditions: no rotation (f = 0), constant Coriolis parameter f, constant variation of coriolis parameter with latitude (β plane approximation). His results were similar for the first two situations (f =0 and f = constant). In the third case (β effect), his results yielded a westward intensification of currents. This means the change of 'f' with latitude is the main responsible factor for westward intensification as shown in case 3 of right side Fig.below.

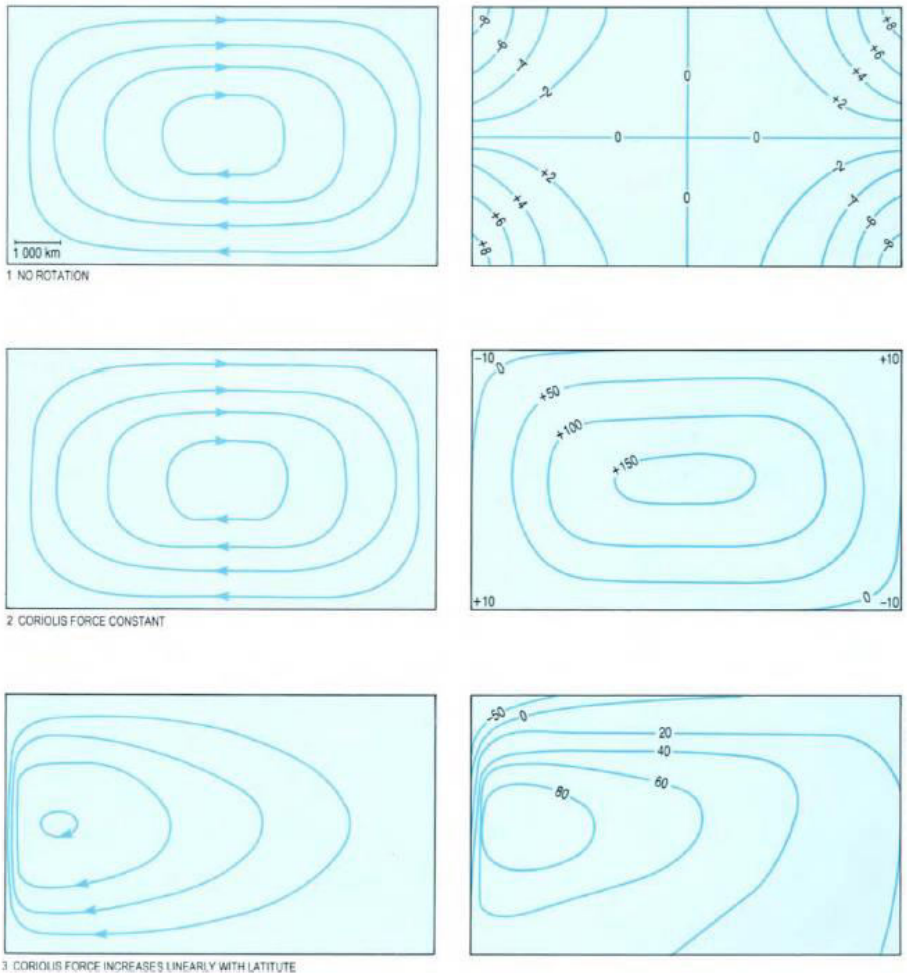

Fig.5.8. Stommel's calculations. Case 1:Left side Non rotating earth (f =0) and right side resulting circulation in the ocean. Case 2: Left side constant rotation of earth (f = const), and right side resulting circulation in the ocean; Case 3: Left side real earth rotation (f increases with latitude), and right side resulting circulation in the ocean

The striking difference in the shape of the sea surface of Fig.5.8 between (case1) and (case 2) (on the right hand side diagrams) is that a large sea surface topography is found at the centre in case of (case 2) whereas there is no such situation in (case 1).This is because of the action of the coriolis force. In order to have equilibrium, the sea surface would adjust to have balance with the horizontal pressure gradient forces.

Looking at the left side of the diagrams (of Fig.5.8), it is clear that just existence of coriolis force (case2) do not bring any intensification but with the variation of coriolis force (case 3)brings change in intensification of streamlines.

Thus Stommel showed that the intensification of western boundary currents is due to increase of coriolis force with increase of latitude (case 3).

5.6. Conservation of angular momentum (vorticity):

In the western part of the oceans, the wind induced relative vorticity is the same as that in the eastern part (Fig.5.9). On the western side, however, the currents move north wards, which make 'f' increase. To conserve absolute vorticity, ζ must decrease, i.e. northward motion on the western part of the oceans acquires anticyclonic (negative) vorticity. Analogously, southward motion in the eastern part of the oceans, produce cyclonic (positive) vorticity. Note that on the eastern part, the wind induced vorticity and the relative vorticity arising from southward flow are of opposite sign and tend to balance each other. On the other hand, over the western part, the vorticity induced by northward currents and the wind induced vorticity are of the same sign. Then, to maintain vorticity balances at the east and west, there has to be a large source of positive vorticity on the west.

The direction of Sverdrup flow (equatorward or poleward) is dictated by the Ekman pumping as the flow is geostrophic. That is, an equatorward flow means that the sea surface is high in the west and low in the east and vice versa (Fig.5.2) as the force balance is between pressure gradient force and Coriolis force. Thus the small terms in the momentum equation that we neglect in geostrophic balance are important when thinking about the very slow evolution of the flow.

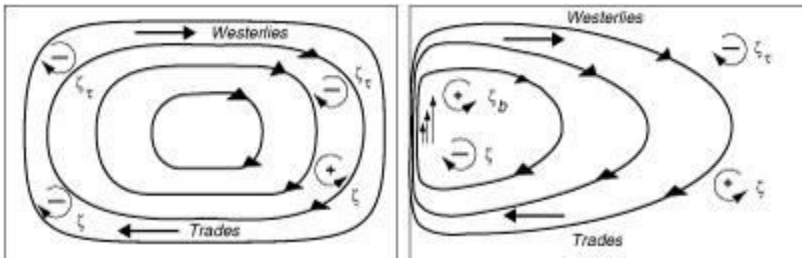

Figure 5.9 The balance of potential vorticity can clarify why western boundary currents are necessary. **Left:** Vorticity input by the wind ζ_{τ} balances the change in relative vorticity ζ in the east as the flow moves southward when f decreases; but the two do not balance in the west where ζ must decrease as the flow moves northward and f increases. **Right:** Vorticity in the west is balanced by relative vorticity ζ_b generated by shear in the western boundary current.

The Ekman layer transports drive circulation in the ocean interior through the Sverdrup transport mechanism. The Ekman layer is the thin frictional layer at the top of the ocean, driven directly by the wind. The whole interior ocean is treated as *inviscid*, that is without friction.

Since the wind varies, for instance with latitude (westerlies and trades), the Ekman transport at right angles to the wind also varies. This means there are convergences and divergences in the (horizontal) Ekman transport. Where there is convergence, there must be vertical velocity downward, escaping from the Ekman layer. Where there is divergence, there must be vertical velocity upward, feeding the Ekman transport. We think of these downward and upward velocities as "squashing" or "stretching" the water column beneath the Ekman layer (i.e. most of the ocean depth).

What is the effect of stretching or squashing? The ocean is a rotating fluid (rotating because of the earth). Therefore it has lots of angular momentum. Stretching and squashing act on the angular momentum, like a spinning skater pulling in or spreading out her arms, and hence

spinning faster or slowly. (conservation of angular momentum, involving the rotation rate and the moment of inertia, which has to do with how tall/thin or short/fat the spinning body is).

The only important component of the angular momentum (vorticity) of the ocean water columns is the local vertical component. This is because the water layers involved in the general circulation are very thin and vertically stratified compared with their horizontal extent, so that the horizontal velocities (parallel to surface of earth) are much stronger than the vertical velocities (order cm/sec versus 10^{-4} cm/sec). The angular momentum (vorticity) has two separate and important components - one is due to local "vorticity" in the flow itself (strong eddying) and the other is due to just the rotation of the earth, which gives everything on the earth angular momentum. These two pieces are called the *relative vorticity* and the *planetary vorticity*.

In the general circulation, relative vorticity is not important over most of the ocean, with the only notable exceptions being in the very strong western boundary currents and in the east-west equatorial currents. The planetary vorticity (local vertical component) is largest and positive (in the sense of the right-hand rule) at the north pole. It is largest and negative at the South Pole. It is zero on the equator. Therefore the important component of the angular momentum increases northward, from large/negative at the south pole through 0 at the equator to large/positive at the north pole.

When the frictional Ekman layer exports water downward (very small downward vertical velocity), at the top of the ocean, it squashes the water columns, which must then spin more slowly. This can be accomplished by either spinning more slowly in the location of the water column ("inducing negative relative vorticity"), or moving to another latitude where the local rotation rate (parallel to the local vertical) is slower - this would be equatorward. If on the other hand there is Ekman divergence, then the water columns are "stretched", and the column must spin faster, either in place or by moving to higher latitude.

5.7. Western boundary currents.

Stommel used wind patterns between 15^0 and 45^0N. His addition of friction allowed a closed circulation across the entire basin, in contrast to Sverdrup's solution that was restricted to eastern boundary. Stommel's results can also be understood in terms of potential vorticity equation as below.

Consider the area of the westerlies and the trade winds in the ocean as shown in Fig.5.10 below. The distribution of wind stress tends to cause anticyclonic (negative vorticity) as shown below

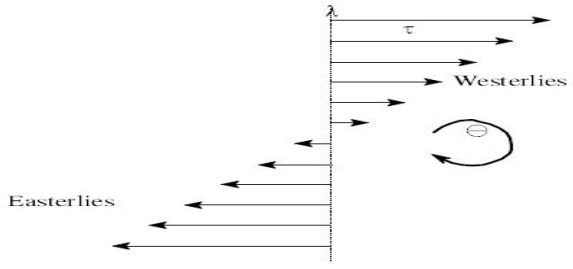

Fig.5.10. Generation of anticyclonic gyre due to Low latitude Easterlies and middle latitude Westerlies

Intensification of western boundary currents may also be explained in terms of vorticity balance as shown in Fig.5.11. It is more convenient to work with vorticity than with linear current flow, because horizontal pressure gradient forces which lead to complications need not be considered.

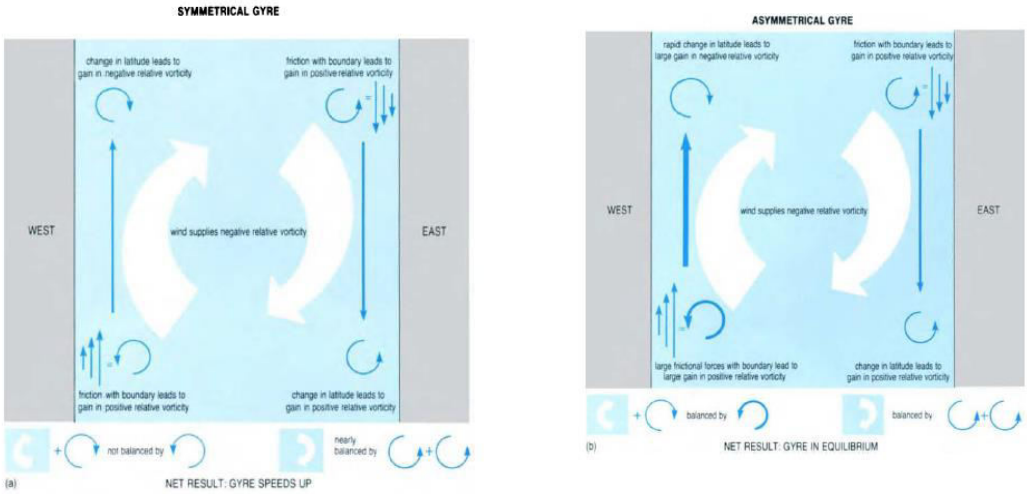

Fig.5.11. Vorticity balance in: (a) a symmetric gyre ; and (b) in asymmetric gyre

The most obvious factor affecting the relative vorticity of the water in the gyre is the wind. The wind field is symmetrical and acts to supply negative (clockwise) vorticity in the Northern Ocean gyre (Fig.5.11a) (say North Atlantic).

The next factor to be considered is the change in latitude. Water moving northwards on the western side of the gyre is moving into regions of larger positive planetary vorticity (f) and hence acquires negative relative vorticity (ζ) (Fig5.11 b). Similarly water moving southwards on the eastern side of the gyre is moving into regions of smaller positive planetary vorticity and so loses negative relative vorticity. However, as more water moves northwards than it moves southwards, the net change in relative vorticity of water due to the change in latitude in the entire gyre is zero.

Then what is acting to counteract the negative (clockwise) tendency supplied by the wind stress, so that the gyre does not speedup indefinitely. The answer is friction. We know that wind driven circulation is confined to the upper layers and is not frictionally bound to the sea floor, but there will be significant friction with the coastal boundaries as a result of horizontal eddies. If we can calculate the vorticity balance using the appropriate value of eddy coefficient of viscosity (A_h), it is clear that frictional forces should be large to provide sufficient positive relative vorticity to balance the negative relative vorticity providedby the wind stress.

The net Sverdrup transport added up across the ocean (along a parallel of latitude) must be returned in a narrow flow somewhere. The transport of this narrow flow is the same and in the opposite direction to the transport across the whole ocean width (Fig.5.12); therefore the velocities are much larger than in the ocean interior.

The return flow must ALWAYS be on the western side, regardless of northern or southern hemisphere. Why? Consider the subtropical gyres, where Sverdrup transport is equatorward. The wind through friction is putting "negative" vorticity into the subtropical ocean, through downward Ekman pumping that send the water columns towards lower rotation, e.g. towards the equator. For a steady state, which the general circulation is, this vorticity must be removed somewhere. It is removed through friction in a narrow boundary current. Why "narrow"? Because friction acts best on high of velocity, which you would get in a narrow flow, and because the return flow has to be narrow enough to escape forcing by the Ekman pumping. A frictional boundary current has zero velocity along the boundary, and strong velocity offshore. If the boundary current for the northern hemisphere subtropical gyre is on the west, then the relative vorticity of the boundary current is positive (paddlewheel sense). Thus the frictional boundary current puts positive vorticity into the ocean, which balances the negative vorticity put in by the Ekman pumping. This exact argument works for the low pressure regions as well (subpolar gyre, with northward Sverdrup transport and southward western boundary current). It also works in the southern hemisphere.

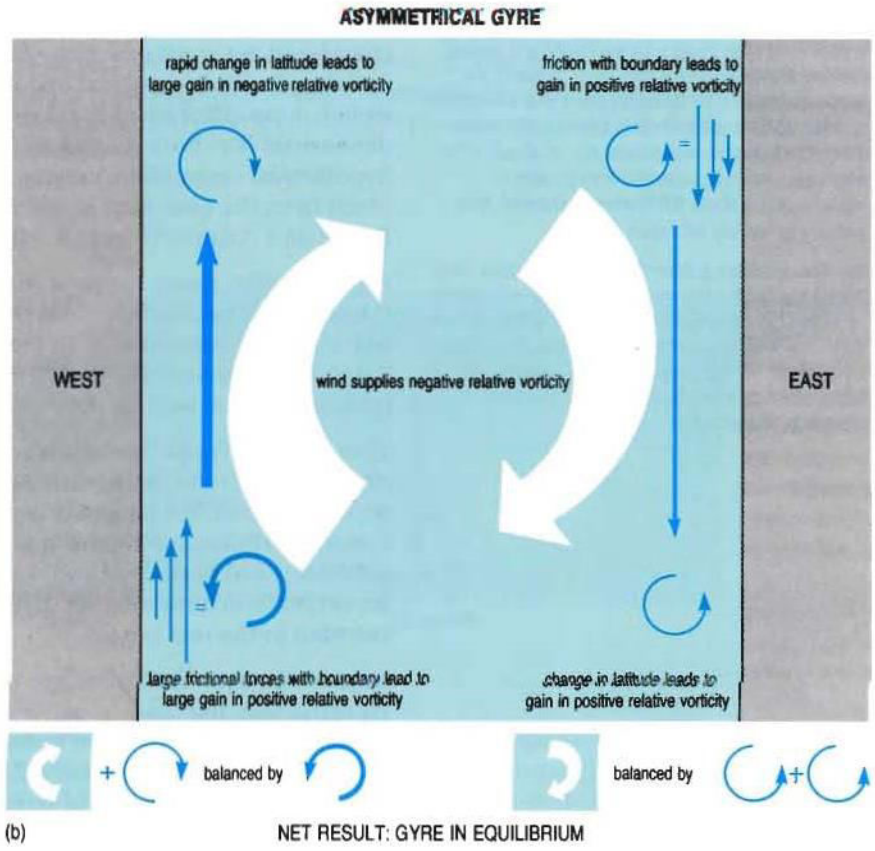

Fig.5.12 Western and eastern boundary currents developed due to vorticity balance

The resulting strong, narrow western boundary currents returning all of the interior transport back to the latitude where it started. The Gulf Stream, Kuroshio, Oyashio, Labrador Current, etc, presented at the beginning of this lecture, are examples of such wind-driven circulation western boundary currents. Because of various other factors, including just inertia, the western boundary

currents are generally stronger than is required to simply return the interior flow. This results in an overshoot of the western boundary current at the latitude where it should end if it were very frictional. Thus the Kuroshio and Gulf Stream, for instance, separate and flow far out to sea before finally dying out.

The simulation of wind driven circulation over North Pacific Ocean by Munk also shows the clear westward intensification as shown in Fig 5.13 below.

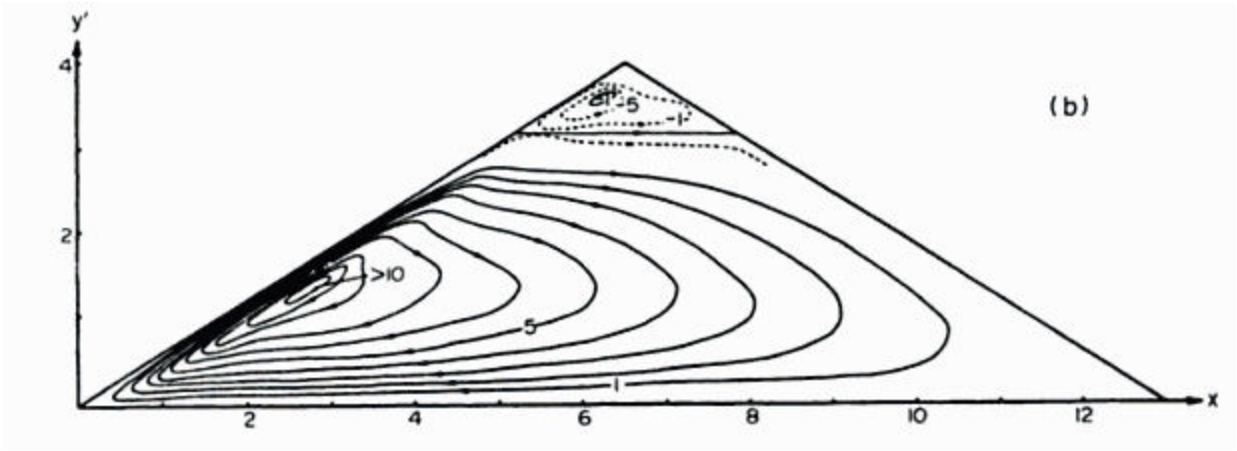

Fig.5.13 . Computed transport streamlines for a triangular ocean from 15^0 to 60^0N by Munk (1 dyne cm^{-2} = 0.1 Pa; 1 dyne cm^{-3} = Pa m^{-1})

5.8. Munk's contribution:

Munk combined the basic features contributed by Ekman, Sverdrup and Stommel to provide the first comprehensive solution of the wind driven circulation, using the real wind field and with the drag coefficient (step function) C_D. He used two friction terms:

a) Vertical friction, associated with vertical shear to convey momentum from the wind stress applied at the surface into the Ekman layer
b) Lateral friction, associated with horizontal shear so that the ocean would remain in a steady state of circulation.

He finished up with a fourth order differential equation describing the circulation as:

$$A.\nabla^4\psi - \left(\beta.\frac{\partial\psi}{\partial x}\right) - curl_z.\tau = 0$$

$$\beta M_y = \nabla \times \tau - A\nabla^4\psi \qquad \text{.....(76)}$$

Where A is the eddy viscosity coefficient for lateral friction for mass transports, ∇^4 is the two dimensional biharmonic operator (= $\frac{\partial^4}{\partial x^4} + 2.\frac{\partial^4}{\partial x^2\,\partial y^2} + \frac{\partial^4}{\partial y^4}$) ; ψ the mass transport stream function. In words it can be described as:

(Vorticity from lateral stresses) – (Planetary vorticity) – (windstress curl) = 0

The three terms in the equation (76) are not equally important all over the ocean. In the west, where the currents are strong, the first and second terms are important, while for the reminder of the ocean the second and third are important. Note that this is a fourth order equation (it contains four partial derivatives) and so its solution can satisfy four boundary conditions. This is the solution for a rectangular ocean and is somewhat stylished. Later Munk and Carrier solved for a triangular ocean which more nearly represents the shape of North Pacific as shown in Fig 5.13.

Munk's derivation:

Munk added lateral friction to the Sverdrup equation : $\therefore \beta M_y = \nabla_z \times \tau_0$

Starting with the basic hydrodynamic equation of Sverdrup:

$$\int_{-D}^{0} \frac{\partial p}{\partial x} dz = \int_{-D}^{0} f.\rho.v + \int_{\tau_D}^{\tau_0} d\tau_x , \ \rightarrow \quad = f.M_y + \tau_{x0} + L.F$$

$$\int_{-D}^{0} \frac{\partial p}{\partial y} dz = -\int_{-D}^{0} f.\rho.u.dz + \int_{\tau_0}^{\tau_0} d\tau_y \ \rightarrow \quad = -f.M_x + \tau_{y0} + L.F \ \text{.....(78)}$$

Where L.F is lateral friction

Or $\frac{\partial \chi}{\partial x} = f.M_y + \tau_x + L.F$; $\frac{\partial \chi}{\partial y} = -f.M_x + \tau_y + L.F$

Substituting the values of L.F and re writing:

$$-f.M_y = -\frac{\partial \chi}{\partial x} + \tau_x + \int_{Bottom}^{surfac} \rho A \frac{\partial^2 u}{\partial x^2} \, dz + \int_{Bottom}^{surfac} \rho A \frac{\partial^2 u}{\partial y^2} \, dz$$

$f.M_x = -\frac{\partial \chi}{\partial y} + \tau_y + \int_{Bottom}^{surfac} \rho A \frac{\partial^2 v}{\partial x^2} \, dz + \int_{Bottom}^{surfac} \rho A \frac{\partial^2 v}{\partial y^2} \, dz$ ……(79)

Here eddy coefficient 'A' is taken as constant in all directions and the integral terms can be written as:

$$\int_{Bottom}^{surfac} \rho A \frac{\partial^2 u}{\partial x^2} \, dz = A \, \frac{\partial^2 M_x}{\partial x^2}$$

Similarly

$$\int_{Bottom}^{surfac} \rho A \frac{\partial^2 u}{\partial y^2} \, dz = A \, \frac{\partial^2 M_x}{\partial y^2}$$

$A \, \frac{\partial^2 M_x}{\partial x^2} + A \, \frac{\partial^2 M_x}{\partial y^2} = A \, \nabla_H^2 \, M_x$ similarly $A \, \frac{\partial^2 M_y}{\partial x^2} + A \, \frac{\partial^2 M_y}{\partial y^2} = A \, \nabla_H^2 \, M_y$

The equations (79) can be re written as:

$f.M_y = \frac{\partial \chi}{\partial x} - \tau_x - A\,\nabla_H^2 M_x$ .....(80)

$f.M_x = -\frac{\partial \chi}{\partial y} + \tau_y + A\,\nabla_H^2 M_y$ .....(81)

Differentiating eqn (80) with respect to 'y' and differentiating eqn (81) with respect to 'x' and on adding we get

$\frac{\partial}{\partial y}(f.M_y) + \frac{\partial}{\partial x}(f.M_x) = \frac{\partial \tau_y}{\partial x} - \frac{\partial \tau_x}{\partial y} + \frac{\partial}{\partial x}(A\,\nabla_H^2 M_y) - \frac{\partial}{\partial y}(A\,\nabla_H^2 M_x)$ .....(82)

We can write the last two terms as:

$$\frac{\partial}{\partial x}(A\,\nabla_H^2 M_y) - \frac{\partial}{\partial y}(A\,\nabla_H^2 M_x)$$

$$A\frac{\partial}{\partial x}\left(\frac{\partial^2}{\partial x^2} + \frac{\partial^2}{\partial y^2}\right)\left(-\frac{\partial \psi}{\partial x}\right) - A\frac{\partial}{\partial y}\left(\frac{\partial^2}{\partial x^2} + \frac{\partial^2}{\partial y^2}\right)\left(\frac{\partial \psi}{\partial y}\right)$$

On expanding and simplifying we can write:

$$-A\left\{\frac{\partial^2 \psi}{\partial x^2}\left(\frac{\partial^2}{\partial x^2} + \frac{\partial^2}{\partial y^2}\right) + \frac{\partial^2 \psi}{\partial y^2}\left(\frac{\partial^2}{\partial x^2} + \frac{\partial^2}{\partial y^2}\right)\right\}$$

$-A\left\{\frac{\partial^4 \psi}{\partial x^4} + 2.\frac{\partial^4 \psi}{\partial x^2 \partial y^2} + \frac{\partial^4 \psi}{\partial y^4}\right\} = -A\nabla^4\psi$ .....(83)

The middle term in the left hand side is called as two dimensional biharmonic operator. Substituting equation (83) in equation (82) and then simplifying we can write:

$\frac{\partial}{\partial y}(f.M_y) + \frac{\partial}{\partial x}(f.M_x) = \frac{\partial \tau_y}{\partial x} - \frac{\partial \tau_x}{\partial y} - A\nabla^4\psi$

$\frac{\partial}{\partial y}(f.M_y) + \frac{\partial}{\partial x}(f.M_x) = \nabla \times \tau - A\nabla^4\psi$

Rewriting again $f\left(\frac{\partial M_x}{\partial x} + \frac{\partial M_y}{\partial y}\right) + M_y\frac{\partial f}{\partial y} + M_x\frac{\partial f}{\partial x} = \nabla \times \tau - A\nabla^4\psi$ .....(84)

In this eqn (84) first term and third term vanishes as $\left(\frac{\partial M_x}{\partial x} + \frac{\partial M_y}{\partial y}\right) = 0$ is equation of continuity of mass, $\frac{\partial f}{\partial x} = 0$ because variation of coriolis parameter in the zonal (x) direction is zero. Taking $\frac{\partial f}{\partial y} = \beta$

$\beta M_y = \nabla \times \tau - A\nabla^4\psi$ .....(85)

Equation (85) is called Munk's equation. Munk assumed that the currents went to zero near the bottom or that the bottom was level and the bottom stress was level and the bottom stress was negligible because the currents are very small in deep water. Munk also assumed that in the west the friction

terms associated with horizontal shears in the currents are important. The vanishing of curl τ at certain latitudes breaks the flow into gyres.

Fig.5.14a below shows the pattern of ocean circulation that Munk calculated in North Pacific Ocean. If this pattern is compared with the global surface circulation of any Northern Oceans (like North Atlantic or North Pacific), it bears a strong resemblance to the actual circulation like gyres, North Equatorial current, Equatorial counter current, westward intensification etc.

Thus in many ways, Munk's model of ocean circulation (Fig.5.14a) reproduces the circulation pattern in the real ocean. This means that the oceanic processes considered by Munk are important. They are flow of water into different latitudes (i.e. regions in which the coriolis force is different) and horizontal and vertical frictional forces which are important in determining the large scale current patterns that result from the wind in the real oceans.

Models of ocean circulation are being improved and refined all the time using the equation of motion. In this regard Fofonoff's analysis of interior transport also is worth to be noted.

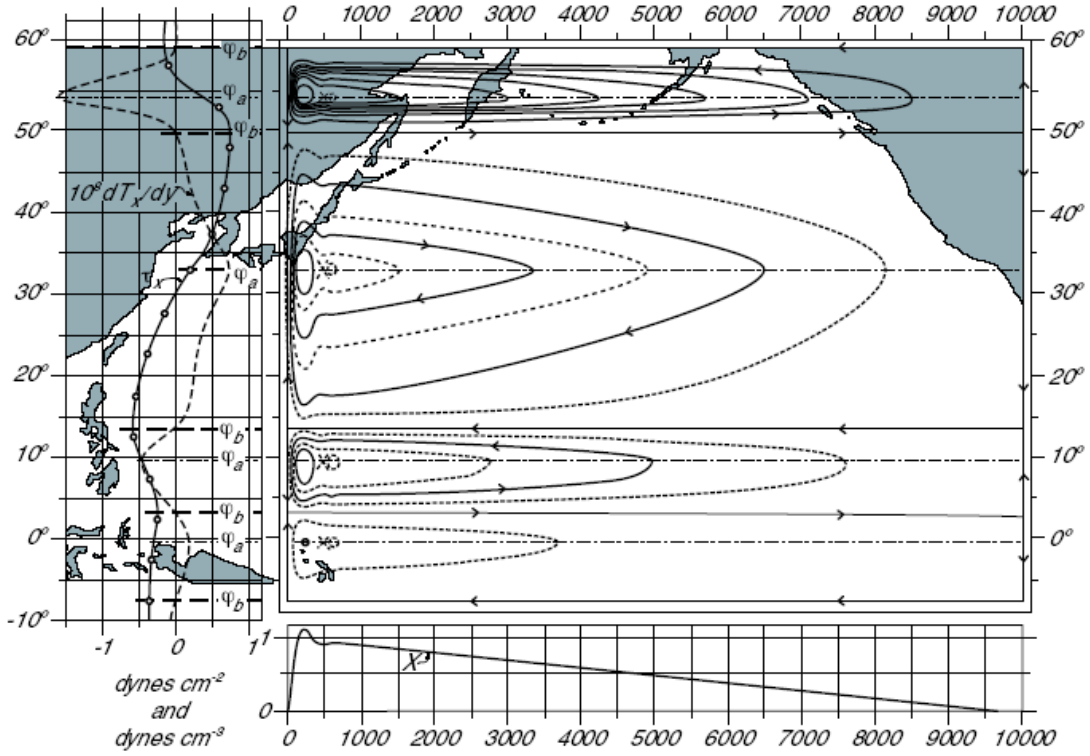

Fig.5.14a . Schematic configuration of current & gyres driven by wind in Pacific calculated by Munk in 1950. **Left Fig**: The full line is Mean annual wind stress (τ_x) over the Pacific and dashed line is its curl. ϕ_b is the northern and southern boundaries of the gyres, where M_y = 0 and curl τ = 0. ϕ_0 is the center of the gyre. **On the right upper** : computed mass transport stream function (ψ) for a rectangular ocean for the observed wind stress. Contour interval is 10 Sverdrups ($1\,Sverdrup = 10^6 m^3 s^{-1}$). The total transport between the coast and at any point (x,y) is $\psi(x,y)$. **On the right Lower**: North-South component of mass transport

Though the circulation derived by Sverdrup and Stommel bear a strong resemblance to the circulatory system of subtropical gyres, these circulation models were extended and made even more realistic by the work of Munk. Like Stommel, Munk used a rotating rectangular ocean and assumed that the coriolis

force varied linearly with latitude, but he extended the ocean to include latitudes upto 60^0 and the equatorial zone. He also balanced the relative vorticity supplied by wind, change of latitude and friction, but improved on the representation of both friction and the wind. He hasn't considered friction only with coastal boundaries like Stommel but friction associated with both lateral and vertical current shear. Thus he included the effect of eddy viscosity in both the horizontal and the vertical dimensions (both A_h and A_z). Instead of using the curl of the hypothetically varying wind, he used the curl that results from the real winds of Pacific and Atlantic Oceans.

Fig.5.14 b shows the pattern of ocean circulation that Munk calculated depicting the different currents. If this pattern is compared with the global surface circulation of any Northern Oceans (Fig.5.14 c) (like North Atlantic or North Pacific), it bears a strong resemblance to the actual circulation like gyres, North Equatorial current, Equatorial counter current, westward intensification etc.

Thus in many ways, Munk's model of ocean circulation (Fig.5.14a and b) reproduces the circulation pattern in the real ocean. This means that the oceanic processes considered by Munk are important. They are flow of water into different latitudes (i.e. regions in which the coriolis force is different) and horizontal and vertical frictional forces which are important in determining the large scale current patterns that result from the wind in the real oceans.

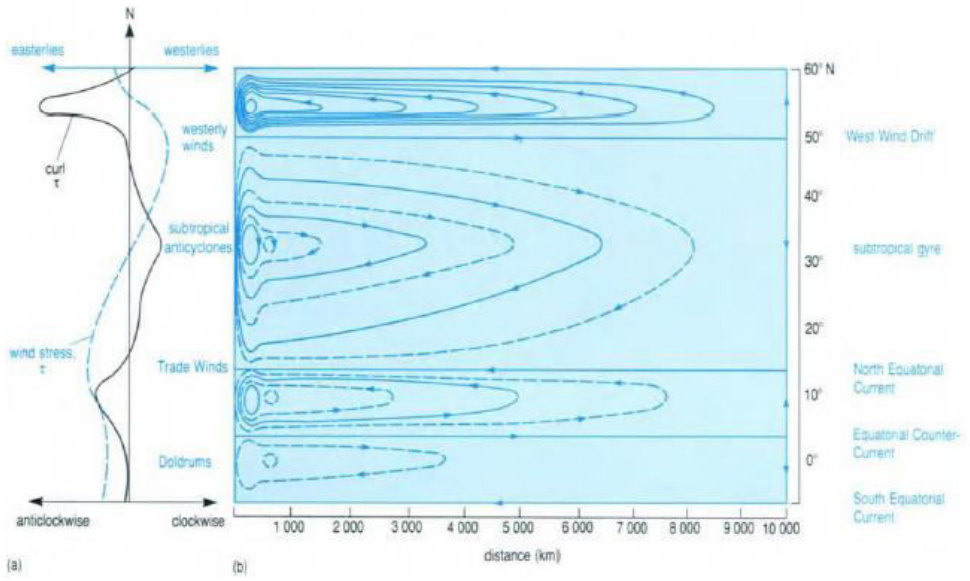

Fig.5.14. (b): The blue curve is the average annual zonal wind stress τ_0 for the Pacific and Atlantic Oceans. The black curve is the curl of the wind stress $(\nabla_z \times \tau_0)$. By definition this curl τ_0 is at a maximum at those latitudes where the wind stress curve shows the greatest change with latitude e.g. at about 55^0N where the wind stress changes from easterly to westerly, and at about 30^0N where it changes from westerly to easterly.

(b): The circulation pattern that Munk calculated using the values of curl τ_0 shown in (a). The volume transport between adjacent solid lines is$10^7 m^3 s^{-1}$. The greatest meridional flow occurs where curl τ_0 is at a maximum i.e. at 55^0N, 30^0 N and 10^0N. At these latitudes, the flow is southwards or northwards, rather than eastwards or westwards.

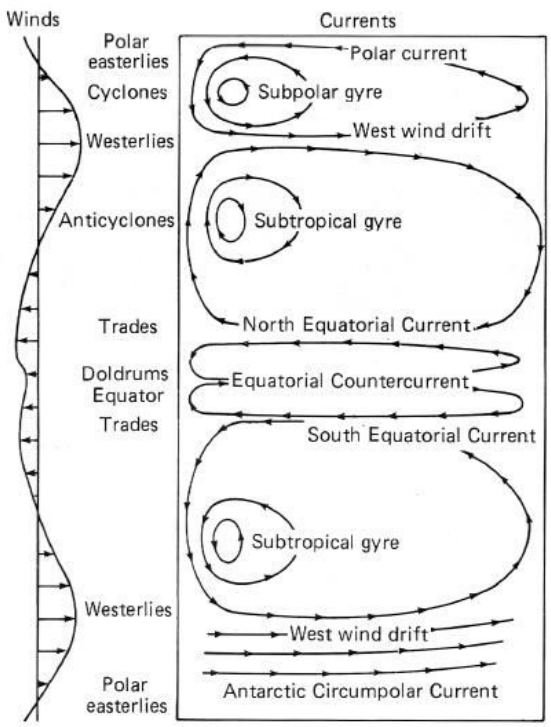

Fig.5.14c Schematic configuration of current gyres driven by wind in Pacific by Munk

Lecture Series of Berhampur University in Physical Oceanography
By Prof.A.S.N.Murty

Chapter – 6

Oceanic Wind Waves

4.0. Introduction:

Successive crests with intervening troughs advance in an undulatory motion are called waves. Waves are considered in two categories. They are forced waves and free waves. A forced wave propagates as long as the generating force acts and once the generating force is removed the wave stops whereas a free wave continues to propagate even after the removal of the generating force.

It is clear by watching a floating bottle on the sea surface, as shown in Fig.4.1, that more or less it moves up and down as the crest and trough passes over it. This gives us the meaning that wave is only an oscillation from the mean sea surface and doesn't transport much of a mass.

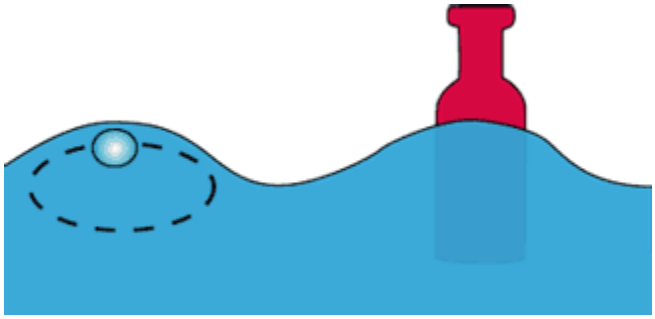

Fig.4.1. A bottle on the sea surface describes the wave profile

As the wave crest approaches, the bottle moves forward with the crest, pause as the trough approaches and move backward in the trough nearly to its original position. Of course, during the same time it has risen to the top of the crest and fallen to the bottom of the trough. The combined motion is very nearly like a circular as seen in the Fig.4.1.

If the vertical difference between crest to trough is wave height (H)(Fig.4.2) and the time required for the bottle to complete its circle and return to its original position is wave period (T), then the diameter of the circle would be equal to its wave height (H). Then the speed of the water particle is $C_p = \frac{\pi H}{T}$. As there is no direct relation between wave height and wave period wide ranges of water particle speeds can occur for the same time period. However, if the particle speed is compared with the wave speed $C_w = L/T$ we get,

$$\frac{C_p}{C_w} = \frac{\pi H}{L} = 3\frac{H}{L} = 3steepness$$

As wave heights are much smaller than the wave lengths, when they approach the coasts the wave height enormously increases and so they break. Stokes sets up an upper

limit for wave breaking as $\frac{H}{L} > \frac{1}{7}$ which means the water particle speed is less than the 3/7 of the wave speed before the wave breaks.

Waves can be distinguished basing on the shape of the profile. If the profile of a wave moves relative to the medium, it is a progressive wave. If the profile doesn't move, but merely oscillates in one place relative to the medium, it is a standing wave. A wave in which the particle motion is entirely parallel to the direction in which the wave moves is called a longitudinal wave. One in which the motion is entirely perpendicular is called a transverse wave. Ocean surface waves belong to neither of these classes as these are theoretical profiles and as ocean waves are formed due to combination of several profiles and bands called spectrum.

While the crest of the wave is the highest point of water above the mean water level, the trough is the lowest point below the water level. In the case of sinusoidal wave the crest and the trough are displaced symmetrically from the mean level and so the height of the wave is twice the amplitude or crest height as shown in Fig.4.2.

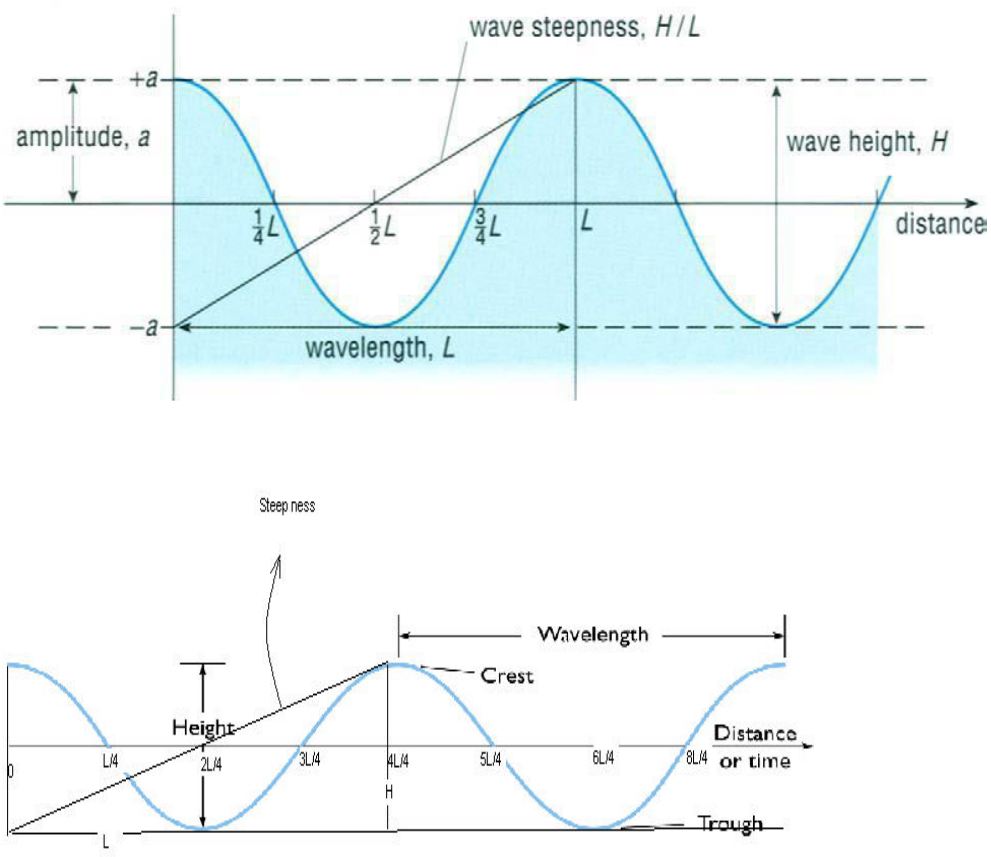

Fig.4.2. wave parameter in Sinusoidal wave form

But this is not true in the case of a trochoid as shown in Fig.4.3. The wavelength,L, is the horizontal distance between two crests and the period,T, is the time

interval between the passage of two successive crests past a fixed point. The wave velocity or Celerity,C, is the ratio of wave Length to time period (L/T).

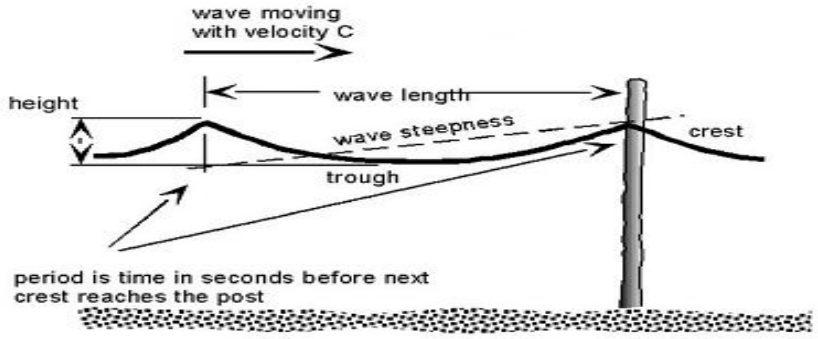

Fig.4.3. Wave parameters in a trochoidal form

In the Ocean waves are generated due to various forces. The normal day to day waves are generated due to wind and so they are called wind waves. The restoring force for *small amplitude* waves is either surface tension or gravity and so they are also called *gravity waves*. But for the *finite or nonlinear* waves the restoring force is gravity. There are also some unusual long waves in the ocean. The waves generated due to storms called *storm surges*. Earth quakes, submarine land slides, volcanic eruptions or isostatic and eustatic movements of the earth's crust cause *tsunamis* and the astronomical forces cause tides which are very long waves. There are also standing waves occur in harbors, bays and estuaries called *seiches* due to storm waves, tides or any other oceanic or atmospheric forcings. In fact waves can occur at any interface or boundary both at the surface or subsurface of the ocean. The interface at the surface of the ocean is air and sea surface. All types of waves occur at the sea surface as shown in Fig. 4.4 as the wave spectrum. The waves occur at the subsurface are called *internal waves* as shown in fig.4.3. They are also called *dead water* because during World War 2, the ships used to be hindered at some places in the oceans. At that time the reason for this hindrance was not known and so they called it as dead water. These internal waves are caused due to tides, turbidity currents, winds, ships in motion, seiches etc.

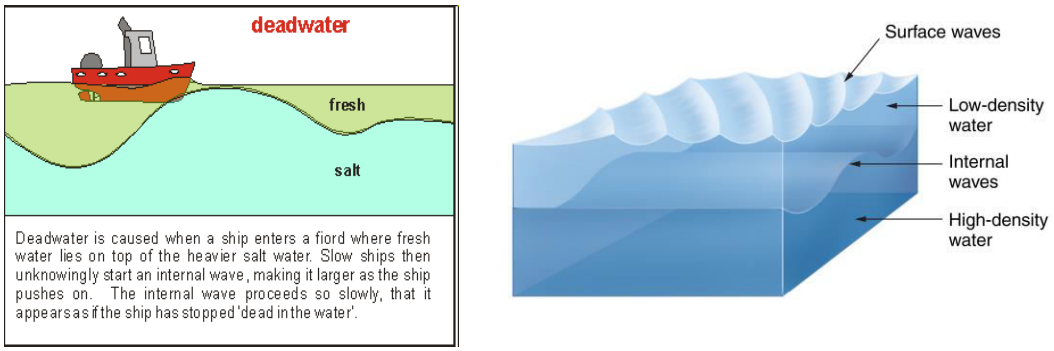

Fig.4.3. Internal waves.

The ocean surface waves are classified basing on their periods as shown in the table 4.1(a &b) and the curve representing the relative amounts of energy with their associated generating forces as shown in Fig.4.4 (a,b and c) is the spectrum of ocean waves.

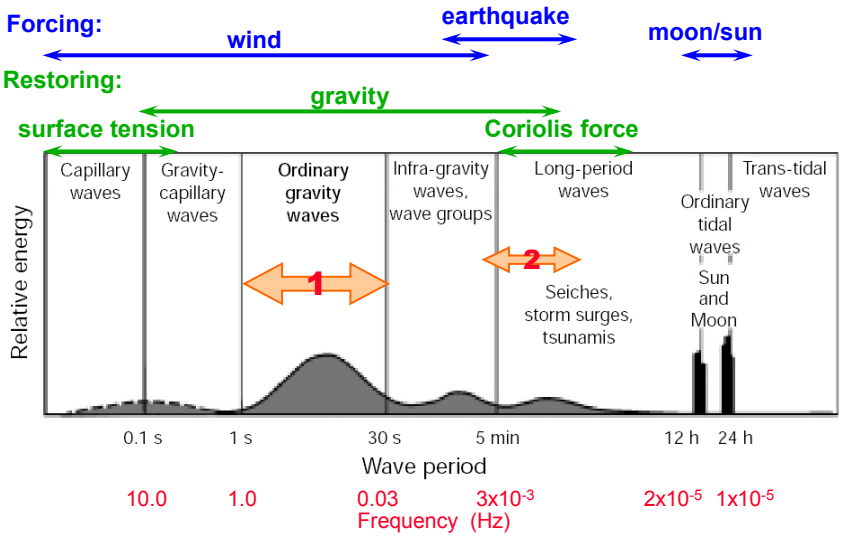

Fig.4.4a Wave spectrum classification basing on period (frequency)

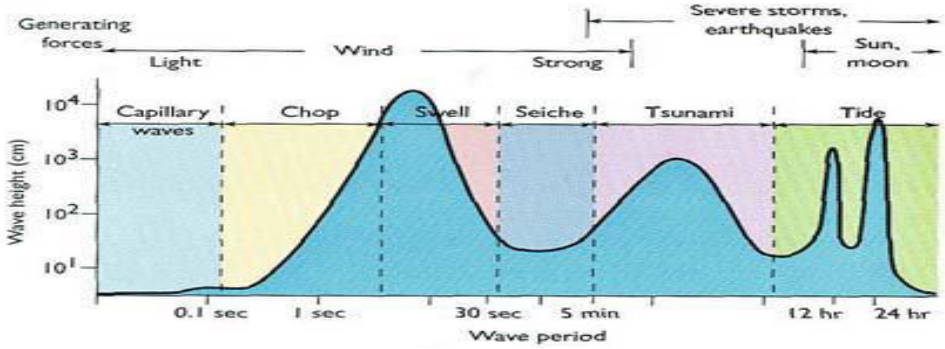

Fig.4.4b Idealized wave spectrum

Table 4.1a. Types of waves in the ocean

Name	Typical Periods	Wave lengths	Forcing Mechanism
Ripples	< 0.2 s	10^{-2} m	wind on sea surface
Sea	0.2 - 9 s	~130 m	"
Swell	9 - 30 s	100s of m	"
Internal	minutes to several hours	1 - 300 m	current shear on stratification
Planetary and Topographic	hours to days	100-1000s km	bathymetry/atmospheric pressure/Coriolis
Tsunamis	15 minutes to 1 hour	few 100s km	seismic
Tides	several hours	several 100s - few 1000s km	gravitational (moon and sun mainly)

Waves are classified in a spectrum according to their wave periods, from the very smallest period "capillary" waves (with period less than 0.1 sec) to "ocean swells" (period about 15 sec) and tsunamis (period about 20 min). The amount of energy in a particular wave class is determined by the typical wave height in that class. The different forces that cause different types of waves and their restoring forces are indicated above and in Fig.4.4.c as per the table 4.1b.

Table:4.1b: classification of waves basing on the period.

S.No.	Wave name	Period
1.	Capillary waves	< 0.01 sec
2.	Ultra gravity waves	0.01sec-1.0sec
3.	Gravity waves	1sec-30sec
4.	Infra Gravity waves	30sec-5 min
5.	Long waves	5 min-12 hrs
6.	Tidal waves	12 hrs-24 hrs
7.	Trans tidal waves	> 24 hrs.

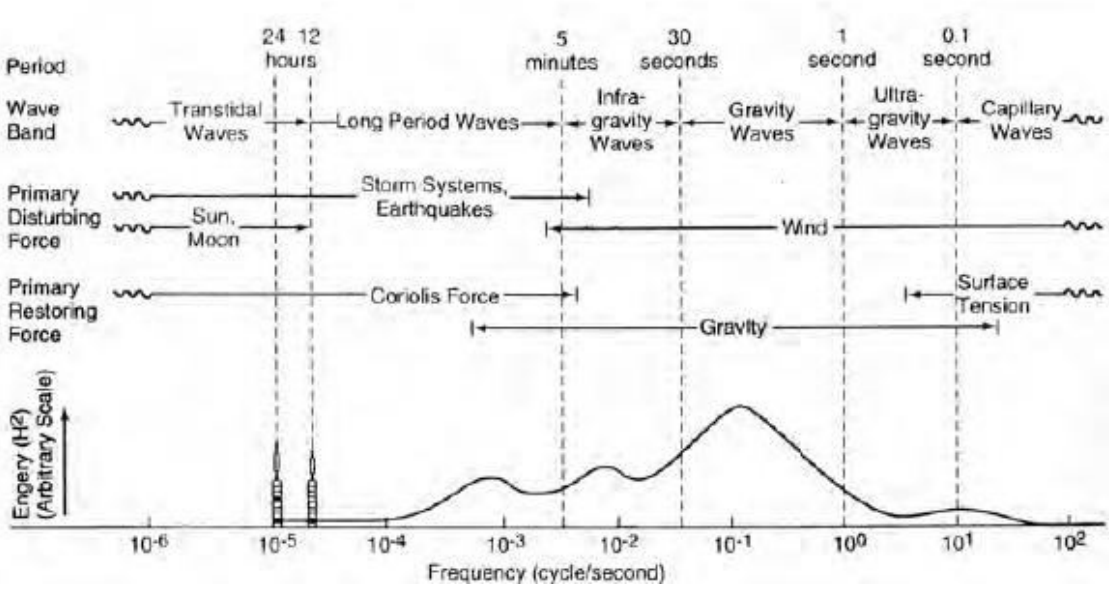

Fig.4.4c. wave spectrum in the oceans

4.1. Wave generation by wind:

If a light breeze springs-up over a calm seas surface the first response of the water is marked by the random appearance of small, darkened, ruffled patches called *cat's-paws.* The cat's paws then turn out to be wavelets as wind strength increases. The reason for the development of wavelets is mainly due to distortion of the sea surface caused due to the drag and other viscous effects as mentioned by Jeffreys as shown in Fig.4.5. Once the wind blows over water the drag should setup a current along the downwind.

The region of blowing wind is called *generating area.* The development of waves ultimately depends on three factors *speed, duration* and *fetch* of the wind. The duration of time that the wind acts on the water surface is called the wind duration. The distance over which wind blows called fetch. A minimum speed, duration and fetch is necessary for the

development of wavelets. When these minimum conditions over steady state reach then the sea is called *fully arisen sea.*

The first wavelets appear in the fully arisen sea are *capillary waves* which are only a few centimeters in length and a few meters in height. The capillary waves, though small, wrinkle the sea surface. This wrinkling is restricted by the surface tension. However, if the wind continues to blow, the capillary waves grow in size and become gravity waves.

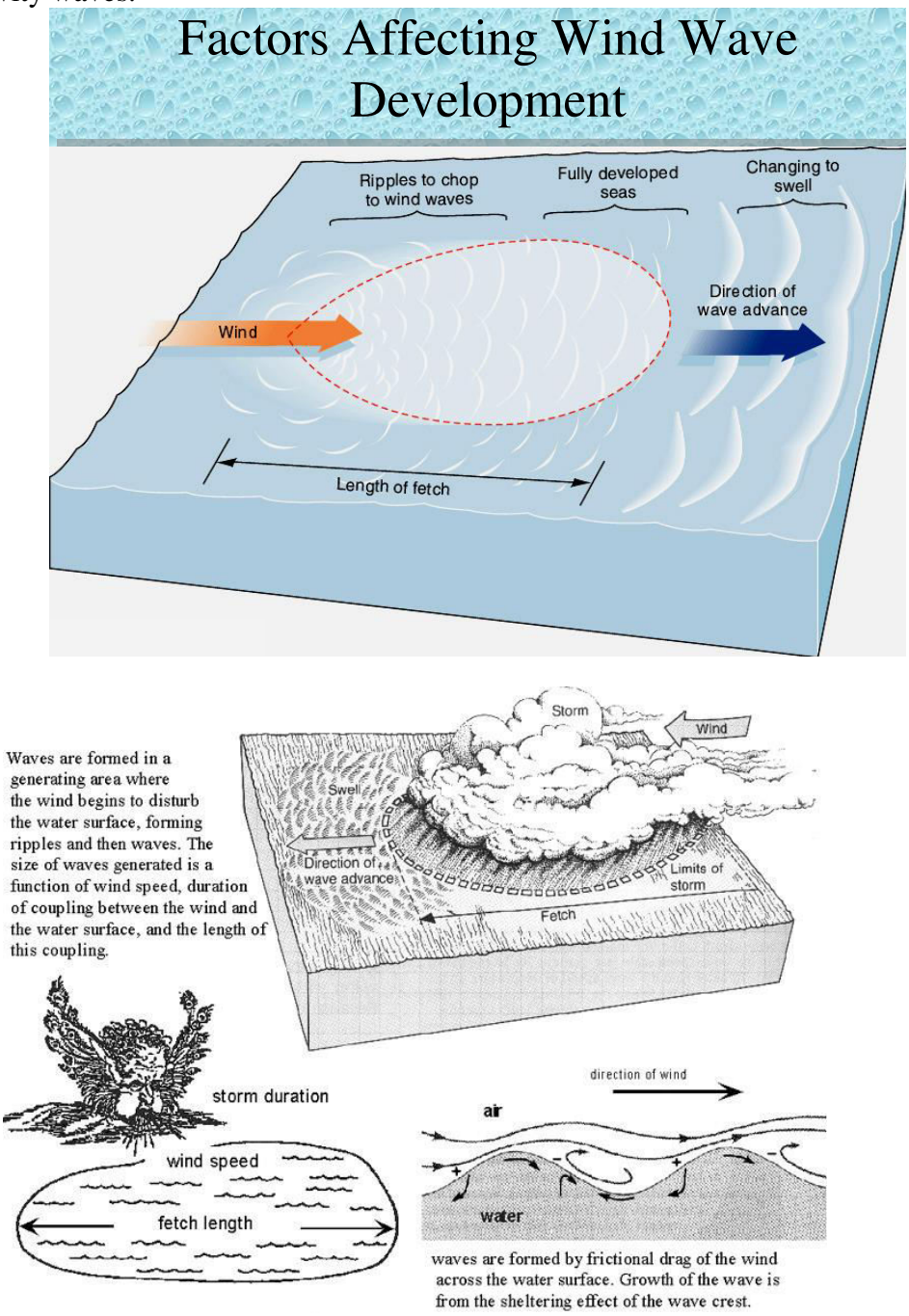

Fig.4.5: Generating area and wave generation mechanism

4.2. Theories of wave generation:

Though many theories were developed, actually the transfer of energy from wind to waves, and the resulting wave growth, is not completely understood. The wave may get energy from the direct push of the wind on their upwind faces if they are remaining slower than the wind.

4.2.1: The sheltering theory of Jeffrey's:

The sheltering theory of Jeffreys (1925) assumes that the air flow is laminar over the wind ward slope of the wave and turbulent on the lee side slope that the lee side of the wave form is sheltered by the crest and that low velocities are found there. The normal pressure is thus said to differ between the windward and leeward faces. If the wind velocity exceeds the wave velocity, energy is transferred from the air to the water. Tangential friction is ignored in the theory. One important parameter in the analysis is the "sheltering coefficient-S" which is related to the proportion of the wind ward slope of the wave which offers resistance to the wind. The value of S is given as 0.27.

Jeffreys theory accounts reasonably satisfactory for the initial generation of waves, when their steepness is very low, but as the waves increase in steepness the value of 'S' appears too great.

If a strong wind blows against an obstacle the wind exerts a pressure on the wind ward side of the obstacle but on the leeward side there will be suction. Similarly when the wind blows over a sequence of waves the pressure of the wind will be greater on the windward slope than on the leeward slope that is sheltered by the crest. This condition can prevail only if the waves travel at a velocity smaller than the speed of the wind. On the basis of these arguments, Jeffreys found that wave can grow only if

$C(W-C)^2 \geq \frac{4\gamma g(\rho-\rho''}{S\rho'}$ where W is wind velocity, C wave velocity; γ=kinematic viscosity of water; ρ and ρ' = densities of water and air ; S = sheltering coefficient (non dimensional.

At a given wind velocity the term $C(W-C)^2$ is maximum when C = W/3. So substituting for C the above equation becomes

$$(W)^3 \geq \frac{27\gamma g(\rho-\rho''}{S\rho'}$$

This equation determines the weakest wind which can raise any wave. Jeffreys conducted wind measurements over small lakes in order to determine the lowest velocity of the wind at which small waves appear. Hr found that only at a speed of the wind a little greater than one meter per second distinct waves seem to appear. Thus substituting this value of 'W' in the above equation the sheltering coefficient w found to be about 0.27 which is related to the proportion of the windward slope of the wave offering resistance to the wind.. This value seems to have been too great. This theory also can not account

for the original generation of waves from a flat surface, although it does seem to apply better in the early stages of wave generation than when the waves become large.

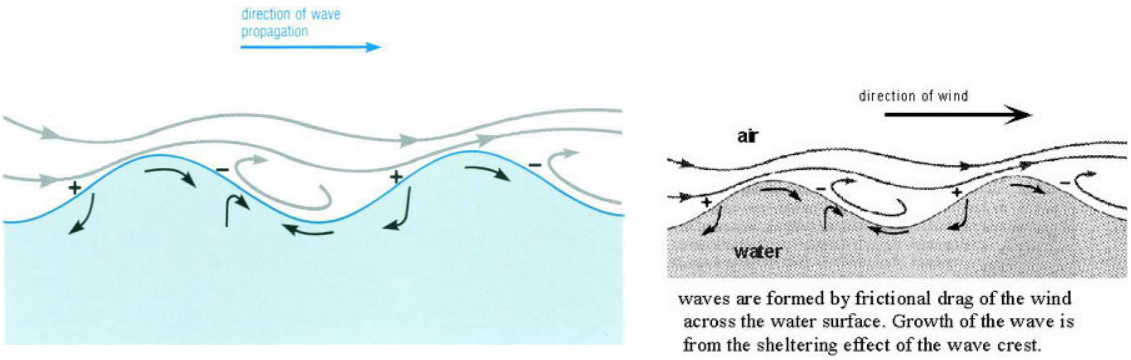

Fig.4.6 Jeffreys sheltering theory

Fig.4.6.(+) indicates higher pressure, minus (-) indicates lower pressure due to sheltering of the crest. Circular arrows indicate the formation of eddies due to pressure difference. Small black arrows indicate the water particle movement. Large wavy arrows indicate the wind flow

b) Sverdrup & Munk theory:

The next great advance in the theory of wave generation in deep water was by H.U.Sverdrup and W.H.Munk. The theory is based on rough turbulent flow which occurs when the wind speed exceeds 7m/s. Above this velocity ripples of small dimension are formed on the wave surface and these alter the type of surface from hydrodynamically smooth to rough. The air flow is considered to be similar to that suggested by Jeffreys, as eddies form in the lee side of the wave. The sheltering coefficient used is about 1/20 of Jeffreys, that is 0.013.

According to this theory waves grow because energy is transferred from the wind to waves. This transfer takes place by two processes namely, transfer by pressure difference and transfer by tangential stress of the wind (R_T in Fig 4.7). The energy which is imparted to the wave is used in part to increase its height and in part to increase its velocity of progress. When the wave velocity is less than the wind velocity, wave receives energy from both the pressure difference and the tangential stress. If, however, the wave velocity exceeds the wind velocity the wave still gains energy by tangential stress but it loses energy through pressure difference because it has to overcome the air resistance.

It is suggested that the tangential stress of the wind, which is an important factor in this theory varies with the square of the wind velocity above a certain value. The waves acquire energy from the wind by tangential stress when the water particles move in the same direction as the wind, and lose energy when the particles move against the wind, but because of mass transport, there is a net gain of energy. The wave velocity is much greater than the velocity of the particles within the wave, and it is thus possible for the wave velocity to exceed that of the generating wind. The limit would be reached when the particle velocity equaled the wind speed. When the waves are moving faster than the generating wind the energy transfer is in two directions. The waves are gaining energy by tangential stress but are losing it by the pressure of the wave form on the wind. Energy is also converted into heat by turbulence. The wave will continue to grow until the loss of

energy equals the gain. The whole energy of the tangential and normal stress of the wind goes into the wave and causes an increase of wave height and wave length. The increase in wave height is more important when the wave is moving lower than the wind, but when the wave speed exceeds the wind velocity most of the energy goes to increase the wave velocity. The proportion of energy increasing the height and length is determined by the relation between the wave steepness and the wave age.

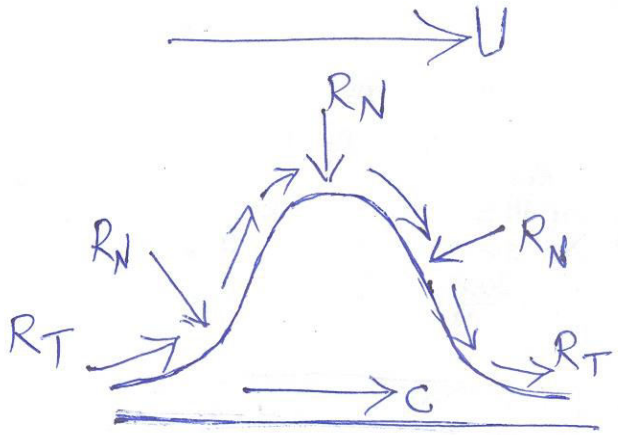

Fig.4.7. Transfer of wind energy to wave through tangential (R_T) and normal stresses (R_N)

The average rate at which energy is transferred to a wave by normal pressure (R_N) is equal to

$$R_N = \frac{1}{L}\int_0^L p_z w_0 dx$$ where w_0 = - kac Cos k (x-ct) is the vertical component of the particle velocity at the surface and p_z is the normal pressure (surface tension) acting on the sea surface.

The average rate at which energy is transmitted to the waves by tangential stress is equal to

$$R_T = \frac{1}{L}\int_0^L \tau u_0 dx$$ where u_0 = kac Sin k (x-ct) denotes the horizontal component of particle velocity at the sea surface and $\tau = \rho C_d U^2$ is the wind stress and 'U' is the wind speed and ρ is air density. Here C_d is the drag coefficient. Various experiments and observations have been made leading to different values of C_d as a function of wind speed. However, a number of authors agreed to put at 1.25×10^{-3} for wind speeds less than 6 m/s and 2.6×10^{-3} for wind speeds greater than 6 m/s.

According to the above the energy of waves can increase only if the rate at which energy is added by both normal and tangential stresses of the wind ($R_N + R_T$), exceeds the rate at which energy is dissipated by viscosity. The energy added by the wind goes into building the wave height and increasing the wave speed.

That is $R_H + R_C = R_N \pm R_T$ where R_H is the portion of energy transformed into wave height and R_c is that portion of energy transformed into wave speed.

c) O.M.Phillips:

One of the most promising theories was put forward by O.M.Phillips in1957. He assumes that a turbulent wind at a given moment starts to blow over a surface previously at rest. The pressure on the surface fluctuates in a distribution which is a stationary random function pf position and time. The study aims to discover the properties of the surface displacement at subsequent periods.

The random distribution assumed by Phillips involves a type of resonance. The turbulent nature of the wind is an essential factor in the growth of waves and causes random stresses on the water surface. These include both normal and tangential stresses. It is true that winds blowing over water do not consist of streams of air in steady and uniform motion but rather of an irregular series of 'puffs' and 'lulls' carrying eddies and swirls distributed in a disordered manner. Eddies, in the air stream, are carried by the wind and change as they move, so that the stress distribution moves across the surface with a certain velocity dependent on the wind speed. This convection velocity of the stress fluctuations is defined as the velocity of the frame of reference, U_c, in which their frequency scale is least, or their time scale is greatest. This velocity is equal to the wind velocity as measured from a ship.

The fluctuating pressure upon the water surface is held responsible for the birth and early growth of the waves, an analysis of the surface should show a wide variety of wave numbers and frequencies in both two dimensional space and time. The components of the pressure fluctuations acting on the surface generate small forced oscillations. These fluctuations affect the component of the amplitude on the surface. If the pressure distribution includes components whose wave numbers and frequencies coincide with possible dimensions of free surface waves a type of resonance is setup, and the continued presence of these particular frequencies in the pressure distribution will generate surface waves whose amplitude will increase. Thus it is asserted that the frame of reference is not changing in character but is moving with the convection velocity, and if one of the wave frequencies generated is moving with the same velocity, then the two move together and growth can continue. This, however, ignores the evolution of the stress pattern and so is an over simplification. If the pressure pattern is changing slowly the growth of the wave lets is reduced.

At first the surface may be assumed to have no effect on the pressure distribution, but this will not last for long. Small ripples will soon form and these have a considerable effect on the vertical velocity distribution. The long gravity waves do not appear to influence the pressure distribution. The viscosity of the water is ignored, which is probably justified for all but the shortest waves. The motion is then irrotational. The results apply when the mean square slopeis small so that the surface boundary conditions can be considered linear. At later stages of growth the non linear effects may become important.

In the initial generation of waves the minimum velocity is given by the equation

$C_{\min} = \left(4gT_s \frac{1}{\rho}\right)^{\frac{1}{4}}$ where ρ is the water density, T_s is the surface tension at the interface and C_{min} is the minimum velocity. The wave length of the critical waves is about:

$L_{cr} = 2\pi\left(T_s \frac{1}{\rho g}\right)^{\frac{1}{2}}$ For water if ρ = 1 gm/c.c; T_s = 73 gm/sec^2 and g = 980 cm/sec^2, C_{min} = 23 cm/sec and L_{cr} = 1.7 cm.

According to Phillips theory of 1957, the main problem of wave generation is related the distribution of pressure on the moving, random water surface under the influence of a turbulent wind. The pressure fluctuations are of two kinds. One is produced by the turbulent eddies in the wind and the other is induced by the air flow over the irregular surface. The total pressure pattern is the sum of these two. The first, the turbulent pressures, provide energy input over a wide spectral range, while the second, the directly induced pressure, provides a selective feed-back which allows certain components to grow rapidly.

4.3. **Seas and Swells**:

Waves that are generated in the generating area are called *seas*. The generating area is chaotic and confusing contains high energy. All the seas that are generated in the generating area gets nullified sometimes and some resulting waves will come out of this generating area and can travel to far off distances up to the coasts. These long period waves that come out of the generating areas and reach the coasts are called *swells*.

Sea waves are usually shorter period (higher frequency) than *swell*. Generally 10 seconds (0.1 cycles per second) can be taken as the demarcation period from sea to swell. *Sea* is shorter in length, steeper, and more rugged and confused in state than the swell as shown in the Fig.4.8 (a to d).

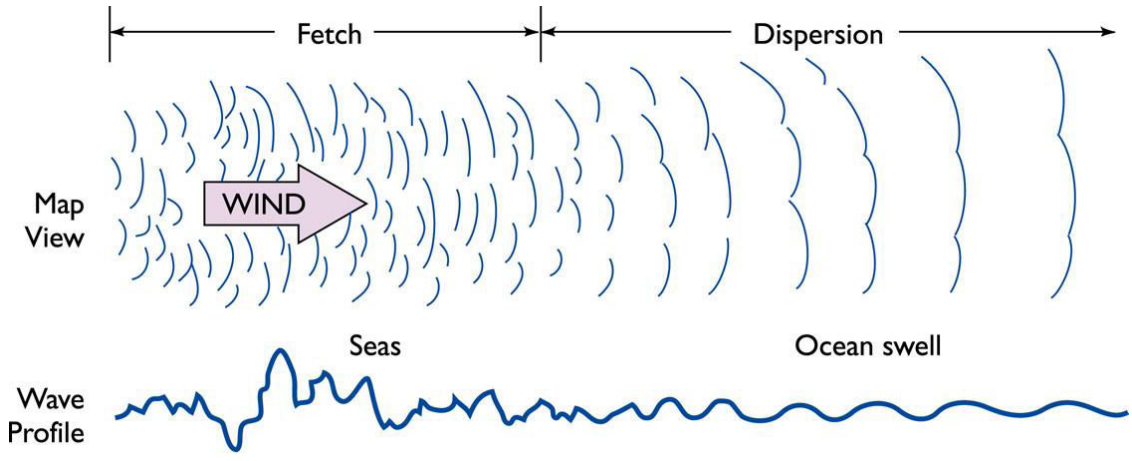

Fig.4.8a: Transformation of sea in the generating area to swell

Seas in the generating area

Swell at the shore

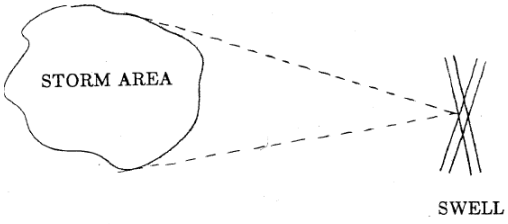

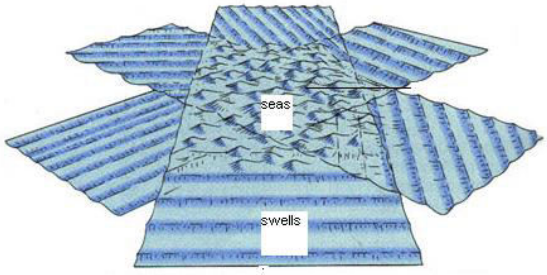

Fig.4.8b. Seas and swells in a generating area

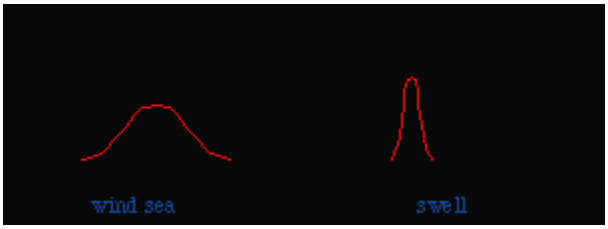

Fig.4.8c spectra of sea and swell

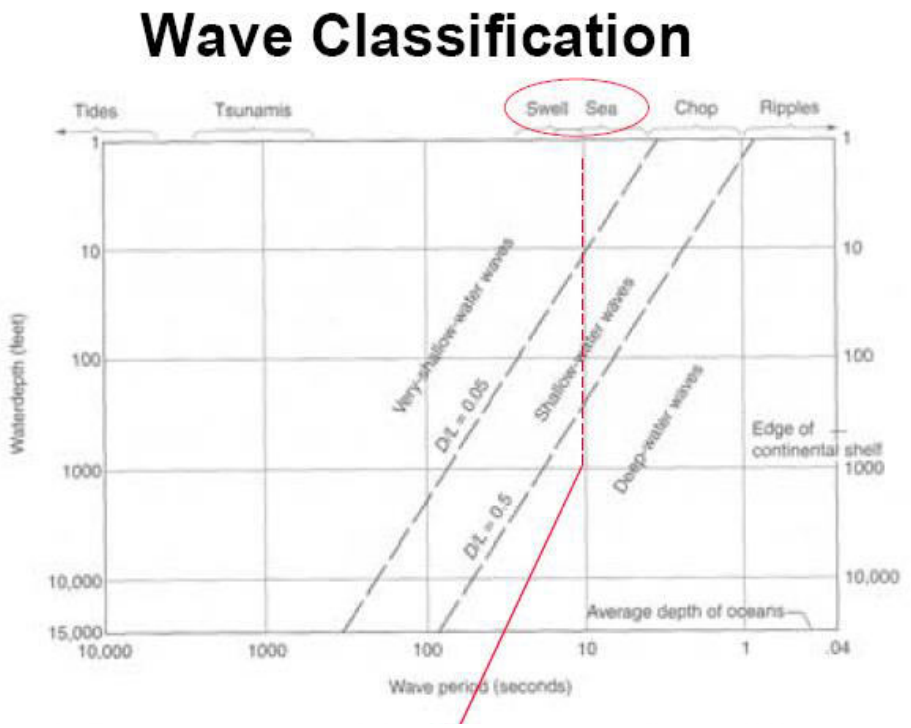

Speed of swell waves = wave length/period = 1000ft/10 seconds = 100ft/sec ~ 30 m/s
Man's walking speed = 4800 ft/1200 seconds = 4 ft/sec ~ 1 m/s. This means swell speed is 30 times more than that of man.

Fig.4.8d. Note how 'swell' tend to have larger time period (T) and length (L), while 'sea' has smaller T and L. The wave speed for a period of T = 10 seconds comes to 30m/s.

Waves of different lengths run at different speeds, so that waves of different sizes combine and recombine in a constantly changing interference pattern. Once waves have escaped from the wind that made them, they can run for several days with very little loss of energy. That is how we are always able to see waves on the coast even if wind speeds are sometimes zero.

The waves always tend to run in groups due to interference. The grouping of high and low waves is called *surf beat*. The velocity with which these groups of waves move called *group velocity*. As waves grow in height they also grow in length in the early part of their history. Even after the height is stopped growing, the length continues to grow as it propagates in the ocean. Thus the steepness is more during early part of the wave formation than the later part. Observations show that the wave steepness varies from 0.1 to 0.008 from the formation of wave to its later part. However, as the wave enters the shallow water, Stokes put a maximum possible wave steepness (H/L) at 1/7 = 0.143.

4.4. **Wave Breaking:**

There are two main sets of conditions in which waves break. The first is when wind blows over the waves in deep water and the second is when waves arrive at the shore over a sloping bottom. The long period swell waves or Stokes waves of finite

amplitude finally run ashore and break up into surf when the steepness exceeds one in seven. In an unbroken wave the orbital velocity of water particles at the crest is less than that of the wave as shown in Fig.4.9. If the velocity of water particles at the crest exceeds the wave velocity it will break away from the wave profile. As the waves enter into shallow water (the ratio of water depth to wave length, d/L, the relative depth, is less than 1/20), the wave length and velocity decreases and period remains same and wave height enormously increases as the wave energy is conserved as shown in Fig.4.10.

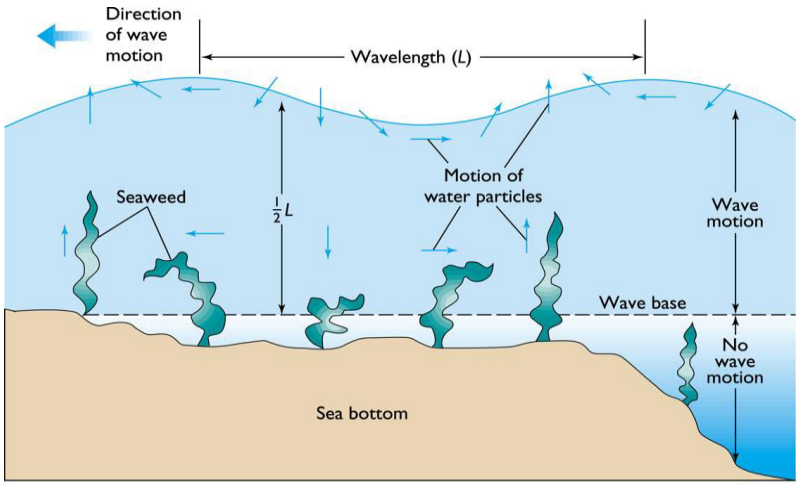

Fig.4.9. Arrows indicate the water particle motion relative to wave motion

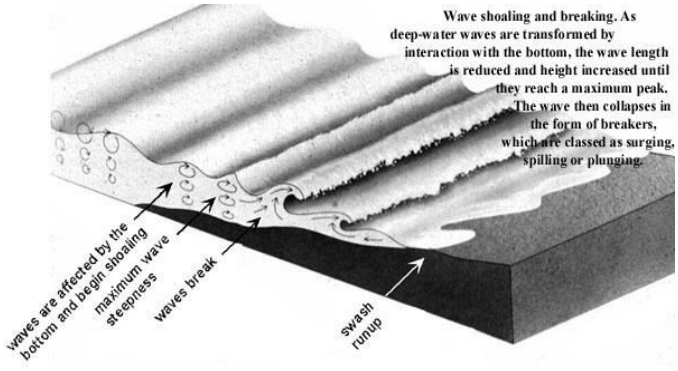

Fig.4.10. wave transformation as it enters from deep to shallow water

When the wave enters shallow water over a shoaling bottom their wave length is reduced and their height is increased with a resulting increase in steepness. When the waves reach a depth of 1 to 1.5 times of their height generally the particle velocity at the crest is equal to the wave velocity and so they break. The exact ratio of wave height to water depth (H/d) at which the wave breaks depends on the deep water steepness of the

waves and the slope of the beach. The types of breakers described are spilling, plunging, surging and collapsing as shown in Fig.4.11 & 4.13.

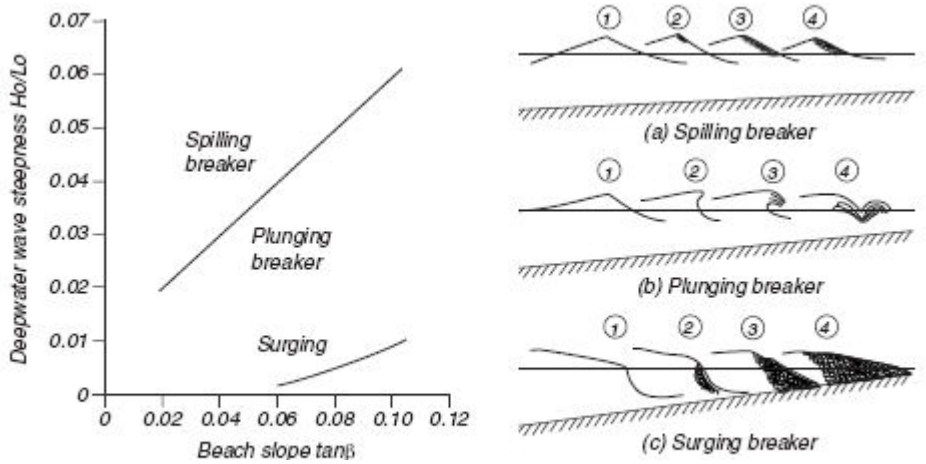

Fig.4.11. Classification of different types of breakers as a function of beach slope to wave steepness

In swell waves on a gently sloping bottom, the typical relation of wave height to water depth at the outer edge of the breakers is 0.78 for short period steep waves its value is 0.6. So storm waves break farther in the sea than the long swell waves of the same height at the coast.

Breakers on evenly sloping beaches may be of two kinds. They are plunging and spilling. The plunging breaker has a well rounded back and a concave front like a hook. A plunging breaker goes to pieces in a few seconds, leaving very little of wave form. A long swell with a steepness of less than 0.005 and an offshore wind are conducive to the formation of plunging breakers. In contrast, spilling breakers are concave on both faces, so that the wave profile resembles a cycloid. The spilling breaker takes more time than the plunging breaker for completely destroying the wave shape. Waves with steepness of more than 0.01, often produce spilling breakers, particularly, when there is an offshore wind. Instead some breakers come out of the mixture of both kinds of plunging and spilling and break more than once. Such breakers are called surging breakers which do not actually break but surge up steep braches. This breaker may break three or four times before the wave form is completely destroyed. The collapsing breaker also is another variety of the mixture of these two main categories.

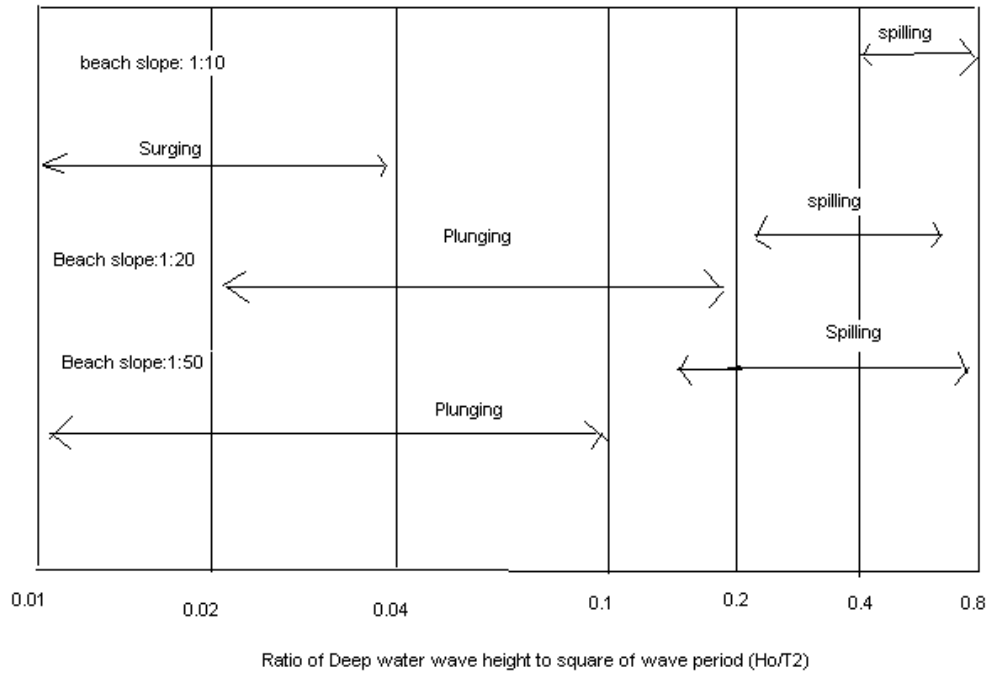

Fig. 4.12. Diagram showing the relation between breaker type, beach slope and steepness of Deep water waves

The boundary between spilling and plunging breakers occurs at a higher ratio between open sea wave steepness and wave length for a steeply sloping beach than for a gently sloping beach. To produce spilling breakers on a steep beach, the deep sea wave steepness must be relatively high, and conversely to produce plunging breakers on a gently sloping beach, the deep sea wave steepness must be relatively low. The diagram in Fig.4.12 shows a relation between plunging, surging and spilling breakers. It may be noted here that the gentler sloping beaches do not have surging breakers. The surging and collapsing breakers are only a mixture of the original plunging and spilling breakers. The plunging breaker collapses and the spilling breaker surges depending on the wind and slope of the beach.

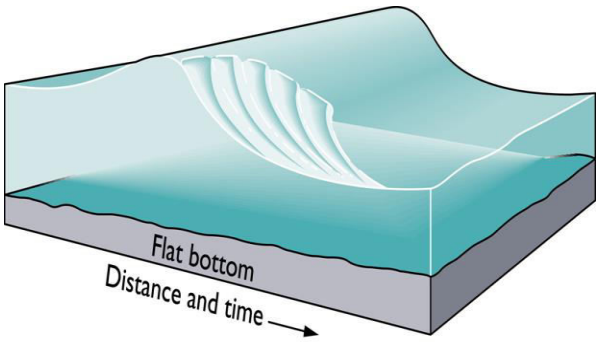

(a) SPILLING BREAKER

Surging Breaker

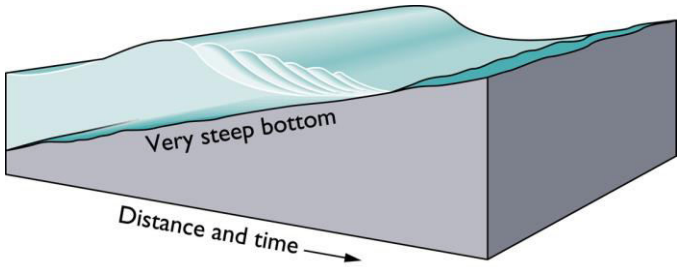

Plunging Breaker

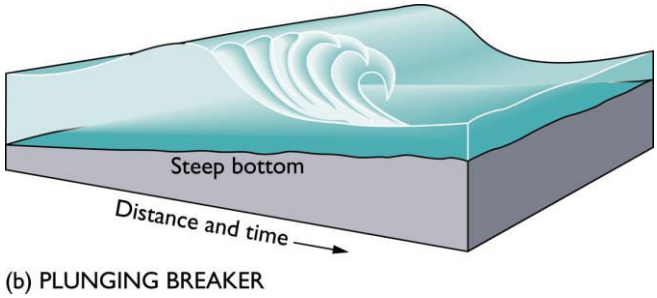

Fig.4.13. Different types of breakers

4.5. Small Amplitude wave theory:

4.5.1. **Merits and demerits of small amplitude wave theory:**

The first restriction imposed for small amplitude wave theory is that the profile is assumed as sinusoidal. Infact no ocean wave follows this restriction. The second restriction is that this sinusoid has small amplitude. When the word small is used naturally doubt arises this word small is relative to what? This is not specified in small amplitude wave theory.

Explicitly we mean here that the wave height H is small compared with the wave length L. that is H/L < 1. If this is true $|n| < 1$ for all x, since H/2 = a, is the largest value ever attained by $|n|$.

Small amplitude wave theory might be best described in practical terms as a first order approximation to the complete theoretical description of wave behavior. Since it is an approximation of the true behavior, however, it is necessary to have an estimate of the

magnitude of error involved in its use. But in many practical situations this error is negligible, but in other cases like wave breaking small amplitude wave theory does not even predict the existence of the phenomenon.

4.6. **Derivation involved in small amplitude wave theory:**

The small amplitude theory for two dimensional free, periodic gravity wave is developed by linearizing the equation that defines the free surface boundary condition. Along with this using the bottom boundary condition, a periodic velocity potential is sought that satisfies the requirements for irrotational flow. This velocity potential is then used to derive the equations for various wave characteristics like wave celerity, particle and group velocity, pressure, energy etc.

4.6.1. **Assumptions involved in the derivation of small amplitude waves:**

i) The water is homogeneous, incompressible and surface tension forces are negligible. Thus there are no internal gravity or pressure waves affecting the flow, and the surface waves being considered are larger than that size where capillary effects are important (i.e. wave lengths greater than 3 cm.)

ii) Flow is considered irrotational and so velocity potential exists which satisfy the Laplace equation. Thus there is no shear stress at the air-sea interface or at the sea bottom and so the fluid slips freely at the bottom.

iii) The bottom is considered impermeable and horizontal and so doesn't move. So the bottom can not add or remove energy to the propagating wave. A separate bottom boundary conditions are defined.

iv) The pressure along the air-sea interface is considered constant. Thus no wind pressures exist and hydrostatic pressure differences due to surface elevation differences are negligible.

v) A surface boundary condition is imposed to linearize the squares of the velocities involved in the Bernoulli's equation.

vi) The wave amplitude is small compared to wave length and water depth. This assumption is most important since the particle velocities are related to wave amplitude and the wave velocity is related to the fluid depth and wave length, this implies that particle velocities are small compared to the wave velocity.

4.7. **Derivation of small amplitude wave equation:**

4.7.1. **Euler's Equation of motion**:

In order to understand the Euler's equation of motion two types of forces are to be considered. They are surface and body forces. The force acting on the surface of an element is surface force and the force depending on the bulk or mass of the fluid is body force. The surface force can be resolved into two components one parallel to the surface and the other perpendicular to it. The parallel component gives the shear force and the perpendicular component gives pressure force. Under frictionless conditions, the shear force can be neglected and so the only surface force remains is pressure force. Gravity is considered as the principal body force in the present study.

The equation of motion can be written as:

$$X - \frac{1}{\rho}\frac{\partial p}{\partial x} = \frac{du}{dt}$$

$$Y - \frac{1}{\rho}\frac{\partial p}{\partial y} = \frac{dv}{dt} \quad \text{…….(4.1)}$$

$$Z - \frac{1}{\rho}\frac{\partial p}{\partial z} = \frac{du}{dt}$$

Where X, Y and Z are the body forces per unit mass in the respective directions. Please note here while X and Y are Coriolis accelerations is acceleration due to gravity. These equations were first published by Euler in 1775 and so are known as Euler's equation of motion.

4.7.2. **Existence of velocity potential:**

The velocity potential or potential function φ is a function of space and time, the derivative of which in a given coordinate direction is the force in that direction.

The velocity potential by definition is related to the tree components of velocity as

$$u = -\frac{\partial \varphi}{\partial x}, v = -\frac{\partial \varphi}{\partial y}, w = -\frac{\partial \varphi}{\partial z} \quad \text{……..(4.2)}$$

If a velocity potential exists the flow must be irrotational, that is the vorticity is zero ($\zeta = 0$).This can be shown by obtaining derivatives of the three velocities as shown below:

$$ie. \frac{\partial u}{\partial z} = \frac{\partial}{\partial z}\left(-\frac{\partial \varphi}{\partial x}\right) = -\frac{\partial^2 \varphi}{\partial x \partial z} \quad \text{Similarly,} \quad \frac{\partial w}{\partial x} = \frac{\partial}{\partial x}\left(-\frac{\partial \varphi}{\partial z}\right) = -\frac{\partial^2 \varphi}{\partial x \partial z}$$

This means $\frac{\partial u}{\partial z} = \frac{\partial w}{\partial x}$ ……(4.3)

this implies $\frac{\partial w}{\partial x} - \frac{\partial u}{\partial z} = 0 \Rightarrow \zeta = 0$

4.7.3. **Laplace Equation:**

For treatment of wave equation only two dimensional motion in the x-z plane will be considered. For compressible two dimensional motion in the x,z plane the equation of continuity is:

$$\frac{\partial u}{\partial x} + \frac{\partial w}{\partial z} = 0 \quad \text{……(4.4)}$$

If in addition the flow is irrotational, the velocity potential exists so by substituting equation (4.2) in equation (4.4), we can write:

$$\frac{\partial^2\varphi}{\partial x^2}+\frac{\partial^2\varphi}{\partial z^2}=0 \quad \ldots\ldots(4.5)$$

This equation is known as the Laplace equation of continuity. Any solution for the water wave motion must obey this continuity relationship.

4.7.4**. Bernoulli's equation:**

Considering the Euler's equation of motion (4.1) in x-z coordinate system;

$$\begin{aligned} x-\frac{1}{\rho}\frac{\partial p}{\partial x}&=\frac{du}{dt}=\frac{\partial u}{\partial t}+u\frac{\partial u}{\partial x}+w\frac{\partial u}{\partial z}\\ z-\frac{1}{\rho}\frac{\partial p}{\partial z}&=\frac{dw}{dt}=\frac{\partial w}{\partial t}+u\frac{\partial w}{\partial x}+w\frac{\partial w}{\partial z}\end{aligned} \quad \ldots\ldots.(4.6)$$

The body force per unit mass (z) is restricted to acceleration due to gravity only here. So the other body force x = 0.

$\therefore x=0$ and z = - g ……(4.7)

We can write 'g' in a derivable form as $z=-g=-\frac{\partial}{\partial z}(gz)$ …..(4.8)

We can also write using the concept of φ: $-\frac{\partial u}{\partial t}=\frac{\partial^2\varphi}{\partial x\partial t}$ and $-\frac{\partial w}{\partial t}=\frac{\partial^2\varphi}{\partial z\partial t}$ ….(4.9)

Substituting equations (4.7), (4.8),(4.3) and (4.9) in (4.6) we get

$$\begin{aligned} -\frac{1}{\rho}\frac{\partial p}{\partial x}&=-\frac{\partial^2\varphi}{\partial x\partial t}+u\frac{\partial u}{\partial x}+w\frac{\partial w}{\partial x}\\ -\frac{\partial}{\partial z}(gz)-\frac{1}{\rho}\frac{\partial p}{\partial z}&=-\frac{\partial^2\varphi}{\partial z\partial t}+u\frac{\partial w}{\partial x}+w\frac{\partial w}{\partial z}\end{aligned} \quad \ldots\ldots(4.10)$$

Re writing again using $u\frac{\partial u}{\partial x}=\frac{1}{2}\frac{\partial}{\partial x}(u^2)$ and $w\frac{\partial w}{\partial z}=\frac{1}{2}\frac{\partial}{\partial x}(w^2)$ &

$\frac{1}{\rho}\frac{\partial p}{\partial x}=\frac{\partial}{\partial x}\left(\frac{p}{\rho}\right)$ and $\frac{1}{\rho}\frac{\partial p}{\partial z}=\frac{\partial}{\partial z}\left(\frac{p}{\rho}\right)$, Equations (4.10) turns out to be:

$$\begin{aligned} \frac{\partial}{\partial x}\left[-\frac{\partial\varphi}{\partial t}+\frac{1}{2}(u^2+w^2)+\frac{p}{\rho}\right]&=0\\ \frac{\partial}{\partial z}\left[-\frac{\partial\varphi}{\partial t}+\frac{1}{2}(u^2+w^2)+\frac{p}{\rho}+gz\right]&=0\end{aligned} \quad \ldots\ldots(4.11)$$

On integrating (4.11) we will get

$$\left[-\frac{\partial\varphi}{\partial t}+\frac{1}{2}\left(u^2+w^2\right)+\frac{p}{\rho}\right]=F(x,t)$$
$$\left[-\frac{\partial\varphi}{\partial t}+\frac{1}{2}\left(u^2+w^2\right)+\frac{p}{\rho}+gz\right]=F(z,t) \quad \text{.....(4.12)}$$

To find the constants F(x,t) and F(z,t) subtracting the equations of (4.12) one from the other then

F(z,t) – F(x,t) = gz or F(x,t) = F(z,t)-gz .....(4.13)

Replacing the constant of 4.13 in (4.12) we get only one equation i.e.,

$$\left[-\frac{\partial\varphi}{\partial t}+\frac{1}{2}\left(u^2+w^2\right)+\frac{p}{\rho}+gz\right]=F(z,t) \quad \text{……(4.14)}$$

Since the fluid motion is affected only by pressure gradients the constant F(z,t) is not a variable constant through out the fluid at any time 't' and so can be taken as zero

$$\left[-\frac{\partial\varphi}{\partial t}+\frac{1}{2}\left(u^2+w^2\right)+\frac{p}{\rho}+gz\right]=0 \quad \text{……(4.15)}$$

This is called generalized Bernoulli's equation

For steady flows which do not change with time at a fixed locality $\frac{\partial\varphi}{\partial t}=0$,So equation (4.14) reduces to : $\left[\frac{1}{2}\left(u^2+w^2\right)+\frac{p}{\rho}+gz\right]=cons\tan t$. This is called the steady state Bernoulli's equation.

4.7.5. **Boundary conditions:**

Kinematic Boundary condition: At any boundary whether it is fixed (sea bottom) or free (the sea surface) the water is free to deform under the influence of any force. So certain physical conditions must be satisfied by the fluid velocities. These conditions on the water particle kinematics are called kinematic boundary condition. The physical interpretation here is at any surface or interface, there cannot be any flow across the surface, because it is a barrier.

Bottom Boundary condition (BBC): The lower boundary is described as z = - h for a two dimensional wave where the origin is located at the still water level and 'h' represents the depth. If the bottom is impermeable, the condition holds good is as below as the bottom does not move with time.

From equation (4.2) we know $w=-\frac{\partial\varphi}{\partial z}$. This must be equal to zero on z = - h as vertical velocity ceases at the sea bottom.

$$\therefore w = -\frac{\partial \phi}{\partial z} = 0 \quad \text{.....(4.16)}$$

Dynamic free surface Boundary condition (DFSBC): This boundary condition can be easily fixed on a rigid surface but it cannot be fixed on a free surface like air-water interface because they cannot support variations in pressure. So a dynamic boundary condition is thus required on any free surface to prescribe the pressure distribution.

The condition for a dynamic free surface boundary is that the pressure on the free surface be uniform along the wave form which means it is constant and is equal to zero. So Bernoulli's equation (eqn.4.15) can be applied.

$$\left[-\frac{\partial \varphi}{\partial t} + \frac{1}{2}\left(u^2 + w^2\right) + \frac{p}{\rho} + gz \right] = 0$$

As 'η' is the instantaneous elevation of free surface, here z = η because on the surface η is the surface of oscillation from the mean sea surface and the sea surface pressure starts from zero (p = 0). Small amplitude theory further based upon the assumption that all motions are so small that the above equation may be linearized. In particular this assumes that the squares of the velocity components u^2 and w^2 are negligible in compared to the remaining terms. Then the equation (4.15) reduces to give the boundary condition on the free surface as:

$$-\frac{\partial \phi}{\partial t} + g(+\eta) = 0$$

Or $\eta = \frac{1}{g}\frac{\partial \phi}{\partial t}$ on z = 0 .....(4.17)

This means when there is no elevation also this boundary condition is valid but not $\eta \neq 0$.

4.7.6. Solution of the wave problem:

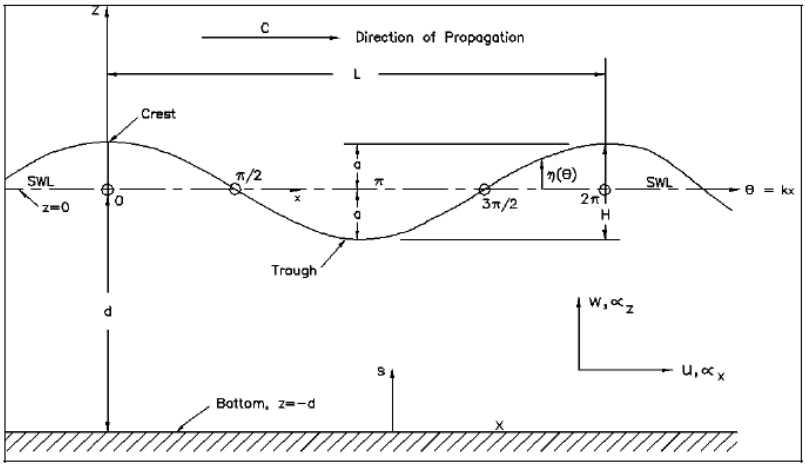

Fig.4.14. A simple, progressive wave as it passes a fixed point

A progressive wave may be represented by the variables x (spatial) and t (temporal) or by their combination (phase), defined as $\theta = kx - \sigma t$, where k and σ are wave number and frequency respectively. The values of θ vary between 0 and 2π. A simple, periodic wave of permanent form propagating over a horizontal bottom may be completely characterized by the wave height H wavelength L and water depth d.

As shown in Figure 4.14, the highest point of the wave is the *crest* and the lowest point is the *trough*. For linear or small-amplitude waves, the height of the crest above the still-water level (SWL) and the distance of the trough below the SWL are each equal to the wave amplitude a. Therefore $a = H/2$, where H = *the wave height*. The time interval between the passage of two successive wave crests or troughs at a given point is the *wave period T*. The *wavelength L* is the horizontal distance between two identical points on two successive wave crests or two successive wave troughs.

Other wave parameters include $\sigma = 2\pi/T$ the *angular* or *radian frequency*, the *wave number* $k = 2\pi/L$, the *phase velocity* or *wave celerity* $C = L/T = \omega/k$, the *wave steepness* $\varepsilon = H/L$, the *relative depth d/L*, and the *relative wave height H/d*.

The governing second order differential equation for the fluid motion under a periodic two dimensional water wave is the Laplace equation (4.5), which holds throughout the fluid domain consisting of one wave.

$$\frac{\partial^2 \varphi}{\partial x^2} + \frac{\partial^2 \varphi}{\partial z^2} = 0$$

To solve this equation use the method of separation of variables. As the velocity potential (potential function) is a function of x,z and t, let suppose its solution is φ such that it is a function of x, z and t. Then we can write the velocity potential (φ) as:

Φ (x,z,t) = X(x).Z(z).T(t) ……..(4.18)

Double differentiating (4.18) with respect to x and z and on substitution in it we can write

$$\frac{\partial^2 \varphi}{\partial x^2} + \frac{\partial^2 \varphi}{\partial z^2} = X''ZT + XZ''T = 0$$

Dividing throughout by XZT and rewriting, we get

$$X''ZT = -XZ''T$$

$$\frac{X''}{X} = -\frac{Z''}{Z} = -K^2$$ where K is some constant. Then we can write two differential equations as:

X" + K^2X = 0

Z" - K^2 Z = 0

Then the general solution of the first one is X = A cos kx + B sin kx and the second one is Z = $Ce^{kz} + De^{-kz}$. On substituting in(4.18) and writing

Φ(x,z,t) = (A cos kx + B sin kx).($Ce^{kz} + De^{-kz}$).T(t)

Since the desired solutions are simple harmonic in time, it is reasonable to express T(t) as cos(σ t) or sin(σ t) where (σ = 2π/T)

$\Phi(x,z,t) = (A \cos kx + B \sin kx).(Ce^{kz} + De^{-kz}). \text{Cos } (\sigma t)$

$= (A \cos kx + B \sin kx).(Ce^{kz} + De^{-kz}). \text{Sin } (\sigma t)$

Expanding the terms and considering each one as solution, we can write as

$\Phi_1 = (Ce^{kz} + De^{-kz}) (A \cos kx. \text{Cos } \sigma t)$ .....(4.19)

$\Phi_2 = (Ce^{kz} + De^{-kz}) (B \text{ Sin } kx. \text{ Sin } \sigma t)$

$\Phi_3 = (Ce^{kz} + De^{-kz}) (B \text{ Sin } kx. \text{ Cos } \sigma t)$

$\Phi_4 = (Ce^{kz} + De^{-kz}) (A \cos kx. \text{ Sin } \sigma t)$

These four separate elementary combinations of the terms which are periodic in x and t and themselves are solutions to Laplace's equation. To find the constantsA,B,C.D we have to use the boundary conditions. Let us consider first φ_1 (eqn 4.19) and try to find the constants so that in a similar fashion rest other potential functions φ_2, φ_3 and φ_4 can be determined.
For applying the bottom boundary condition (equation 4.16) to equation (4.19), differentiate equation 4.19 with respect to z then we get

$\frac{\partial \varphi_1}{\partial z} = k (Ce^{-kz} + De^{-kz}) (A \cos kx. \text{Cos } \sigma t)$

According to equation 4.16 on **z = -d**, $\frac{\partial \varphi_1}{\partial z} = 0$

$\therefore \frac{\partial \varphi_1}{\partial z} = k (Ce^{-kd} - De^{kd}) (A_1 \cos kx. \text{Cos } \sigma t) = 0$

This means that as A_1 and k can not be equal to zero, $(Ce^{-kd} - De^{kd})$ must be equal to zero
$(Ce^{-kd} - De^{kd}) = o$ or $C = D e^{2kd}$

Substituting this value of C in equation 4.19 after much manipulation we can write

$\Phi_1 = (A \cos kx. \text{Cos } \sigma t) (D e^{2kd} e^{kz} + De^{-kz}) =$

$= (A \cos kx. \text{Cos } \sigma t)\left[2\frac{(De^{kd}.e^{k(d+z)} + De^{kd}.e^{-k(d+z)}}{2} \right]$

$= 2 A D e^{kd} \text{Cosh } k(d+z). \text{Cos } kx. \text{Cos } \sigma t$ .....(4.20)

To find the constant A in equation 4.20, apply the surface boundary condition (equation 4.17). To do that differentiate equation 4.20 with respect to 't' then

$\frac{\partial \varphi_1}{\partial t}$ = - 2 σ A D e^{kd} Cosh k(d +z). Cos kx. Sin σ t

According to 4.17 on Z = 0, $\frac{1}{g}\frac{\partial \varphi_1}{\partial t} = \eta$

$\therefore \frac{1}{g}\frac{\partial \varphi_1}{\partial t} = \eta = -\frac{2\sigma A}{g}$ D e^{kd} Cosh k(d). Cos kx. Sin σ t ……..(4.21)

we know from the equation of η = a sin(σ t – k x) that η = a , when (Cos kx. Sin σ t) = 1 using this condition we can write 4.21 as

$a = -\frac{2\sigma A}{g}$ D e^{kd} Cosh k(d). Or 2 A D e^{kd} = $-\frac{ag}{\sigma \cosh kd}$ substituting this value in equation (4.20)

$\Phi_1 = -\frac{ag}{\sigma \cosh kd}$ Cosh k(d +z). Cos kx. Cos σ t

Here the constant $k = \frac{2\pi}{L}$ is wave number and $\sigma = \frac{2\pi}{T}$ is wave radian frequency.

Similarly if all the other φ's in equation 4.19 are evaluated we get

$\Phi_2 = +\frac{ag}{\sigma \cosh kd}$ Cosh k(d +z). Sin kx. Sin σ t

$\Phi_3 = -\frac{ag}{\sigma \cosh kd}$ Cosh k(h +z). Sin kx. Cos σ t

$\Phi_4 = +\frac{ag}{\sigma \cosh kd}$ Cosh k(h +z). Cos kx. Sin σ t

As mentioned earlier these elementary solutions may be combined linearly and due to the linearity of Laplace equation the combination in various ways or with one another will also be a solution to the problem. Suppose the subtraction of φ_1 from φ_2 gives rise to:

$\Phi = (\varphi_2 - \varphi_1) = +\frac{ag}{\sigma \cosh kd}$ Cosh k(d +z).Cos (k x – σ t) …….(4.22)

If ($\varphi_4 - \varphi_3$) is used we can get

$\Phi = (\varphi_4 - \varphi_3) = +\frac{ag}{\sigma \cosh kd}$ Cosh k(d +z).Sin (k x – σ t)

Either of the equations can be used for potential function representing the wave solution. The wave parameters of wave celerity, Length and period can be extracted from this potential function.

4.7.7. Wave celerity, length and period:

The rate of rise of water surface can be written as: $w = \frac{d\eta}{dt} = \frac{\partial \eta}{\partial t} + u\frac{\partial \eta}{\partial x} + w\frac{\partial \eta}{\partial z}$

Since we are dealing with waves of very small amplitude, the surface slope elevation $\frac{\partial \eta}{\partial x}$ is negligibly small and so can be neglected. On Z = 0, $\frac{\partial \eta}{\partial z}$ does not exist and so

$$w = \frac{\partial \eta}{\partial t} \quad \text{on z} = 0$$

Relating this with the dynamic free surface boundary condition (equation 4.17) and the velocity potential (equation 4.2) we can write:

$$\eta = \frac{1}{g}\frac{\partial \phi}{\partial t} \qquad \Rightarrow \frac{\partial \eta}{\partial t} = \frac{1}{g}\frac{\partial^2 \phi}{\partial t^2} = w \quad \text{on z} = 0 \quad \text{We know} \quad \text{w} = -\frac{\partial \varphi}{\partial z} \quad \text{on z} = 0$$

$$\therefore -\frac{\partial \varphi}{\partial z} = \frac{1}{g}\frac{\partial^2 \phi}{\partial t^2} \quad \text{on z} = 0 \quad \text{…….(4.23)}$$

To Apply equation (4.23) on to the equation (4.22) we have to partially differentiate 4.22 with respect to z and then partially double differentiate 4.22 with respect to ‘t’ and then equate and simplify.

Double differentiation of 4.22 with respect to ‘t’:

$$\frac{1}{g}\frac{\partial^2 \varphi}{\partial t^2} = -\, a\sigma \frac{Coshk(d+z)}{Coshkd} Cos(kx - \sigma t) \quad \text{…….(4.24)}$$

Differentiating 4.22 with respect to ‘z’ gives rise to:

$$-\frac{\partial \varphi}{\partial z} = -\, kag \frac{Sinhk(d+z)}{\sigma Coshkd} Cos(kx - \sigma t) \quad \text{……(4.25)}$$

Equating (4.24) and (4.25) using the relation 4.23, on simplification we get:

$\sigma^2 = gk \tanh k(d+z)$ on z =0 this tends to

$\sigma^2 = gk \tanh(kd) \Rightarrow gk \tanh(r)$ ……..(4.26)

where kh = r is the asymptote of the hyperbolic wave profile.

We know the equation of free moving surface of wave profile as:

$$\eta = aSin(kx - \sigma t) = \frac{H}{2} Sin(\frac{2\pi}{L}x - \frac{2\pi}{T}t) \quad \text{…….(4.26a)}$$

where, a = amplitude which is half of the wave height, H. Let suppose Kx – σ t is constant, then Kdx – σ dt = 0 or Kdx = σ dt $\Rightarrow \frac{dx}{dt} = \frac{\sigma}{k} = \frac{2\pi/T}{2\pi/L} = \frac{L}{T} = c$,

$\therefore c = \frac{\sigma}{k} \Rightarrow \sigma^2 = k^2 c^2$, substituting the value of σ^2 from equation (4.26) we get

$$c^2 = \frac{g}{k}\tanh(kd)$$

$$\Rightarrow \frac{L^2}{T^2} = \frac{gL}{2\pi}\tanh(kd) \Rightarrow \frac{L}{T} = \frac{gT}{2\pi}\tanh(kd) = c \quad \text{.....4.27}$$

Similarly, $L = \frac{gT^2}{2\pi}\tanh(kd)$

4.7.8. Classification of waves according to relative depth:

As the wave approaches from deep water to shallow, the wave profile changes as given in Fig.4.15

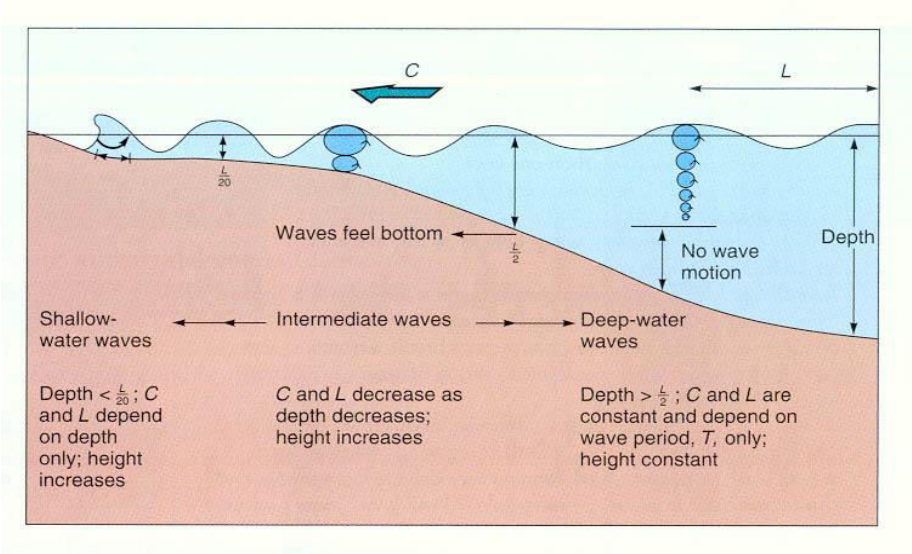

Fig. 4.15 Classification of waves as they approach the coast from deep water

Ocean waves are generally classified according to a parameter called 'relative depth'. It is the ratio of the water depth (d) to the wave length (L). This ratio d/L is called the 'relative depth'.

The table 4.1 and Fig.4.13a gives Classifications made according to the magnitude of *d/L* and the resulting limiting values taken by the function *tanh (2πd/L)*. Note that as the argument of the hyperbolic tangent r = kd = 2πd/L gets large, the tanh (r) approaches 1, and for small values of kd, tanh (kd) tends to kd.

Table 4.1. Wave classification according to relative depth

Range of d/L	Range of r = Kd=2πd/L	Types of waves
0 to 1/20	0 to π/10	Shallow water waves (Long waves)
1/20 to ½	π/10 to π	Intermediate waves
½ to ∞	π to ∞	Deep water waves (short waves0

The simplifications which occur in the various wave equations arise by replacing the hyperbolic functions by their asymptotes for the particular range of relative depth are listed below in the table 4.2.

Table 4.2. Approximations for hyperbolic functions

Function	Asymptotes	
	Shallow water	Deep water
Sinh kd	Kd	$\frac{e^{kd}}{2}$
Cosh kd	1	$\frac{e^{kd}}{2}$
Tanh kd	Kd	1

The deep and shallow water expressions can be obtained by using the simplifications resulted due to the asymptotes as given in table 4.2 and Fig.4.16 & 4.17.

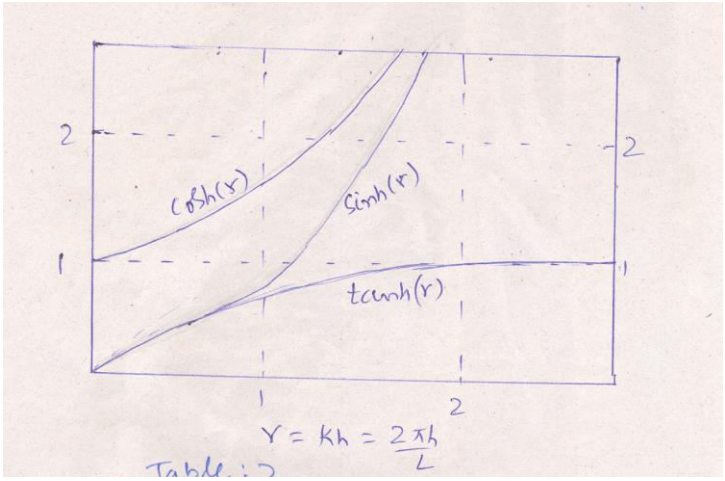

Fig.4.16a.The variation of asymptotes of hyperbolic sin, cos and tan as per table 4.2

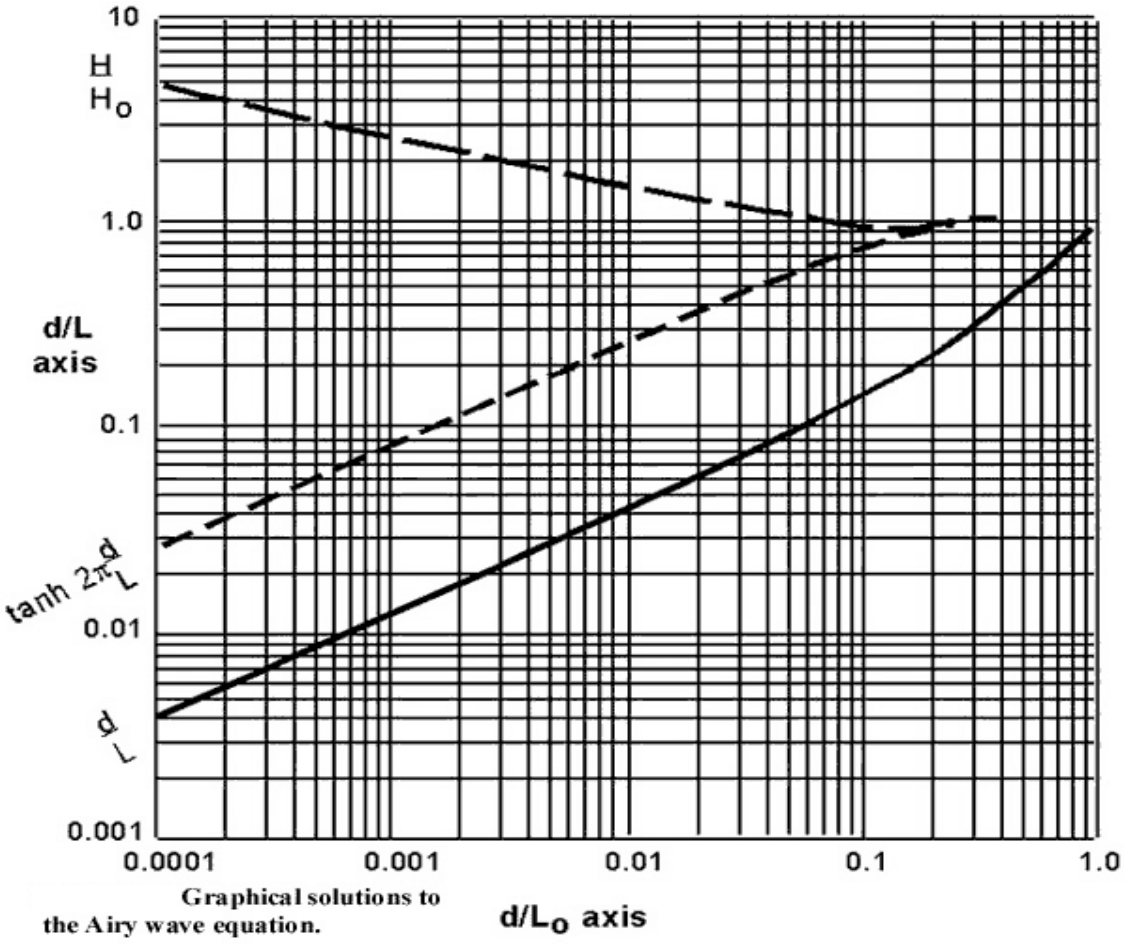

Fig.4.16b. Asymptotic variation for shallow and deep water relative depths

$$C^2 = gT/2\pi,\ C^2 = gL/2\pi(\text{ deep})$$
$$C^2 = gd\ (\text{Shallow})$$

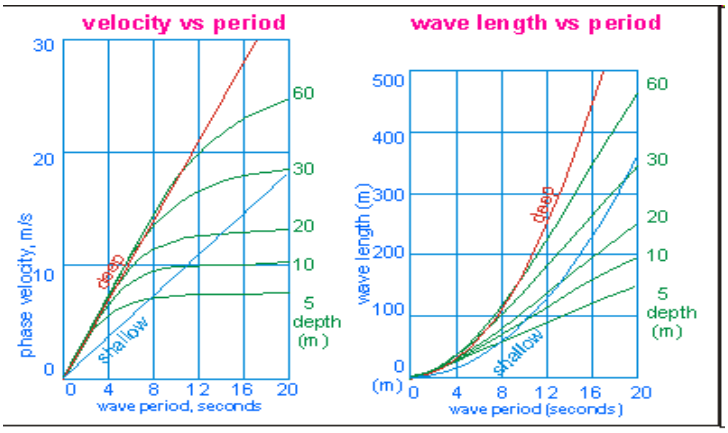

Fig.4.17 wave velocity versus length

Shallow water wave equation:

The shallow water condition from table 4.27 is Tanh kd → kd, so the equation 4.27 turns out to

$$C^2 = gd \quad \text{……..(4.28)}$$

This equation implies that wave velocity is independent of wave length and depends only on the water depth.

Deep water wave equation:

The deep water condition from table 4.2 is tanh kd → 1 and so equation 4.27 turns out to be

$C_o^2 = g/k_o$ as we know $k_o = 2\pi/L_o$; $C_0 = \frac{gT}{2\pi}$, $L_0 = \frac{gT^2}{2\pi}$ ……..(4.29)

The suffix zero indicates the deep water conditions. The celerity and wave length for deep water conditions are therefore independent of water depth. One should note here that 'T' doesn't vary with the local depth of water.

If $g = 9.8$ m/s^2 and $\pi = 3.14$ then $\frac{g}{2\pi} = 1.56$

then $C_0 = 1.56T$ and $L_0 = 1.56\ T^2$ ……..(4.30)

Question:1.

a) what is speed of wave in deep water if its period is 20 seconds (Ans = 31.2m/s)
b) What is the speed of wave in deep water if its wave length is 312 m (Ans = 22.1 m/s)
c) At what speed will each of the waves referred in 'a' and 'b' travel in water of 12 meters deep.

Ans for 'c':

In the case of (a): T = 20 seconds, so $L = 1.56 \times 20^2 = 624$ m

When d = 12 m, d/L = 12/624 = 1/52, according to table 4.1, this 1/52 comes under shallow water category ie.between 0 to 1/20. so shallow water wave velocity equation is to be used. Then the wave velocity according to equation 4.2 is $C = \sqrt{gd} = \sqrt{9.8 \times 12} =$ 10.8 m/s

Similarly in case of (b), L = 312 m; so d/L = 12/312 = 1/26 which is also less than 1/20. so this also comes under shallow water category. So $C = \sqrt{gd} = \sqrt{9.8 \times 12} = 10.8$ m/s

This example implies that in shallow water where d/L < 1/20 all waves travel at the same speed when they reach to that particular depth.

For example the speed of tsunami in deep water at a depth of 5 km in the deep ocean is $C = \sqrt{gd} = \sqrt{9.8 \times 5000} = 70$ m/s = 252 km/hr.

Question 2:

A generating area consists of 'seas' of wavelength 6m and 'swells' of wave period of 22 seconds i) calculate the speed of 'seas' and 'swells' ii) when these seas and swells propagate against a current of 5.0 m/s in a bay whether these can overcome and pass through it or not?

Ans:
Seas:

Seas are short waves or deep water waves. So the equation is $C^2 = \frac{gL}{2\pi} = 1.56 \times 6$ or C= 3.06 m/s. But the deep water velocity in groups (group velocity) is $C_g = C/2 = 3.06/2 =$ 1.5 m/s

Swells:
Swells are also generated in the generating area. So deep water wave equation used is $C = \frac{gT}{2\pi} = 1.56 \times 22 = 34.32$ m/s. The deep water group velocity is $C_g = C/2 = 34.32/2 =$ 17.16 m/s
Propagation in the Bay against the current 5.0 m/s:

The group speed of seas is 1.5 m/s whereas the current speed is 5 m/s. so seas can not overcome the current. Whereas the swells can overcome because their group speed is 17.16 m/s that is much greater than the current speed.

Question 3:

The ship Sagar kanya is a 146 m long Research Vessel of NIO. In one of her cruises in Indian Ocean, it was moving at a reduced speed of 5.14 m/s and that the waves took 6.3 seconds to pass the ship from stern to bow. Then calculate

i) the apparent speed of over taking waves
ii) the actual wave speed, wave length and steepness if the wave height reported by the ship was 34 m.

Ans:

i) the apparent speed of overtaking waves = Ship length/period of passing waves = 146/6.3 = 23.17 m/s
ii) Actual wave speed = Apparent speed of waves + The ships speed = 23.17 + 5.14 = 28.31 m/s
iii) Actual wave length = L = $C^2/1.56 = 28.31^2/1.56 = 513.75$ m (since in deep water $C^2 = \frac{gL}{2\pi} = 1.56L$)

iv) Actual wave period = T = C/1.56 = 28.31/1.56 = 18.14 seconds (since $C = \frac{gT}{2\pi} = 1.56T$)

v) The steep ness = H/L = 34/513.75 = 0.066 which is a very steep wave.

4.8. **Orbital motion of wave particles in a progressive wave:**

The velocity potential for a small amplitude progressive wave traveling in the positive x direction in an inviscid fluid is (Equation 4.22)

$$\Phi = (\varphi_2 - \varphi_1) = + \frac{ag}{\sigma \cosh kd} \text{ Cosh k(d +z).Cos (k x} - \sigma \text{ t)}$$

By definition of velocity potential, the horizontal and vertical components of velocity potential are given in equations 4.2 as $u = -\frac{\partial \varphi}{\partial x}, w = -\frac{\partial \varphi}{\partial z}$

So differentiating partially equation 22 with respect to x and z we get u and w as

$$u = + \frac{agk}{\sigma \cosh kd} \text{ Cosh k(d +z).sin (k x} - \sigma \text{ t)} \quad \text{.....(4.31)}$$

$$= \frac{\pi H}{T} \frac{Coshk(d+z)}{Coshkd} Sin(kx - \sigma t) \; (\because L = \frac{gT^2}{2\pi}, K = \frac{2\pi}{L}, \sigma = \frac{2\pi}{T}, a = \frac{H}{2} \text{ and so } \frac{agk}{\sigma} = \frac{\pi H}{T})$$

$$w = - \frac{agk}{\sigma} \frac{Sinhk(d+z)}{Coshkd} Cos(kx - \sigma t) = - \frac{\pi H}{T} \frac{Sinhk(d+z)}{Coshkd} Cos(kx - \sigma t) \text{ .....(4.32)}$$

These equations (4.31 & 4.32) represent the velocity components within the wave at any depth z. At a given depth the velocities are seen to be harmonic in both x and t. At a given phase angle ($\theta = kx - \sigma t$), the hyperbolic functions of z (i.e. cosh and sinh) cause an exponential decay of the velocity components with distance down from the free surface. This is shown in the Fig.4.18 for the phase angles at which the components are the largest. As the depth z = -L/2 is reached, the velocities become negligibly small and below this depth there is essentially no motion.

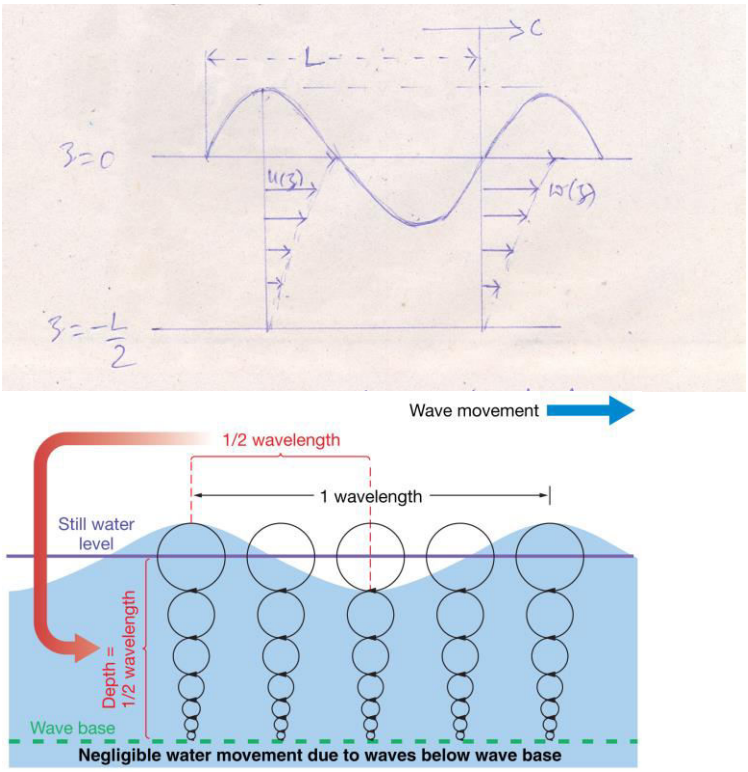

Fig.4.18 hyperbolic decrease of particle velocities up to wave base where the depth, z = -L/2

4.8.1. The particle displacements and paths of orbits:

The horizontal and vertical particle displacements from the mean positions are denoted as ζ and Є respectively.

The velocity field during the period "T' can be obtained by integrating the equations (4.31 and 4.32).

$$\zeta = \int u dt = \frac{agk}{\sigma^2}\frac{Coshk(d+z)}{Coshkd}.\text{Cos (k x-}\sigma\text{ t)}$$

$$\varepsilon = \int w dt = -\frac{agk}{\sigma^2}\frac{Sinhk(d+z)}{Coshkd}.\text{Sin (k x-}\sigma\text{ t)}$$

We know from equation (4.26), σ^2 = gk tanh kd, on substituting we get

$$\therefore \zeta = a\frac{Coshk(d+z)}{Sinhkd}\text{Cos (k x-}\sigma\text{ t)}$$

$$\varepsilon = a\frac{Sinhk(d+z)}{Sinhkd}\text{Sin (k x-}\sigma\text{ t)}$$

Put $A = a\frac{Coshk(d+z)}{Sinhkd}$ and $B = a\frac{Sinhk(d+z)}{Sinhkd}$ …….(4.33)

then we can write: $\frac{\zeta^2}{A^2}+\frac{\varepsilon^2}{B^2}=1$

This is the equation of an ellipse with a major semi-axis of 'A' and a minor semi-axis of 'B'. Hence the particle paths, in general, are elliptical in shape as shown in Fig.4.19. The specific form of the particle paths for shallow and deep water conditions can be determined by examining their axes A and B.

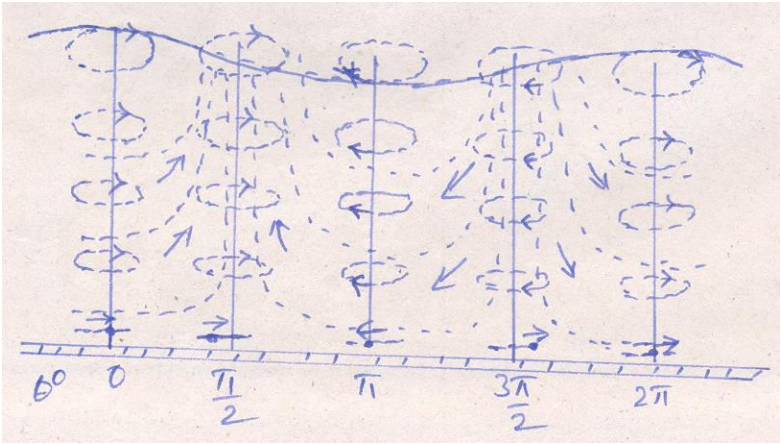

Fig.4.19. Orbital motion of particles in a progressive wave

4.8.2. Deep water case:

$A = a\frac{Coshk(d+z)}{Sinhkd}$,

For deep water from table 4.2 Cosh k(d+z) $\rightarrow \frac{e^{k(d+z)}}{2}$ and Sinh (kd) $\rightarrow \frac{e^{kd}}{2}$

On substitution, $A = ae^{kd}$

Similarly, $B = a\frac{Sinhk(d+z)}{Sinhkd}$

for deep water Sinh k(d+z) $\rightarrow \frac{e^{k(d+z)}}{2}$ and Sinh (kd) $\rightarrow \frac{e^{kd}}{2}$

On substitution, $B = ae^{kd}$

This means $A = B = ae^{kd}$. The major and minor semi axes are equal in deep water implies the orbital paths are no more elliptical but circular in such a way that the orbits decrease exponentially as shown in Fig.4.20a

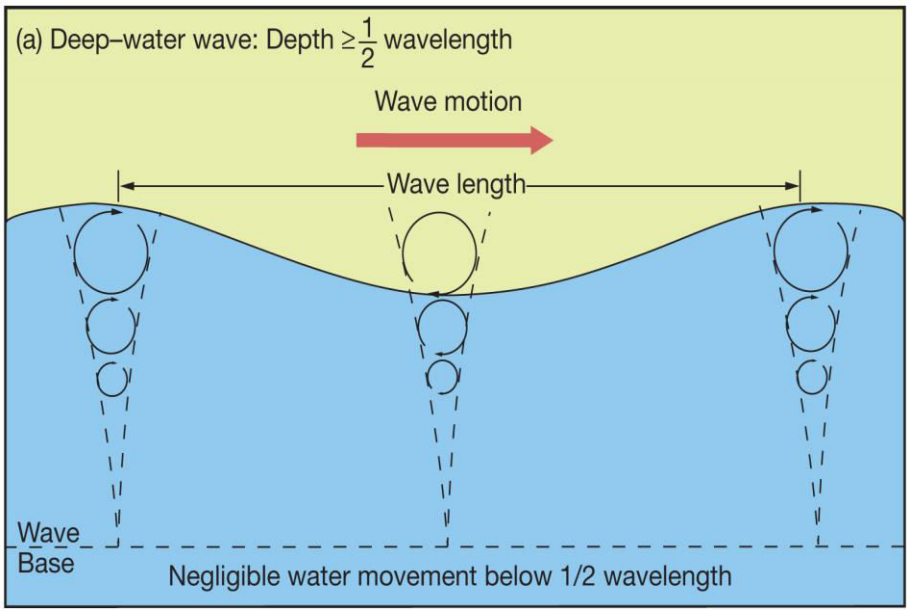

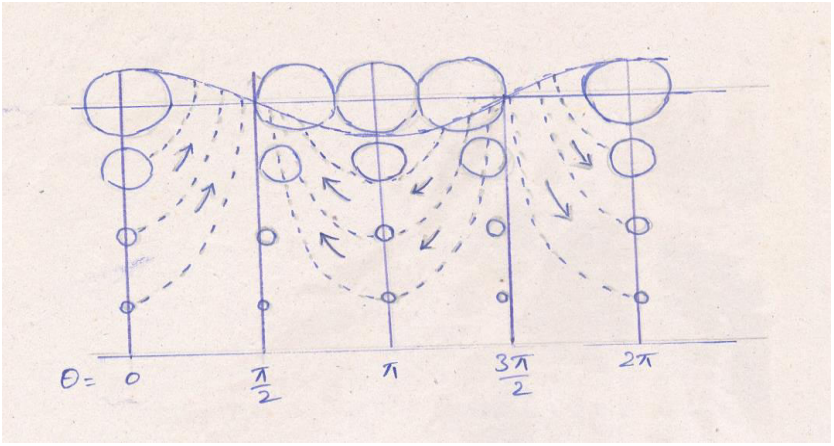

Fig.4.20 Orbital motion of wave particle motion in deep water waves

The individual water particles move in closed circular orbits with radii (ae^{kd}) decreasing exponentially with depth below the sea surface. The Fig. 4.20 depicts the orbits, instantaneous orbital velocities and streamlines (dashed lines) in a deep water wave.

Just ahead of the crest there is an area of convergence and just behind the crest an area of divergence. Hence the surface rises ahead of the crest and falls behind it. This qualitatively describes the progress of the wave.

4.8.3. Shallow water case:

The values of A and B for shallow water condition can be obtained by applying the condition of table 4.2 to the equations (4.33).

$$A = a\frac{Coshk(d+z)}{Sinhkd} \quad ,$$

For shallow water from table 4.2 Cosh k(d+z) → 1 and Sinh (kd) → kd

$$\therefore A = \frac{a}{kd}$$

$$B = a\frac{Sinhk(d+z)}{Sinhkd}$$ for shallow water Sinh k(d+z) → k (d+z) and Sinh (kd) → kd

$$\therefore B = \frac{a(d+z)}{d}$$

This means the particle paths of shallow water waves are *elliptical* with a major semi-axis of A = a/kd and a minor semi-axis of B = a(d+z)/d as shown in Fig.4.21. The same condition is applicable to Intermediate waves or transitional waves and the total figure showing the orbital motion for deep, intermediate and shallow water waves is as shown in Fig. 4.22.

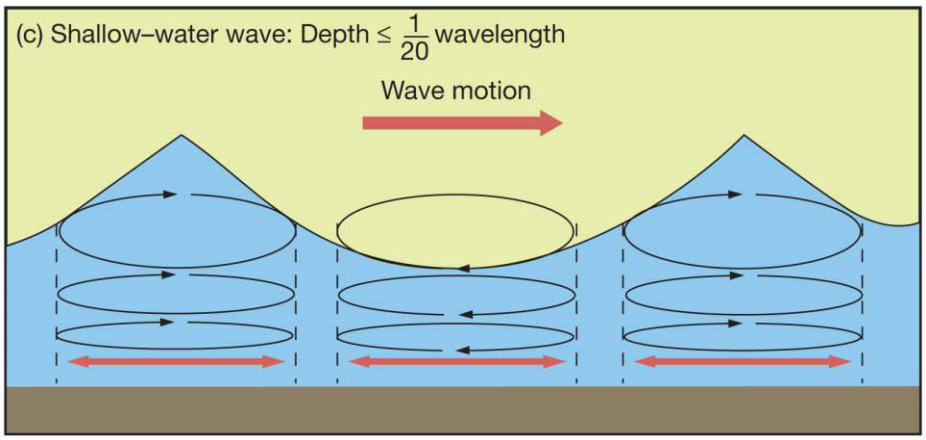

Fig.4.21. Orbital motion of particles in shallow water wave

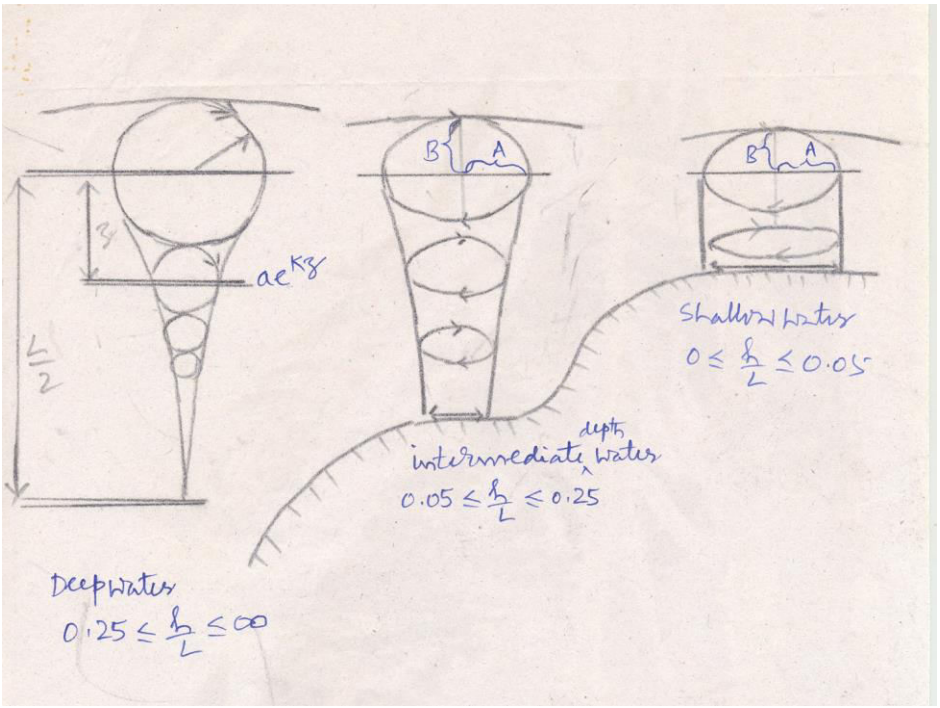

Fig.4.22 .Orbital motion of water particle motion in deep, intermediate and shallow water waves

4.9. Differences between surface waves (short waves) and Long waves (shallow water waves):

S.No	Character of the wave	Surface waves	Long waves
1.	Velocity	i. Progressive,standing free or forced waves ii. Dependent on wave Length $C^2 = \frac{gL}{2\pi}$	i. Progressive,standing free or forced waves ii. Dependent on water depth $C^2 = gd$
2.	Movement of water Particles in a Vertical plane	Orbital motion of water particles is circular. The Radii of theses circles decrease with depth. Motion is imperceptible at a depth equal to half of its wave length.	The motion is in ellipses. While the size of the ellipses decrease with depth and flattened, at a depth of half the wave length the ellipses become so flat like a line and so particles move back and forth.
3.	Pressure distribution	Below the depth of perceptible motion of water particles the pressure is not influenced by the wave	The wave influences the pressure distribution in the same manner at all depths.
4.	Influence of earth's rotation	Negligible	Can not be neglected if the period of wave approaches the period of earth's rotation.

4.10. Pressure of a progressive wave:

We have seen that the integrated and linearized equation of motion for irrotational motion of an incompressible fluid can be written from Bernoullils equation (equation 4.15) as:

$$\left[-\frac{\partial \varphi}{\partial t}+\frac{p}{\rho}+gz\right]=0 \quad \text{.....(4.34)}$$

The velocity potential for a progressive wave moving in the positive x direction (equation 4.22), can be differentiated with respect to 't' and substituting in the equation (4.34) we get:

$$\frac{p}{\rho}=g\frac{\cosh k(d+z)}{\cosh kd}a\sin(kx-\sigma t)-gz \quad \text{.....(4.35)}$$

Using the wave profile equation $\eta = a \sin(\sigma t - k x)$, equation 4.35 can be modified as:

$$p=\gamma\left[\eta\frac{\cosh k(d+z)}{\cosh kd}-z\right] \quad \text{.....(4.36)}$$

In equation (4.36), $\gamma=\rho g$ and z is negative downward from mean water level. The quantity $\frac{\cosh k(d+z)}{\cosh kd}=K_p$ is called the pressure response factor and K_p is less than unity for all depths below the mean water level. Equation (4.36) is not valid for all positive z, though it exists under the crest above the mean water level because of the boundary condition. If we recall that in free surface boundary condition we set p = 0 at the surface but in determining φ we applied this surface boundary condition at z = 0, rather than z = η at the peak level of the profile of the crest. Because of this inconsistency we will restrict our discussion of equation (4.36) to the region of negative z only.

Equation (4.36) can further be simplified as:

$$\frac{p}{\gamma}=K_p\eta-z \quad \text{.....(4.37)}$$

where $\frac{p}{\gamma}$ is pressure head, K_p is pressure response factor and z is elevation head. This can be readily interpreted physically in comparison with the familiar relationships of hydrostatics. The second term ($K_p\eta$) represents the negative one-to-one correspondence between pressure head ($\frac{p}{\gamma}$) and elevation head (z) associated with hydrostatic pressure distribution. The first term ($\frac{p}{\gamma}$) provides a positive or negative (depending on wave phase) deviation from the hydrostatic produced by the vertical accelerations accompanying the orbital motions.

Looking first at the limiting values of z, equation (4.37) turns out to:

i) at z = 0 and $\frac{p}{\gamma}=\eta$, the equation 4.37 is equal to:

$\eta = \eta K_p \rightarrow \eta (1 - K_p) = 0$ which means $K_p = 1$

It would thus be consistent to assume the pressure to be hydrostatic for positive z.

ii) at z = -d (below the mean water level) the equations 4.36 or 4.37 turns out to:

$$\frac{p}{\gamma} = \frac{\eta}{\cosh kd} + d \qquad \text{.....(4.38)}$$

as $K_p = \frac{1}{\cosh kd}$ $\because \cosh 0 \rightarrow 1, \cosh(z+d) \rightarrow \cosh(d-d) \rightarrow \cosh 0 \rightarrow 1$

Thus the hydrostatic bottom pressure as given by the equation (4.38) turns out to be:

$$\frac{p}{\gamma} = \eta + d \quad (\text{as cosh kd} \rightarrow 1)$$

For wave phases at which η is negative (under the trough) the bottom pressure is thus greater than the hydrostatic pressure (h – η) since $h - \frac{\eta}{\cosh kd} > \text{h} - \eta$

Conversely for positive 'η' (under the wave crest)

$$h + \frac{\eta}{\cosh kd} < \text{h} + \eta$$

Which means the bottom pressure is less than hydrostatic pressure under the wave crest. The Figure 4.23 below represents these arguments of resulting vertical pressure distribution.

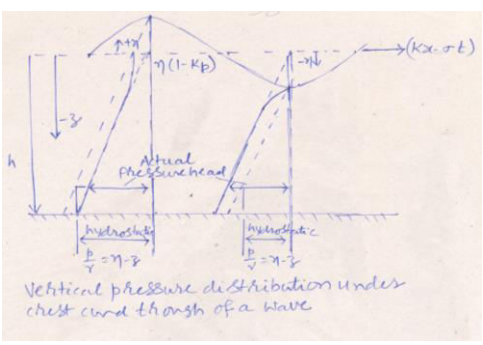

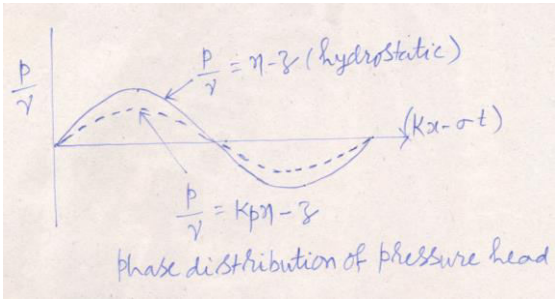

Fig.4.23. VerticalPressure distribution under crest and trough of a wave

4.11. Wave Energy:

The total energy contained in a wave consists of two kinds viz., the potential energy, resulting from the position of the wave and the displacement of the free surface from mean sea level and the kinetic energy due to the fact that the water particles throughout the fluid are moving. The total energy and its transmission are of importance in determining how waves change in propagating toward shore, the power required to generate waves, and the available power for wave energy extraction.

Potential energy:

Potential energy occurring in waves is the result of displacing a mass from a position of equilibrium against a gravitational field. When water is at rest with a uniform free surface elevation, it can be shown readily that the potential energy is minimum. However, a displacement of an assemblage of particles resulting in the displacement of the free surface will require that work be done on the system and results in an increase in potential energy.

We will derive the average potential energy associated with a sinusoidal wave by considering a strip of unit depth in the y-direction in a two dimensional wave.

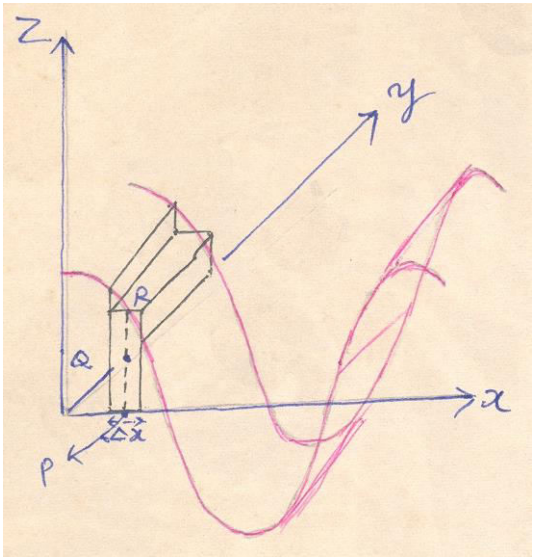

Fig.4.24. Calculation of potential energy

The potential energy of a column of water PR (Fig.4.24) at height 'η' with width Δx is the weight of the water column.

$\therefore$ The area of the column = $\Delta x.\ \eta$

If this area is multiplied by the thickness in y direction, then it gives the volume of the fluid within the strip (column). Since the thickness of the column in y direction is unity, the volume of the fluid in the column is $\Delta x.\ \eta.\ 1$

Mass of the fluid = $\rho.\ \Delta x.\ \eta$

Where ρ is the density of sea water. The centre of gravity of water in the strip is at 'Q' that is, at half the height ($\frac{\eta}{2}$).

The potential energy is = $mgh = (\rho.\ \Delta x.\ \eta).g.\ \frac{\eta}{2} = \frac{1}{2}\rho.g.\ \Delta x.\ \eta^2$

The average P.E per unit horizontal area is found by integrating over a wave length.

$$\therefore \text{P.E} = \int_0^L \frac{\rho g}{2}\eta^2 dx$$

The horizontal area covered by the wave of length L and thickness unity in y direction is (L × 1 = L) units. So the average potential energy per unit horizontal surface area is

$$\text{P.E} = \frac{g}{2L}\int_0^L \rho.\eta^2.dx$$

If the fluid has constant density, then

$$\text{P.E} = \frac{g\rho}{2L}\int_0^L \eta^2.dx$$

But we know $\eta = a\cos(kx - \sigma t)$ for progressive wave

$$\therefore \text{P.E} = \frac{\rho g a^2}{2L}\int_0^L \cos^2(Kx-\sigma t)dx, \text{ putting L} = 2\pi/K$$

$$\therefore \text{P.E} = \frac{\rho g a^2}{4\pi}\int_0^{2\pi/k} \cos^2(Kx-\sigma t)kdx$$

$$= \frac{\rho g a^2}{4\pi}\int_0^{2\pi/k} \frac{1+\cos 2(kx-\sigma t)}{2}kdx$$

$$= \frac{k.\rho g a^2}{2(4\pi)}\{\int_0^{2\pi/k} dx + \int_0^{2\pi/k} \frac{1+\cos 2(kx-\sigma t)}{2}kdx\}$$

$$= \frac{k.\rho g a^2}{8\pi)}\left\{[x]_0^{2\pi/k} + \left[\frac{Sin2(kx-\sigma t)}{2k}\right]_0^{2\pi/k}\right\} =$$

$$\frac{k.\rho g a^2}{8\pi)}\left\{\left(\frac{2\pi}{k}-0\right)+\frac{1}{2k}\left[\sin 2\left(k.\frac{2\pi}{k}-\sigma t\right)-\sin 2(k.0-\sigma t)\right]\right\}$$

$$= \frac{k.\rho g a^2}{8\pi)}\left\{\left(\frac{2\pi}{k}\right)+\frac{1}{2k}[-\sin 2\sigma t+\sin 2\sigma t]\right\} = \frac{k.\rho g a^2}{8\pi}.\frac{2\pi}{k} = \frac{\rho g a^2}{4} \quad \text{.....(4.39)}$$

Kinetic Energy:

The kinetic energy of the wave is due to moving particles in the wave.

We know K.E = $\frac{1}{2}mv^2 = \frac{1}{2}\rho(u^2+v^2) = \int_0^L\int_0^{-d}\frac{1}{2}(u^2+w^2)dxdy$

We know the particle velocities as from equations (4.31 & 4.32)

u = $+\frac{agk}{\sigma \cosh kd}$ Cosh k(d +z).Cos (k x – σ t)

w = - $\frac{agk}{\sigma}\frac{Sinhk(d+z)}{Coshkd}Sin(kx-\sigma t)$

substituting and writing

K.E =

$$\int_0^L\int_0^{-d}\frac{\rho}{2}\left[\frac{agk}{\sigma}\frac{1}{\cosh kd}\right]^2\left[Cosh^2k(d+z)Cos^2(kx-\sigma t)+Sinh^2k(d+z).Sin^2(kx-\sigma t)\right]dxdz$$

Using the trigonometric identities just as was done earlier, this can be recasted as

$$\text{K.E} = \frac{\rho}{2}\left[\frac{agk}{\sigma}\frac{1}{\cosh kd}\right]^2\frac{1}{2}\int_0^L\int_0^{-d}\left[Cosh2k(d+z)+Cos2(kx-\sigma t)\right]dxdz$$

On integration further simplification, it yields to : K.E = $\frac{1}{4}\rho g a^2$ ……(4.40)

Total Energy:

The total energy per unit width of the crest in a wave is P.E + K.E

$= \frac{1}{4}\rho g a^2 + \frac{1}{4}\rho g a^2 = \frac{1}{2}\rho g a^2 = \frac{1}{8}\rho g H^2$ ($\because a = \frac{H}{2}$) ……(4.41)

Energy flux:

Small amplitude waves do not transmit mass as they propagate across a fluid, as the trajectories of the water particles are closed. However, all waves do transmit energy. The rate at which the energy is transferred is called the energy flux "Ŧ" and for linear waves it is the rate at which work is being done by the fluid on one side of a vertical section. For the vertical section AÁ in the Fig.4.25, the instantaneous rate at which work is being done by the dynamic pressure P_D (= P + ρgz) per unit width in the direction of wave propagation is:

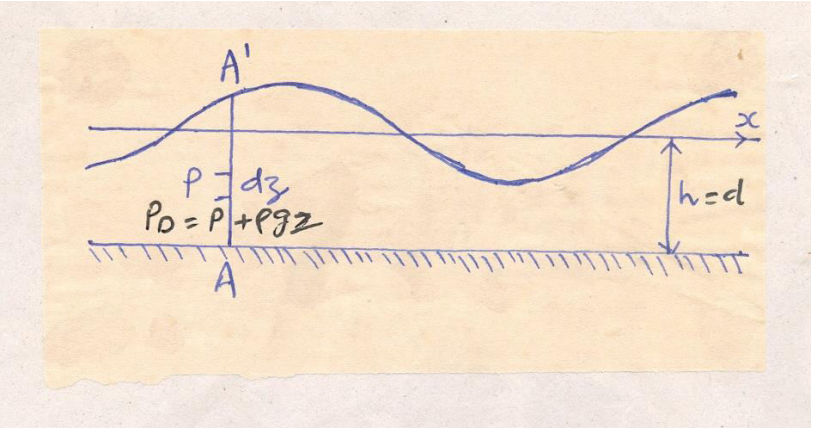

Fig. 4.25. Plan view for wave energy flux

$$F = \int_0^{-d} P_D . u dz$$

$$F = \int_0^{-d} (P + \rho g z) . u dz \quad \ldots\ldots\ldots (4.42)$$

The average energy flux is obtained by averaging over a wave period

$$F = \frac{1}{T} \int_0^T \int_0^{-d} P_D . u dz dt \quad \ldots\ldots (4.43)$$

Substituting the values of P from equation (4.36), η from equation (4.26a) and u from equation (4.31) in 4.42 and then substituting in eqn (4.43) we get:

$$F = \frac{1}{T} \int_0^T \int_0^{-d} \left[\rho g \eta \frac{Coshk(d+z)}{Coshkd} \right] \left[\frac{agk}{\sigma} \frac{Coshk(d+z)}{Coshkd} Sin(kx - \sigma t \right] dz dt$$

$$= \frac{1}{T} \int_0^T \int_0^{-d} \left[\rho g \eta \frac{Coshk(d+z)}{Coshkd} \right] \left[\eta \sigma \frac{Coshk(d+z)}{Sinhkd} \right] dz dt \qquad \left(\because \sigma^2 = gk \tanh kd \right) \ldots (4.44)$$

To retain the terms upto the second order in wave height, it is only necessary to integrate up to the mean free surface, on integration the equation reduces to

$$F = \frac{\rho g \sigma}{4k} \left(\frac{H}{2} \right)^2 \left[\frac{2kd + Sinh2kd}{Sinh2kd} \right] = \left(\frac{1}{8} \rho g H^2 \right) \left(\frac{\sigma}{k} \right) \left[\frac{1}{2} \left(1 + \frac{2kd}{Sinh2kd} \right) \right]$$

$$= (E)(C)\ (N) = E\, C_g \quad \ldots\ldots\ldots\ldots\ldots\ldots\ldots\ldots\ldots\ldots (4.45)$$

Where CN = C_g is the group velocity at which the energy is transmitted. Thus it is evident from group velocity

$$\frac{C_g}{C} = N = \left[\frac{1}{2} \left(1 + \frac{2kd}{Sinh2kd} \right) \right] \quad \ldots\ldots\ldots\ldots\ldots\ldots (4.46)$$

The factor N has deep and shallow water asymptotes and has the values ½ and 1 respectively. The energy flux 'F' has the unit of power and for this reason it is some times referred to as the 'wave power'.

An alternate formula used for estimation of wave power from the spectrum is

$$P = \frac{\gamma g}{64\pi} H_S^{\,2} T_Z \text{ watts} \quad \ldots\ldots\ldots\ldots\ldots (4.47)$$

Where γ = Specific weight of sea water (10.05 newtons /m^3), g = 9.8 m/s^2, H_S = Significant wave height in meters, T_Z = zero crossing period in seconds.

Relative Depth	Shallow Water $\frac{d}{L} < \frac{1}{20}$ $kd < \frac{\pi}{10}$	Transitional Water $\frac{1}{20} < \frac{d}{L} < \frac{1}{2}$ $\frac{\pi}{10} < kd < \frac{\pi}{2}$	Deep Water $\frac{d}{L} > \frac{1}{2}$ $kd > \frac{\pi}{2}$
1. Wave profile	Same As >	$\eta = \frac{H}{2}\cos\left[\frac{2\pi x}{L} - \frac{2\pi t}{T}\right] = \frac{H}{2}\cos\theta$	< Same As
2. Wave celerity	$C = \frac{L}{T} = \sqrt{gd}$	$C = \frac{L}{T} = \frac{gT}{2\pi}\tanh\left(\frac{2\pi d}{L}\right)$	$C = C_0 = \frac{L}{T} = \frac{gT}{2\pi}$
3. Wavelength	$L = T\sqrt{gd} = CT$	$L = \frac{gT^2}{2\pi}\tanh\left(\frac{2\pi d}{L}\right)$	$L = L_0 = \frac{gT^2}{2\pi} = C_0 T$
4. Group velocity	$C_g = C = \sqrt{gd}$	$C_g = nC = \frac{1}{2}\left[1 + \frac{4\pi d/L}{\sinh(4\pi d/L)}\right]C$	$C_g = \frac{1}{2}C = \frac{gT}{4\pi}$
5. Water particle velocity			
(a) Horizontal	$u = \frac{H}{2}\sqrt{\frac{g}{d}}\cos\theta$	$u = \frac{H}{2}\frac{gT}{L}\frac{\cosh[2\pi(z+d)/L]}{\cosh(2\pi d/L)}\cos\theta$	$u = \frac{\pi H}{T}e^{\left(\frac{2\pi z}{L}\right)}\cos\theta$
(b) Vertical	$w = \frac{H\pi}{T}\left(1+\frac{z}{d}\right)\sin\theta$	$w = \frac{H}{2}\frac{gT}{L}\frac{\sinh[2\pi(z+d)/L]}{\cosh(2\pi d/L)}\sin\theta$	$w = \frac{\pi H}{T}e^{\left(\frac{2\pi z}{L}\right)}\sin\theta$
6. Water particle accelerations			
(a) Horizontal	$a_x = \frac{H\pi}{T}\sqrt{\frac{g}{d}}\sin\theta$	$a_x = \frac{g\pi H}{L}\frac{\cosh[2\pi(z+d)/L]}{\cosh(2\pi d/L)}\sin\theta$	$a_x = 2H\left(\frac{\pi}{T}\right)^2 e^{\left(\frac{2\pi z}{L}\right)}\sin\theta$
(b) Vertical	$a_z = -2H\left(\frac{\pi}{T}\right)^2\left(1+\frac{z}{d}\right)\cos\theta$	$a_z = -\frac{g\pi H}{L}\frac{\sinh[2\pi(z+d)/L]}{\cosh(2\pi d/L)}\cos\theta$	$a_z = -2H\left(\frac{\pi}{T}\right)^2 e^{\left(\frac{2\pi z}{L}\right)}\cos\theta$
7. Water particle displacements			
(a) Horizontal	$\xi = -\frac{HT}{4\pi}\sqrt{\frac{g}{d}}\sin\theta$	$\xi = -\frac{H}{2}\frac{\cosh[2\pi(z+d)/L]}{\sinh(2\pi d/L)}\sin\theta$	$\xi = -\frac{H}{2}e^{\left(\frac{2\pi z}{L}\right)}\sin\theta$
(b) Vertical	$\zeta = \frac{H}{2}\left(1+\frac{z}{d}\right)\cos\theta$	$\zeta = \frac{H}{2}\frac{\sinh[2\pi(z+d)/L]}{\sinh(2\pi d/L)}\cos\theta$	$\zeta = \frac{H}{2}e^{\left(\frac{2\pi z}{L}\right)}\cos\theta$
8. Subsurface pressure	$p = \rho g(\eta - z)$	$p = \rho g\eta\frac{\cosh[2\pi(z+d)/L]}{\cosh(2\pi d/L)} - \rho g z$	$p = \rho g\eta e^{\left(\frac{2\pi z}{L}\right)} - \rho g z$

Group velocity:

Consider two waves moving in the positive x direction whose periods are different.

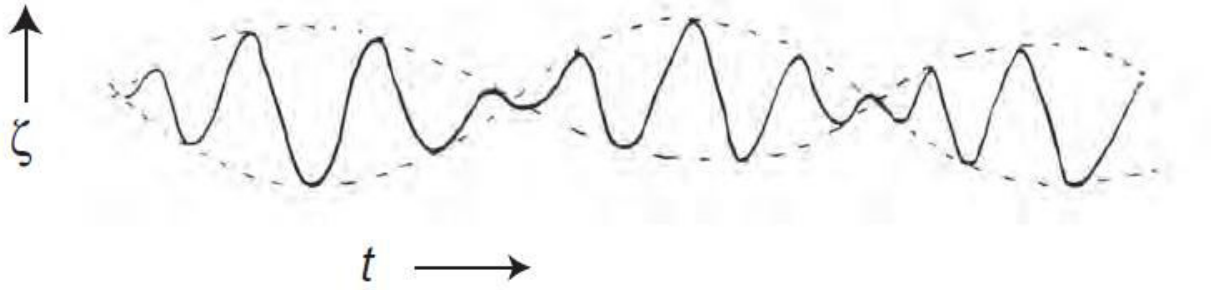

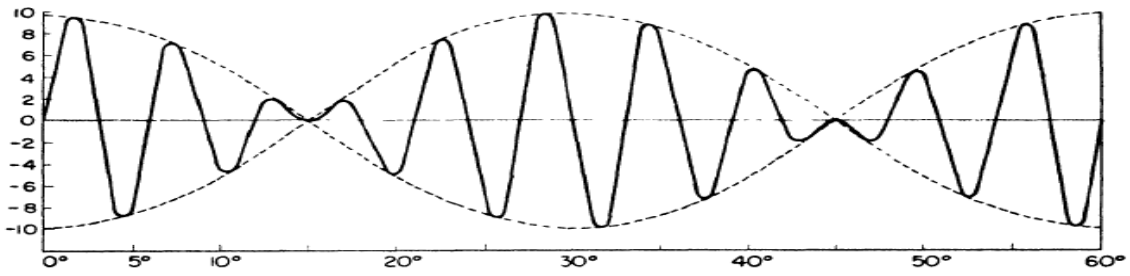

Fig.4.26. Group velocity envelope

Then $\eta_1 = a_1 \text{Sin}(k_1x - \sigma_1 t + \delta_1)$ and $\eta_2 = a_2 \text{Sin}(k_2x - \sigma_2 t + \delta_2)$

Then the composite wave is $\eta_T = \eta_1 + \eta_2$

So $\eta_T = a_1 \text{Sin}(k_1x - \sigma_1 t + \delta_1) + a_2 \text{Sin}(k_2x - \sigma_2 t + \delta_2)$

This equation represents a wave train. If the two components of this wave train are assumed for simplicity to have equal amplitudes and to be in phase at the origin of (kx-σt), then the average amplitude of the wave train is $\frac{a1+a2}{2}$ = a and $\delta_1 = \delta_2 = 0$

$\eta_T = a\{\text{Sin}(k_1x - \sigma_1 t) + \text{Sin}(k_2x - \sigma_2 t)\}$

$\eta_T = 2a\,\text{Sin}\{\frac{(k1x-\sigma_1 t)+(k2x-\sigma_2 t)}{2}.\text{Cos}\frac{(k1x-\sigma_1 t)-(k2x-\sigma_2 t)}{2}\}$

$= 2a\{\text{Sin}[\frac{(k1+k2)x}{2} - \frac{(\sigma_1+\sigma_2)t}{2}].\text{Cos}\frac{(k1-k2)x}{2} - \frac{(\sigma_1-\sigma_2)t}{2}\}$

When K_2 is slightly smaller than K_1, σ_2 is also slightly smaller than σ_1 and the difference between each is also small. Hence the values of $\frac{(k1+k2)}{2}$ and $\frac{(\sigma_1+\sigma_2)}{2}$ are essentially the wave number and wave radian frequency of the composite wave. The cosine term represents a slowly varying term in the above equation which only modulates the sine term.

We can see that this composite wave (Fig.4.26) takes the form of a series of Sine waves the amplitude of which varies slowly between 0 and 2a according to the Cosine factor. The points of zero amplitude of the wave envelope thus separate groups of individual waves. These nodal points are located by finding the zeros of the cosine factor

$\text{Cos}(2m+1)\frac{\pi}{2} = 0$ which implies $\eta_T = 0$

$\text{Cos}\frac{(k1-k2)x}{2} - \frac{(\sigma_1-\sigma_2)t}{2} = \text{Cos}(2m+1)\frac{\pi}{2} = 0$ which means $\frac{(k1-k2)x}{2} - \frac{(\sigma_1-\sigma_2)t}{2} = (2m+1)\frac{\pi}{2}$

Or $x(k_1 - k_2) = (2m+1)\pi + (\sigma_1 - \sigma_2)t$

Or $X_{node} = \frac{(\sigma_1-\sigma_2)t}{(k_1-k_2)} + \frac{(2m+1)\pi}{(k_1-k_2)}$

Since the position of all nodes is a function of time, they are not stationary. At t = 0 there will be nodes at (putting m 0,1,2,….)

$X = \frac{\pi}{(k_1 - k_2)}, \frac{3\pi}{(k_1 - k_2)}, \frac{5\pi}{(k_1 - k_2)}, \ldots\ldots$

Thus the distance between one node to another is $dx = \frac{2\pi}{(k_1 - k_2)} = \frac{L_1 L_2}{(L_2 - L_1)}$ { since $K_1 = \frac{2\pi}{L_1}$ and $K_2 = \frac{2\pi}{L_2}$}.

The speed of propagation of the nodes associated with this wave group is given by

Group velocity $C_g = \frac{dXnodes}{dt} = \frac{(\sigma_1 - \sigma_2)}{(k_1 - k_2)} = \frac{d\sigma}{dk}$

Solution: $C_g = \frac{d\sigma}{dk} = \frac{d}{dk}(Ck)$ { since $C = \frac{\sigma}{k}$}

So $C_g = \frac{d}{dk}(Ck) = \frac{d}{dk} k\sqrt{\frac{g}{k}\tanh kd} = \frac{d}{dk}\sqrt{gk\tanh kd} = \frac{d}{dk}[gk\tanh kd]^{-1/2}$

On differentiating

$= \frac{1}{2}[gk\tanh kd]^{-1/2}$ {gkd sech^2 (kd) + g tanh (kd) .1}

$= \frac{1}{2}\frac{g}{\sqrt{gk\tanh kd}}$ { kd. $\frac{1}{\text{Cosh}^2 kd} + \frac{Sinh\ kd}{\text{Cosh kd}}$} on further simplification of dividing and subtracting by $\sqrt{k}$ we can write

$= \frac{1}{2}\frac{g}{\frac{\sqrt{k}}{\sqrt{k}}\sqrt{gk\tanh kd}}$ { kd. $\frac{1}{\text{Cosh}^2 kd} + \frac{Sinh\ kd}{\text{Cosh kd}}$}

$= \frac{1}{2}\frac{g}{k\sqrt{\frac{g}{k}\tanh kd}}$ { kd. $\frac{1}{\text{Cosh}^2 kd} + \frac{Sinh\ kd}{\text{Cosh kd}}$} $= \frac{g}{2k}\frac{1}{C}\{\frac{kd + \frac{1}{2}\text{Sinh kd}}{\text{Cosh}^2 kd}\}$

On separating and simplifying within the brackets we can write

$= \frac{g}{2k}\frac{1}{C}\{\frac{2\,\text{Sinh kd Cosh kd}}{2\,\text{Cosh}^2 kd}\}\{1 + \frac{2kd}{\text{Sinh 2kd}}\} = \frac{g}{2k}\frac{1}{C}\tanh kd\,\{1 + \frac{2kd}{\text{Sinh 2kd}}\}$

We know $C^2 = \frac{g}{k}\tanh kd$ substituting this in the above equation we get

$C_g = \frac{C}{2}\{1 + \frac{2kd}{\text{Sinh 2kd}}\}$

From the above equation, it is clear that the group velocity is half the phase velocity and $\frac{Cg}{C}$ can be seen to have the value $\frac{1}{2}$ in deep water and approach to a limiting value of unity in shallow water.

4.12. Finite amplitude Wave theories:

The generation of waves depends on the transference of energy from the wind to the sea. Some of the theories that explain how wind transfers energy for generation of waves is given below.

The simplest wave theory is the *first-order, small-amplitude*, or *Airy* wave theory which will hereafter be called *linear theory*. Many engineering problems can be handled with ease and reasonable accuracy by this theory. For convenience, prediction methods in coastal engineering generally have been based on simple waves. For some situations, simple theories provide acceptable estimates of wave conditions.

When waves become large or travel toward shore into shallow water, higher-order wave theories are often required to describe wave phenomena. These theories represent *nonlinear waves*.

There are five wave theories that are commonly applied to describe wave motion on the sea. The general wave profile, its application and related references are given below:

i) Airy waves (Sinusoidal waves) (Fig.4.27): This theory is applied to waves of small amplitude in deep water. References are Laplace (1776) and Airy(1845).

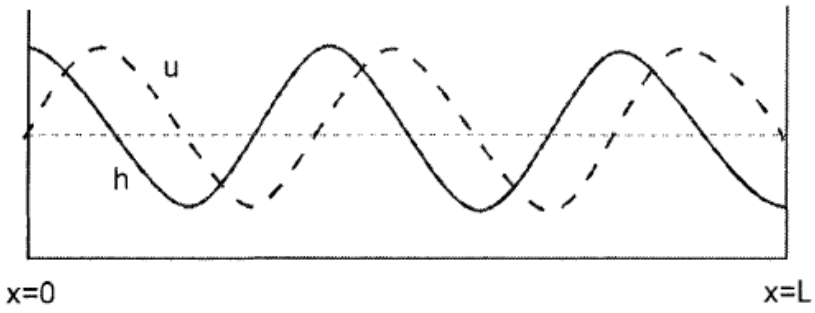

Fig.4.27. Airy waves of Sinusoidal character

Airy wave theory represents the simplest formulation but because of the assumptions involved in the derivation its application should be limited to waves of small amplitude. This theory is actually strictly true only for the limiting case of waves of zero height. For waves of appreciable height this theory does not hold good.

The linear theory that is valid when waves are infinitesimally small and their motion is small also provides some insight for finite-amplitude periodic waves (nonlinear). However, the linear theory cannot account for the fact that wave crests are higher above the mean water line than the troughs are below the mean water line. Results obtained from the various theories should be carefully interpreted for use in the design of coastal projects or for the description of coastal environment.

Laplace (1776) presented the first satisfactory treatment of waves of small amplitude in water of arbitrary depth. Airy (1845) later developed a theory for irrotational waves traveling over a horizontal bottom in any depth of water. In the derivation of this theory the equations are linearized and so this theory is often referred to as *linear wave theory.* Airy wave theory represents the simplest formulation but because of the assumptions involved in the derivation its application should be limited to waves of small amplitude. The theory is actually strictly true only for the limiting case of waves of least height. Where waves of appreciable height are involved more complex wave theories are required.

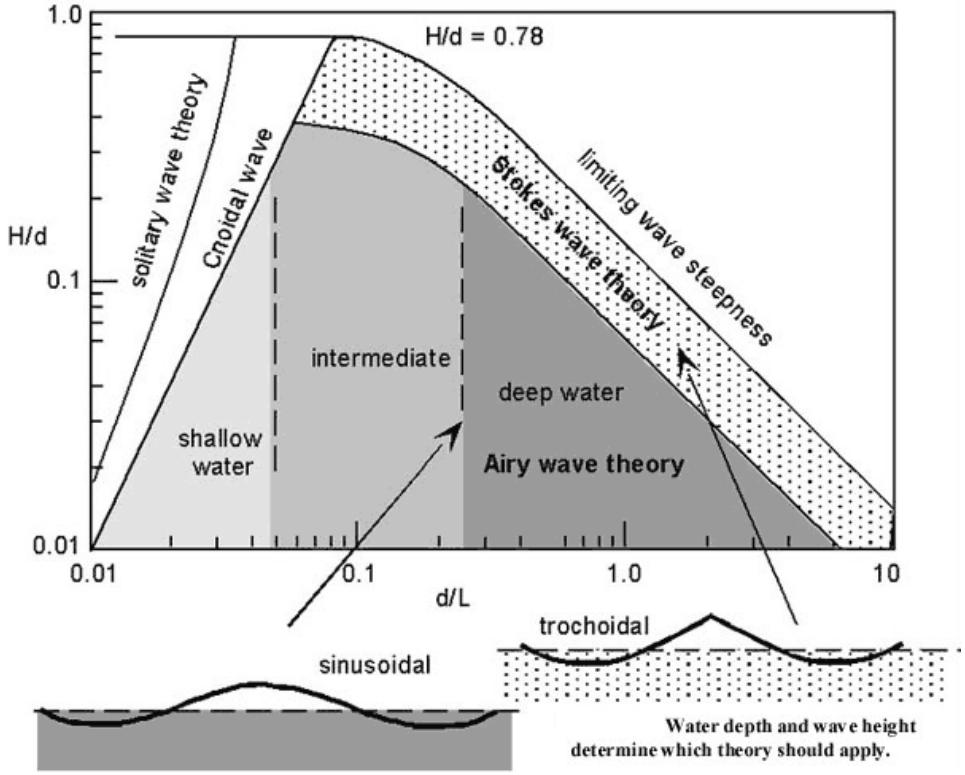

Fig.4.28. Nonlinear of Finite amplitude waves

ii) Stokes and Gerstner waves (trochoidal): This theory is applied to waves of finite amplitude in deep, intermediate and shallow water. More than half the wave height is above the mean water level for trochoidal wave as shown in Fig.4.29.

Just before the time of breaking, the crest would form a cusp with an angle of 120^o between the tangents to the two faces of the crest as shown in Fig.4.8. The references are Gerstner (1802), Stokes (1847), Froude (1862), Rankine (1863) and Rayleigh (1877).

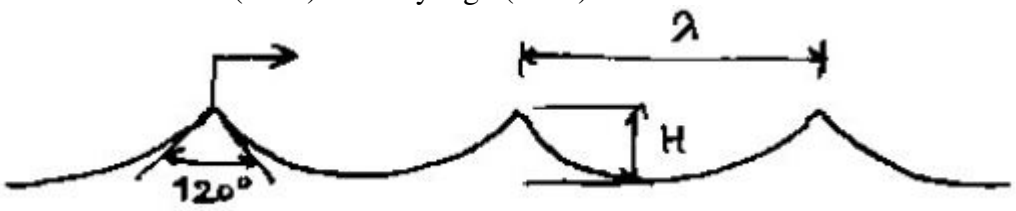

Fig.4.29. Stokes or Gerstner waves

Airy wave theory omits terms involving the wave height to the second (H^2) and higher orders. If the wave height is large, such an approximation is not adequate, and so it is necessary to retain the higher order terms. Stokes in 1847 considered waves of small, but finite height progressing over still water of finite depth and presented a second

order theory. The solutions he obtained are approximate and in the form of series with coefficients that require considerable detailed calculations. The method of Stokes has since been extended to third and fifth orders later by other workers.

To the second order approximation, the wave profile of the Stokes wave is given by

$$\eta = \frac{H}{2} Cos(kx - ct) + \frac{\pi}{8}\frac{H^2}{L}\frac{Cosh(kd[2 + Cosh(2kd)]}{[Sinh(kd)]^3} Cos[2(kx - \sigma t)] \quad \text{.....(4.48)}$$

Which in deep water ($d/L_o > ¼$) reduces to

$$\eta_0 = \frac{H_0}{3} Cos 2\pi\left(\frac{x}{L_o} - \frac{t}{T}\right) + \frac{\pi H_0^{\,2}}{4L_0} Cos 4\pi\left(\frac{x}{L_o} - \frac{t}{T}\right) \quad \text{.....(4.49)}$$

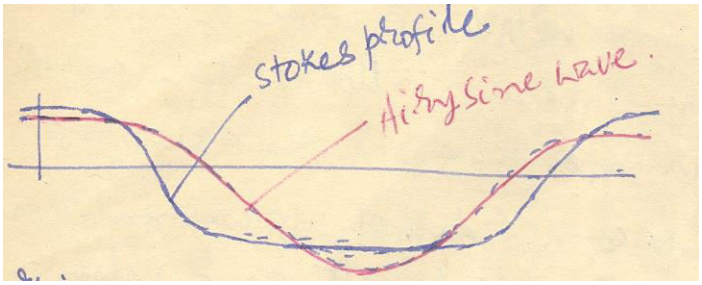

Fig.4.30. Comparison of Stokes and Airy wave profiles

It is seen that if H/L is small, the profile reduces to the sinusoidal form given by the Airy wave theory. For finite height waves there is an additional term added onto the basic sinusoidal shape. The effect of this term is shown in the above Figure 4.30 where a finite wave form is compared to a sine wave with the same height. The added term enhances the crest amplitude and detracts from the trough amplitude, so that the Stokes wave profile has steeper crests separated by flatter troughs than does the sinusoidal Airy wave as shown in the fig above. The waves are symmetrical about vertical planes through crests and troughs. The shallower the water, the more pronounced the peaks of the wave and flatter the toughs. The general shape of the Stokes wave more closely conforms to the profile of swell waves as they enter shallow water and begin to transform. To the second order of approximation, the equations of wave length and velocity are the same as those for the linear Airy wave theory.

To the third order of approximations, the wave velocity is dependent on the wave height as well as on the period and water depth which is given by:

$$C = \frac{gT}{2\pi}\tanh\left(\frac{2\pi d}{L}\right)\left[1 + \left(\frac{\pi H}{L}\right)^2 \frac{7 + 2Cosh^2\left(\frac{4\pi d}{L}\right)}{8Sinh^4\left(\frac{2\pi d}{L}\right)}\right] \quad \text{.....(4.50)}$$

This relationship corresponds to that developed by Hunt in 1953. It is seen that if $(H/L)^2$ is small, the second term in the parenthesis vanishes and the relationship reduces to the equation 4.27.of Airy waves.

In deep water the above equation (4.50) approximates to

$$C = \frac{gT}{2\pi}\left[1+\left(\frac{\pi H_0}{L_0}\right)^2\right] \quad \text{.....(4.51)}$$

A finite wave slope H_o/L_0 will cause a slight increase in C_0 over that calculated with Airy wave theory. The maximum value that the deep water steepness H_o/L_0 can achieve is approximately 1/7. At greater values the wave is unstable and breaks. For this limiting value of H_o/L_0 we have $\left[1+\left(\frac{\pi H_0}{L_0}\right)^2\right]$ = 1.20 which is 20% increase due to the finite wave height. At more steepness values the finite height produces only a slight increase in C_0.

The components of water particle velocities are given by

$$u = \frac{\pi H}{T}\frac{Cosh[k(z+d)]}{Sinh(kd)}Cos(kx-\sigma t)+\frac{3}{4}\left[\frac{\pi H}{L}\right]^2 C\frac{Cosh[2k(z+d)]}{[Sinh(kd)]^4}Cos[2(kx-\sigma t)] \text{.. .(4.52)}$$

$$w = \frac{\pi H}{T}\frac{Sinh[k(z+d)]}{Sinh(kd)}Sin(kx-\sigma t)+\frac{3}{4}\left[\frac{\pi H}{L}\right]^2 C\frac{Sinh[2k(z+d)]}{[Sinh(kd)]^4}Sin[2(kx-\sigma t)] \text{..(4.53)}$$

The first terms in the relationships for 'u' and 'w' in equations (4.52 & 4.53) are the same as the equations obtained in Airy wave theory. The second term is positive under the wave crest and trough and negative ¼ and 3/4th wavelengths from the crest. The effect of this second term is to increase the magnitude but shorten the duration of the velocity under the crest, and decrease the magnitude but lengthen the duration of the velocity under the trough as shown in fig 4.31 below. This effect is observed in waves in shallow water.

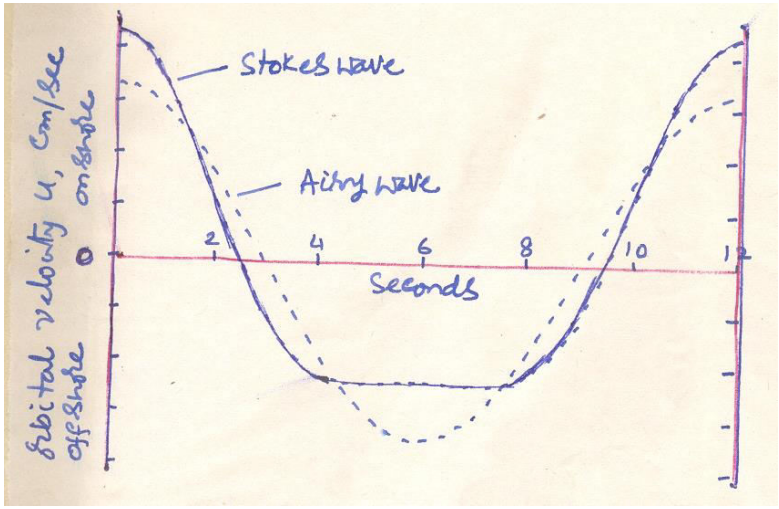

Fig.4.31. Change of shape of the profiles and the associated orbital velocity

An interesting departure of the Stokes wave from the Airy wave is that the particle orbits are not closed. This leads to a non periodic drift or mass transport in the direction of wave advance, the associated velocity being given by:

$$\bar{U} = \frac{1}{2}\left[\frac{\pi H}{L}\right]^2 C \frac{Cosh[2k(z+d)]}{[Sinh(kd)]^2} \quad \text{..... (4.54)}$$

which in deep water reduces to $\bar{U}_0 = \left[\frac{\pi H_0}{L_0}\right]^2 C_0 e^{2kz}$ .....(4.55)

Integration of the above equation(4.55) with depth yields to the discharge "q" which is the volume transported forward per unit wave crest length per unit time as:

$$q = \int_{-d}^{0} \bar{U}_0 dz = \frac{\pi}{4}\frac{H_0^2}{T} \text{ (cm}^3\text{/cm.Sec)} \quad \text{.....(4.56)}$$

The above results for the Stokes mass transport were derived for a channel of infinite length and constant depth, with no consideration of viscosity. The discharge equation (4.56) is very low.

The net shoreward velocity near the bottom, given by Longuet –Higgins (1953) is

$$\bar{U}_0 = \frac{5}{4}\left[\frac{\pi H}{L}\right]^2 C \frac{1}{[Sinh(kd)]^2} \quad \text{.....(4.57)}$$

This is important for understanding transport of sediment toward the beach.

For any given water depth and wave period there is an upper limit to the wave height of the Stokes wave at which the wave becomes unstable and breaks. The Stokes criterion for wave breaking is that the water particle velocity at the crest be just equal to the wave propagation velocity C. It is apparent that if the wave is so large that the crest water particle velocity exceeds C, then the wave would topple forward and break. Stokes determined that this breaking condition corresponds to a crest angle of 120^0. Mitchell (1893) found that for deep water this condition could also be expressed as a limiting wave steepness

$$\left[\frac{H_0}{L_0}\right]_{\max} = 0.142 \cong \frac{1}{7}$$

Gerstner or Trochoidal waves:

First solution of periodic waves of finite height was developed by Gerstner in 1802. His solution is limited to waves in water of infinite depth. From the equations he developed, Gerstner concluded that the surface profile is trochoidal in shape. Later Froude (1862) and Rankine (1863) developed further.This theory has wide application to civil engineers and naval architechts because the solutions are exact and equations are simple to use. The solutions also satisfy the pressure conditions at the water surface and

continuity. The experimental studies also demonstrate that the surface profile of the trochoidal wave closely approximates the actual profile of waves on a horizontal bottom.

Formation of trochoid:

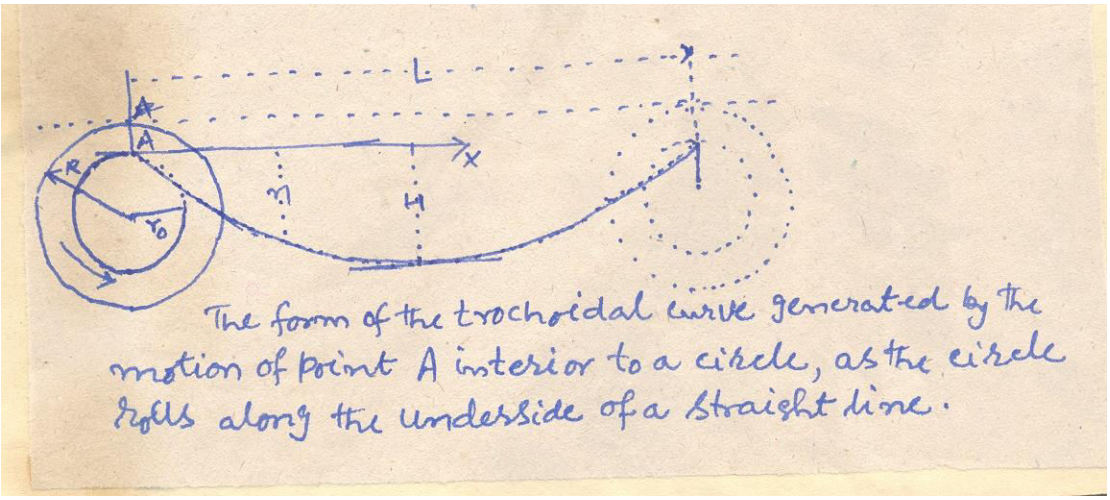

Fig.4.32. Formation of a trochoid

The trochoid curve is generated by the motion of a point 'A' interior to a circle, as the circle rolls along the underside of a line. Referring the figure, if R is the radius of the circle, then the wave length will be $L = 2\pi R$ (the radius of the circle is 1/k). The wave height will be $H = 2r_o$, where r_o is the radial distance from the circle center to the point'A'. For an angle of rotation θ, the surface depression below crest level is

$$\eta = \frac{H}{2}(1-\cos\theta)$$

While the horizontal distance of the surface from the origin at the crest is

$$x = L\left[\frac{\theta}{2\pi} + \frac{H}{2L}Sin\theta\right]$$

As H/L becomes small (as point 'A' approaches the center), the surface profile becomes nearly that of the Stokes wave, and with H nearly zero the shape tends toward a sine wave. Hence in the limit, the wave corresponds to a deep water Airy wave.

The positions of the crest and trough relative to the still-water level are:

Height of the crest $= \frac{H}{2} + \frac{\pi H^2}{4L}$

Depth of the trough $= \frac{H}{2} - \frac{\pi H^2}{4L}$

Thus it is clear that the crest is more than half the wave height above the still-water level and the trough is less than half below the still water level.

The particle orbits of the trochoidal wave are $d = S = H e^{kz}$ which is same as deep-water Airy waves whose orbits are circular and their diameters decrease exponentially with depth. The wave length and phase velocity expressions are also the same as those for a deep –water Airy wave. The energy is given by

$$E = \frac{1}{8}\rho g H^2 \left[1 - \frac{1}{2}\left(\frac{\pi H}{L}\right)^2\right]$$

If the equations for the trochoid are expanded into a series, it is found that the first three terms are the same as those in the Stokes solution. It may be noted here that the trochoid theory is limited to water of infinite depth.

iii) Cnoidal wavetheory: This is also applied to waves of finite amplitude in deep, intermediate and shallow water. The references are Korteweg and Devries (1895) and Keller (1949). The shape of the wave profile is as shown in Fig.4.33.

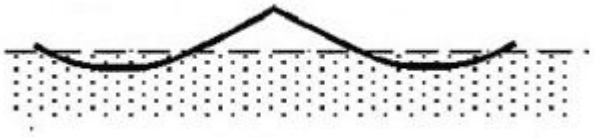

Fig.4.33. Cnoidal wave profile

iv) Solitary wave theory: The application is for isolated crests (Fig.4.34) of finite amplitude moving in shallow water. The references are Scot-Russell (1844), Bousinesq (1871), Rayleigh (1876) and Mc Cowan (1891).

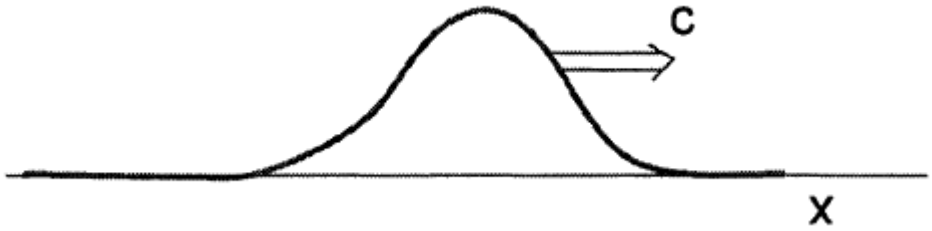

Fig. 4.34. Solitary wave profile showing isolated crests with grazing troughs

The solitary wave, as its name suggests, is a progressive wave consisting of a single crest (Fig.4.34). So it is not oscillatory like that of the simple harmonic waves. Therefore there is no wave period and length associated with the solitary wave. While this wave is not useful in describing the periodic wind waves, when ocean wave enters the shallow water sometimes their crests peak-up and are separated by wide flats and form solitary waves. As in the shallow water the wave depends on the water depth than on the period, so is the case in the case of solitary wave. Thus it has more application in near shore region. The character of the solitary wave was first described by J.Scott

Russell in 1844 by producing in a laboratory tank by suddenly releasing a mass of water at one end of the tank.

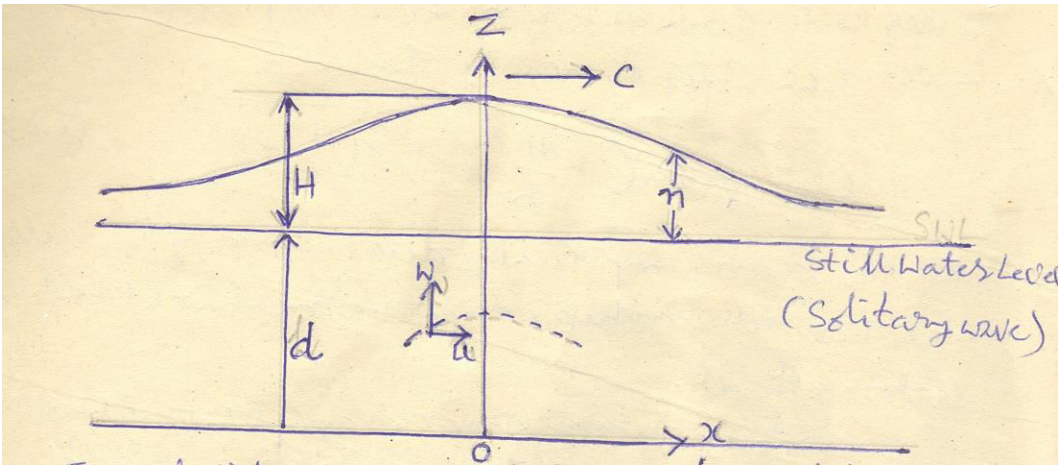

Fig.4.35. Profile Notations of the solitary wave

For the orbital velocities, the solution of McCowan may be used. The profile and notation of the solitary wave is shown in the above Figure 4.35 and the equation is

$$\eta = H \sec h^2\left(\frac{x}{d}\sqrt{\frac{3}{4}\frac{H}{d}}\right) \ldots\ldots\ldots\ldots (4.58)$$

Where η is the vertical coordinate above the still water line at a horizontal distance x from the crest; H is the wave height and d is the water depth below the still water level. The wave velocity is given by Laiton (1959) to higher order as:

$$C = \sqrt{gd\left[1+\frac{1}{2}\frac{H}{d}-\frac{3}{20}\left(\frac{H}{d}\right)^2+.....\right]} \ldots\ldots\ldots\ldots\ldots\ldots (4.58)$$

This equation (4.58) is seen to be greater than the velocity of the shallow water Airy wave. The solitary wave takes the finite height as below by neglecting the higher order terms in the above equation

$$C = \sqrt{gd\left[1+\frac{H}{d}\right]} = \sqrt{g[d+H]} \ldots\ldots\ldots\ldots\ldots\ldots (4.59)$$

This equation (4.59) was empirically determined by Russell (1844). The above two equations (4.58 & 4.59) depart somewhat at higher values of H/d (r).

As the solitary wave advances into shoaling water, the wave height progressively increases until a condition is reached at which the wave becomes unstable and breaks. This instability is again reached when the particle velocity at the crest equals the wave velocity 'C. Also the angle at the crest is 120^0.

Using these criteria, Mc Cowan (1894) further demonstrated theoretically that

$\left[\frac{H}{d}\right]_{max} = r_b = 0.78$ at the critical point of breaking.

The total energy (sum of potential and kinetic) of solitary wave per unit crest length is given by

$$E_{solitary} = \frac{8}{3\sqrt{3}} \rho g \left(\frac{H}{d}\right)^{3/2} d^3$$

Basing on the above solutions, the particle velocities obtained are

$$u = NC \frac{1 + \cos\left(M \frac{z}{d}\right) Cosh\left(M \frac{x}{d}\right)}{\left[\cos\left(M \frac{z}{d}\right) + \cosh\left(M \frac{x}{d}\right)\right]^2}$$

$$w = NC \frac{\sin\left(M \frac{z}{d}\right) \sinh\left(M \frac{x}{d}\right)}{\left[\cos\left(M \frac{z}{d}\right) + \cosh\left(M \frac{x}{d}\right)\right]^2}$$

The values of M and N are given by the following figure (Fig.4.36) as functions of H/d. The solitary wave is considered as a wave of translation, that is, the water particles move only in the direction of wave advance and there is no return flow.

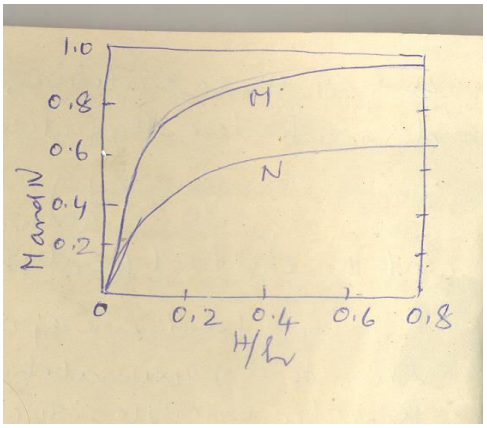

Fig.4.36. The variation of values of M and n with respect to wave height to water depth (H/h or H/d)

Problem 1:

a) In deep water waves, what is the energy per square metre of a wave field made up of waves with an average amplitude of 1.3m ($\rho = 1.03 \times 10^3$ kgm^{-3})
b) What would be the wave power in KW/m of crest length if the waves had a steepness of 0.04 (1 watt = 1JS^{-1} and one kilowatt = 10^3 watts)
c) Also calculate wave power in shallow water.

Answer:

a) Energy $E = 1/8\ \rho g H^2 =$ $1/8 \times 9.8 \times 1.03 \times 10^3 \times (2.6)^2 = 8.529 \times 10^3$ J/m^2

b) Wave power: P = group velocity × wave energy per unit area

Given steepness = H/L = 0.04, we know H = 2.6; L = 2.6/0.04 = 65m

Phase velocity in deep water = C = $\sqrt{\frac{gL}{2\pi}} = \sqrt{1.56 \times 65} = 10.07 m/s$

Group velocity in deep water = half of phase velocity; $C_g = C/2 = 10.07/2 = 5.035$ m /s

Wave power = E.C.n = $EC_g = 8.529 \times 10^3 \times 5.035 = 42.7 \times 10^3$ J/m/s = 42.7×10^3 watts/m=42.7 Kw/m

c) wave power in shallow water = P = E.C.n = E.C as n = 1 in shallow water
= $8.529 \times 10^3 \times 10.07 = 85.4 \times 10^3$J/m/s = 85.4 kw/m

Problem 2:

A wave of period 10 seconds approaching the shore has a height of 1m in deep water. Calculate a) the wave speed and group speed in deep water b) the wave steepness in deep water c) the wave power per meter of crest in water of 2.5 m deep

Ans:

a) the deep water wave celerity, $C^2 = gL/2\pi$ or $C = gT/2\pi = 1.56 \times T = 1.56 \times 10 = 15.6$ m/s

Wave measurement

Visual observations of the heights of waves reaching the shore may be made by noting the rise and fall of the sea surface against a vertical scale. The period may be determined by measuring the time interval between the arrivals of successive crests at a fixed point. To estimate the wave length directly it is necessary to be able to see a whole wave as it travels along a fixed structure such as a jetty or sea wall.

Measurements of waves in the form of a record of the height of the water surface against time may be made in various ways. The changing water level may be measured by a float or indirectly by the change in electrical capacitance or resistance as the water level moves along a wire or set or contacts. Other types of wave gauges operate by measuring the change of pressure at a fixed point as the waves pass above it. Such a gauge may be attached to a fixed structure above the bottom or may be laid on the sea bed. The amplitude of the pressure oscillation due to a wave of given surface amplitude decreases with distance below the surface and allowance for this must be made in converting the pressure oscillation to surface movement.

The vertical component of acceleration of a floating object, such as a buoy (as shown in Fig.4.37) may be measured by a suitable accelerometer and then a double integration, carried out electronically, will give the vertical displacement. The ship borne wave recorder, described by Tucker (1956), measuring the vertical movement of a point on the ship's hull and a pressure gauge, measuring the movement of water relative to that point. Various types of wave recorders were described by Draper (1961, 1967).

Measurements by the above types of instruments yield a record of sea surface height as a function of time, from which various mean values, statistical properties and

energy spectra may be derived. However, they do not give any information on the direction of travel of waves. For this purpose an array of recorders may be used, using the principle of wave interference, as in a directional radio aerial array, to determine the direction. Alternatively, one may employ an instrument measuring the components of slope of sea surface, such as the pitch and roll buoy or by measuring the two components of wave particle velocity, from which the direction of travel may be determined.

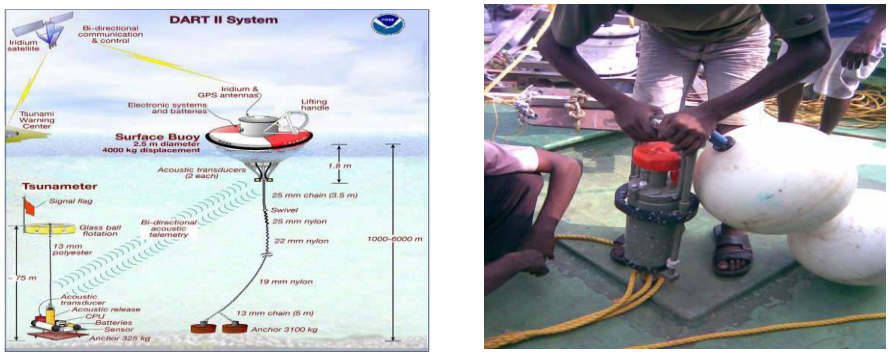

Fig. 4.37. Wave rider buoy (left) and a wave gauge (right)

In addition to instruments mounted in fixed positions, or on buoys or onboard ship, there are several methods of measuring waves by remote sensing methods. Stereoscopic photographs from air craft can be used to determine the directional wave spectrum. Radar reflections from surface waters, normally regarded as disturbing clutter, may be used to measure wave properties, employing suitable transmission and reception techniques, from shore based stations or from air craft. Remote sensing from satellites can also be applied to the measurement of wave properties over large areas of sea.

WAVE FORECASTING

Importance of wave forecasting:

The wave forecasting for practical purposes has gained importance during World War II for planning and landing operations of different naval ships and submarines, particularly on the shallow beaches. It is also important from both the design and operational point of view.

The calculation of wave characteristics from the weather maps is known as hindcasting. This hindcasting technique is useful for obtaining statistical information on the possible wave conditions expected at a given location. This statistical information is also useful for choosing the equipment needed or for choosing the suitable time of the year for marine operations.

Wave forecasting may also be used to predict the wave dimensions at a given location on a day-to-day basis. This information can be used whether a dredge can operate, a mobile offshore oil platform can be moved, a barge can be towed etc.

Forecasting procedures:

There are several procedures to predict waves. While there are two broad techniques, there are a few others based on statistical techniques. The two main methods are significant or SMB (Sverdrup, Munk and Bretschneider) method and the other one is

spectrum or PNJ (Pierson, Neuman and James) method. Similar methods were also developed in Great Britain by Darbyshire in 1963 and Wilson.

SMB (Sverdrup, Munk and Bretschneider) Method:

The SMB method was developed for site specific forecasts during world war II for amphibious operations in 1944. In this method the wave forecasting parameters presented are evolved from theoretical considerations, but the actual relationships required certain basic data for the determination of various constants and coefficients. Hence this method is semi-theoretical and semi-empirical.

The SMB method entails two important parameters. They are significant wave height and significant wave period. These two are considered important because around which the wave energy is concentrated.

The significant wave height is the mean or average wave height of the highest one third of all the waves present in the wave train. The significant wave period represents the mean period of the significant wave height.

This method works on duration and fetch limited cases. In the duration limited case, the significant height ($H_{1/3}$) and significant wave period ($P_{1/3}$) depend on the wind duration. In fetch limited case, which is quasi-steady state, the wave dimensions depend upon the fetch. So before forecasting it is necessary to distinguish between these two cases and proceed accordingly. A third case of wind-speed limited also introduced under 'fully developed sea'.

The wave parameters required for SMB method can be obtained from dimensional considerations as detailed below:

The factors on which the wind wave parameters for deep water depend are the wind velocity U, the fetch 'F' and the wind duration 't'. the wave parameters required are wave height 'H' and wave period 'T' such that in deep water the wave length and celerity (velocity) are:

$L = \frac{g}{2\pi} T^2$ and $C = \frac{g}{2\pi}$T

So 'C' and 'H' are functions as below:

C = f_1 (U,F,t, g) …….. (4.60)

H = f_2 (U,F,t, g) …….. (4.61)

The above two equations contain five variables and two dimensional units. Hence equation (4.60) can be written as:

$0 = F_1[(C\,U^a g^b)(F\,U^c g^d)(t\,U^e g^f)]$

Equating to unity the sum of the exponents for the corresponding dimensions we can get

$$0 = F_1\left[\left(\frac{C}{U}\right)\left(\frac{gF}{U^2}\right)\left(\frac{gt}{U}\right)\right]$$

Or

$$\frac{C}{U} = \psi_1\left[\left(\frac{gF}{U^2}\right),\left(\frac{gt}{U}\right)\right] \quad \text{…….. (4.62)}$$

In a similar manner equation (4.61) can be written as:

$$\frac{gH}{U^2} = \psi_2\left[\left(\frac{gF}{U^2}\right),\left(\frac{gt}{U}\right)\right] \quad \text{…….. (4.63)}$$

Equations (4.62) and (4.63) represent the wave generation parameters for deep water, based on dimensional considerations, $\psi_1, and\ \psi_2$ are functional relations that must be determined by the help of wave data.

The quantities $\frac{gH}{U^2}, \frac{C}{U}, \frac{gF}{U^2}$ and $\frac{gt}{U}$ respectively are the parameters of wave height, velocity, fetch and wind duration. The wave speed parameter $\left(\frac{C}{U}\right) = \left(\frac{gt}{2\pi U}\right)$ can also be used as $\frac{gt}{2\pi U}$ as T can be easily measured than the wave speed.

Using the above dimensionless parameters Bretschneider revised the original forecasting relations of Sverdrup and Munk utilizing much additional wave data. So these forecasting relationships have acquired the name SMB method.

Wilson method:

When the state of the sea is limited by fetch (or wind duration) if the fetch is unlimited, one would expect the spectrum. Then the significant wave height and period are the functions of fetch as well as the wind speed. The two variables may be combined by introducing the concept of 'dimensionless fetch' as defined by $\frac{gF}{U^2}$. The prediction equations may then be expressed in dimensionless form, giving the dimensionless significant wave height $\frac{gH_S}{U^2}$ and dimensionless wave velocity $\frac{C}{U}$. Where U is wind speed and H_S is significant wave height. Keeping this concept in view, the following empirical forecasting equations were derived by Wilson in 1966.

$$\frac{C}{U_{10}} = 1.37\left[1 - \left\{1 + 0.008F^{1/3}\right\}\right]^{-5} \quad \text{.....(4.64)}$$

$$\frac{gH_S}{U_{10}^2} = 0.30\left[1 - \left\{1 + 0.004F^{1/2}\right\}\right]^{-2} \quad \text{.....(4.65)}$$

These equations (4.64 & 4.65) are valid only for large values of F. for small values of F the equations given are

$H_S \propto F^{1/2}$ and $T_m \propto F^{1/3}$

Where T_m is the period corresponding to the maximum frequency.

Darbyshire method:

Most wave prediction schemes have been developed for waves generated in deep water. So Darbyshire (1963) deduced that there were significant differences in the properties of waves generated in deep and shallow waters for the same speed and fetch. Therefore he produced separate prediction schemes for the two cases. So he prepared nomograms that gives prediction for significant wave height and zero upcrossing period (T_Z) in coastal waters (shallow waters) as functions of wind speed and fetch or duration. Nomograms also were prepared for prediction of deep water waves separately by PNJ (1955), Bretschneider (1970) and Darbyshire (1963). The nomograms of Darbyshire (1963) for fetch limited and duration limited cases are as shown in Fig.4.38 and 4.39 respectively.

How to use this Nomogram for prediction:

To predict the wave height, enter with wind speed at left hand side, move across until the limiting fetch (ordinate) or duration (dashed lines) whichever is reached first. Then estimate the height between the two solid wave height curves.

Problem: a) Fetch limited case:

Estimate the significant wave height if a wind speed of 30 m/s blows for 36 hours over an extent of 300 km.

Ans:

Starting with 30 m/s on left hand side ordinate and proceed towards right hand side until either F = 300 km or t = 36 hrs whichever first is reached. When we proceed along 30 horizontal first it touches 300 km ordinate as 36 hrs dashed line is far ahead (which is not shown in the nomogram). The point of intersection of 30 m/s and 300 km is in between 8 and 10 m solid curves. As it is close to 8 m, it may be around 8.3 m.

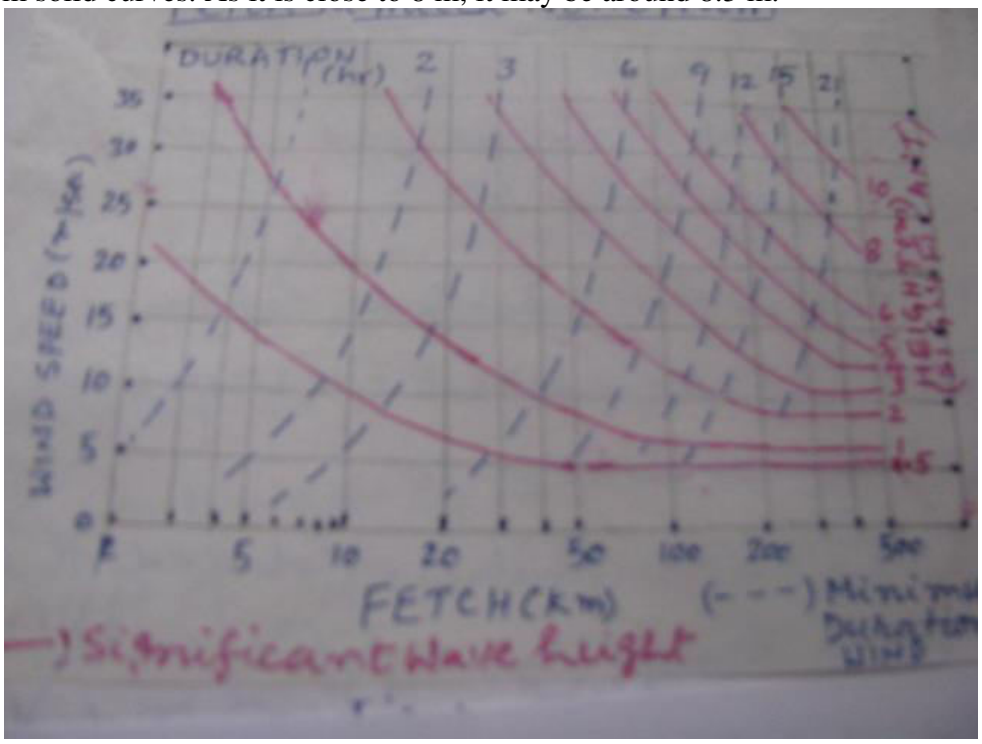

Fig.4.38. Fetch limited Nomogram for prediction of significant wave height (Deep water wave forecasting curves). red curves: Significant wave height; dashed curves: Minimum duration (hrs) lines.

b) Duration limited case:

Find the significant wave height and period if the wind speed is 30 m/s blown over a stretch of 1000 km for 21 hours.

Ans:

Taking the wind speed 30 m/s move horizontally in the duration limited nomogram (Fig.2). Then we can find that t = 21 hrs is reached first as 1000 km fetch is farther off. So the meeting point of 30 m/s and 21 seconds is on 11 seconds significant period. Hence significant wave period is T_S = 11 seconds.

From Fig.1 we can find significant wave height using wind speed 30 m/s and significant wave period duration 11 seconds. The meeting point of 30 m/s and 11 seconds is between 6 and 8 m curves which comes to 6.5 m.

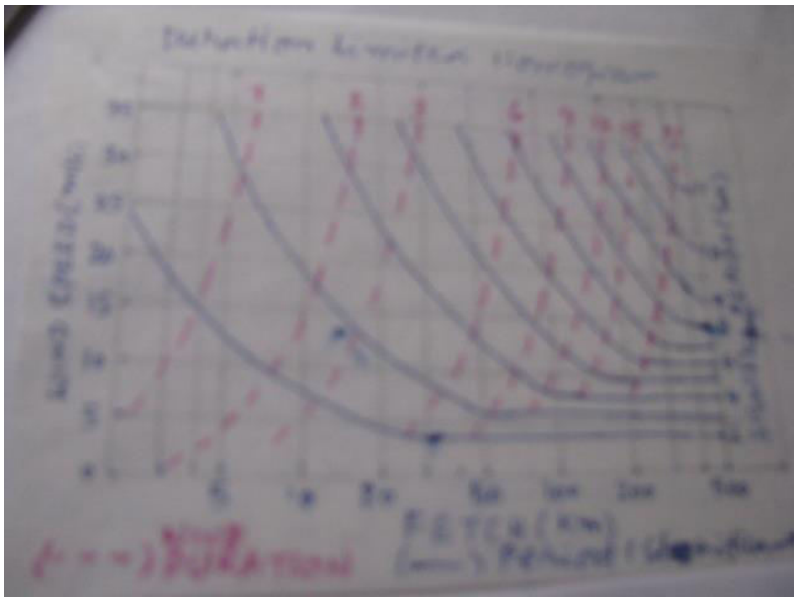

Fig.4.38: Nomogram for duration limited case for prediction of significant wave height (Deep water wave forecasting curves).

PNJ method or Spectrum method of wave forecasting

Prior to the development of PNJ method, Neumann proposed a theoretical wave spectrum based on a great abundance of individual wave observations. From the wind and wave observations, Neumann computed the parameters H/T^2 and T/U and derived the relation:

$$\frac{H}{gT^2} = Constant\ e^{-\{\frac{gT}{2\pi U}\}^2}$$

The parameter H/T^2 is related to wave steepness and T/U is related to the wave age. Where H is wave height, U the wind speed and T is the individual apparent wave period which is defined as the time between two successive zero up-crossings of the wave spectrum.

From this empirical relationship, Neumann derived the theoretical spectrum of wave energy 'E' called 'one number'. From these results he concludes for unlimited fetch and duration for a fully developed sea, the wave height is equal to some constant times the wind velocity to the power of 5/2.

$$H = constant\ U^{5/2}$$

The concept of the wave spectrum is certainly a great advance in trying to understand the nature of wave generation. It is shown that the waves generate from the high frequency side of the spectrum and with this concept the relationships for the young and the transient state of the sea can be derived. That is, these developed relations are called co-cumulative power spectra from which 'E' values can be predicted.

Longuet-Higgins later derived the theoretical wave distribution that is related to E-values as:

Average wave height data (in feet)

i) The most frequent wave height = $1.41\sqrt{E}$

ii) The average wave height (H) = 1.772 $\sqrt{E}$

iii) Significant wave height $(H_{1/3})$ = 2.832 $\sqrt{E}$

iv) Average of the height of 1/10 th of the highest waves $(H_{1/10})$ = 3.600 $\sqrt{E}$

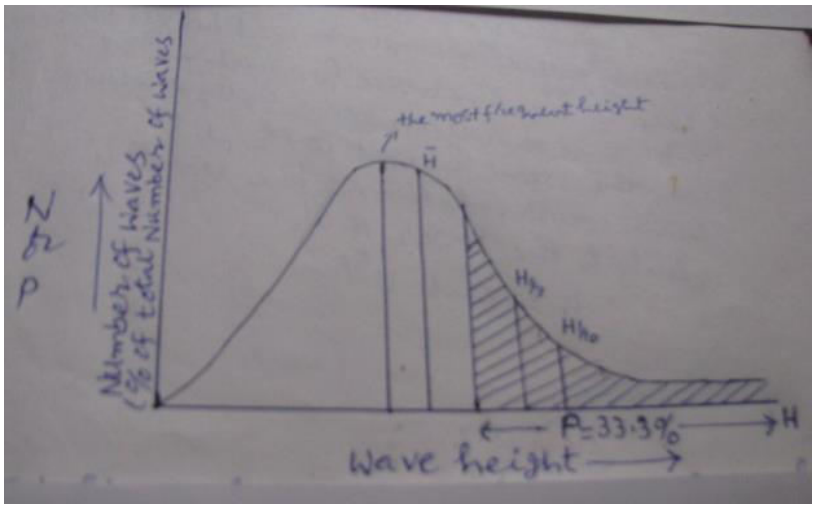

Fig.4.39 Distribution of different wave heights in a histograph

The Figure (4.39) shows the distribution of wave heights in a histograph which is a graph of number of waves (or percentage of total waves) in each wave height range.

The significant wave description is a simple and practical means of dealing with problems in wave forecasting. As the waves in the sea are very complex and made up of many variable heights and periods, one important wave height which represents the spectrum is important, that is significant wave height as shown in the above figure.

The significant wave height is the average of the highest one third of the waves in a given wave train which is a statistical parameter used by both SMB and PNJ methods. Whereas the significant wave period is the average period of the highest one-third wave heights and is used only by SMB method while PNJ uses a mean apparent wave period and ranges in wave period.

Further the average wave height ($\overline{H}$), the significant wave height $(H_{1/3})$ and the average of the highest 10% of waves $(H_{1/10})$ are related as:

$$(\overline{H}) = 0.625\, H_{1/3}$$

$$H_{1/10} = 2.03\, \overline{H} = 1.27\, H_{1/3}$$

Longuet-Higgins found these relations and said about 16 or 17% of the waves will be higher than the significant wave height.

Material needed for wave forecasting according to PNJ:

1. Weather map and weather data
2. Co-cumulative spectra
3. Dispersion diagrams
4. Angular spreading factor diagrams
5. Height table

Steps in preparing a wave forecast:

1. Analyze the weather map
2. Forecast the Co-cumulative spectrum in the storm area
3. Determine the type of storm and filter required and evaluate observed quantities needed for the filter.
4. Evaluate θ_4 and θ_3
5. Evaluate angular spreading factor
6. For various times of observation find frequency and range of periods present.
7. Find the value of 'E' present at point of observation owing to the effect of dispersion by subtracting the value of 'E' at the upper frequency from the value of E at the lower frequency.
8. Multiply by angular spreading factor to find the forecast value of E.
9. From E compute the needed height data like significant, most frequent, average or 1/10 th of the height using Longuet-Higgins statistics.

Calculation of 'one number' E:

To compute E, the value of the wave records is read off at a hundred or so equally spaced points with any arbitrary zero reference level. An average value is computed from these values and this average is subtracted from each of the original readings. Then each resultant number is squared and then the total is found. Then this total if multiplied by two is called the number 'E'.

Example,

Let suppose the wave data is n_1 n_2, n_3, and so on upto n_i. Then the average of these values is say $\bar{n}$. Then the difference of average from each of the wave data is $(n_i - \bar{n})$. Then the square of the difference is $(n_i - \bar{n})^2$. Then twice the sum of the squares of all values (variance)is "E"

$$E = 2\left[\sum_{i=1}^{i}(n_i - \bar{n})^2\right]$$

Problem:

Calculate ($\bar{H}$), $(H_{1/3})$, and $(H_{1/10})$ for the following data

Wave height	1	2	3	4	5	6	7	8
Number of waves	7	33	30	20	7	3	1	1

Ans:

S.No	Wave height	No. of waves	Cumulative value	Wave height × Number of waves	$H_{1/3}$	$H_{1/10}$
1.	1	7	102	1× 7 = 7		
2.	2	33	102-7=95	2×33 = 66		
3.	3	30 (28 + 2)	95-33=62	3×30=90	3×2=6	
4.	4	20	62-30=32	4×20=80	4×20=80	
5	5	7	32-20=12	5×7=35	5×7=35	5×5=25
6	6	3	12-7=5	6×3=18	6×3=18	6×3=18
7	7	1	5-3=2	7×1=7	7×1=7	7×1=7
8	8	1	2-1=1	8×1=8	8×1=8	8×1=8
Total		102		311	102/3=34	

Average wave height = 311/102 = 3.0 ft.

Significant wave height H1/3 (102/3 =34) = $\frac{6+80+35+18+7+8}{(2+20+7+3+1+1)\div 3} = \frac{154}{34}$ = 4.5 ft.

Average height of 1/10 th of highest H1/10 = $\frac{25+18+7+8}{5+3+1+1)} = \frac{58}{10}$ = 5.8 ft

Reliability and limitation in wave forecasting methods:

The value of the day-to-day forecasts has been subject to criticism by marine operators due to their consistencies and so they must be used with caution.

On comparing the two methods of SMB and PNJ, no method is appreciably better than the other. It is difficult to compare the results of the two methods forecasting, as each set of forecasting curves is based largely upon its own set of original data and none of which can be considered to be adequate. There is no theoretical set of forecasting curves. These empirical and semi-empirical procedures rely on physical measurements. These physical measurements in the open ocean are few and unreliable. Infact there is not much difference between the spectrum method and significant method as far as the results are concerned.

Though at present considerable data has been obtained and used for the open ocean wave forecasting according to SMB method, still it is difficult to make reliable predictions for large fetches. The scatter of data is large and so it is difficult to see how predictions can be made more reliable. Additional information on the effect of air-sea temperature difference will improve the forecasts in future.

The relationships among winds and sea are not precise, especially when considering the moving fetches (moving storms) and varying wind fields. The numerical effects of these must be determined and incorporated in the wave forecasting data for a reliable forecast.

Lecture Series of Berhampur University in Physical Oceanography
By Prof.A.S.N.Murty
Chapter – 7

OCEAN TIDES

The tides are the longest oceanic waves and are characterized by the rhythmic rise and fall of sea-level over a period of half a day (called semi diurnal tides) or a day (called diurnal tides). The oceanic tides on earth are caused due to gravitational attraction of Sun and moon. The rising tide is usually referred to as the flood tide and the falling tide is called as the ebb tide. Figure 2.1 is a tidal record, showing regular vertical movements of the water surface relative to a mean level, over a period of about a month.

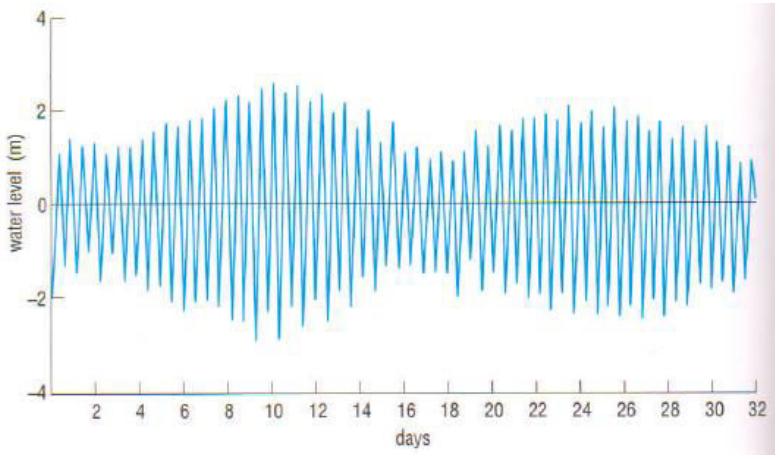

Fig.1. A typical 30-day semi diurnal tidal record showing oscillations in water level with a period of about 12.5 hours

Tide Producing force:

The tide producing force (hatched thick arrow in Fig.2) is the resultant force between gravitational and centrifugal forces between earth and moon.

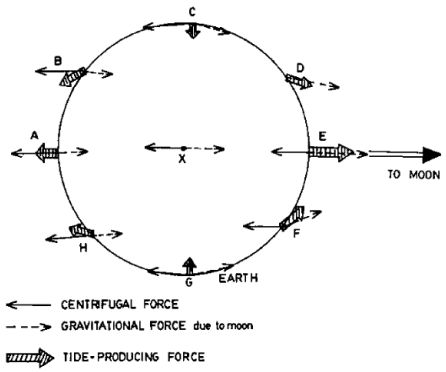

Fig.2 Tide producing force is the resultant of gravitational and centrifugal forces between earth and moon

From Figure 2 above it is clear that the magnitude of the gravitational force exerted by the moon on the earth is not the same at all points on earth, because all

these points are not at the same distance from the moon. While the gravitational force of the moon is largest at point 'E', it is the weakest at point 'A' as Point E is closest and A is farthest from the moon. So while the gravitational force is dominant in one half of the earth facing the moon, the centrifugal force is dominant than gravitational force in the other half of the earth away from the moon. In addition, the direction of the moon's gravitational force at all points on the earth is directed towards the center of the moon. So only on the equatorial diameter the gravitational force (dashed arrow in Fig.2) is straight and at other places it is inclined. As the tide producing force (hatched thick arrow in Fig.2) is the difference between gravitational and centrifugal forces, it also is directed in the same way as that of gravitational force.

Similarly Sun also acts in the same way on the earth's surface. But as the Sun is far away its influence is relatively small when compared to that of the moon.

Computation of tide producing force at any latitude:

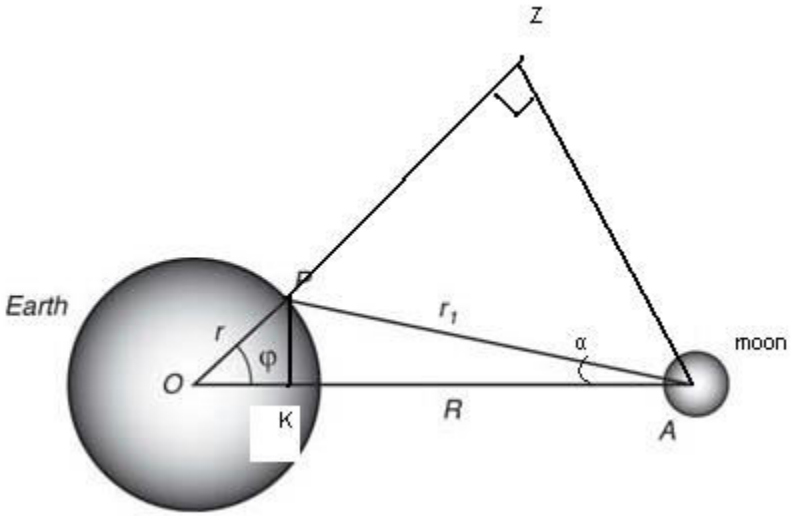

Fig.3.Computation of Tide producing force at any latitude

From the figure, let 'P' be any point on the earth's surface at which tide producing force is to be calculated. Let O and A denote the centers of the earth and the moon respectively. Other abbreviations are as mentioned in the figure.

Attraction of moon at point O of the particle 'μ' on the earth (OA) = $\frac{G\mu m}{R^2}$ ……(1.7.5)

Attraction of moon at point 'P' on mass 'μ' (PA) = $\frac{G\mu m}{r_1^2}$ ……..(1.7.6)

Where 'R' and 'r_1' are the distances of points O and P from A.

Let each of these forces are resolved into a vertical component along the radius OP and a horizontal component perpendicular to it in the plane OPA. Denoting the angles AOP and OAP as φ and α respectively, we can write equations (1.7.5) and (1.7.6) as

Attraction at O in the direction OP (radial or vertical component) = $\frac{G\mu m}{R^2}\cos\varphi$ ….(1.7.7)

Attraction at O perpendicular to OP (tangential or horizontal component = $\frac{G\mu m}{R^2}Sin\varphi$ …….(1.7.8)

Attraction at P in the direction P to Z(where 'Z' is extension of OP) =

(Vertical, PZ) = PM cos (α + φ) = $\frac{G\mu m}{r_1^{\,2}}Cos(\alpha+\varphi)$ ……(1.7.9)

Attraction at P perpendicular to the direction P to Z =

(horizontal PZ) = $\frac{G\mu m}{r_1^{\,2}}Sin(\alpha+\varphi)$ ……(!.7.10)

The attraction at point O, center of the earth of equations (1.7.7) and (1.7.8) shows the centrifugal forces of the earth. As the tide generating force is the difference between gravitational attraction and the centrifugal forces, we get tide generating forces by subtracting equation (1.7.7) from (1.7.9) for vertical component and equation (1.7.8) from (1.7.10) for horizontal component.

$$F_V = Gm\mu\left[\frac{Cos(\alpha+\varphi)}{r_1^{\,2}} - \frac{Cos\varphi}{R^2}\right] \quad \ldots\ldots\ldots\ldots \quad (1.7.11)$$

$$F_H = Gm\mu\left[\frac{Sin(\alpha+\varphi)}{r_1^{\,2}} - \frac{Sin\varphi}{R^2}\right] \quad \ldots\ldots\ldots\ldots\ldots\ldots (1.7.12)$$

Since the angle α is very small for all practical purposes we can write PA = KA or if we substitute the projection of r_1 on R, we can write KA = R – r cosφ, where r is the radius of the earth taken as unity as it is very small compared to R.

Further from right angled triangle PZA,

$$\text{Cos}\,(\alpha+\varphi) = \frac{PZ}{PA} = \frac{OZ-OP}{KA} = \frac{R\cos\varphi - r}{R - r\cos\varphi} \quad \ldots\ldots.(1.7.13)$$

$$\text{Similarly, } \sin(\alpha+\varphi) = \frac{ZO}{PO} = \frac{R\sin\varphi}{R - r\cos\varphi} \quad \ldots\ldots\ldots\ldots\ldots\ldots\ldots..(1.7.14)$$

Substituting equation (1.7.13) in (1.7.11) we get,

$$F_V = Gm\mu\left[\frac{R\cos\varphi - r}{(R - r\cos\varphi)^3} - \frac{Cos\varphi}{R^2}\right]$$

$$= \frac{Gm\mu}{R^3}\left[\frac{R\cos\varphi - r}{\left(1 - \frac{r^3}{R^3}\cos^3\varphi - 3\frac{r}{R}\cos\varphi + 3\frac{r^2}{R^2}\cos^2\varphi\right)} - \frac{Cos\varphi}{1}\right]$$

Neglecting the higher order terms of $\frac{r}{R}$ as 'r' is negligibly small compared to 'R'

$F_V = \frac{Gm\mu}{R^3}\left[\frac{r(3\cos^2\varphi - 1)}{\left(1 - 3\frac{r}{R}\cos\varphi\right)}\right]$ neglecting again $\frac{r}{R}$ term we get

$$= \frac{Gm\mu}{R^3}\left[\frac{r(3\cos^2\varphi - 1)}{(1)}\right]$$

$F_V = \frac{Gm\mu}{R^3}3\left(\cos^2\varphi - \frac{1}{3}\right)$ ($\because$ r is taken as unity) ……..(1.7.15)

Similarly substituting equation (1.7.14) in (1.7.12) and simplifying we get

$F_H = \frac{Gm\mu}{R^3}\frac{3}{2}\sin 2\varphi$ .. …… (1.7.16)

These formulae (eqns 1.7.15 and 1.7.16) show that the tide producing force of the moon at any point on the earth depends on the zenith angle of the moon (φ) and the moon's distance from the earth (R). As the R value at perigee (357,000 km) and apogee (407,000) is different tidal forcing is not constant always.

The vertical component F_V attains its maximum value at $\varphi = 0$ and 180^o when the moon is in zenith and Nadir points (from equation 1.7.15).

The horizontal component F_H attains its maximum value when $2\varphi = 90^o$ or 270^o or $\varphi = 45^0$ or 135^o (from equation 1.7.16).

The vertical component of tide producing force (F_V) is in the same direction of gravitation and therefore it doesn't have any effect on the water particle and so is neglected. Whereas the horizontal component of the tide producing force (F_H) will not be affected by gravity and so it will tend to drag the water particle in the ocean horizontally. This is called the tractive force.

Fig.4a shows how the horizontal component of the tide producing force is distributed over the earth's surface when the moon is on the equatorial plane. In Fig.4b the water particles facing the moon are dragged towards it and the other particles (shaded area) are dragged away from it. On any latitudinal circle (A_1A_5) the variation of tractive force is significant (Fig.4b). At point A_2 facing the moon it is directed south. When the point has moved to point A_4 the force is zero and when it has moved to A_5 the force is again equal and opposite. This explains why two high tides (A_2 and A_5) occur and two low tides (A_4 and its opposite) occur in one full rotation of the earth.

The sun produces a similar effect but relatively small tide producing force compared to the moon due to far off distance. When the two forces of sun and moon coincide it produces a maximum tide generating force and it is called spring tide. This happens twice during a period of 29.5 days. When these two bodies act at right angles the tide generating force is least. This least (minimum) force produces neap tide. This also happens twice during 29.5 days.

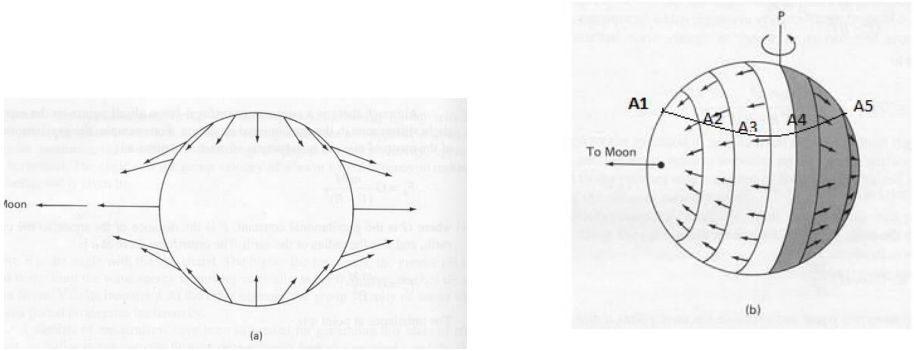

Fig.4.a) Distribution of the total tide generating forces for a cross section of the earth. b) the horizontal component of the tide generating force at the earth's surface

Types of Tide:

There are different types of tides. Low tide, High tide, diurnal, semidiurnal and mixed type of tide, spring tide and neap tide etc..

Along the coast of Africa as shown in Fig.5, the tides are semidiurnal and the range increases from Cape Town, South Africa (1.8 m) to Daressalam,Tanzania (4m). The tidal range grandually increases from the coast of Egypt (Suez) to Aden, Oman (Muscat) and Iraq (Shat –Al-Arab) while at Bushire (Iran coast) it decreases.

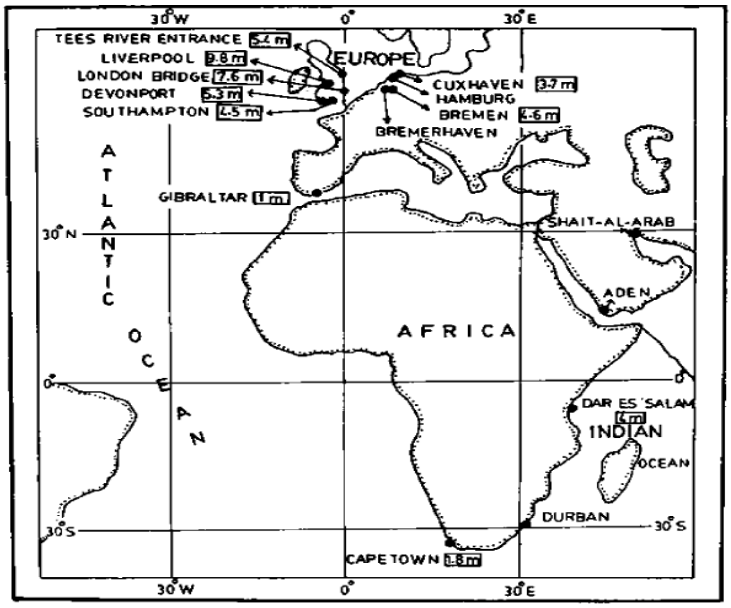

Fig. 5.Tidal ranges along the coast of Africa and Middle East

With regard to the number of times of occurrences of tide they are classified as Diuranl, semidiurnal and mixed type. If one High tide and one Low tide occur in a day (24 hours) it is called diurnal and if two high and two low tides occur in a day (fig.7) then they are called semidiurnal tides. If both are mixed they are called mixed tides as shown in Fig.6

For example,

i) Immingham (England), semidiurnal

ii) SanFrancisco (U.S.A), mixed type but dominant semidiurnal

iii) Manila (Phillippines), mixed type but dominant diurnal type.

iv) Do-San (Vietnam), full diurnal type. Here the period from one high tide to next high tide is 24 hours 50 minutes.

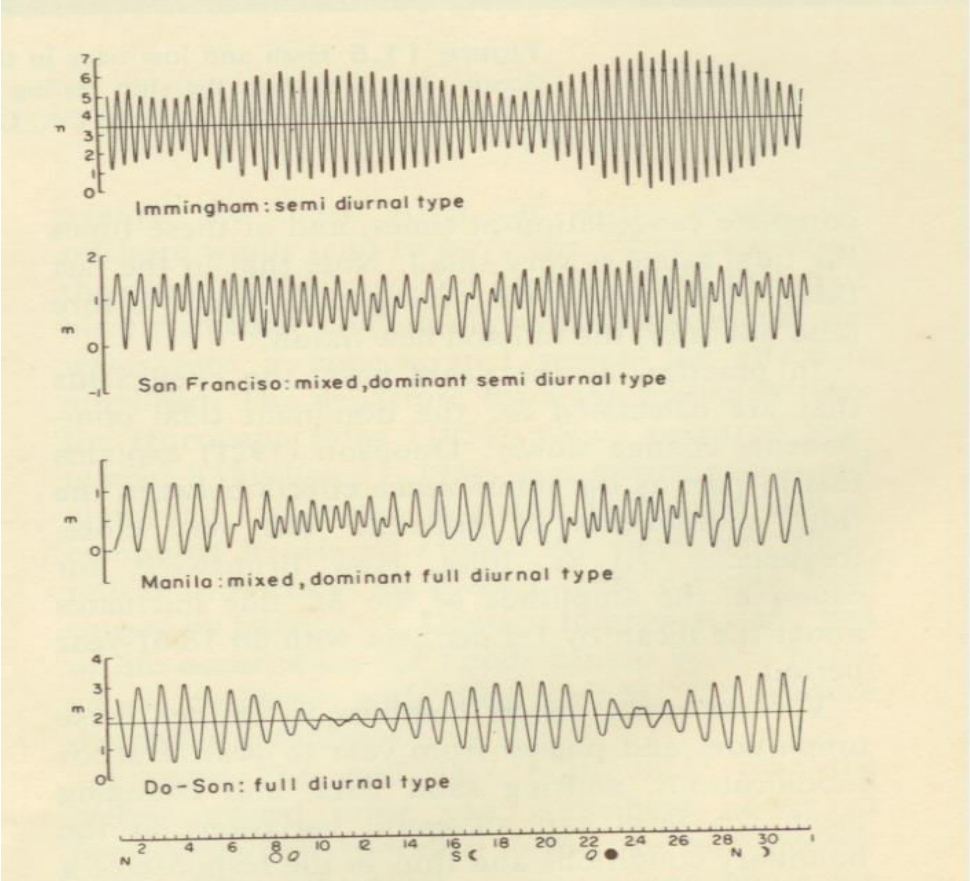

Fig.6.Example of shape of tidal curves in case of semidiurnal, diurnal and mixed tides at different palces. The phases of the moon are indicated on the days in the x axis. 'N' shows the maximum northern declination of the moon; 'S' shows the maximum southern declination and 'Q' the time when the moon crosses the equator.

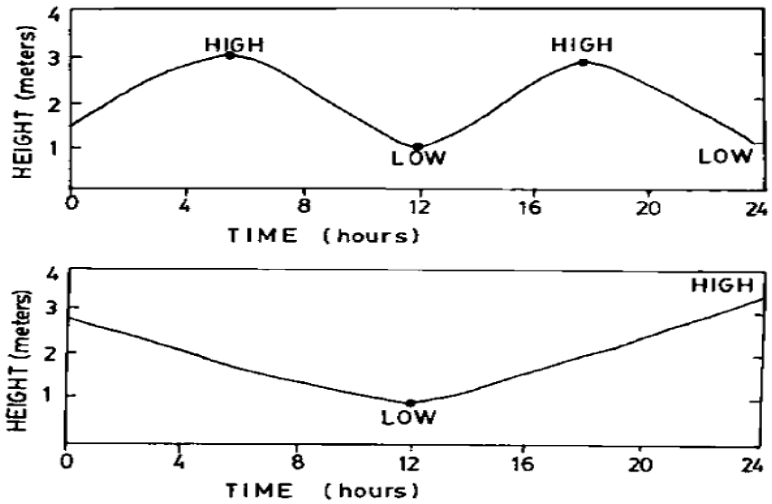

Fig.7. Shapes of semidiurnal and diurnal tidal curves in a day

At any place, the tide generally has two cycles in a lunar month (29.5 days). In the lunar month, the earth faces full or new moon and the moon is in quadrants. When the

moon is full or new, we get spring tides (highest tides) and when the moon is in quadrants, we get neap tides (Lowest tides) as shown in Fig.8.

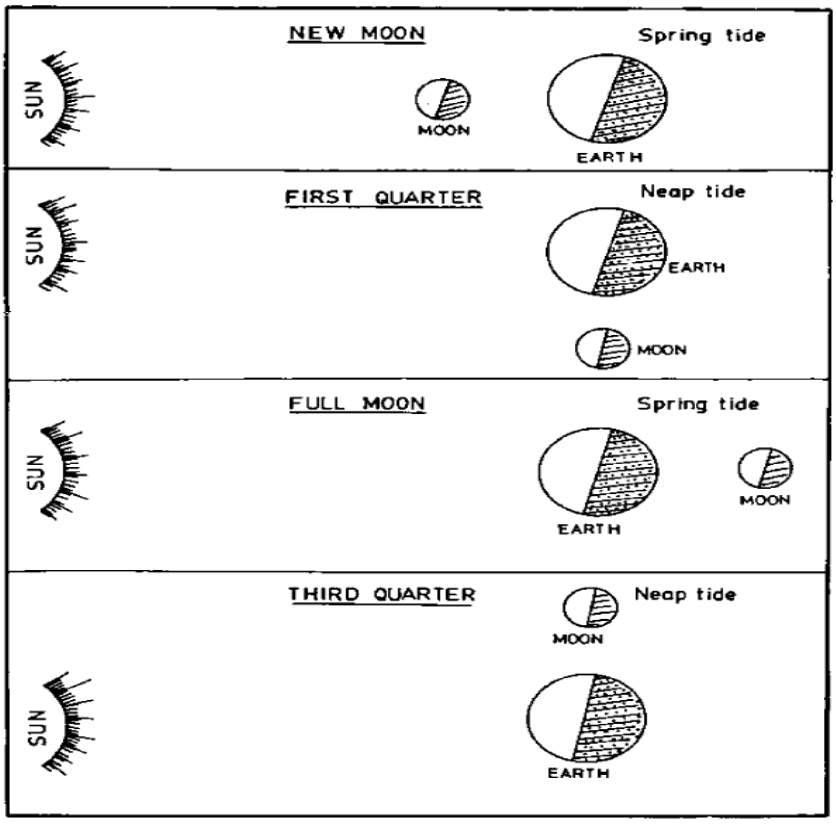

Fig.8. Spring and neap tides depending on the position of the moon

Interaction of Solar & Lunar tides:

In order to understand the interaction between solar and lunar tides, Fig.9 may be considered. In Figure 2.12(a) and (c),the tide-generating forces of the Sun and Moon are acting in the same directions, and the solar and lunar equilibrium tides coincide, i.e. they are in phase, so that they reinforce (anhance) each other. So the tidal range produced is larger than the average, i.e. the high tide is higher and the low tide is lower. Such tides are known as spring tides. When spring tides occur, the Sun and
Moon are said to be either in *conjunction* (at new Moon - Figure 2.12(a)) or in *opposition* (at full Moon - Figure 2.12(c)).

On the other hand in Figure 2.12(b) and (d), the Sun and Moon act at right angles to each other, the solar and lunar tides are out of phase, and do not reinforce each other. The tidal range is correspondingly smaller than average. These tides are known as neap tides, and the Moon is said to be in **quadrature** when neap tides occur. The complete cycle of events in Figure 2.12 takes 29.5 days.

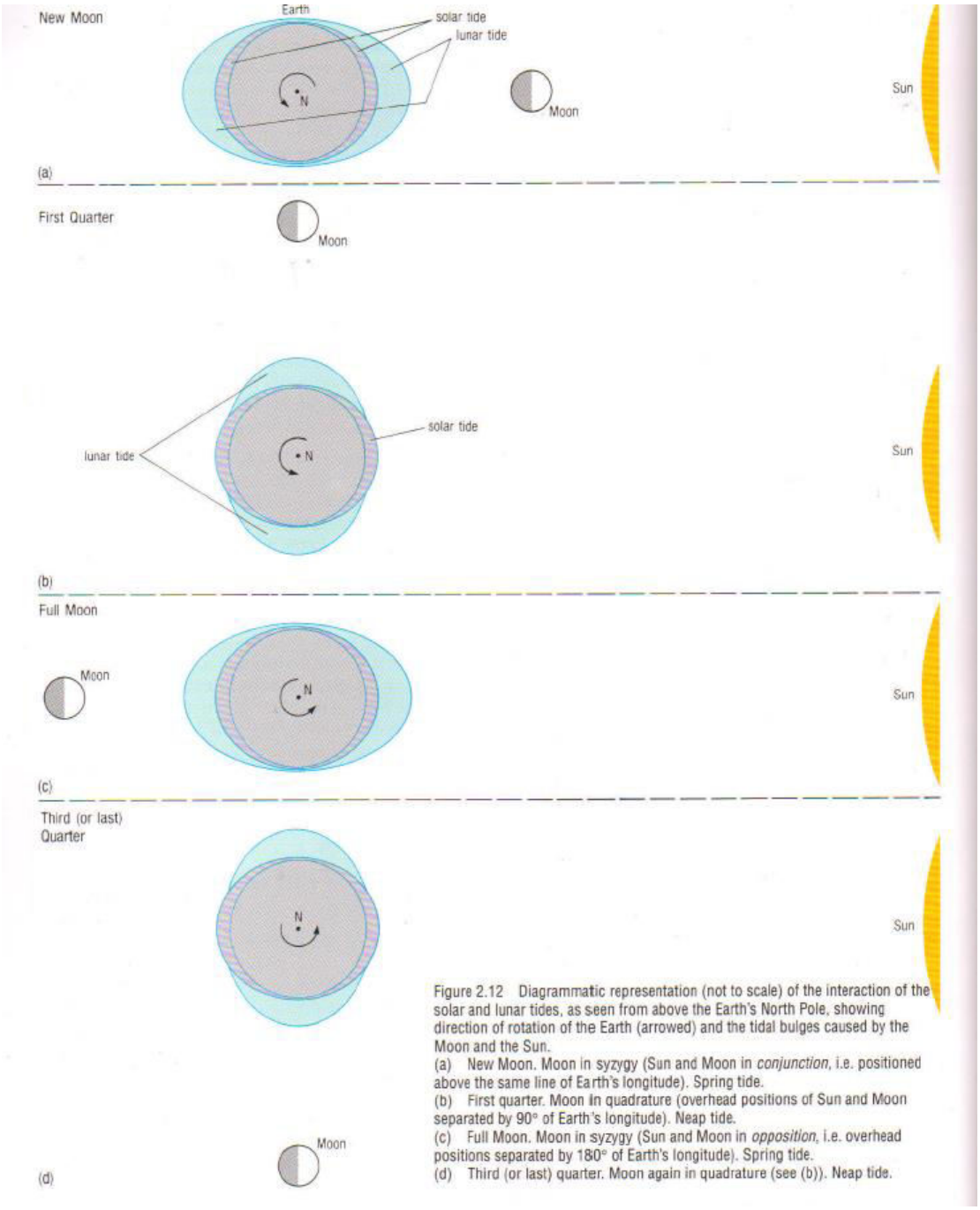

Figure 2.12 Diagrammatic representation (not to scale) of the interaction of the solar and lunar tides, as seen from above the Earth's North Pole, showing direction of rotation of the Earth (arrowed) and the tidal bulges caused by the Moon and the Sun.
(a) New Moon. Moon in syzygy (Sun and Moon in *conjunction*, i.e. positioned above the same line of Earth's longitude). Spring tide.
(b) First quarter. Moon in quadrature (overhead positions of Sun and Moon separated by 90° of Earth's longitude). Neap tide.
(c) Full Moon. Moon in syzygy (Sun and Moon in *opposition*, i.e. overhead positions separated by 180° of Earth's longitude). Spring tide.
(d) Third (or last) quarter. Moon again in quadrature (see (b)). Neap tide.

Fig.9.Interaction of solar and lunar tides as seen from above the earth's north pole. a) New moon: Spring tide; b) First quarter: Neap tide; c) Full moon: Spring tide; d0 third or last quarter: Neap tide.

Measurement of Tide:

Tides are measured using an instrument called tide gauge as shown in Figure.14

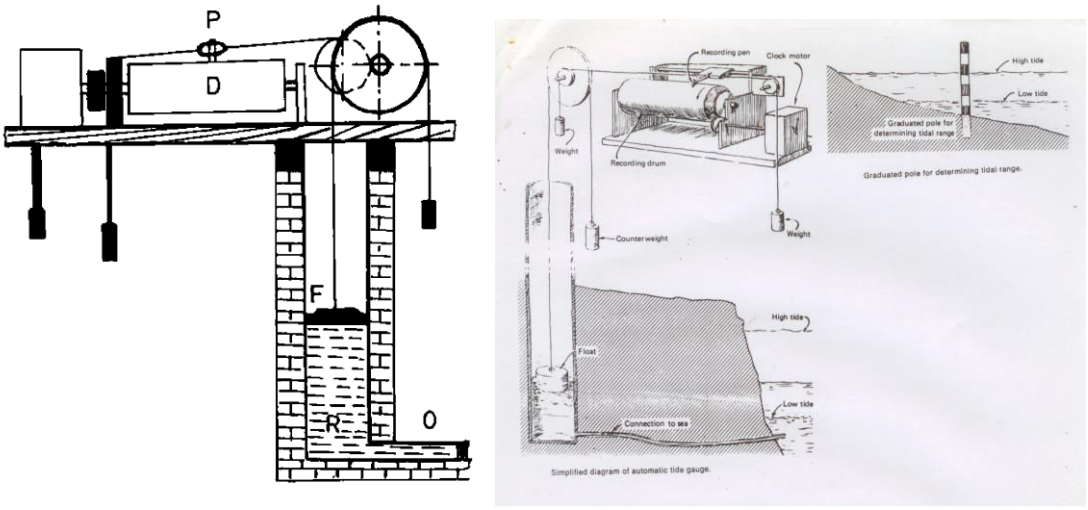

Fig.10. Tide gauge and its parts.

The tide gauge shown in Fig.10 consists of a float (F), which operates in the float well (R), to which the slow moving tide has free access. The more rapid waves caused by winds are filtered out by means of the relatively small size of the pipe (canal) (O) connecting the well to the ocean. The rising and falling of the float (F) turns a screw on the gauge which moves a pen (P) to and fro across a wide strip of paper on a drum (D) which is moved forward by clockwork. The combined motion of pen and paper gives a continuous graph showing the rise and fall of the tide. Generally this entire assembly will be housed in a shelter as shown in Fig.11. This shelter is built on a pier (a bridge type in the ocean bank). The graph drawn by the tide gauge is monthly and so every month the chart is to be changed.

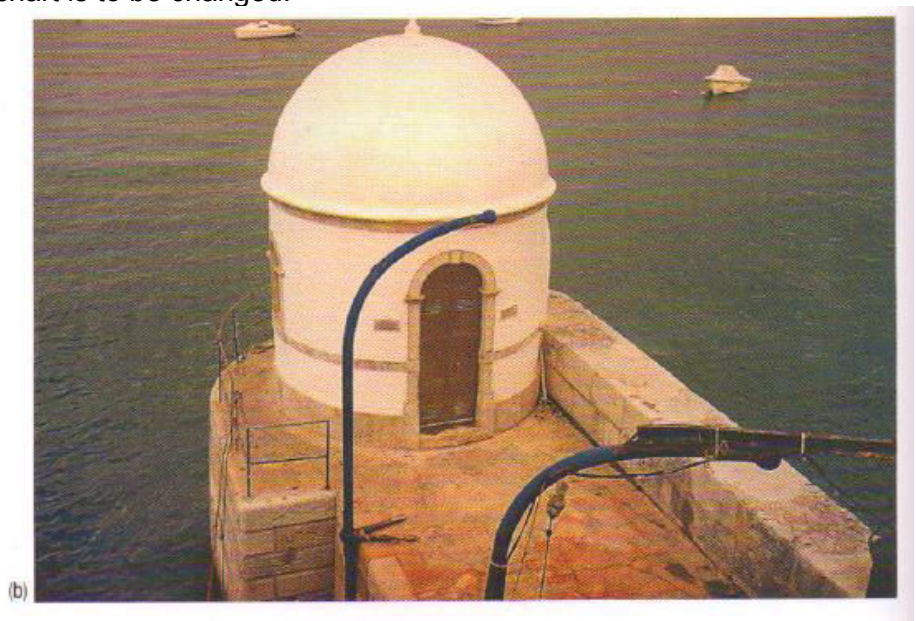

Fig.11. The pier (bridge) and the house where the tide-guage is kept in the back waters of the ocean.

Tide predicting machine:

Using the tide predicting machine shown in Fig.12a, tides can be predicted in advance. Usually yearly tidal heights and times of occurrence at each important coastal place are predicted and published in a book. This information is highly useful for navigators in the

ocean. It uses a harmonic equation for prediction. Each circle shown in the machine is a key for each partial tide M_2, S_2, K_1, O_1 etc. Depending upon the speed of each partial

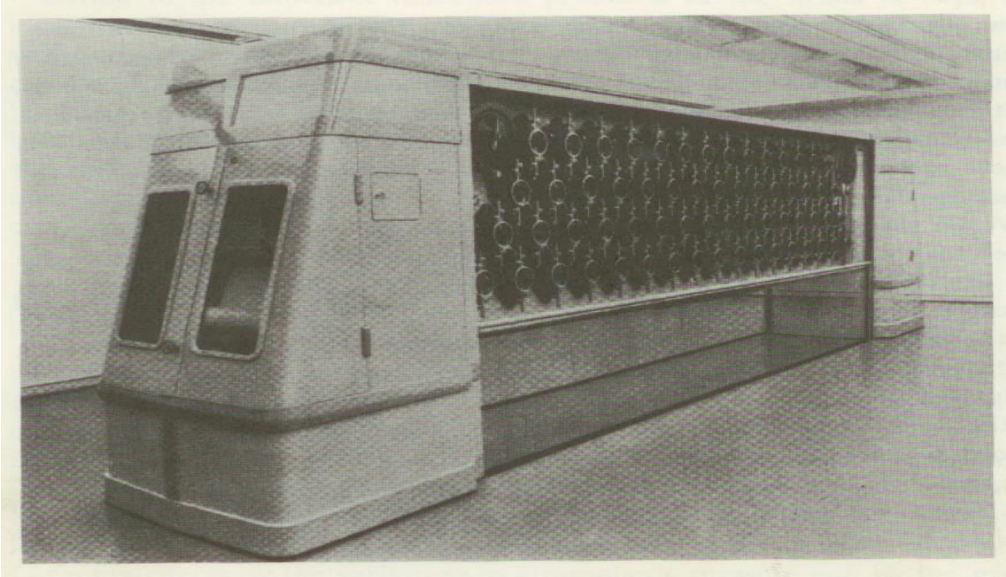

Fig.12.(a) Large Kelvin tide predicting machine located at Survey of India, Dehra Dun, India.

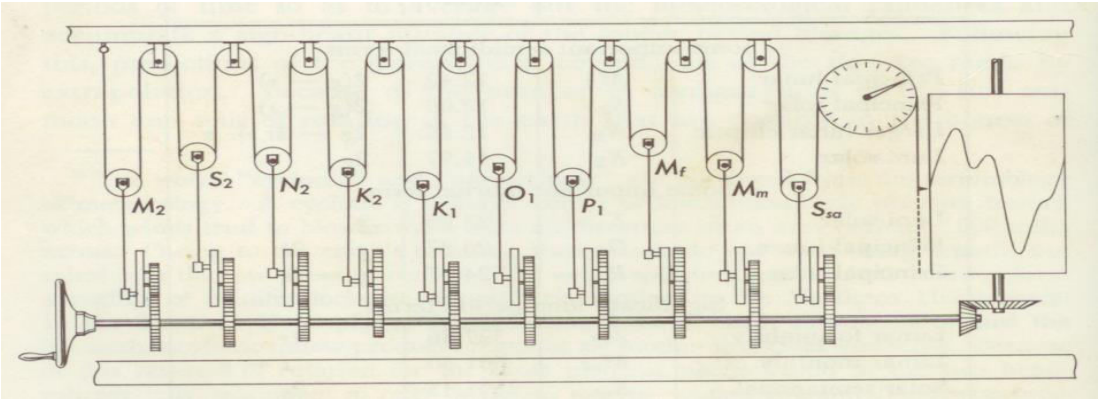

Fig.12 (b) Arrangement of the working parts of different pulleys for different partial tides in the Kelvin tide predicting machine.

Tide, each pulley (Fig.12b) is rotated that many times and finally a chart will be drawn by the pen and clock drum attached to the machine. The curve drawn on the chart by the machine is the tide predicting chart. Using this tide chart, time, height of the tide can be obtained and published in a book format. But now a days nobody is using this tide predicting machine and the tidal predictions are done using a super computer.

Tidal maps:

Tide waves run around in circles (clockwise and counter clock wise in both hemispheres) around islands, and certain other points in the sea, called **nodes**. The map shown in Fig. 13 here shows the tides circling around their nodes in 30º increments (12 parts to 25/2 hours) in the directions of the solid arrows. Each solid line connects tide levels in the ocean that are at the same phase. The dotted lines show tide amplitude (half tide height) in cm. This early model has been shown to agree with reality and, for its time, has been a remarkable achievement of computational mathematics. From this map one can see that some places in the world (the nodes) have no tides, others have two (12 lines) and a few other places one (24 lines).

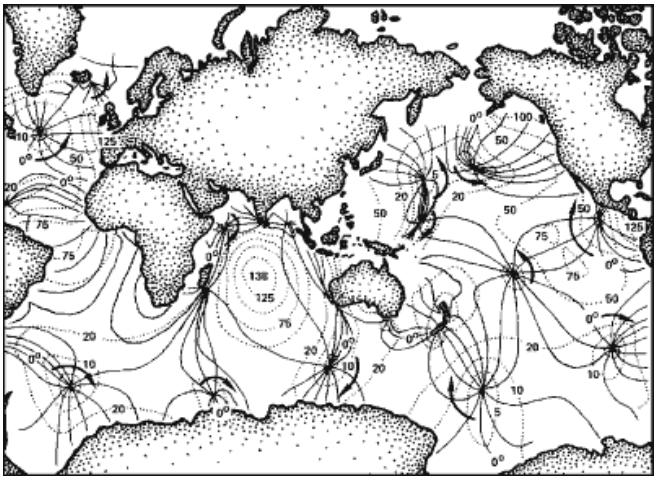

Fig.13 Tidal chart of the world.

Since the TOPEX/Poseidon satellite has been measuring surface height data, the oscillating surface of the oceans due to moon tides could be measured and mapped (Fig.14). Note that the nodes correlate with areas of no tide change, except where these rotate around islands such as New Zealand and Madagascar. Highest tidal ranges are found where continental coasts distort the tide wave.

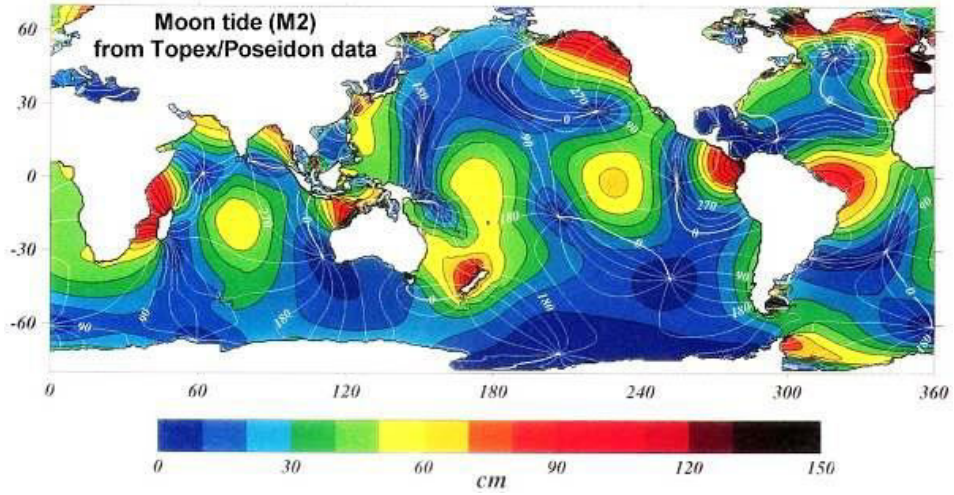

Fig.14.M2 tide obtained from the Topex/Poseidon satellite data. Note high tidal ranges are found in the south east coast of Africa.

Tidal characteristics:

- Tide waves follow shorter paths in twelve hour rotations, **never exceeding the maximum wave speed** of about 800 km/hr.
- Tide waves **do not bounce off continents** by hitting them squarely. Instead, they follow along their coasts.
- There is **no starting and stopping** but a continuous motion. The standing waves absorb minimal energy.
- There is **no balancing bulge**. Instead, tide waves run in twelve hour circles.
- There can be **none, one or two tides per day**.
- The **time of high tide depends both on the lunar cycle and the place on Earth**.
- Tide waves are **standing waves**, expending the least energy.

Tidal effects and natural impacts:

- Without tides, dunes cannot form. Tides expose sea sand to the wind, which blows it into dunes.
- Tides create an area of rocky shore where specialized organisms have evolved. Tides thus increase the biodiversity of the coast (limpets, barnacles, oysters, etc.)
- Tides create large areas for specialized organisms within harbours and embayments (sand and mud flats, mangroves, etc.). Such areas may act as nurseries for various marine species.
- Tides create currents that mix the water so that surface plankton is spread and bottom nutrients re-surface. This makes plankton available throughout the year.
- Tides create currents that transport plankton to sessile filter feeders such as clams, sponges, seasquirts, etc. It creates very rich habitats where currents pass.
- Tides create currents that transport and mix coastal sediments. Without them, the coast would be more sensitive to sewage disposal and runoff from the land. It would support fewer people.

Lecture Series of Berhampur University in Physical Oceanography
By Prof.A.S.N.Murty

Chapter – 8

Rossby & Kelvin waves in the oceans

Rossby waves in the oceans:

Kelvin waves are relatively fast. But there are slower waves in nature under rotating homogeneous fluids.

For large wave formations (such as cyclonic and anticyclonic vortices and Gulf stream meanders), it is necessary to consider the meridional change in 'f'.

We know $f = 2\Omega \sin\phi$

If the y coordinate is oriented in the meridional direction and is measured from a reference latitude ϕ_0 (some where in the middle of the wave) then

$$\phi = \phi_0 + \frac{y}{a} \quad \ldots\ldots\ldots\ldots\ldots\ldots\ldots\ldots(1)$$

Where a is the radius of the earth (6371 km). Then equation (1) can be expanded using Taylor's series as

$f = f_0 + \frac{\partial f_0}{\partial \phi}\Delta\phi + \frac{\partial^2 f_0}{\partial \phi^2}\frac{(\Delta\phi)^2}{\angle 2} + \ldots..$ Limiting upto terms in the right hand side

$$f = f_0 + \frac{\partial f_0}{\partial \phi}\Delta\phi = 2\Omega\sin\phi_0 + 2\Omega\cos\phi_0\frac{y}{a}$$

$$f = f_0 + \beta_0 y \quad \ldots\ldots\ldots\ldots\ldots\ldots\ldots\ldots(2)$$

Where $f_0 = 2\Omega\sin\phi_0$ and $\beta_0 = \frac{2\Omega\cos\phi_0}{a}$ is called β parameter or Rossby parameter.

Typical mid latitude values on earth are $f_0 = 8\times10^{-5}S^{-1}$, $\beta_0 = 2\times10^{-11}m^{-1}S^{-1}$

The Cartesian frame work where β plane is not retained and considered along latitude circle is called f-plane.

Note that the β plane representation is validated at mid latitudes only if the $\beta_0 y$ term is small compared to the leading f_0 term. In terms of meridional length scale L, this implies

$\beta = \frac{\beta_0 L}{f_0} << 1 (\because L << a)$ This dimensionless ratio is called planetary number. In such case $\frac{\partial f_0}{\partial y} = \beta$ can be taken as constant. This is called β plane approximation.

Derivation :

$$\frac{du}{dt} = -\alpha \frac{\partial p}{\partial x} + fv \quad \text{or} \quad \frac{\partial u}{\partial t} + u\frac{\partial u}{\partial x} + v\frac{\partial u}{\partial y} + w\frac{\partial u}{\partial z} = fv - g\frac{\partial z}{\partial x}$$

Neglecting the non linear terms and putting (z = η) we can write

$$\frac{\partial u}{\partial t} - fv = -g\frac{\partial \eta}{\partial x} \quad \text{.....(3)}$$

Substitute eqn (2) in eqn (3)

$$\frac{\partial u}{\partial t} - (f_0 + \beta_0 y)v = -g\frac{\partial \eta}{\partial x} \text{.....(4)}$$

$$f_0 v = g\frac{\partial \eta}{\partial x} + (\frac{\partial u}{\partial t} - \beta_0 yv) \text{ .....(5)}$$

Similarly 'y' equation can be written as

$$f_0 u = -g\frac{\partial \eta}{\partial y} - (\frac{\partial v}{\partial t} + \beta_0 yu) \text{ .....(6)}$$

Writing equations (6) and (5) as

$$u = -\frac{g}{f_0}\frac{\partial \eta}{\partial y} - \frac{1}{f_0}(\frac{\partial v}{\partial t} + \beta_0 yu) \text{ .....(7)}$$

$$v = \frac{g}{f_0}\frac{\partial \eta}{\partial x} + \frac{1}{f_0}(\frac{\partial u}{\partial t} - \beta_0 yv) \text{.....(8)}$$

Substitute equations (7) and (8) in equation (4)

$$\frac{\partial}{\partial t}\left[-\frac{g}{f_0}\frac{\partial \eta}{\partial y} - \frac{1}{f_0}\frac{\partial v}{\partial t} - \frac{1}{f_0}\beta_0 yu\right] - f_0 v - \beta_0 y\left[\frac{g}{f_0}\frac{\partial \eta}{\partial x} + \frac{1}{f_0}\frac{\partial u}{\partial t} - \frac{1}{f_0}\beta_0 yv\right] = -g\frac{\partial \eta}{\partial x}$$

On further simplification

$$\frac{1}{f_0}\frac{\partial}{\partial t}\left[-g\frac{\partial \eta}{\partial y}-(\frac{\partial v}{\partial t}+\beta_0 yu)\right]-f_0 v-\frac{\beta_0 y}{f_0}\left[g\frac{\partial \eta}{\partial x}+(\frac{\partial u}{\partial t}-\beta_0 yv)\right]=-g\frac{\partial \eta}{\partial x} \quad \ldots\ldots\ldots(9)$$

Neglecting the terms in the small brackets, we can write the eqn (9) as

$$\frac{g}{f_0}\frac{\partial^2 \eta}{\partial t \partial y}-f_0 v-\frac{\beta_0 g}{f_0}y\frac{\partial \eta}{\partial x}=-g\frac{\partial \eta}{\partial x} \quad \ldots\ldots\ldots\ldots\ldots\ldots\ldots\ldots\ldots(10)$$

Similarly writing the 'y' component we get

$$\frac{g}{f_0}\frac{\partial^2 \eta}{\partial t \partial x}+f_0 u-\frac{\beta_0 g}{f_0}y\frac{\partial \eta}{\partial y}=-g\frac{\partial \eta}{\partial y} \quad \ldots\ldots\ldots\ldots\ldots\ldots\ldots\ldots\ldots(11)$$

Substituting (7) and (8) into eqn (11) we get

$$\frac{\partial}{\partial t}\left[\frac{g}{f_0}\frac{\partial \eta}{\partial x}+\frac{1}{f_0}\left\{\frac{\partial u}{\partial t}-\beta_0 yv\right\}\right]+f_0 u+\beta_0 y\left[-\frac{g}{f_0}\frac{\partial \eta}{\partial y}-\frac{1}{f_0}\left\{\frac{\partial v}{\partial t}-\beta_0 yu\right\}\right]=-g\frac{\partial \eta}{\partial y} \quad \ldots(12)$$

I II

(Neglecting the small terms I & II) ,Equations 10 and 11 can be written as

$$u=-\frac{g}{f_0}\frac{\partial \eta}{\partial y}-\frac{g}{f_0^{\,2}}\frac{\partial^2 \eta}{\partial t \partial x}+\frac{\beta_0 g}{f_0^{\,2}}y\frac{\partial \eta}{\partial y} \quad \ldots\ldots\ldots\ldots\ldots\ldots\ldots\ldots\ldots(13)$$

$$v=\frac{g}{f_0}\frac{\partial \eta}{\partial x}-\frac{g}{f_0^{\,2}}\frac{\partial^2 \eta}{\partial t \partial y}-\frac{\beta_0 g}{f_0^{\,2}}y\frac{\partial \eta}{\partial x} \quad \ldots\ldots\ldots\ldots\ldots\ldots\ldots\ldots..(14)$$

The first terms on the right hand side are geostrophic velocities and the other two small terms are called ageostrophic terms.

Substituting equations (13) and (14) in equation of continuity (eqn 15)

$$\frac{\partial \eta}{\partial t}+h\left[\frac{\partial u}{\partial x}+\frac{\partial u}{\partial y}\right]=0 \quad \ldots\ldots\ldots\ldots\ldots\ldots\ldots..(15)$$

For substitution of eqn (13) and (14) in eqn (15):

<u>Differentiate eqn (13) with respect to 'x'</u>

$$\frac{\partial}{\partial x}(u) = \frac{\partial}{\partial x}\left[-\frac{g}{f_0}\frac{\partial \eta}{\partial y} - \frac{g}{{f_0}^2}\frac{\partial}{\partial t}\left(\frac{\partial \eta}{\partial x}\right) + \frac{\beta_0 g}{{f_0}^2} y \frac{\partial \eta}{\partial y}\right]$$

Similarly differentiating eqn (14) with respect to 'y':

$$\frac{\partial}{\partial y}(v) = \frac{\partial}{\partial y}\left[\frac{g}{f_0}\frac{\partial \eta}{\partial x} - \frac{g}{{f_0}^2}\frac{\partial}{\partial t}\left(\frac{\partial \eta}{\partial y}\right) - \frac{\beta_0 g}{{f_0}^2} y \frac{\partial \eta}{\partial x}\right]$$

On simplifying we get $\frac{\partial u}{\partial x} + \frac{\partial v}{\partial y} = -\frac{g}{{f_0}^2}\frac{\partial}{\partial t}\left(\frac{\partial^2 \eta}{\partial x^2} + \frac{\partial^2 \eta}{\partial y^2}\right) - \frac{\beta_0 g}{{f_0}^2}\frac{\partial \eta}{\partial x}$ .....(16)

Substituting eqn (16) in eqn (15) we get

$$\frac{\partial \eta}{\partial t} + h\left[-\frac{g}{{f_0}^2}\frac{\partial}{\partial t}\left(\frac{\partial^2 \eta}{\partial x^2} + \frac{\partial^2 \eta}{\partial y^2}\right) - \frac{\beta_0 g}{{f_0}^2}\frac{\partial \eta}{\partial x}\right] = 0$$

Put $\frac{gh}{{f_0}^2} = R^2$ (Baroclinic Rossby radius of deformation)

$$\frac{\partial \eta}{\partial t} - R^2 \frac{\partial}{\partial t}\left(\frac{\partial^2 \eta}{\partial x^2} + \frac{\partial^2 \eta}{\partial y^2}\right) - \beta_0 R^2 \frac{\partial \eta}{\partial x} = 0$$

or $\frac{\partial \eta}{\partial t} - R^2 \frac{\partial}{\partial t}\left(\nabla_H{}^2 \eta\right) - \beta_0 R^2 \frac{\partial \eta}{\partial x} = 0$ .....(17)

To solve eqn (17), assume the wave profile (η) solution as

$$\eta = \eta_0 e^{i(kx+ly-\sigma t)} \quad \text{.....(18)}$$

Where k = east-west wave number, and l = north-south wave number.

Differentiate equation (18) with respect to 't' then double differentiate with respect to 'x' and 'y' and then substitute in eqn (17) and simplify.

Differentiation of (18) w.r.t 't':

$$\frac{\partial \eta}{\partial t} = \eta_0(-i\sigma)e^{i(kx+ly-\sigma t)} \quad \text{.....(19)}$$

Double differentiation of (18) w.r.t 'x':

$$\frac{\partial \eta}{\partial x} = \eta_0 (ik) e^{i(kx+ly-\sigma t)} \quad , \qquad \frac{\partial^2 \eta}{\partial x^2} = \eta_0 \left(i^2 k^2\right) e^{i(kx+ly-\sigma t)} \quad \text{.....(20)}$$

Double differentiation of (18) w.r.t 'y':

$$\frac{\partial^2 \eta}{\partial y^2} = \eta_0 \left(i^2 l^2\right) e^{i(kx+ly-\sigma t)} \quad \text{.....(21)}$$

Substituting 19,20 and 21 in 17:

$$\eta_0 (-i\sigma) e^{i(kx+ly-\sigma t)}$$
$$-R^2 \left[\frac{\partial}{\partial t} \left\{ \eta_0 \left(i^2 k^2\right) e^{i(kx+ly-\sigma t)} \right\} + \eta_0 \left(i^2 l^2\right) e^{i(kx+ly-\sigma t)} \right] - \beta_0 R^2 \left[\eta_0 (ik) e^{i(kx+ly-\sigma t)} \right] = 0 \quad \text{.....(22)}$$

I II III

Further simplification of (22) : I + II = III

Simplification of II:

$$-R^2 \left[\frac{\partial}{\partial t} \left\{ \eta_0 \left(-k^2\right) e^{i(kx+ly-\sigma t)} \right\} + \eta_0 \left(-l^2\right) e^{i(kx+ly-\sigma t)} \right] \qquad (\because i^2 = -1)$$

On differentiation w.r.t 't' and simplifying

$$-R^2 \eta_0 e^{i(kx+ly-\sigma t)} \left[i\sigma \left(k^2 + l^2\right) \right] \quad \text{.....(23)}$$

Substituting 23 in 22 and simplifying:

$$\eta_0 e^{i(kx+ly-\sigma t)} \left[(-i\sigma) - R^2 \left(i\sigma k^2 + i\sigma l^2 \right) - \beta_0 R^2 (ik) \right]$$

since $\eta = \eta_0 e^{i(kx+ly-\sigma t)}$ according to (18)

or $$\sigma = -\frac{\beta_0 k}{\left(1/R^2\right) + (k^2 + l^2)} \quad \text{.....(24)}$$

Note that if β corrections were not retained $(\beta_0 = 0)$ the frequency (σ) would have been zero which corresponds to steady state geostrophic flow on the f-plane.

By tracing the time derivatives as small terms ($\frac{\partial u}{\partial t} - \beta_0 yv$) and II in eqn (12) (i.e., assumed a small temporal Rossby number R <<1), we have retained only the low frequency (< f_0) for these waves to develop.

The zonal phase speed of Rossby wave can be obtained from the eqn (24) as

$$C_x = \frac{\sigma}{k} = -\frac{\beta_0 R^2}{1 + R^2(k^2 + l^2)} \quad \text{.....(25)}$$

This C_x is always negative implying the phase propagation is in the negative x direction. This means its propagation is towards west.

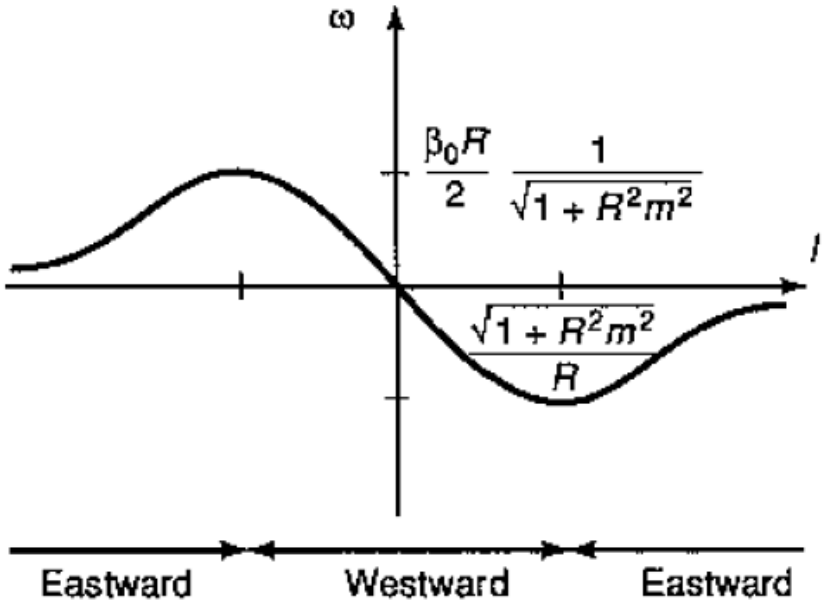

Fig.1. Dispersion relation of Rossby waves. The frequency Ω is plotted against the zonal wave number 'l' at constant meridional wave number m. As the slope of the curve reverses, the direction of zonal propagation and its associated energy also changes.

The meridional phase speed $C_y = \frac{\sigma}{l}$ is undetermined since the wave number (l) has either sign under the root. Thus for very long waves for which 1/k and 1/l are larger then R, equation (25) will become:

$$C_{x(\max)} = -\beta_0 R^2 = -\beta_0 \frac{gh}{f_0^{\,2}} \quad \text{.....(26)}$$

This is the maximum speed allowed for Rossby waves

Mechanism of propagation of Rossby waves:

Let us consider five parcels of water on the same latitude moving on a β-plane as shown in Fig.2.

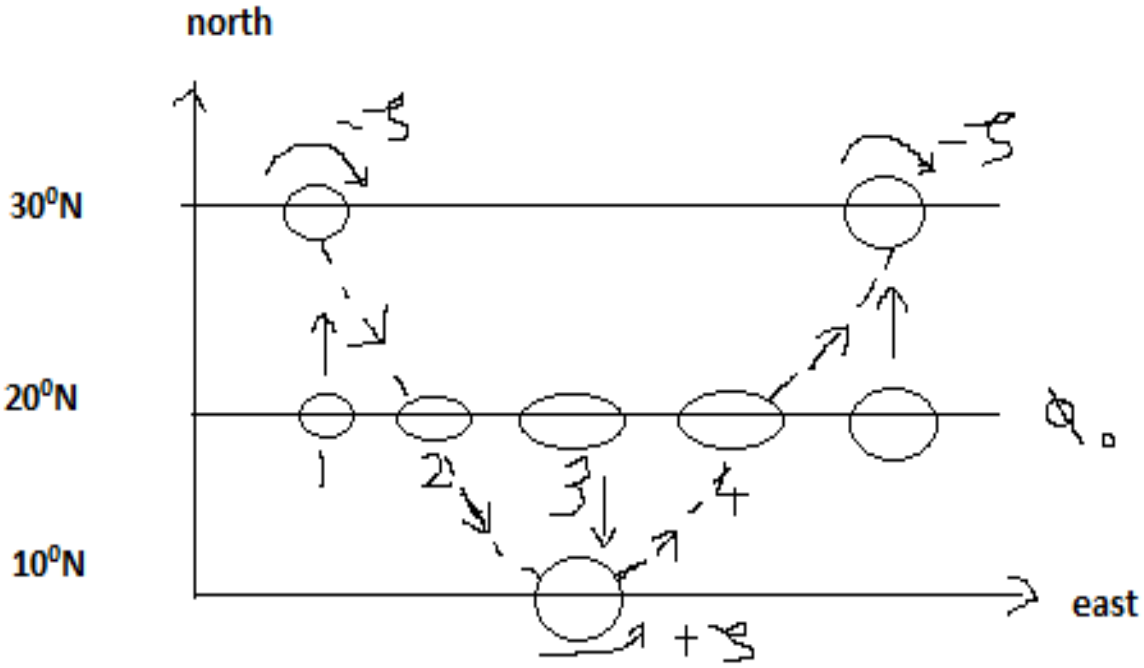

Fig.2. Mechanism of generation and propagation of Rossby waves

Let two parcels 1 and 5 have gone towards higher latitude (30^0N) while the parcel 3 has moved toward lower latitude to 10^0N. Let the water depth (h) is constant. Thus the water column length is constant. Then the potential vorticity $\left[\frac{\zeta + f}{h} = const\right]$ is conserved.

The two parcels moved to higher latitudes (30^0N) develops negative relative vorticity ($-\zeta$) as 'f' increased. This means parcel (1 & 5) acquires anticyclonic (clockwise) rotation. Whereas parcel 3 acquires cyclonic rotation as it acquires positive relative vorticity ($+\zeta$) due to decrease of 'f'.

Thus 1,3,5 parcels develop an eastward tending wave field. This flow field disturbs the parcels 2 and 4. When the parcels 1,3,5 are restored under stability

considerations, the parcels 2 and 4 will tend to move on the β-plane. Let suppose the parcel '2' has a tendency to go lower latitude (toward 10^0N) and the parcel 4 has a tendency to go toward higher latitude (30^0N) side in the next instant. Then the wave profile shifts toward west progressing westward as shown by solid profile in the figure 3.

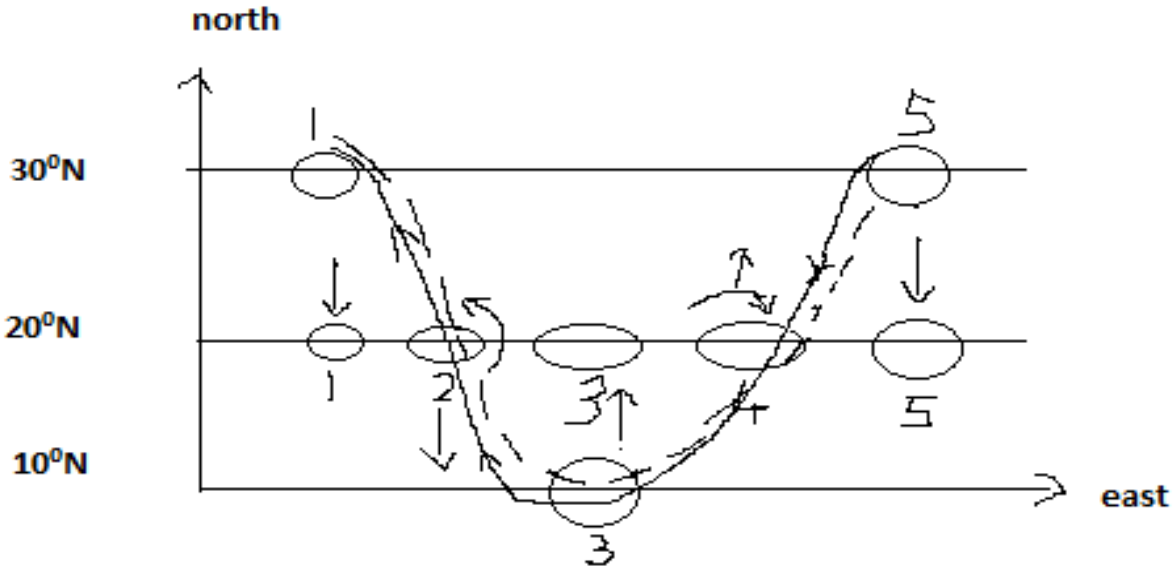

Fig.3. Reverse propagation to show the to-and –fro motion of Rossby waves

Note that these waves are called Rossby waves and they are transverse waves. This means the particles mover perpendicular to the direction of propagation. The restoring force of this wave is the north-south gradient of potential vorticity $\left[\frac{\zeta + f}{h}\right]$.The gradient can be either due to variation of 'f' or 'h'.

The Rossby waves are two kinds. They are tropospheric Rossby waves and the other are continental shelf waves.

When the variation of 'h' dominate the variation of 'f', topography comes into picture and so they are called *topography waves*. However, variations in topography may lead to wave trapping (concentration of wave energy in between shallow depths). Then these are called shelf waves. The gravity waves also can be trapped near the shelf. Then they are called *edge waves*.

The variation of 'f' also under shallow depths of long waves may lead to trapping near the equator. Then they are called *equatorial waves*.

Salient points on Rossby waves:

1. The phase speed C_x is always negative (eqn 25). This means the wave propagates westward.
2. The group velocity at which the energy of a wave packet propagates is defined by $\frac{\partial\sigma}{\partial k}$ and $\frac{\partial\sigma}{\partial l}$ is the gradient of function σ in k and l wave number plane. It is thus perpendicular to the circles of constant σ. The group velocity vector is directed inward toward the center. Therefore longwaves (small 'k' and 'l' point near the origin) have westward propagating group velocities, whereas shorter waves(larger 'k' and 'l' point on the opposite side of the circle) have eastward energy propagation as shown in Fig.4.

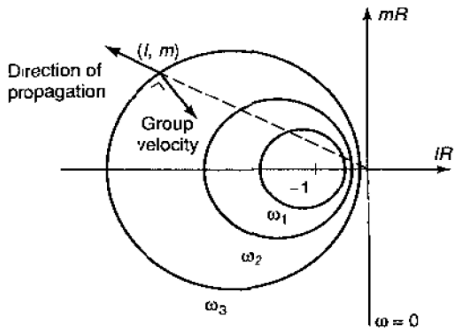

Fig.4. Geometric representation of the planetary – wave dispersion relation. Each circle corresponds to a single frequency, with frequency increasing with decreasing radius. The group velocity of (l.m) wave is a vector perpependicular to the circle at point (l,m) and dircted toward its center.

3. Thus as far as energy propagation is concerned it can be either direction

   i)i.e., when $\frac{\partial\sigma}{\partial k} < 0$ for low 'k' (long waves) = westward

   ii) when $\frac{\partial\sigma}{\partial k} > 0$ for short waves = eastward

4. Lines of constant frequency (σ) in the (K, l) wave number space are circles defined by

$\left(K+\frac{\beta_0}{2\sigma}\right)^2+l^2=\left(\frac{{\beta_0}^2}{4\sigma^2}-\frac{1}{R^2}\right)$ These circles are illustrated in Fig.4. such circles exist only if their radius is a real number.

i.e., ${\beta_0}^2>4\sigma^2$ this implies the existence of maximum frequency $|\sigma|_{\max}=\frac{\beta_0 R}{2}$ beyond which planetary waves do not exist.

5. The wave length limits for long waves is k, l <<1
6. They strictly propagate westward with a maximum speed of $C_{x(\max)}=-\beta_0 R^2$ (when k, l <<1) as mentioned in equation 26.
7. These are non dispersive (frequency linear function of wave number) waves.
8. Rossby wave phase speed decrease as it moves away from the equator (as β decreases). Wave crest also changes to crescent shaped.
9. These are considered as sub-inertial waves because their maximum frequency is always less than 'f'. So the periods of these waves may be weeks to months.
10. Right close to the equator within ($\pm 5^0$), they have greater acceleration. The equator acts as a wave guide like Kelvin waves. These Rossby waves sometimes are refracted by the strong gradient of 'f'. Then bend back towards the equator into the wave guide and develop as a standing wave moving westward. Fastest moving meridional standing wave mode moves westward at C/3.
11. All these types of long waves (Kelvin waves, Rossby waves, shelf waves, equatorial waves, poincare waves, topographic waves etc.) play an important role in the adjustment of ocean circulation on climate scales.
12. Rossby wave propagates westward relative to the mean zonal flow. The wave speed depends on the zonal and meridional wave numbers. Therefore Rossby waves are dispersive waves whose phase speeds increase with wave length.

The frequency of Rossby waves is compared with other waves as given below:

S.No	Type of wave	Frequency	
		Waves per second	Waves per day
1.	Sound waves	10^3	10^8
2.	Long gravitational waves	10^{-1}	10^4
3.	Inertial waves	10^{-2}	10^3

4.	Cyclone	10^{-5}	10^{0}
5.	Rossby	10^{-6}	10^{-1}

The above table shows that in the case of a cyclone the frequency 10^0 per day which means 10 waves pass in a day. Whereas the frequency in the case of Rossby waves is 10^{-1} per day (1/10) which means to pass one wave 10 days it will take.

Try this Problem:

If the Ocean is 4 km deep, what is the Rossby wave speed at latitude 45^0 for a wave of 10,000 km zonal wave length? (Take $\beta_0 = 2\times10^{-11} m^{-1}s^{-1}$ and $f_0 = 8\times10^{-5} s^{-1}$)

Ans: We know the Rossby wave velocity equation as,

C $= -\beta_0 \frac{gh}{f_0^2}$ substitute all the values in the equation and simplify.

$C = \frac{2\times10^{-11}9.8\times4\times10^3}{(8\times10^{-5})^2} = 122.5\ m/s$

Kelvin Waves:

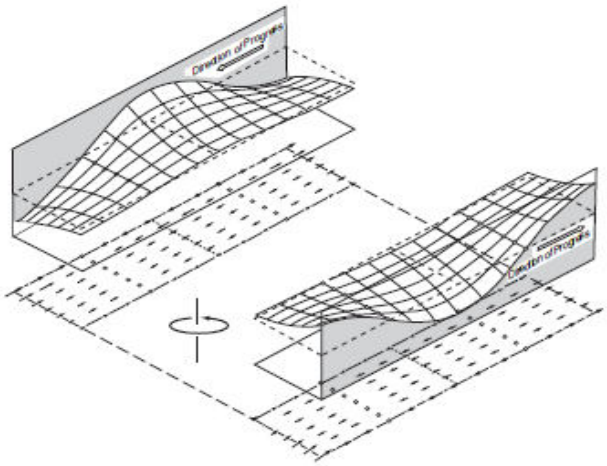

Fig.5. Northern Hemisphere Kelvin waves on opposite sides of a channel that is wide compared with the Rossby radius. In each vertical plane parallel to the coast, the currents(shown by arrows) are entirely within the plane and are exactly the same as those for a long gravity wave in a non-rotating channel. However, the surface elevation varies exponentially with distance from the coast in order to give a geostrophic balance. This means Kelvin waves move with the coast on their right in the Northern Hemisphere and on their left in the Southern Hemisphere.

The Kelvin wave is a large scale wave motion of great practical importance in the Earth's atmosphere and oceans. The Kelvin wave is a special type of gravity wave that is affected by the earth's rotation and trapped at the equator or along lateral vertical boundaries such as coastlines or mountain ranges.

The existence of Kelvin wave relies on a) gravity and stable stratification for sustaining a gravitational oscillation, b) significant coriolis acceletation and c) the presence of vertical boundary or equator.

An important property of Kelvin wave is its unidirectional propagation. The Kelvin wave moves equatorward along a western boundary, poleward along a eastern boundary and cyclonically (N.H) and anticyclonically (in S.H) in a closed boundary.

The wave amplitude is largest at the boundary and decays exponentially with distance from it. At the equator, Kelvin waves always propagate eastward, reaching their maximum magnitude at the equator and decaying exponentially with increasing latitude as shown in fig.1.

There are two types of Kelvin waves. Boundary trapped and equatorially trapped. Each type is further subdivided into surface and internal Kelvin waves. Surface Kelvin waves are barotropic and internal Kelvin waves are baroclinic. Internal Kelvin waves are often found in the layer of large density gradients. For example in the oceanic thermocline zone these internal waves exist. Whereas in the layer of inversion zone, these waves can exist in the atmosphere.

Atmospheric Kelvin waves play an important role in the adjustment of the tropical atmosphere to convective latent heat release, in the atmospheric quasi-biennial oscillation and in the generation and maintenance of Madden- Julian oscillation. OceanicKelvin waves play a critical role in tidal motion and in generating and sustaining the ElNini and southern oscillation phenomena. Kelvin waves can also be generated as storm surges when a cyclone crosses a low lying coastal region. Internal coastyal Kelvin waves can also be induced due to coastal upwelling.

Equatorially trapped Kelvin waves:

Matsuno in 1966 showed that the eastward propagating Kelvin wave is a possible free solution to the perturbation equations of the shallow water on an equatorial β plane, provided that meridional velocity (v = 0) vanishes. This is called equatorially trapped Kelvin wave because it is similar to the coastally trapped Kelvin wave but the equator serve as a boundary.

The equatorial Kelvin wave moves eastward only. The speed of the Kelvin wave is like the shallow water gravity wave $C = \sqrt{gd}$. Because the coriolis parameter changes sign on either side of the equator, eastward flow occurs on both sides of the equator. This would induce equatorward Ekman Net transport causing convergence and meridional pressure gradient at the equator.

Because of the conservation of momentum in the north-south direction requires a geostrophic balance between the eastward velocity and the meridional pressure gradient force. This geostrophic balance results in the perturbation zonal velocity reaching a

maximum on the equator and decay with increasing distance from the equator as shown in Fig.6.

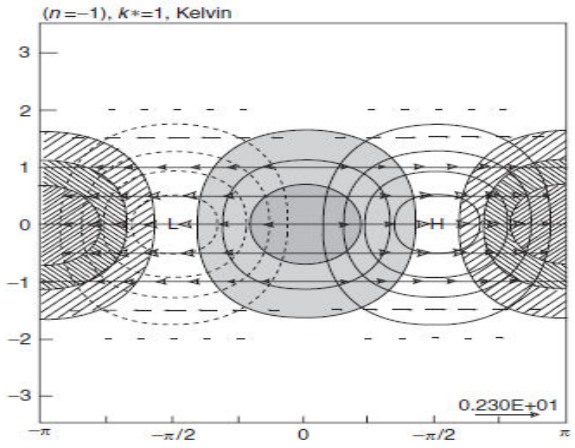

Fig.6. Equatorial kelvin wave. Hatched semi circles near the equator denotes convergence. Centre circle denotes divergence. Unshaded contours are for geopotential with a contour interval of 0.5 units. Negative contours are dashed.

The tide waves traveling along continents is transmitted in the form of barotropic Kelvin waves such that the cotidal lines rotate anticlockwise (cyclonic) in the higher latitudes side in the N.H and clockwise in the S.H. For shallow seas and coastal waters the Rossby radius is about 200 km.

When a Kelvin wave moves through a region in which the fluid depth or the coriolis parameter varies and the wave energy flux remains constant then the amplitude of the wave varies in proportion to $\left[\frac{f}{d}\right]^{1/2}$. Thus the wave amplitude increases when it moves into shallow water.

Variable longshore winds, internal density gradients play a vital role in generating Kelvin waves. Equatorial Kelvin waves play a vital role in thermocline adjustment.

The equatorial Kelvin waves play an essential role in the ENSO cycle. A westerly wind anomaly (lateral wind shear) excites downwelling Kelvin waves, which propagate into the eastern Pacific suppressing thermocline and ceases upwelling during El Nino as shown in Fig.7

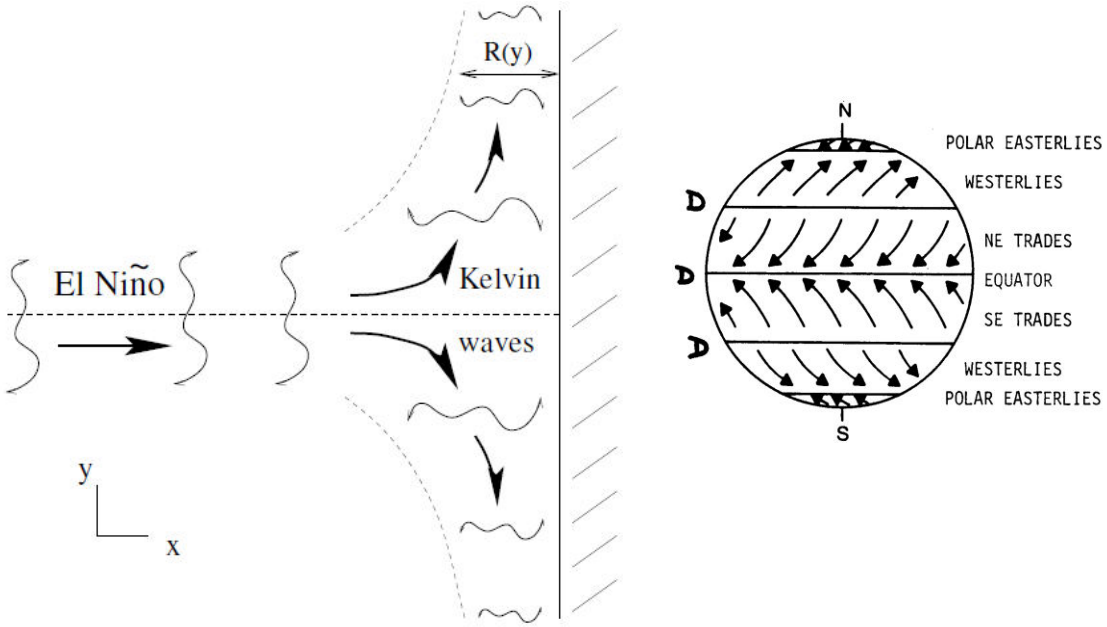

Fig.7. The generation of poleward propagating Kelvin wave along eastern oceanic boundary by equatorial variability (during ElNino). The thick solid arrows indicate the Kelvin wave propagation direction. The curved arrows indicate the width of the Kelvin wave in the perpendicular direction. The deformation radius $R = \sqrt{gd}/f$ decreases with increase of latitude since f increases. Note the offshore decay scale (shown by dashed curve) of the wave decreases exponentially. The balance of horizontal pressure gradient and coriolis gives the flow in the meridional. Convergence occurs near the boundary due to Ekman Net transport.

Internal Kelvin wave:

The horizontally propagating internal or baroclinic Kelvin wave behaves in the same manner as the surface wave except that the motion varies with depth as shown in Fig.8.

For internal Kelvin waves, the pressure gradient force normal to the lateral boundary arises from the tilt of the interface and is balanced by the coriolis force such that the vertical differential flow is parallel to the boundary. In the ocean, the typical speed of internal coastal boundary Kelvin wave is of the order of 1 m/s and the Rossby radius of deformation (C_0/f) is of the order of 10 km in the mid latitude.

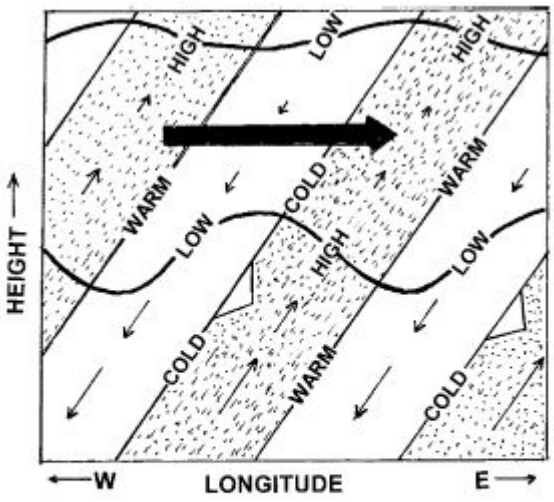

Fig.8. Longitude – height section along the equator showing pressure, temperature and wind perturbations for a thermally damped Kelvin wave. Heavy wavy lines indicate material lines, short blunt arrows show phase propagation. Areas of high pressure are shaded. Length of small thin arrows is proportional to the wave amplitude which decreases with height due to damping. The large shaded arrow indicates the net mean flow acceleration due to the wave stress divergence

Derivation of Kelvin wave:

Take the equation of motion and continuity:

$$\frac{du}{dt} = -\alpha \frac{\partial p}{\partial x} + fv$$

$$\frac{dv}{dt} = -\alpha \frac{\partial p}{\partial y} - fu$$

$$\frac{\partial u}{\partial x} + \frac{\partial v}{\partial y} + \frac{\partial w}{\partial z} = 0$$

Assumptions:

1. Let us assume the ocean is barotropic (ρ = constant)
2. The horizontal pressure gradients are expressed in terms of surface elevation (η) gradients to incorporate the rise and fall of the free surface.
3. An eastern boundary exists such that the meridional velocity, v = 0
4. In the horizontal equations, w = 0
5. Non linear terms are neglected.

Zonal component:

$$\frac{\partial u}{\partial t} + u\frac{\partial u}{\partial x} + v\frac{\partial u}{\partial y} = fv - \alpha \frac{\partial p}{\partial x}$$

Using the assumptions 2, 3,4 and 5 and using hydrostatic equation $\alpha\partial p = g\partial z$,this zonal component reduces to

$$\frac{\partial u}{\partial t} = -g\frac{\partial z}{\partial x} = -g\frac{\partial \eta}{\partial x} \quad \text{.....(1)}$$

Meridional component:

$$\frac{\partial v}{\partial t} + u\frac{\partial v}{\partial x} + v\frac{\partial v}{\partial y} + w\frac{\partial v}{\partial z} = -fu - \alpha\frac{\partial p}{\partial y}$$

Using the assumption of 3 and hydrostatic assumption it becomes

$$fu = -g\frac{\partial z}{\partial y} = -g\frac{\partial \eta}{\partial y} \quad \text{.....(2)}$$

Equation of continuity:

$$\frac{\partial u}{\partial x} + \frac{\partial v}{\partial y} + \frac{\partial w}{\partial z} = 0 \qquad \int_{-h}^{\eta}\left(\frac{\partial u}{\partial x} + \frac{\partial v}{\partial y}\right)dz = -\int_{-w_h}^{w_\eta} dw$$

on integrating we get

$$\left[\frac{\partial u}{\partial x} + \frac{\partial v}{\partial y}\right][z]_{-h}^{\eta} = -\left[w_\eta - w_{-h}\right] = -w_\eta$$ since at z = -h, w_{-h} =0 which means vertical velocity vanishes at the sea bottom.

$$\therefore w_\eta = \frac{dz}{dt} = \frac{d\eta}{dt} = \frac{\partial \eta}{\partial t} \qquad (\because \text{ non linear components neglected})$$

$$\therefore \frac{\partial \eta}{\partial t} = -(h+\eta)\left[\frac{\partial u}{\partial x} + \frac{\partial v}{\partial y}\right] \quad \text{.....(3)}$$

Putting $(h+\eta) = D$, equation 3 can be written as

$$\therefore \frac{\partial \eta}{\partial t} = -D\left[\frac{\partial u}{\partial x}\right] \qquad (\because \text{ v =0 is assumed})$$

So the three required equations for the derivation of Kelvin waves are: 1,2 and 3.

$$\frac{\partial u}{\partial t} = -g\frac{\partial \eta}{\partial x} \quad \text{.....(1)}$$

$$fu = -g\frac{\partial \eta}{\partial y} \quad \text{.....(2)}$$

$$\frac{\partial \eta}{\partial t} = -D\left[\frac{\partial u}{\partial x}\right] \quad \text{.....(3)}$$

Solution:

Find one equation for 'η' using (3) and (1).

Differentiate eqn. (3) with respect to (w.r.t) 't':

$\frac{\partial}{\partial t}\left[\frac{\partial \eta}{\partial t}\right] = -D\frac{\partial}{\partial t}\left[\frac{\partial u}{\partial x}\right]$ which can be written as $\frac{\partial^2 \eta}{\partial t^2} = -D\left[\frac{\partial^2 u}{\partial x \partial t}\right]$ ……(4)

Differentiate eqn. (1) with respect to (w.r.t) 'x':

$\frac{\partial}{\partial x}\left(\frac{\partial u}{\partial t}\right) = \frac{\partial}{\partial x}\left[-g\frac{\partial \eta}{\partial x}\right]$ which can be written as $\frac{\partial^2 u}{\partial x \partial t} = -g\frac{\partial^2 \eta}{\partial x^2}$ ……(5)

From eqn (4) and (5) we can write:

$\frac{\partial^2 \eta}{\partial t^2} = -gD\left[\frac{\partial^2 \eta}{\partial x^2}\right] = 0,$ put gD = C^2 then we can write

$\frac{\partial^2 \eta}{\partial t^2} = -C^2\left[\frac{\partial^2 \eta}{\partial x^2}\right] = 0$ ……..(6)

The solution of eqn (6) can be written as $\eta = a_{(y)}e^{i(kx-\sigma t)}$ ……(7)

Where a = amplitude of the wave, k = wave number ($\frac{2\pi}{L}$) and σ = wave radian frequency ($\frac{2\pi}{T}$) such that L = wave length and T = time period of the wave.

Equation (7) is a wave equation. For Kelvin waves it is further assumed that the wave travels along the wall (coast in the case of oceans) e^{ikx} with the asymptote $e^{i(kx-\sigma t)}$.

Solving equation (7):

Combine equation (1) and (2): To do this

Differentiate eqn (2) w.r.t "t"

$f\frac{\partial}{\partial t}(u) = \frac{\partial}{\partial t}(-g\frac{\partial \eta}{\partial y})$ which is equal to $f\frac{\partial u}{\partial t} = -g\frac{\partial^2 \eta}{\partial y \partial t}$ ……(8)

Substitute eqn (1) in (8) $f\left[-g\frac{\partial \eta}{\partial x}\right] = -g\frac{\partial^2 \eta}{\partial y \partial t}$ which is equal to

$f\left[\frac{\partial \eta}{\partial x}\right] - \frac{\partial^2 \eta}{\partial y \partial t} = 0$ ……(9)

Using equation (7) and (9) solve for η:

Differentiate eqn (7) w.r.t "x"

$$\frac{\partial \eta}{\partial x} = a(ik)e^{i(kx-\sigma t)} \quad \text{……..(10)}$$

Differentiate eqn (7) w.r.t "t":

$$\frac{\partial \eta}{\partial t} = a(-i\sigma)e^{i(kx-\sigma t)} \quad \text{…….(11)}$$

Further differentiate eqn (11) w.r.t 'y'

$$\frac{\partial^2 \eta}{\partial y \partial t} = (-i\sigma)e^{i(kx-\sigma t)}\frac{\partial a}{\partial y} \quad \text{……..(12)}$$

Substituting (10) and (12) in (9) and simplifying:

$fkdy = -\sigma \frac{da_{(y)}}{a}$ on integrating we get $\int \frac{da_{(y)}}{a} = \left[-\frac{fk}{\sigma}\right]\int dy$ ……(13)

$$\therefore \ln(a_y) = \left[-\frac{fk}{\sigma}\right]y + \ln C \quad \text{……(14)}$$

The additive integration constant 'C' can be eliminated by a proper reexamination of 'y' coordinate. Eqn (14) can be written as

$\therefore \ln\left(\frac{(a_y)}{C}\right) = \left[-\frac{fk}{\sigma}\right]y$ which is equal to $a_{(y)} = Ce^{-\frac{fk}{\sigma}y}$

to find 'C' , when y $y \to 0, C = a_{(0)} = \eta_0$ (say)

$$\therefore a_{(y)} = \eta_0 e^{-\frac{fk}{\sigma}y} \quad \text{…….(15)}$$

Substituting eqn (15) in eqn (7)

$$\eta = \eta_0 e^{-\frac{fk}{\sigma}y} e^{i(kx-\sigma t)} \quad \text{……(16)}$$

Expanding (16) further

$$\eta = \eta_0 e^{-\frac{fk}{\sigma}y}\left[\cos(kx-\sigma t) + i\sin(kx-\sigma t)\right] \quad \text{…….(17)}$$

Eqn(17) has real and imaginary parts. The imaginary part is zero(as in left hand side there is no imaginary part). So taking only the real part we can write

$\eta = \eta_0 e^{-\frac{fk}{\sigma}y}\left[\cos(kx-\sigma t)\right]$ .We know $C = \frac{\sigma}{k}$ is the wave celerity. Then we can write

$$\eta = \eta_0 e^{-\frac{y}{R}}\left[\cos(kx-\sigma t)\right] \quad \text{……(18)}$$

Equation (18) is called the Kelvin wave profile equation.

Where $R = \frac{C}{f}$ ……..(19)

is called the Rossby radius of deformation.

We already put v = 0 ……(20)

And $C^2 = gD$ or $C = \sqrt{gD}$ ……(21)

To find 'u':

Differentiate eqn (16) w.r.t to 'y'

$$\frac{\partial \eta}{\partial y} = \eta_0 \left[-\frac{fk}{\sigma} \right] e^{-\frac{fk}{\sigma} y} e^{i(kx-\sigma t)} + e^{-\frac{fk}{\sigma} y} e^{i(kx-\sigma t)} \frac{\partial \eta_0}{\partial y}$$

The second term is zero, since η_0 is constant (η_0 = a_0)

$$\therefore \frac{\partial \eta}{\partial y} = \eta_0 \left[-\frac{fk}{\sigma} \right] e^{-\frac{fk}{\sigma} y} e^{i(kx-\sigma t)} \quad \text{……..(22)}$$

Substitute eqn (22) in eqn (2) and simplfy

$u = \eta_0 \left[\frac{gk}{\sigma} \right] e^{-\frac{fk}{\sigma} y} e^{i(kx-\sigma t)}$, substituting eqn (16) in this we get $u = \eta \left[\frac{gk}{\sigma} \right] = \eta \left[\frac{g}{c} \right]$

But w know from eqn (21) $C = \sqrt{gD}$

$$\therefore u = \eta \left[\frac{g}{\sqrt{gD}} \right] = \eta \sqrt{\frac{g}{D}} \quad \text{……..(23)}$$

So from eqns 18,19,20,21 and 23 we can write Kelvin wave parameters as

$\eta = \eta_0 e^{-\frac{y}{R}} \left[\cos(kx - \sigma t) \right]$ …..(18)

$R = \frac{C}{f}$ Rossby radius of deformation

v = 0

$C = C_g = \sqrt{gD}$ where C_g is group velocity

$u = \eta \sqrt{\frac{g}{D}}$

Explanation:

Case i): If the wave is on the y > 0 side as per equation (18) it becomes

Limit $y \to \infty, \eta = 0$ (finite) $\quad \therefore C = +\sqrt{gD} \Rightarrow \frac{\sigma}{k} > 0$ or $k > 0$ (+ve)

This means the wave travels in the positive (+ve) x direction.

Case ii): If the wave is on the y < 0 side then

Limit $y \to \infty, \eta = 0$ (finite) which means the wave travels in the same mode of direction in either hemispheres.

Case iii) In either case in N.H, f > 0

Properties of Kelvin waves:

1. Kelvin wave is a boundary wave such that it always travels with the boundary (wall/coast) on its right side in N.H and left side in S.H
2. The wave amplitude decreases exponentially away from the boundary
3. The wave is trapped along the boundary by rotation called the wave guide
4. The forces of balance is pressure gradient and coriolis such that horizontal pressure gradient is offshore normal to the coast(shelf)(boundary)
5. Rotation does not affect the particle motion and wave propagation. But only traps the wave at the coast line.
6. The decay scale is C/f and is called as the Rossby deformation radius which is a measure of its decrease in amplitude as it goes northward.
7. The amplitude is greatest at the boundary and decays exponentially away from it.
8. It propagates meridionally such that the coast is on its right side in the N.H (towards high latitudes in N.H) and left side in the S.H (towards low latitudes in S.H)
9. Kelvin waves also occur on either side of the equator due to change in coriolis parameter propagating west to east in both the hemispheres called double Kelvin waves.
10. In a closed boundary Kelvin waves propagates anticlockwise in N.H and clockwise in S.H.

Calculation of length scale of the Rossby deformation radius $\frac{C}{f} = \frac{\sqrt{gD}}{f}$:

i) If D = 5 km = 5×10^3 m and f = 10^{-4} S^{-1} in middle latitudes

$$\therefore R = \frac{\sqrt{gD}}{f} = \frac{\sqrt{9.8 \times 5 \times 10^3}}{10^{-4}} = 2200km$$

ii) If D = 100 m in shallow seas

$$R = \frac{\sqrt{gD}}{f} = \frac{\sqrt{9.8 \times 10^2}}{10^{-4}} = 300km$$

Problem: The Red Sea between Arabian Peninsula and North East African continent has an average depth of 500 m and a coastal perimeter of 2100 km. What is the trapping distance (Rossby deformation radius) and frequency of this wave at 30^0 N latitude?

Ans. $C = \sqrt{gD} = \sqrt{9.8 \times 500} = 70 m/s$

L/T = 70 m/s which means T = L/70 = 2100×10^3 m$\div$ 70 = 30×10^3 seconds = 8hours 20 minutes. This means this Kelvin wave will take 8 hours 20 minutes to travel around the shores of red Sea at 30^0 N latitude. The frequency is given by σ = wave radian frequency ($\frac{2\pi}{T}$).

$$\therefore \sigma = \frac{2\pi}{T} = \frac{2\pi}{30 \times 10^3} = \frac{12}{10^3} \text{ rad/sec}$$

Trapping distance: $R = \frac{\sqrt{gD}}{f} = \frac{\sqrt{9.8 \times 500}}{2 \times 7.3 \times 10^{-5} \times \sin 30} = 10^6 m = 10^3 km$

Lecture Series of Berhampur University in Physical Oceanography
By Prof.A.S.N.Murty

Chapter – 9

ESTUARIES

Estuaries are partially enclosed bodies of water where freshwater (water without salt) meets salty ocean water. Bays, inlets and ocean-flooded river valleys are all examples of estuaries.

Estuaries - Estuary Life

Estuaries are home to an astonishing variety of plants and animals. Crabs and clams of many species make home to these fresh and saltwater mixing zones, each finding the salinity (saltiness) that suits them best.

Horseshoe Crab

Filter feeders are found in all parts of the estuary. They are creatures that pull small bits of organic material, like plankton and larvae, from the water as it moves past them. Horseshoe crabs are one of the older inhabitants of coastal estuaries, living happily and largely unchanged for millions of years.

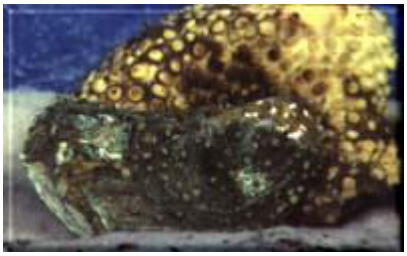

Boring Sponge

Oysters blanket the estuary floors in areas where they use foot secretions to cement themselves to the substrate. Not only are these oysters a rich food source for us, but they are also important food sources to many estuarine creatures. Predatory snails, including Oyster Drills, whelks, sponges, especially the Boring Sponges, and fish all find oysters a tasty treat.

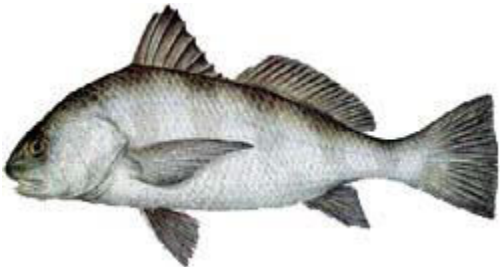

The Black Drum has jaws powerful enough to crush adult oyster shells.

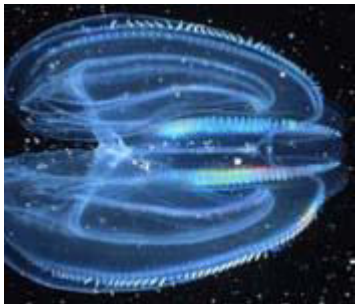

Leidy's Comb Jelly is a jellyfish that eats oyster larvae.

1.0. Introduction:

The word estuary is derived from the latin word ‘aestus’ meaning tide and the adjective ‘aestuarium’ means tidal. This means the body which has much tidal effects are seen. Estuaries are thus partially enclosed bodies of water where freshwater (water without salt) meets salty ocean water as shown in Fig 10. Bays, inlets and ocean-flooded river valleys are all examples of estuaries.

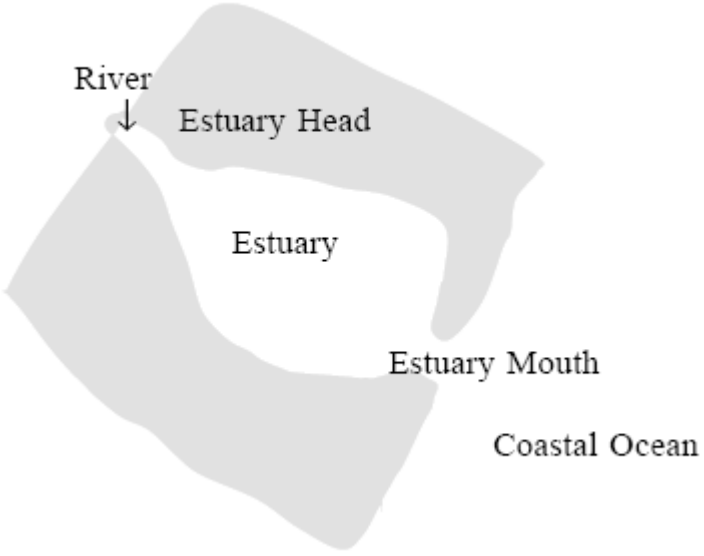

Fig.10. Broad view of a Estuary structure

If the coastal ocean is the region where the continents and the ocean overlap, the estuaries are the place where they really meet. In estuaries, freshwater collected over vast regions of the land pours into an ocean, which sends salt water upstream far beyond the river mouth.

A classical definition of an estuary according to Cameron and Pritchard,(1963) is 'an estuary is a semi enclosed coastal body of water which has free connection with the open sea and within which sea water is measurably diluted with fresh water derived from land drainage'.

Fair Bridge (1980) further explained the estuary as 'it is an inlet of the sea reaching into a river valley as far as the upper limit of tidal rise, usually being divisible into three sectors a) marine lower sector which has free connection with the open sea b) a middle sector which is subjected to strong salt and fresh water mixing and c) an upper fluvial sector which is predominantly characterized by fresh water but subjected to daily tidal action as shown in Fig 11.

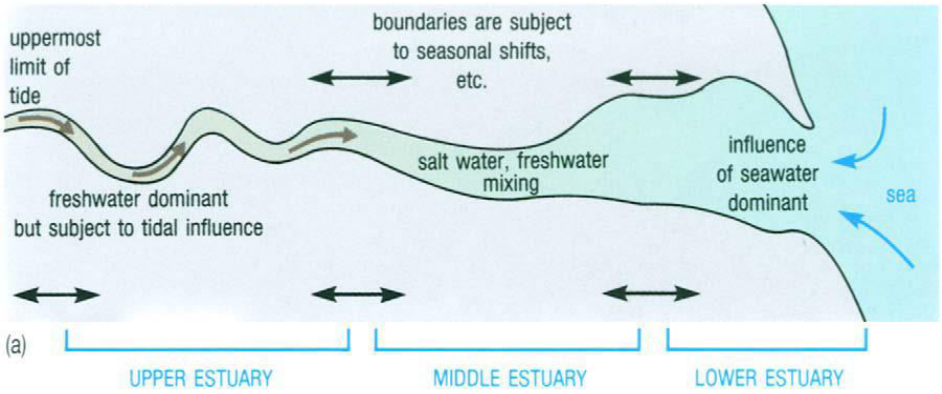

Fig.11.Estuary formed at the river mouth on the sea coast.

Estuaries described by this definition are known as positive estuaries. However, there are three classes of estuaries can be recognized. They are positive, negative and mixed type of estuaries. In order to include all these types of estuaries the definition of estuary is modified as 'it is a narrow, semi enclosed coastal body of water which has a free connection with the open sea at least intermittently and within which the salinity of the water is measurably different from the salinity in the open ocean'.

Most estuaries are geologically very young. They have developed since the last post glacial rise in the places of sea level inundated coast lines and drowned river valleys. They are now being progressively filled with sediment. The life of an estuary is expected to be more if the river transports small amount of sediment and more amount of fresh water where wave and tide action are strong. However, if the sediment discharge is high and there is limited wave and tide action then in course of time estuary vanishes and a delta is formed.

Flood and ebb tides in the estuaries:

As the tide enters into the estuary during high tide, the water level advances and increase the sea level and flood on the banks of the estuary called flood tide which is deflected towards right hand side by the coriolis force and so the direction of arrows bends towards right in Fig.13a. On the other hand during low tide time after 12 hours the

water start receding back towards the sea called ebb tide. Then the arrows bend towards west as shown in Fig.13b.

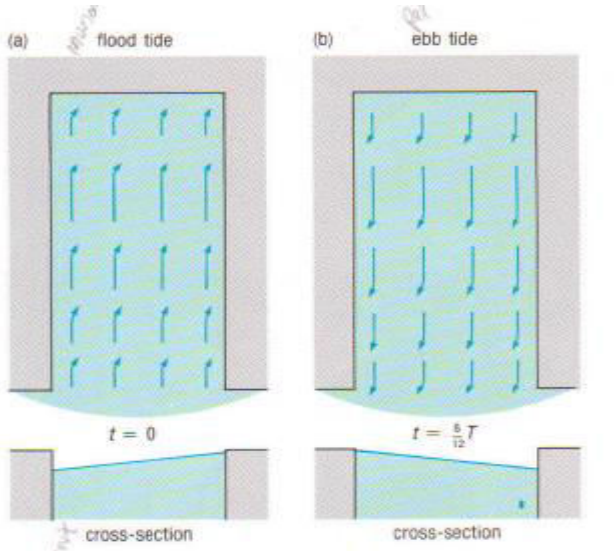

Fig.13. Flood and ebb tides in an estuarine circulation due to high and low tides

As estuaries are considered long and narrow with poor vertical dimensions, the water movement in the vertical is considered zero normal to estuary axis. Hence Coriolis force need not be considered in estuarine circulation but the pressure gradient here balances the frictional forces along the estuary that is caused due to strong tidal currents. In a way it is similar to the circulation in a laboratory tank.

The estuarine salinity field is determined by the balance between advection by the mean flow and turbulent tidal diffusion.

Mathematically this balance is expressed in a non linear differential equation. Non linear dynamic systems are much more difficult to describe than linear systems. This is because the solution to a linear problem can be found by solving simpler problems first and then adding the results. Non linear dynamic systems do not have this additive property, so their solution has to be found in a single attempt including all relevant forces. Thus analyses of dynamics of estuaries are more complicated than that of the open ocean.

So to solve this problem estuaries are classified into different types basing on their circulation characteristics or topography.

1.1. TYPES OF ESTUARIES:

Estuaries are far from uniform in character and the differences are mainly due to variations in tidal range and river discharge, which affect the extent to which saline sea water mixes with fresh water. On this basis the estuaries are broadly recognized into three types as salt wedge, partially mixed and well mixed estuaries.

Pritchard (1952) introduced a classification of estuaries based on topography. They are coastal plane estuaries (drowned river valleys), fjords and bar built estuaries.

1.1.1. Coastal Plane Estuaries:

These are formed by the flooding of river valleys following a rise in sea level over geologic time. They show little sedimentation. So the ancient river valley still determines the estuarine topography. These estuaries are shallow, with depths rarely exceeding 30 m or so and mostly located in the temperate climate zones. Examples of this are the Chesapeake Bay in Maryland and the harbor in Charleston, South Carolina

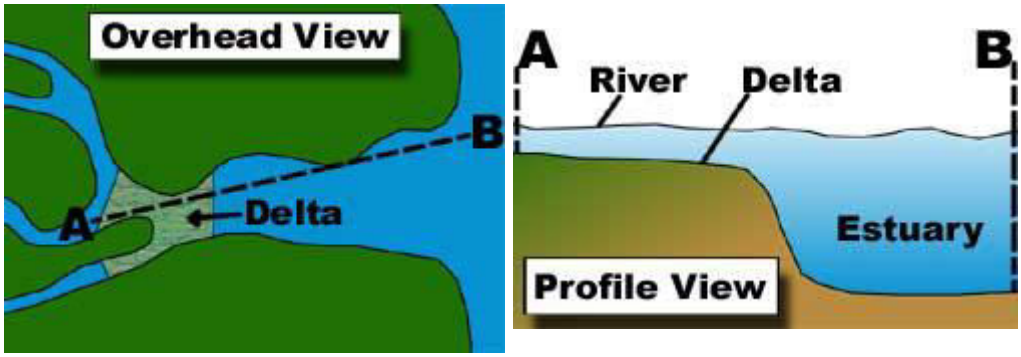

1.1.2. Bar built estuaries:

Bar-built estuaries are drowned river valleys with a high sedimentation rate. They form when a shallow lagoon or bay is protected from the ocean by a sand bar or barrier island. They are thus mostly very shallow, with depths of a few meters. They often branches into two such as a shallow water way or a lagoon extending towards the mouth. The most characteristic feature of bar-built estuaries is accumulation of sediment near the mouth of the estuary and forming a bar. Most of the Indian estuaries along east coast are bar-built estuaries. Thus they are common in subtropics and tropics. These are alsofound along the Eastern Seaboard and the Gulf Coast of North America.

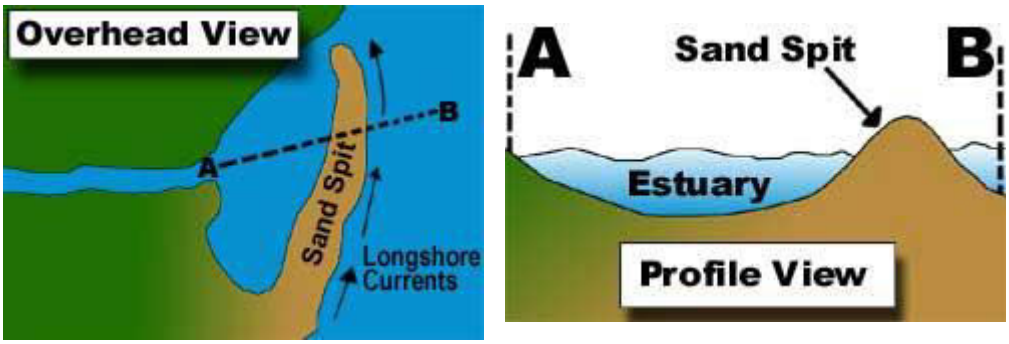

1.1.3. Fjords:

These are also U-shaped river valleys deepened by glaciers during the last ice age. The scouring of the valley floor results in very deep estuaries. So

the depth of fjords sometimes exceeds 800 m or so. The most characteristic feature of fjord is the existence of a shallow sill at the mouth formed by accumulated rock at the glacier front. The sill depth can be between 40 m and 150 m. True fjords are also found in the temperate zones. Fjords are found in areas with long histories of glacier activity, like northern Europe, Alaska and Canada.

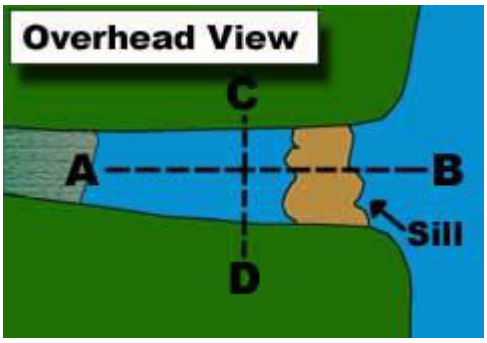

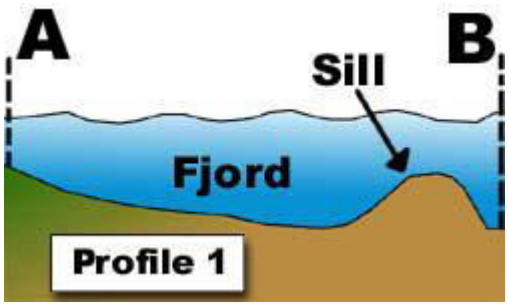

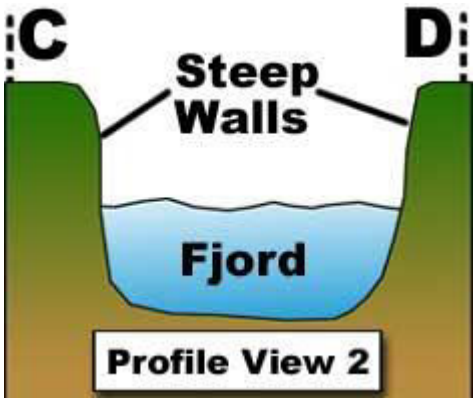

Most of today's estuaries formed because the sea level has slowly risen during the last 18,000 years, drowning river valleys and filling in glacial

2. **Tectonic Estuaries** are caused by the folding or faulting of land surfaces. These estuaries are found along major fault lines, like the San Francisco Bay area in California.

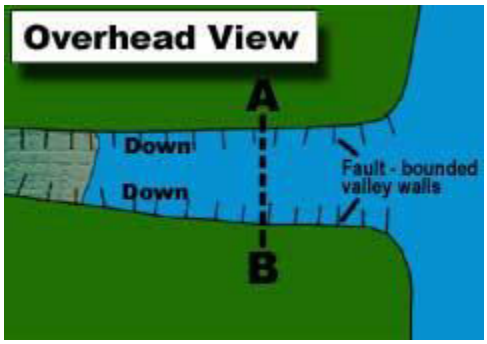

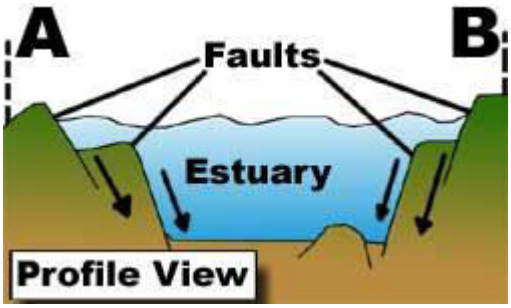

3. **Classification of estuaries basing on circulation**:

However, the above classification has limited use and practically far different from the circulation characteristics. As estuaries are predominantly controlled by tidal

currents and mixing of fresh water and salt water varies with time, season and space, they are classified, for scientific study purpose, into three types. They are salt wedge, partially mixed and well mixed type of estuaries

However, in recent times, another type of classification followed is basing on salinity stratification in estuaries as shown in Fig.1. The salt content of the estuary depends on the difference in volume of river water (R) that enters at one end of the estuary and leaves at the other end (mouth). In other words the salinity field is controlled by the balance between advection of fresh water and diffusion of salt. This diffusion is achieved through turbulence caused by tides.

The type of turbulence that occurs in an estuary is determined by the strength of the tide. This can be expressed by tidal volume (V). The tidal volume is defined as the difference in volume of water brought into the estuary by the flood tide to the ebb tide during a tidal cycle.

By comparing V and R over the same tidal period we derive the first four types of estuaries.

The vertical integral of the average velocity profile multiplied by the cross sectional area of the estuary gives net volume transport (M) which is equal to R divided by the tidal period. So the unit of M is m^3 S^{-1}. The cross sectional average of the vertically averaged mean velocity is given by R/AT, where A is the cross sectional area of the estuary and T is the tidal period. For classification of estuaries the absolute values of R and V is not important but their ratio R/V is important.

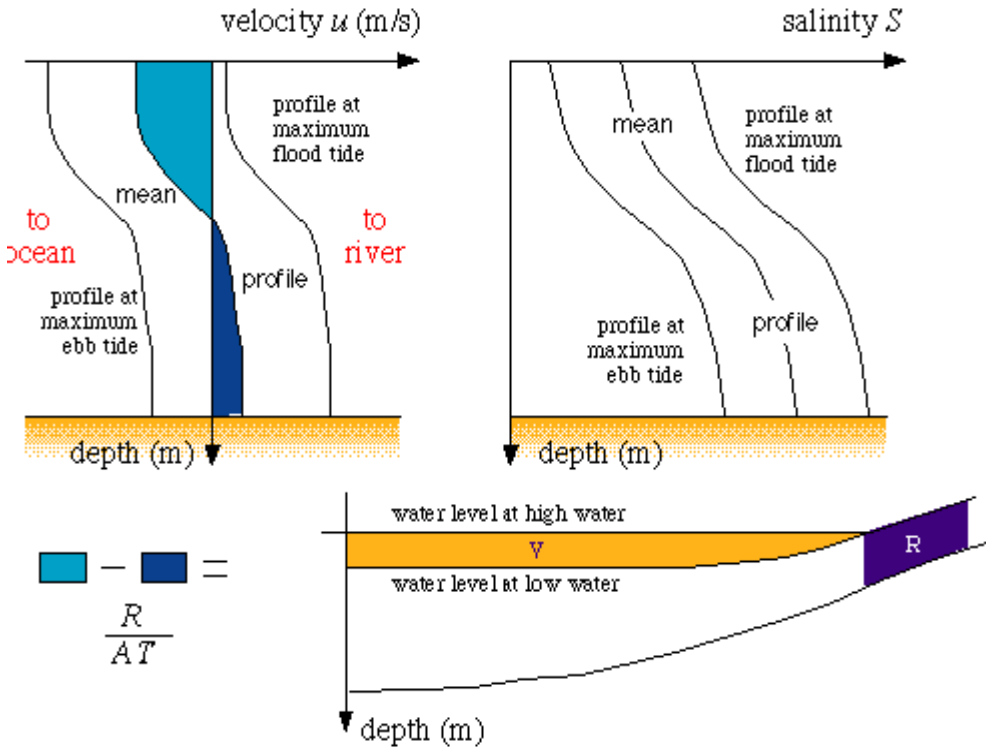

Fig.1.Sketch of variations of current and salinity over a tidal period *T*. As Fresh water flows in the upper layer from River to Ocean so profile is concave. Similarly sea water flows from ocean to river side in the sub surface so profile is convex below. Same situation appears in salinity profile also. The difference between the shaded areas of mean

velocity profile corresponds to $V_R - V_0 = \frac{R}{AT}$ where V_R is Ocean volume in the above(Navy blue hatching) and V_0 is ocean volume below(Royal blue hatching), R is river volume, A cross sectional area of estuary and T tidal period.

Top diagrams: velocity and salinity profiles at maximum flood and ebb tides and after averaging over *T*; bottom diagram: the relationship between tidal volume *V* and fresh water volume *R*.

3.1.1. Salt wedge estuaries:

These types develop where a river discharge (R) is much higher than tidal volume (V). The less dense river water spreads out horizontally in the top layer towards the sea while the more dense sea water flows upstream below the surface as shown in fig.2.

Hence between the two layers a boundary (wedge) or front is formed. Between the fresh water and sea water there are very sharp density and salinity gradients develop so that a stable halocline develops and the two water types do not mix easily. However, because one layer of water is moving over another layer, a shear stress occurs at the interface, producing turbulence at the base of the fresh water which generates a series of internal waves along the interface (salt wedge). Typical R/V ratios for salt wedge estuaries are more than unity.

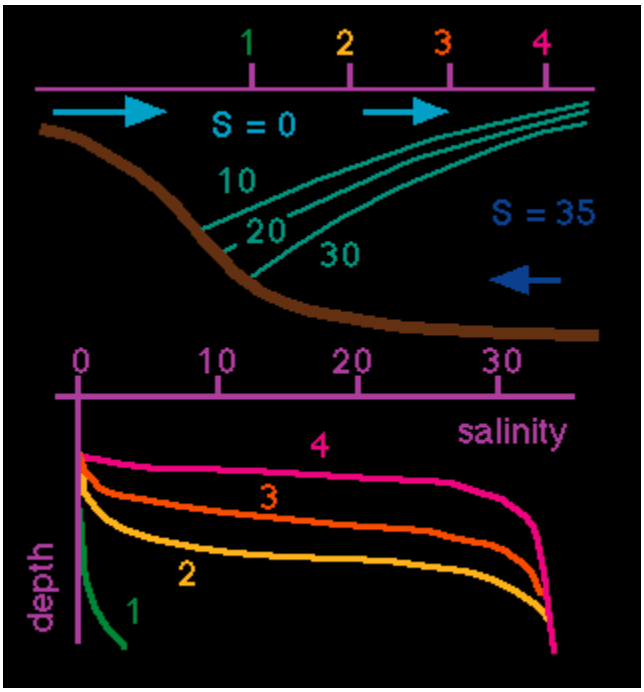

Fig.2. Salinity in a salt wedge estuary. Top Figure: Surface salinity is close to zero at all stations (1 to 4), bottom salinity close to oceanic. Bottom figure: vertical salinity profiles for stations 1-4.

3.1.2. Highly stratified estuary:

These estuaries occur where rivers discharge into the sea with a moderate tidal range as shown in Fig.3. Tidal currents are significant and so the whole water moves up and down with flood and ebb tide. Thus in this estuary tidal volume (V) increases over river discharge volume (R) then the ratio $\frac{R}{V}$ reduces to 0.1 to 1.0. Due to strong tidal forcing, strong current shear develops at the interface that causes entrainment. This current shear creates instabilities in the form of internal waves which become unstable and break. When the tops of the breaking waves separate from the interface they inject salt water into the upper layer. The result is a net upward transport of mass and salt known as entrainment. Actually the definition of entrainment is transport of mass from a less turbulent medium to more turbulent medium.

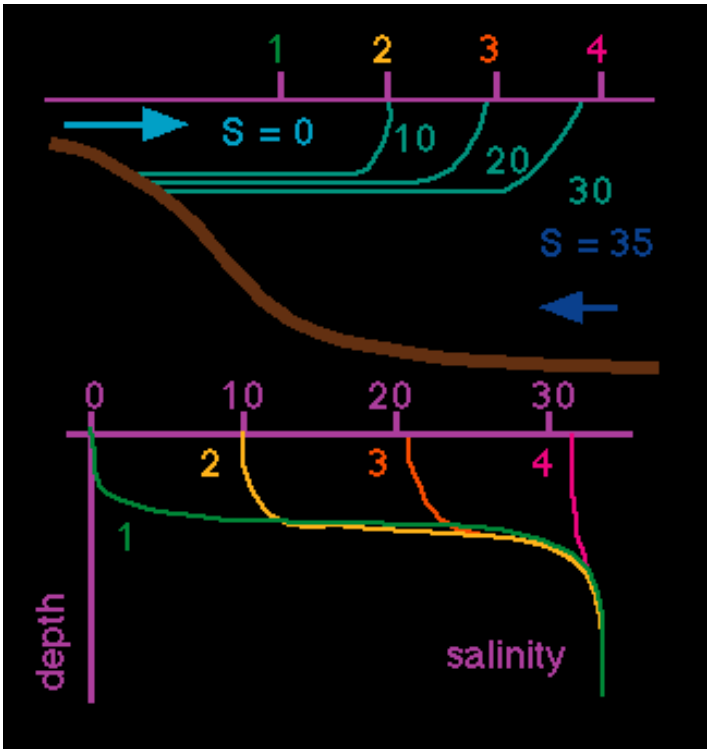

Fig. 3. Upper fig: Salinity in a highly stratified estuary. Lower fig: Surface salinity increases from station 1 to 4, but bottom salinity is close to oceanic at all stations.

The characteristic features of a highly stratified estuary are the salinity in the upper layer increases towards the sea, on account of the addition of salt by entrainment from the lower layer as shown in Fig.4. Thus while salinity will be equal to that of open ocean below the interface, salinity gradually increases towards the mouth above the interface of the surface layer.

Because water is constantly added to the upper layer along the length of the estuary, the interface always lie below and does not come to the surface even at the mouth. This interface is hard to determine from the salinity profile at the mouth and so it is determined by 'zero mean flow'. This zero mean flow is determined through current measurements over a tidal cycle.

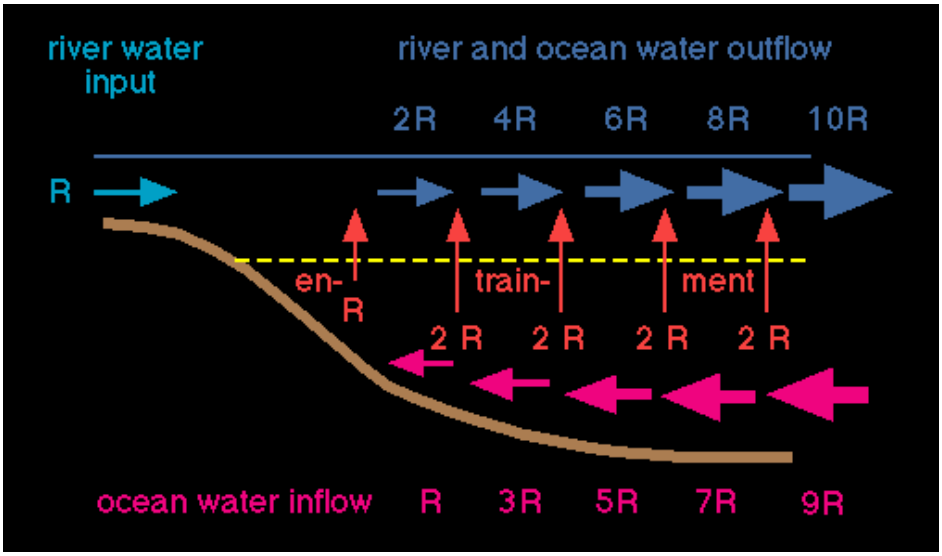

Fig.4. Entrainment in highly stratified estuary: Outflow from the estuary in the upper layer is 10R; this is compensated by inflow of oceanic water of 9R. The net flow at the outer end of the estuary is thus only 1R.

3.1.3. Slightly stratified estuary:

If the tidal volume (V) is further increased to a ratio $\frac{R}{V}$ equal to 0.005 to 0.1 then it is called slightly stratified estuary as shown in Fig.5.

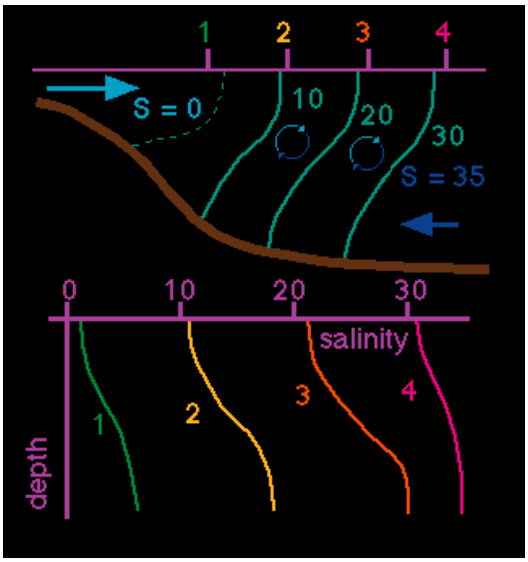

Fig.5. Salinity in a slightly stratified estuary. Top: as a function of depth and distance along the estuary, numbers indicate station locations, mixing between upper and lower layer is indicated by the faint circular arrows; bottom: vertical salinity profiles for stations 1 - 4.

Surface and bottom salinity increase from station 1 to station 4, but surface salinity is always lower than bottom salinity.

The tidal current is so strong that water movement becomes turbulent. Hence entire estuary experience turbulent mixing. As a result water and salt are exchanged between the two layers in both the directions. Thus while salinity in the upper layer increases towards the sea, the salinity in the lower layer decreases towards the estuary head. Vertical salinity profiles show a gradual salinity increase from the surface to bottom, with a maximum gradient near the interface between the two layers and gradual increase from station to station at all depths as the ocean is approached.

3.1.4. Vertically mixed estuary:

If the tidal volume is further increased to the ratio $\frac{R}{V} < 0.005$, turbulent mixing becomes so efficient that locally all salinity differences are nearly eliminated and the estuary turns into vertically mixed estuary (Fig.6).

The characteristics of this estuary are: i) the salinity increases towards the sea but doesn't vary with depth ii) the mean flow is very weak compared to the strong tidal current and is directed towards the sea at all depths iii) penetration of salt into estuary is achieved only by turbulent diffusion iv) the distribution between upper and lower layer can not be made.

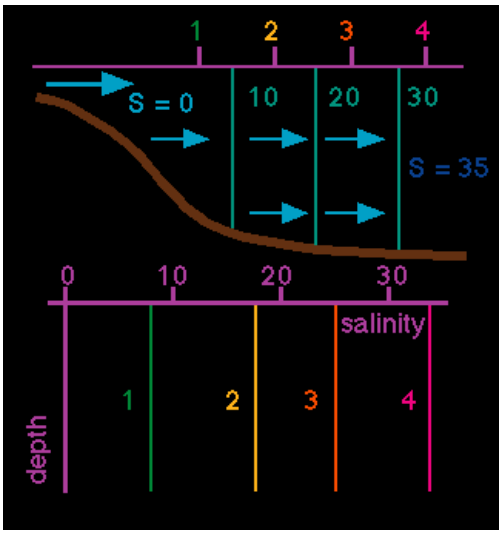

Fig.6. Upper: Horizontal flow of mass & salt from stations 1 to 4, Bottom: vertical salinity profiles from stations 1 to 4

3.1.5. Inverse or Negative estuary:

It is called negative estuary because $\frac{R}{V}$ value is negative (Fig.7). This estuary is understood by assuming that there is no river input and that the estuary is exposed to evaporation which leads to a salinity increase in the surface water at the inner end of the estuary. The associated increase of density causes to sink and flow towards the sea near the bottom. Thus though two layer system exists but the circulation is reverse. That is the flow from sea to river at the surface and river to sea at sub surface which is opposite to positive estuaries.

The characteristics of negative estuary are: i) the salinity in the upper layer decreases towards the sea and the salinity in the lower layer increases towards the river ii) Vertical salinity profiles show a gradual increase from the surface to bottom with a maximum in the vertical gradient near the interface iii) A gradual salinity decrease in the horizontal from river to ocean.

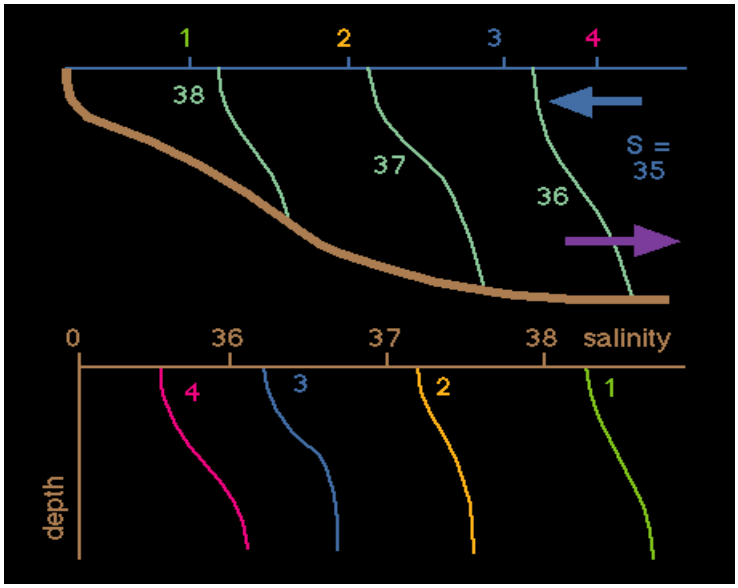

Fig.7.Salinity in an inverse estuary. Bottom: vertical salinity profiles for stations 1 - 4. The circulation is into the estuary at the surface; outflow occurs at sub surface depths. Surface and bottom salinities decrease from station 1 to station 4, but surface salinity is always lower than bottom salinity.

3.1.6. Salt Plug estuary:

In tropical regions generally evaporation exceeds the fresh water input of the river into the estuary is common. Then $\frac{R}{V}$ is just negative. But in arid regions where river run off into the estuary is poor and variable, evaporation is permanently high and so perpetual negative estuarine conditions prevail during dry seasons of the tropics. This type of estuary observed in these situations is known as salt plug estuary (Fig.8).

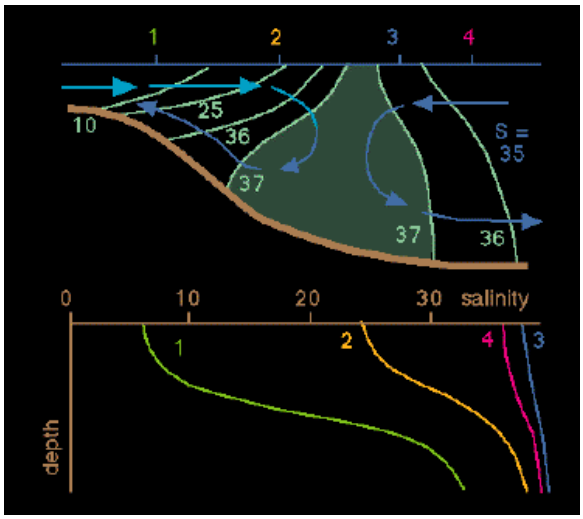

Fig.8. Sketch of a salt plug estuary. Upper: Note that the salt plug (shaded) is at the salinity maximum between stations 2 and 3. Please see the circulation on either side of the salt plug. Bottom: vertical salinity profiles for stations 1 – 4.

An intriguing feature of the salt plug estuary is while it appears that there is a continuity of water as a river entering the sea, really no water passes the salt plug and so very little water reaches the sea. The mean flow goes to zero at the salinity maximum, so the only exchange of water between the two sides is achieved by turbulent diffusion.

This has important consequences for the management of this estuary, since all the material introduced into the estuary on the river side of the salt plug will accumulate in the estuary until the next wet season removes the plug.

2.0. SALT BALANCE TECHNIQUES IN ESTUARIES:

This chapter discusses the methods to derive volume transports from the observations of salinity distribution. Such methods are based on the principle of salt conservation and therefore known as salt balance technique.

The basis for salt balance techniques is the diffusion equation for salt. For a two dimensional estuary it can be written as:

$$\frac{\partial}{\partial x}(us)+\frac{\partial}{\partial z}(ws)-\frac{\partial}{\partial x}\left(K_h\frac{\partial s}{\partial x}\right)-\frac{\partial}{\partial z}\left(K_v\frac{\partial s}{\partial z}\right)=0 \quad \ldots\ldots\ldots\ldots\ldots\ldots\ldots(1)$$

Where u and w are horizontal and vertical component of velocity, S is salinity, K_h and K_v are horizontal and vertical turbulent diffusion (Austausch) coefficients for salt, x is the horizontal coordinate measured positive from the inner end of estuary towards the sea and z is vertical coordinate downward.

The first term in the equation expresses transport of salt by horizontal current (horizontal advection). The second term expresses transport of salt by vertical water movement (vertical advection). The third term represents the net transport of salt from horizontal turbulent mixing and the last term gives the contribution to the salt transport from vertical turbulent mixing. Note that all turbulent mixing is the result of tidal action. Therefore all this depends on strength of the tide.

The equation can be simplified for different classes of positive estuaries. In the case of salt wedge and highly stratified estuary all salt transport is achieved by advection only. So the diffusion equation changes as:

$$\frac{\partial}{\partial x}(us)+\frac{\partial}{\partial z}(ws)=0 \ldots\ldots\ldots\ldots\ldots\ldots\ldots\ldots\ldots\ldots\ldots..(2)$$

The vertical velocity w represents the effect of entrainment from the lower layer into the upper layer.

In the case of the slightly stratified estuary, the movement of salt between upper and lower layer is achieved by turbulent mixing. Horizontal mixing is negligibly small.

$$\therefore \frac{\partial}{\partial x}(us)+\frac{\partial}{\partial z}(ws)-\frac{\partial}{\partial z}\left(K_v\frac{\partial s}{\partial z}\right)=0 \ldots\ldots\ldots\ldots\ldots\ldots.(3)$$

In the case of vertically mixed estuary, it is characterized by vertically uniform property. This means vertical changes vanish. So in this case horizontal advection and tidal turbulent mixing are important.

$$\frac{\partial}{\partial x}(us)-\frac{\partial}{\partial x}\left(K_h\frac{\partial s}{\partial x}\right)=0 \ldots\ldots\ldots\ldots\ldots\ldots\ldots\ldots..(4)$$

In the case of vertically mixed wide estuaries where lateral salinity variations are significant, then the diffusion equation is :

$$\frac{\partial}{\partial x}(us)+\frac{\partial}{\partial y}(vs)-\frac{\partial}{\partial y}\left(K_h\frac{\partial s}{\partial y}\right)=0 \quad \ldots\ldots\ldots\ldots\ldots\ldots(5)$$

2.1. KNUDSEN'S HYDROGRAPHICAL THEOREM (KHT):

The salt transport in estuaries is a balance between two processes horizontal and vertical advection of salt. This makes it possible to derive some simple calculation scheme for the determination of mean circulation. They are based on the principle of conservation of volume and salt known as KHT.

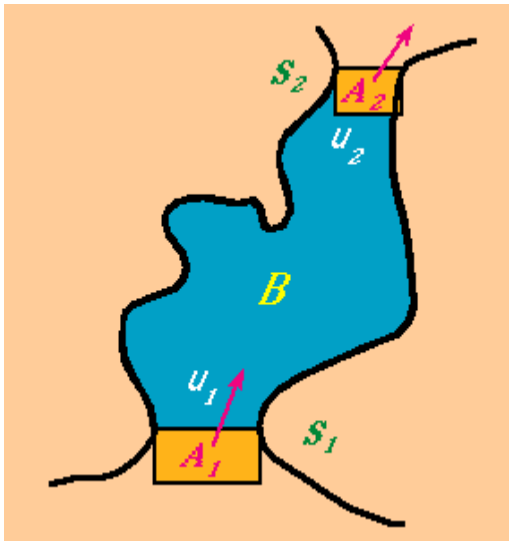

Fig.9. A sketch to illustrate the relationship between through flow velocity and salinity.

Let A_1, u_1 and S_1 are the cross sectional area, velocity and salinity at the entry point and A_2, u_2 and S_2 are the corresponding points at the exit point of the estuary as shown in Fig.9. The cross sectional area is the product of width and depth. If the flow is from $A_1$to A_2 it is positive and if it is reverse negative. Then

i) the volume transport per unit time at the entry point (Voume flux)(Q_1): A_1u_1
ii) the volume transport per unit time at the exit point (Voume flux)(Q_2) : A_2u_2
iii) the amount of salt entering the estuary per unit time (Salt flux) : Q_1S_1
iv) the amount of salt leaving the estuary per unit time (Salt flux at exit point) : $Q_2 S_2$

If there is a rainfall in the estuary, then let the rate of rainfall is r and let the area of the estuary is B. Then the volume of rain water (R) added is Br. In the steady state

condition the amount of water entering the estuary is equal to the amount of water leaving the estuary.

$\therefore Q_1 + R = Q_2$.....(6)

Similarly for conservation of salt: $Q_1 S_1 = Q_2 S_2$ .....(7)

As rain does not add salt rainfall term is not included here. The units used here are length in meters, time in seconds. A_1, A_2 and B are in m^2; u_1, u_2 are in ms^{-1} and convert r from $mmday^{-1}$ to meters $second^{-1}$. Then solving for Q_1, and Q_2 from (6) and (7) we get as:

$$Q_1 = \frac{R}{\frac{S_1}{S_2} - 1} \quad , \qquad Q_2 = \frac{R}{1 - \frac{S_2}{S_1}} \quad \text{.....(8)}$$

A quick inspection of this result shows that if $R > 0$ (rain added to the system), the water moves from the region of high salinity to low salinity because in order to be R positive, Q_1 must be positive. Q_1 will be positive when $S_1 > S_2$. So water moves from A_1 to A_2. Similarly if $S_2 > S_1$, Q_2 is negative and hence $R < 0$. Which means evaporation is more than the rainfall. Then the flow is from A_2 to A_1.Which means the flow is from the river (low salinity) to ocean (high salinity side). Under this condition the concentration of salt (salt plug) will be somewhere on the way.

2.2. ENTRAINMENT:

In a highly stratified estuary higher salinity sea water flows below and lower salinity river water mixture goes above. However mixing at the interface takes place through entrainment (Fig.10).

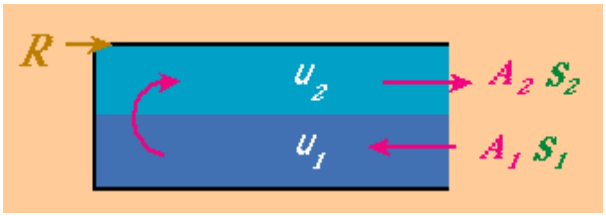

Fig.10. A sketch to derive the mass and salt balance for an estuary through entrainment

If B_e is the area of the estuary, the entrainment velocity or the upward velocity at the interface (w, the upward velocity at the interface) is given by:

$$wB_e = Q_2 = -\frac{S_1}{(S_1 - S_2)} R = \frac{S_1}{(S_2 - S_1)} R \quad \text{.....(9)}$$

The negative sign is assigned as it is rising from high denser water to low denser water.

For example, Fjords are good examples of highly stratified estuaries. The ratio $\frac{S_1}{(S_2 - S_1)}$ in Hardanger fjord of Norway varies between 2 to 6 during summer.

2.3. ITERATIVE KNUDSEN FORMULA:

Using the iteration method we can find the volume transport at second station if we know initial or first station. Let there are two stations (i-1) and i as shown in Fig.11.

let the through flow occurs in upper (top) and lower layer in opposite directions.

Fig.11. Sketch diagram for the iterative Knudsen formula

Then according to steady state principle, what goes in must be equal to what goes out. So we can write:

$$Q_i^T - Q_i^L = Q_{i-1}^T - Q_{i-1}^L \quad \text{.....(10)}$$

Similarly for conservation of salt we can write as:

$$Q_i^T S_i^T - Q_i^L S_i^L = Q_{i-1}^T S_{i-1}^T - Q_{i-1}^L S_{i-1}^L \text{.....(11)}$$

In equation 10 there are four unknowns. If we know two values at one station, we can find Q values at the other station. Solving the equations 10 and 11 we get:

$$Q_i^T = Q_{i-1}^T \frac{1 - \frac{S_{i-1}^T}{S_{i-1}^L}}{1 - \frac{S_i^T}{S_i^L}} \quad \text{similarly} \quad Q_i^L = Q_{i-1}^L \frac{\frac{S_{i-1}^L}{S_{i-1}^T} - 1}{\frac{S_i^L}{S_i^T} - 1} \quad \text{.....(12)}$$

These are known as iteration equations. Once you know the volume transport at any station (i-1), you can obtain at another station (i)

Similarly this technique can be applied if we have salinity data for 0,1,2…(n-1)n stations starting from estuary head (river entry point) to estuary mouth. We can find the volume transport at station 'n' from the volume transport at (n-1), which we find from (n-2). The volume transport at station '0' represents the starting point or initial condition of the iteration scheme which is to be found from the independent argument as below:

Let the volume flux from the river is R and it enters on the upper layer of the estuary. So

$$Q_0^T = R, \qquad S_0^T = 0 \text{.....(13)}$$

Because there is now lower layer at station '0' we can not apply equation 12 to determine Q_1^L. But we know that Q_1^L has to supply the volume flux necessary to increase the volume flux of the upper layer from R at station '0' to Q_1^T at station 1.

$$\therefore Q_1^L = Q_0^T - R \text{.....(14)}$$

Then Q_1^T can be calculated from equation (12) taking i =1 and using equation (13).this gives

$$Q_1^T = R\frac{1}{1-\frac{S_1^T}{S_1^L}} \quad \text{.....(15)}$$

As the salinities, S_1^T and S_1^L, are measured at all stations from 0 to n, Q_1^T can be calculated and for further stations can be calculated using iteration technique.

Problem: calculate volume transports for the following stations using Knudsen's hydrographical theorem for the given salinity data in a highly stratified estuary. Take the river flow rate as 12 m^3S^{-1} when lower layer salinity is constant.

Stn No/ salinity	0	1	2	3	4	5	6
S^T	0	5	10	15	20	25	30
S^L	-	35	35	35	35	35	35

Answer:

Stn No/ Vol transport	0	1	2	3	4	5	6
Q^T m^3 s^{-1}	12	14	16.8	21	28	42	84
Q^L m^3 s^{-1}	-	2	4.8	9	16	30	72

Example 2: When lower salinity varies:

Calculate volume transport for the given salinity data in a slightly stratified estuary

Stn No/ salinity	0	1	2	3	4	5	6
S^T	0	5	10	15	20	25	30
S^L	-	20	25	28	30	33	35

Answer:

Stn No/ Vol transport	0	1	2	3	4	5	6
Q^T m^3 s^{-1}	12	16	20	25.85	36	49.5	84
Q^L m^3 s^{-1}	-	4	8	13.85	24	37.5	72

2.4. THE FLUSHING TIME:

Increased use of estuaries by human population causes pollution in estuaries. So one of the tools used for estuarine management is the concept of flushing time. It is often used to determine how much of a potentially harmful substances an estuary can tolerate before its ecosystem is adversely affected to a significant degree.

2.4.1. Definition of Flushing Time:

In its simplest form, it is defined as the time needed to drain a volume of water (V) through an outlet area A with a current velocity 'u'. Let 'B' is the surface area of the estuary and 'H' is the depth and 'A' is the cross section area of the mouth of the estuary and 'T' is the tidal cycle. Then the volume of water drained out in a tidal cycle is

V = BH = AuT

Quantitatively, the flushing time (t_F) of an estuary can be defined as the time needed to replace its fresh water volume V_F at the rate of the net flow through the estuary by the river water discharge rate R.

$$\therefore t_F = \frac{V_F}{R}$$

As the measurement of fresh water volume is not easy, it can be estimated as

$$\therefore t_F = \frac{f^* V}{R} \quad \text{.....(2)}$$

Where $f^* = \int f dv = \frac{S_0 - S}{S_0}$ .....(3)

Here 'V' is the volume of the estuary, S_o is the oceanic salinity found outside the estuary mouth and S^* is mixed water. Also here while 'f' represents fresh water fraction in a water sample, 'f*'represents the average fresh water fraction.

Calculation of flushing time by equation (2) requires the knowledge of the volume of the estuary (V), rate of river discharge ® and salinity distribution through the entire estuary. The volume of the estuary can be estimated by measuring the bathymetry. The river discharge can be measured at a single point at the inner end of the estuary by a flow meter or current meter.

2.5. TIDAL PRISM METHOD:

The flushing time derived from the tidal prism method represents the shortest possible time during which the entire fresh water fraction of an estuary can be removed.

Tidal prism is the net combined sea and fresh water volume entered into estuary during a tidal cycle.

This method starts from the concept that a sea water volume V_T enters the estuary with the rising tide, while a fresh water volume V_R enters the estuary during a tidal cycle (rising to falling tide) as shown in Fig.12. It assumes that sea water V_T is completely mixed with fresh water V_R at high tide and that the mixed water (V_T + V_R) leaves the estuary during low tide.

If S_o is sea water salinity and S^* is mixed water salinity we can write

$$(V_T + V_R)S^* = V_T S_0$$

$$\therefore S^* = \frac{S_0 V_T}{(V_T + V_R)} \quad \text{.....(4)}$$

Substituting the value of S^* from the equation (3) in (4) we get

$$f^* = 1 - \frac{V_T}{(V_T + V_R)} = \frac{V_R}{(V_T + V_R)} \text{.....(5)}$$

The flushing time according to equation (2) is $t_F = \frac{f^* V}{R}$ where R is rate of river discharge or fresh water volume per unit time. In the tidal prism concept the unit of time is tidal cycle (T).

$$\therefore R = \frac{V_R}{T} \quad \text{.....(6)}$$

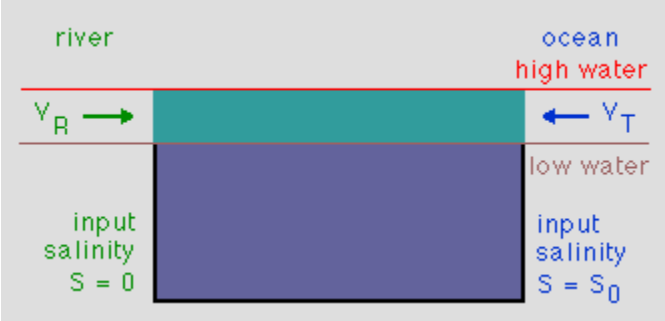

Fig.12. Sketch diagram for the definition of the fresh water and salt water volumes in the tidal prism method. The combined volume $\mathbf{V_T + V_R}$ represents the difference between low water and high water.

Substituting equation (5) and (6) in equation (2) we get

$$t_F = \frac{V\,T}{(V_T + V_R)} \text{.....(7)}$$

This method gained importance as the only two quantities required to be estimated are (V_T+V_R) and V. Whereas in the case of general method extensive observations are needed for measurement of salinity, bathymetry and current or flow and river discharge season wise.

Limitations:

The assumptions of the tidal prism method are never completely met in real estuaries. Mixing of the two waters V_T and V_R is never complete. Some of the mixed water that leaves the estuary during ebb tide may enter again during flood tide.

Tidal prism method is more suitable for slightly stratified and vertically mixed estuaries.

2.6. KNUDSEN'S METHOD:

Another method of estimation of flushing time is due to Knudsen's method. This can be achieved from the salt balance equation of Knudsen's formula.

If R denotes the river discharge rate, Q_B and Q_T are the volume transports of water entering and leaving the estuary at its mouth with respective salinities S_B and S_T, then we can write the continuity of volume and mass (salt) as

$$\begin{aligned} Q_T - Q_B &= R \\ Q_T S_T &= Q_B S_B \end{aligned} \quad \text{.....(8)}$$

Eliminating Q_B from these two equations we can write $Q_B = Q_T - R$.Substituting this in second equation we get

$$Q_T S_T = (Q_T - R) S_B$$

$$\therefore Q_T = \frac{RS_B}{S_B - S_T} \quad \text{.....(9)}$$

But we know the flushing time as $t_F = \frac{V}{Q_T}$ .....(10)

substituting the value of Q_T from equation (9) in equation (10) we get

$$t_F = \frac{V}{R}\left[1 - \frac{S_T}{S_B}\right]$$

Where V is volume of the estuary, R River discharge S_T salinity at the surface and S_B at bottom near any station at the mouth of the estuary.

The main assumption of knudsen's formula is that all the sea water that enters the estuary through the bottom leaves it through upper layer after complete mixing with fresh water.

Limitation :

If the interface is weak and more diffuse the upper layer will not maintain zero salinity at the head then the above formula under estimates the true flushing time.

In practice Knudsen's formula appears more appropriate for highly stratified and salt wedge estuaries.

The following table gives the summary of the three methods:

Method	Formula	Input data	Remarks
General method	$t_F = \frac{f^* V}{R}$	• Estuary volume, bathymetry • Salinity • Rate of river discharge	
Tidal prism method	$t_F = \frac{V\,T}{(V_T + V_R)}$	• Estuary topography(volume) • Sea level (tidal record)	• Under estimates • Suitable for slightly stratified estuaries
Knudesen's method	$t_F = \frac{V}{R}\left[1 - \frac{S_T}{S_B}\right]$	• Estuary topography • Salinity profile at the mouth • Rate of river discharge	• Under estimates • Suitable for highly stratified estuaries

4. ESTUARINE MODELLING:

Man's most intense utilization of the marine environment occurs in the estuary. The estuary has long been considered a reservoir for man's wastes, but its capacity to absorb the waste materials is quickly being reduced. A significant portion of the world's food supply is harvested from the estuary. The distance of inland penetration of seawater varies with the relative strength of the fresh water discharge and the co- oscillating tidal flow resulting from the dynamical interaction with an adjacent coastal sea. So the knowledge of the dynamics that govern the estuarine circulation pattern becomes essential.

4.1. GOVERNING EQUATIONS:

The set of equations that describe the dynamics of a partially mixed estuary is the vertically integrated continuity equation, momentum balance equations, the thermodynamic equation, the salt balance equation, turbulent energy density equation and an equation of state. Here the parameterization of the turbulent processes is considered by the application of a transport equation for the turbulent energy density. The set of equations has been simplified to eliminate the lateral (y) momentum balance equation and all the other lateral derivatives. The simplification process assumes that all variables except the lateral velocity (v) are independent of y and the lateral average of v is zero. These assumptions not only reduce the dimensionality of the problem but permit a physical interpolation for both the turbulent stresses and salt fluxes. The governing equations contain the Bousinesq approximation and the hydrostatic assumption.

Therefore the equation of continuity in the channel is written as:

$$b\frac{\partial H}{\partial t}+\frac{\partial}{\partial x}\left(bH\bar{u}\right)=0 \quad \text{.....(1)}$$

Where (H = ζ + H) is total depth of the channel, b is the breadth of the channel, ζ the elevation of water level over mean level, h depth of the channel and $\bar{u}$ is depth averaged velocity given by:

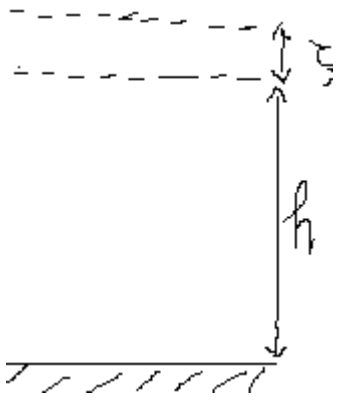

$$\bar{u}=\frac{1}{H}\int_{-h}^{\zeta}u\,dz$$

Here z = $\zeta_{(x,t)}$ and $-h_{(x)}$ refer to the location of the disturbed free surface to the impermeable floor of the channel and its breadth is denoted by b_x.

The momentum equation has the form:

$$\frac{\partial}{\partial t}(bu)+\frac{\partial}{\partial x}(bu^2)\frac{\partial}{\partial z}(buw)=-gb\frac{\partial\zeta}{\partial x}-\frac{b}{\rho_0}\int_z^{\zeta}\frac{\partial}{\partial x}(\rho g)dz+\frac{\partial}{\partial z}[K_M\frac{\partial}{\partial z}(bu)]+\ell(u)\ldots..(2)$$

The letter ℓ is an operator such that $\ell(u)$ simulates the effect of horizontal momentum exchange by turbulent scale motions. The inclusion of such a term is required if there is any anticipated formation of an internal hydraulic jump in the estuary.

The salinity S is determined from the transport equation which has the form:

$$\frac{\partial}{\partial t}(bs)+\frac{\partial}{\partial x}(bus)\frac{\partial}{\partial z}(bws)=\frac{\partial}{\partial z}[K_S\frac{\partial}{\partial z}(bs)]+\ell(u)\ \ldots\ldots\ldots\ldots\ldots\ldots\ldots\ldots(3)$$

Where K_S is exchange coefficient. The term $\ell(s)$ represents the effect of turbulent horizontal salinity flux which is expected to be of secondary importance when compared to the advective salinity flux.

Similarly we can write the transport equation for turbulence energy density, E as:

$$\frac{\partial}{\partial t}(bE)+\frac{\partial}{\partial x}(buE)\frac{\partial}{\partial z}(buE)=bK_M\left(\frac{\partial u}{\partial z}\right)^2+P+\frac{g}{\rho_0}bK_S\frac{\partial\rho}{\partial z}+\frac{\partial}{\partial z}[K_E\frac{\partial}{\partial z}(bE)+\ell(E)-b\varepsilon$$

$\ldots\ldots\ldots\ldots(4)$

The terms on the right hand side are: the first term represents a production of turbulent energy consequent upon vertical shear in the Reynolds averaged flow. The second term represents a production of turbulent energy due to the action of normal eddy stresses. These two terms describe the ways in which the energy is transported from the Reynolds averaged flow to the turbulent energy budget.

For $\frac{\partial\rho}{\partial z} < 0$, the third term represents a sink of turbulent energy resulting from the presence of stable density stratification. The fourth term represents the vertical diffusion of turbulent energy with an eddy coefficient K_E. The fifth term represents the horizontal redistribution of turbulent energy by the turbulence itself. The final term involving ε simulates the dissipation of turbulent energy.

Lecture Series of Berhampur University in Physical Oceanography
By Prof.A.S.N.Murty

Chapter-10

STORM SURGES

A storm surge is defined by N.S.Heaps (1967) as a 'raising or lowering of sea level produced by wind and by changes in atmospheric pressure over the sea associated with a storm'.

Actually the height to which the water level near the coast rises consequent up on the passage of a storm depends on various factors as given by the equation:

$$H = A + B + P + X + F$$

Where 'A' is contribution due to astronomical tides, 'B' is static rise due to barometric pressure drop commonly known as inverted barometric effect which is generally one centimeter of sea level for every one millibar pressure drop, 'P' is the rise due to piling up of water against the coast by winds, 'X' is the mean height of the crests of the individual waves superimposed on the general rise of the sea level and 'F' is the effect of the fore runners.

The effect of waves (X) is important only for seasonal sea level variations but not to the transient storm surges. The effect of waves on sea level will be of the order of a few centimeters while the transient surges are of the order of some hundred centimeters. Hence the effect of 'X' is not important for surges. The last factor 'F', the fore runner, serves as a warning to the coastal people about an impending surge when the storm is a few hundred kilometers away from the coast. Its elevation is also very small.

The astronomical tide 'A' may either enhance the surge if the high tide time and occurrence time of surge coincide. The information on astronomical tide can be obtained fro the tide tables published by survey of India which when the surge and high tide come at a time it has resonance effect other wise its effect is nil.

Thus the final height of the storm surge mainly depends on the piling –up effect (P) due to winds of the storm which need to be computed using the gradient wind equation and the isobar pattern of the cyclone.

1.2. The computation of Piling-up effect (P):

Welander (1957) gave the slope of the equation caused due to wind as:

$$\frac{dZ}{dx} = \frac{\lambda \tau}{\rho_w g h}$$

Where Z is the elevation of the water surface, x is the horizontal coordinate in the direction of wind, τ is wind stress, g is acceleration due to gravity, ρ_w is the density of water (1025 kg m^{-3}), h is the average depth of the basin and λ is the Mannings frictional factor which varies between 1 and 1.5 depending upon the frictional conditions at the sea bottom.

The wind stress τ can be computed using the equation: $\tau = \rho C_d w^2$ where τ is N m^{-2}, ρ_a density of air (1.3 kg m^{-3}) and C_d is the drag coefficient which depends on the height and speed of wind at which it is measured, the stability of the lowest few meters of the atmosphere, the roughness of the sea surface. For Indian Ocean region we can take $C_d = 2.6\times10^{-3}$ when wind speeds are greater than 7 ms^{-1} and it is equal to 1.5×10^{-3} for wind speeds less than 7 ms^{-1}.

Substituting all the above values taking $C_d = 2.6\times10^{-3}$ we can write the welander's equation as: $\frac{dZ}{dx} = 4.2\times10^{-7}\left(\frac{W^2}{h}\right)$. The value of P is obtained by the summation of the slopes $\left(\frac{dZ}{dx}\right)$ generated by the wind stress starting from the origin of the cyclone to the landfall point along the track of the cyclone. Therefore, P is calculated by step wise integration from the initial position to landfall.

$$\therefore P = \sum dZ = 4.2\times10^{-7} W^2 \sum \frac{dx}{h}$$

Problem:

a) Calculate the slope of the sea surface caused due to wind speed of 20 m/s at a depth of 50 m

b) What is the rise of sea level over a distance of 500 km.

Ans: a) $\frac{dZ}{dx} = 4.2\times10^{-7}\left(\frac{W^2}{h}\right) = 4.2\times10^{-7}\left(\frac{20^2}{50}\right) = 33.6\times10^{-7}$

b) $dZ = 33.6\times10^{-7}\, dx = 33.6\times10^{-7} \times 500\times10^{3} = 1.68$ m

2. METHODS OF FORECASTING STORM SURGES:

2.1. Empirical methods:

Prior to the development of numerical models, empirical methods were devised for forecasting the surge level at a particular coastal location by correlating it with meteorological conditions over an area of sea. For example, a formula was obtained by Heaps (1967) for the surge height at Southend, at the mouth of the Thames estuary, in terms of northerly and easterly pressure gradients over the North Sea.

2.2. Mathematical Methods:

The methods for forecasting storm surges now use a suitable model obtained from the basic dynamic equations. The model may be two or three dimensional. If the variation of velocity with depth is retained in the depth integrated equation, then it is called three dimensional model. Two dimensional models may be classified as linearized when several when several approximations are made and non linear if the full equations are used. Though in many cases linearized models give an adequate representation of conditions, but this is not always true. Because in shallow areas where the tidal amplitude or surge height is not small compared with the depth of water and bottom friction effects

are considerable, there is significant interaction between tide and surge and misleading results will come unless the nonlinear terms are retained.

2.2.1. Linearized equations for depth integrated flow:

Assumptions required for linearizing the basic storm surge equations.

1. the elevation ζ remains small compared with the undisturbed depth of water 'h'
2. the convective acceleration terms $\frac{\partial}{\partial x}\left(\frac{U^2}{h+\zeta}\right), \frac{\partial}{\partial y}\left(\frac{U\ V}{h+\zeta}\right)$ are negligible compared with $\frac{\partial U}{\partial t}, \frac{\partial V}{\partial t}$ terms.
3. The components of bottom stress can be linearly related to the components of integrated transport U and V such that setting $\tau_{bx} = \lambda \rho U$ and $\tau_{by} = \lambda \rho V$ where $\lambda = \frac{k}{h} \approx \frac{kC}{h}$ where $k = ARC$
4. Tide generating potential $\bar{\zeta}$ is neglected

Where λ is a coefficient having the dimensions of velocity. The admittance coefficient, A, is a factor of order of unity, R the drag coefficient, C is the depth mean current. 'A' is due to the ratio of bottom velocity to depth mean velocity and includes the factor $\frac{4}{\pi}$.

With these assumptions equations 7 a to c reduces to

$$\frac{\partial U}{\partial t} + \lambda U - fV = -\frac{h}{\rho}\frac{\partial P_a}{\partial x} - gh\frac{\partial \zeta}{\partial x} + \frac{\tau_{sx}}{\rho} \quad \text{.....1a}$$

$$\frac{\partial V}{\partial t} + \lambda V + fU = -\frac{h}{\rho}\frac{\partial P_a}{\partial y} - gh\frac{\partial \zeta}{\partial y} + \frac{\tau_{sy}}{\rho} \quad \text{.....1b}$$

$$\frac{\partial U}{\partial t} + \frac{\partial V}{\partial y} + \frac{\partial \zeta}{\partial t} = 0 \quad \text{.....1c}$$

Note that the coefficient λ which depends on the tidal current amplitude and the depth h is a function of x and y.

2.2.2. Analytical and numerical solutions:

a) Analytical solutions:

A number of analytical solutions have been obtained for areas of simple geometrical shape like shelf adjacent to a straight coast, a closed basin or a channel closed at one end. The wind stress is assumed to be applied suddenly and then maintained at a constant value.

An example of an investigation using analytical solutions is that by Heaps (1965) dealing with storm surges on a continental shelf. A shelf of uniform width and depth was

assumed, bounded by a straight coast on one side and connected with an infinitely deep ocean on the other. A moving wind field was applied and the following cases considered.

i) the response on the shelf to an input surge from the ocean, specified by $\zeta = f(t)$ at x= l

ii) the generation of a surge on the shelf by a steady wind stress suddenly created

iii) the elevation at the coast produced by a wind field with a moving boundary.

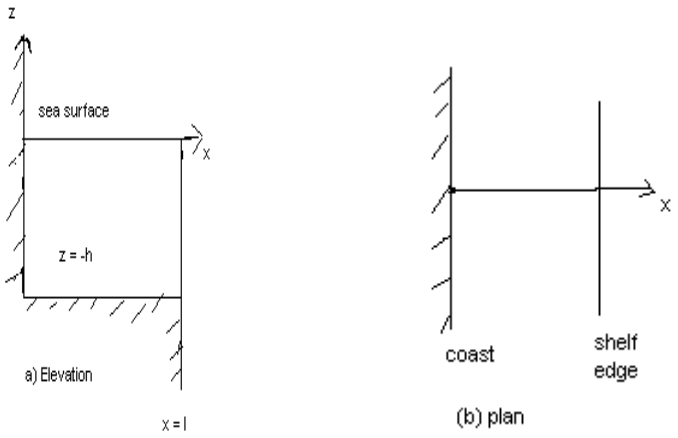

Fig.1

b) Numerical solutions:

For detailed studies of surges in a particular region numerical models are more suitable. The region can be represented by a net work of elementary areas which approximate to the actual coastline at a boundary and which use the actual depths of water in the offshore areas.

An important point in formulating a numerical model is the specification of appropriate boundary conditions. The coast is usually represented as a vertical wall with the condition that transports normal to it, denoted by V_n, is zero. Thus if the normal to the coast is inclined at an angle α to the x-axis as in the figure, the condition is:

$$V_n = U\cos\alpha + VSin\alpha = 0$$

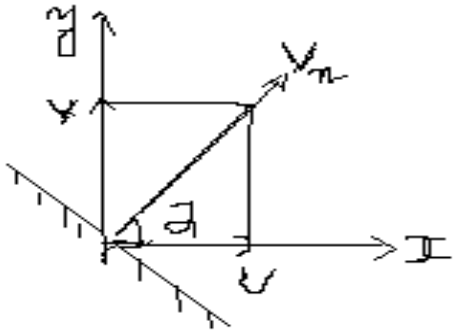

Fig.2

At an open boundary, represented by a straight line separating the modeled region from the open ocean, there are several alternative conditions which may be applied.

a) the elevation may be assumed to be zero i.e. ζ =0
b) The elevation may be prescribed for example from the distribution of atmospheric pressure or by an assumed external surge i.e. $\zeta_{x,y,t}$ is given on the boundary.
c) The normal transport may be prescribed as $V_n = U\cos\alpha + VSin\alpha = F_{x,y,t}$
d) The derivative of the transport normal to the boundary may assumed to be zero i.e. $\frac{\partial V_n}{\partial y_n} = 0$
e) The radiation condition may be applied, stating that any energy reaching the boundary from inside the model travels outwards as a progressive wave, without reflection. This can be expressed as $V_n = \left(gh\right)^{1/2}\zeta$ which is a special case of the more general condition: $V_n = A\zeta$ where A is called the Admittance Coefficient.

2.4. NON LINEAR EFFECCTS ON DEPTH INTEGRATED FLOW:

When the elevation of the water surface (ζ) is no longer small compared with the depth of water (h) the effects of the non linear terms in the equation of motion become significant. Hence to obtain the results sufficiently accurate, the full equations must be used.

The basic hydrodynamic equations of motion are:

$$\frac{du}{dt} = -\alpha\frac{\partial p}{\partial x} + fv + F_x$$
$$\frac{dv}{dt} = -\alpha\frac{\partial p}{\partial y} - fu + F_y \qquad (1)$$

The vertical component equation of motion is

$$\frac{dw}{dt} = -\alpha\frac{\partial p}{\partial z} - g + F_z \qquad (2)$$

In equation (2) $\frac{dw}{dt}$ =0 as the surge is horizontally accelerated in a frictionless medium

$$\therefore \frac{\partial p}{\partial z} = -\rho g$$
$$\int_{p_a}^{p} dp = -\rho g\int_{\zeta}^{z} dz$$
$$\therefore \left(p - p_a\right) = -\rho g\left(z - \zeta\right)$$
$$p = p_a + \rho g\left(\zeta - z\right) \qquad (3)$$

Where p_a is atmospheric pressure

The friction terms here describe the bottom stresses and they are obtained from Reynolds shearing stresses as

$$F_x = \alpha \frac{\partial \tau_x}{\partial z} and F_y = \alpha \frac{\partial \tau_y}{\partial z} \quad \ldots\ldots\ldots\ldots(4)$$

Substituting (3) and (4) in (1) we can write as:

$$\frac{du}{dt} - fv = -\alpha \frac{\partial}{\partial x}\left[p_a + \rho g(\zeta - z).\right] + \alpha \frac{\partial \tau_x}{\partial z}$$
$$\frac{dv}{dt} + fu = -\alpha \frac{\partial}{\partial y}\left[p_a + \rho g(\zeta - z).\right] + \alpha \frac{\partial \tau_y}{\partial z} \quad \ldots\ldots\ldots..(5)$$

Taking z = $\bar{\zeta}$ and $\alpha\rho = 1$ we can write as

$$\frac{du}{dt} - fv = -\alpha \frac{\partial p_a}{\partial x} - g \frac{\partial}{\partial x}\left(\zeta - \bar{\zeta}\right) + \alpha \frac{\partial \tau_x}{\partial z}$$
$$\frac{dv}{dt} + fu = -\alpha \frac{\partial p_a}{\partial y} - g \frac{\partial}{\partial y}\left(\zeta - \bar{\zeta}\right) + \alpha \frac{\partial \tau_y}{\partial z} \quad \ldots\ldots\ldots\ldots..(6)$$

Expanding these equations:

$$\frac{\partial u}{\partial t} + u\frac{\partial u}{\partial x} + v\frac{\partial u}{\partial y} - fv = -\alpha \frac{\partial p_a}{\partial x} - g \frac{\partial}{\partial x}\left(\zeta - \bar{\zeta}\right) + \alpha \frac{\partial \tau_x}{\partial z} \ldots\ldots\ldots..(7a)$$

$$\frac{\partial v}{\partial t} + u\frac{\partial v}{\partial x} + v\frac{\partial v}{\partial y} + fu = -\alpha \frac{\partial p_a}{\partial y} - g \frac{\partial}{\partial y}\left(\zeta - \bar{\zeta}\right) + \alpha \frac{\partial \tau_y}{\partial z} \ldots\ldots\ldots..(7b)$$

Consider the volume transports by integrating through a vertical column from the bottom z = -h to the surge elevation z = ζ as

$$U = \int_{-h}^{\zeta} u dz = u(\zeta + h), u = \frac{U}{\zeta + h}$$
$$V = \int_{-h}^{\zeta} v dz = v(\zeta + h), v = \frac{V}{\zeta + h} \quad \ldots\ldots\ldots\ldots\ldots\ldots\ldots\ldots\ldots\ldots(8)$$

On substituting (8) in (7) we get :

$$\frac{\partial}{\partial t}\left(\frac{U}{\zeta + h}\right) + \frac{\partial}{\partial x}\left[\frac{U^2}{(\zeta + h)^2}\right] + \frac{\partial}{\partial y}\left[\frac{UV}{(\zeta + h)^2}\right] - f\left[\frac{V}{\zeta + h}\right] = -\alpha \frac{\partial p_a}{\partial x} - g \frac{\partial}{\partial x}\left(\zeta - \bar{\zeta}\right) + \alpha \frac{\partial \tau_x}{\partial z} \ldots\ldots\ldots..(9a)$$

$$\frac{\partial}{\partial t}\left(\frac{V}{\zeta + h}\right) + \frac{\partial}{\partial x}\left[\frac{UV}{(\zeta + h)^2}\right] + \frac{\partial}{\partial y}\left[\frac{V^2}{(\zeta + h)^2}\right] + f\left[\frac{U}{\zeta + h}\right] = -\alpha \frac{\partial p_a}{\partial y} - g \frac{\partial}{\partial y}\left(\zeta - \bar{\zeta}\right) + \alpha \frac{\partial \tau_y}{\partial z} \ldots\ldots\ldots..(9b)$$

Multiply both sides by (ζ +h)

$$\frac{\partial U}{\partial t} + \frac{\partial}{\partial x}\left[\frac{U^2}{(\zeta + h)}\right] + \frac{\partial}{\partial y}\left[\frac{UV}{(\zeta + h)}\right] - fV = -\alpha(\zeta + h)\frac{\partial p_a}{\partial x} - g(\zeta + h)\frac{\partial}{\partial x}\left(\zeta - \bar{\zeta}\right) + \alpha(\zeta + h)\frac{\partial \tau_x}{\partial z} \ldots\ldots\ldots..(10a)$$

$$\frac{\partial V}{\partial t} + \frac{\partial}{\partial x}\left[\frac{UV}{(\zeta + h)}\right] + \frac{\partial}{\partial y}\left[\frac{V^2}{(\zeta + h)}\right] + fU = -\alpha(\zeta + h)\frac{\partial p_a}{\partial y} - g(\zeta + h)\frac{\partial}{\partial y}\left(\zeta - \bar{\zeta}\right) + \alpha(\zeta + h)\frac{\partial \tau_y}{\partial z} \ldots\ldots\ldots..(10b)$$

The stress terms $\frac{\partial \tau_x}{\partial z}$ *and* $\frac{\partial \tau_y}{\partial z}$ can be integrated with the limits –h to ζ taking $\tau_{sx}, \tau_{bx}, \tau_{sy}, \tau_{by}$ respectively and writing

Let $\frac{\partial \tau_x}{\partial z} = K_x$ then $\int_{\tau_{bx}}^{\tau_{sx}} \partial \tau_x = \int_{-h}^{\zeta} K_x dz$ where s = surface and b= bottm

$$\therefore K_x(\zeta + h) = (\tau_{sx} - \tau_{bx}), \quad \therefore K_x = \frac{(\tau_{sx} - \tau_{bx})}{\zeta + h}$$

Similarly $\frac{\partial \tau_y}{\partial z} = K_y$ then $\int_{\tau_{by}}^{\tau_{sx}} \partial \tau_y = \int_{-h}^{\zeta} K_y dz$

$$\therefore K_y(\zeta + h) = (\tau_{sy} - \tau_{by}), \quad \therefore K_y = \frac{(\tau_{sy} - \tau_{by})}{\zeta + h}$$

Substituting these in the above equations we get

$$\frac{\partial U}{\partial t} + \frac{\partial}{\partial x}\left[\frac{U^2}{(\zeta + h)}\right] + \frac{\partial}{\partial y}\left[\frac{UV}{(\zeta + h)}\right] - fV = -\frac{1}{\rho}(\zeta + h)\frac{\partial p_a}{\partial x} - g(\zeta + h)\frac{\partial}{\partial x}\left(\zeta - \bar{\zeta}\right) + \frac{(\tau_{sx} - \tau_{bx})}{\rho} \quad \text{.....(11}a\text{)}$$

$$\frac{\partial V}{\partial t} + \frac{\partial}{\partial x}\left[\frac{UV}{(\zeta + h)}\right] + \frac{\partial}{\partial y}\left[\frac{V^2}{(\zeta + h)}\right] + fU = -\frac{1}{\rho}(\zeta + h)\frac{\partial p_a}{\partial y} - g(\zeta + h)\frac{\partial}{\partial y}\left(\zeta - \bar{\zeta}\right) + . \frac{(\tau_{sy} - \tau_{by})}{\rho} \quad \text{.....(11}b\text{)}$$

And the continuity equation remains as it is : $\frac{\partial U}{\partial x} + \frac{\partial V}{\partial y} + \frac{\partial \zeta}{\partial t} = 0$

These equations represent storm surge equations. In these equations the elevation ζ, the transport components U, V refer to the resultant values due to the tidal constituents and the meteorological storm effects of wind stresses at surface and bottom. In coastal waters of limited extent the direct effects of the tide generating potential, represented by $\bar{\zeta}$ can often be neglected.

In these non linear equations ζ, U, V refer to the elevation and transport components due to the tide surge combined.

2.5. EFFECT OF ATMOSPHERIC PRESSURE OF THE CYCLONE:

From equation 7a neglecting the terms acceleration, coriolis, stress and mean ζ terms we can write:

$$-\alpha \frac{\partial p_a}{\partial x} - g \frac{\partial}{\partial x}\left(\zeta - \bar{\zeta}\right) = 0$$

Or $$\frac{\partial}{\partial x}\left(\zeta-\bar{\zeta}\right)=-\frac{\alpha}{g}\frac{\partial p_a}{\partial x}$$ ……..(12)

$$\Delta\zeta=\frac{1}{\rho g}\Delta P_a$$

Thus the increase in elevation above mean level ($\zeta-\bar{\zeta}$) is accomplished by a decrease in pressure of the cyclone. The amount is proportional to $\left(\frac{1}{\rho g}\right)$. This roughly comes to for every one millibar drop of pressure one centimeter rise of sea level.

2.6. WIND STRESS EFFECT:

Considering stress and elevation terms of equation 11a ignoring $\bar{\zeta}$ terms

$$-g(\zeta+h)\frac{\partial}{\partial x}\left(\zeta-\bar{\zeta}\right)+\frac{(\tau_{sx}-\tau_{bx})}{\rho}.=0.$$

$$\frac{\partial}{\partial x}\left(\zeta-\bar{\zeta}\right)=\frac{(\tau_{sx}-\tau_{bx})}{\rho g(h+\zeta)}.$$

Generally for a channel closed at one end such as a gulf, the longitudinal transport U = 0 in the steady state but there will be surface flow in the direction of wind with a compensatory flow in the lower layer, then τ_{bx} can be neglected as the return flow is weak.

$$\therefore\frac{\partial}{\partial x}\left(\zeta-\bar{\zeta}\right)=\frac{(\tau_{sx})}{\rho g(h+\zeta)}$$

However, Manning suggested, in shallow basins $\frac{\partial}{\partial x}\left(\zeta-\bar{\zeta}\right)=\frac{\lambda(\tau_{sx})}{\rho g(h+\zeta)}$ where λ lies between 1 and 1.5. If the elevation ζ remains small compared to the mean depth of water, the above equation becomes

$$\frac{\partial}{\partial x}(\delta\zeta)=\frac{\lambda(\tau_{sx})}{\rho g h}$$ ……(13)

where $\left(\zeta-\bar{\zeta}\right)=\delta\zeta$ represents the elevation above mean sea level as in the figure below

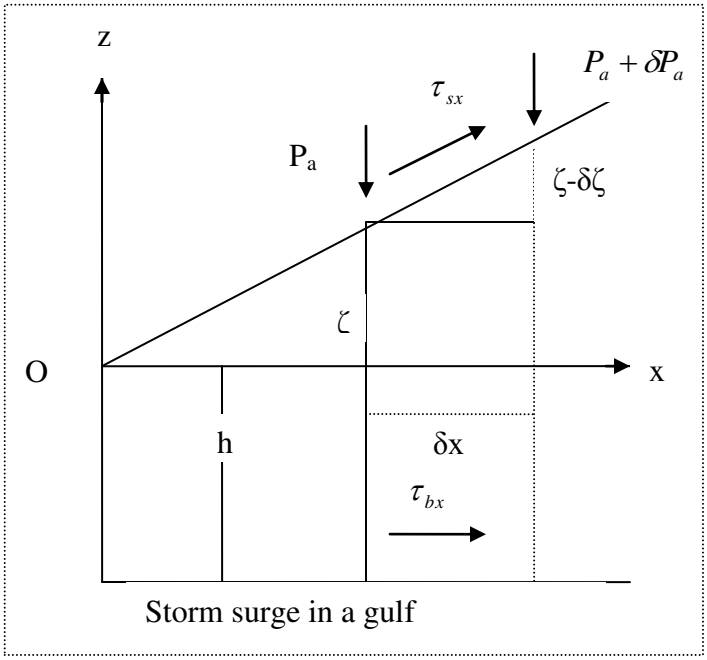

Fig.3. Storm surge in a gulf

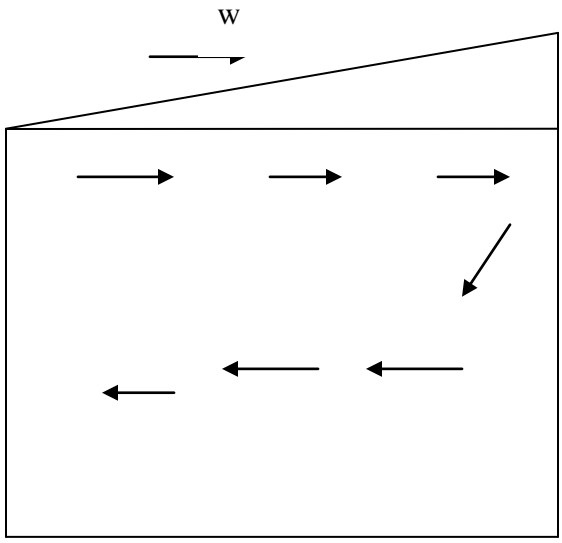

Pattern of currents

Fig.4. Patterns of currents

y

2.5. Bathystrophic Approach for calculation of storm surges:

The technique for the determination of wind induced surge along a straight open coast using the bathystrophic approximation was given by Freeman, Baer and Jung in 1957.

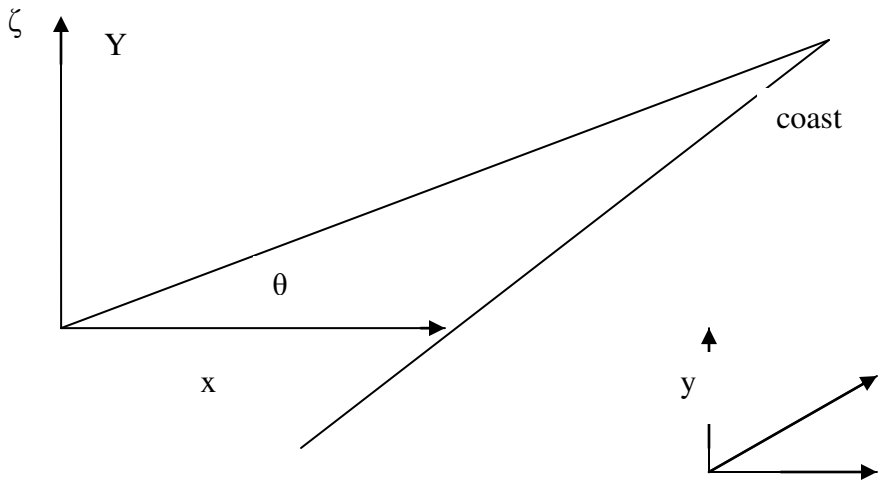

Fig.5

The above figure (2) shows the coordinate system used in this discussion. We shall consider a steady and uniform wind 'W = (w_x, w_y) blowing at an angle θ to the x-axis which is normal to a straight open coast.

The basic assumptions involved in the bathystrophic approximations are

a) there is no sustained onshore transport i.e. $Q_x = 0$ and hence $\tau_{bx} = 0$
b) space derivatives of surge height and volume transport among the y-axis are negligible i.e. $\zeta_y = 0$ and $Q_{y,y} = 0$

c) the advective acceleration terms are negligible
d) the pressure effect is small as only wind effect is considered here. Hence pressure gradient is not considered.

With these assumptions equations 1 a & b changes to:

$$gH\frac{\partial \zeta}{\partial x} = fQ_y + \frac{1}{\rho}\left(\tau_{sx} - \tau_{bx}\right)$$

$$\frac{\partial Q_y}{\partial t} = \frac{1}{\rho}\left(\tau_{sy} - \tau_{by}\right) \qquad \text{---------- (14) (a \&b)}$$

Here H = $\left(h+\zeta\right)$ and V = Q_y

Though non linear acceleration terms do not appear in these equations, still they are non linear due to the presence of stress terms which are quadratic in nature.

The surge due to the pressure field is obtained from equation (12). Hence the effect due to tangential stress field both at the surface and bottom can be obtained by solving equations (14).

The tangential stresses are assumed as follows using quadratic law:

$$\tau_S = K_a \rho |W| W$$

$$\therefore \tau_{Sy} = K_a \rho W^2 Sin\theta \qquad \text{----------(15)}$$

From Fig.2, the component where K_a is drag coefficient of air and along y-axis it is W Sinθ.

The bottom stress τ_b can be related to the resultant bottom current U_b by the quadratic law:

$$\tau_b = K_\rho \rho |U_b| U_b$$

Where K is drag coefficient and U_b is measured at a height of 1 m above the bottom. If U_b is resolved into x and y components as u_b and v_b we can write:

$$U_b^2 = u_b^2 + v_b^2 ; \qquad U_b = \sqrt{u_b^2 + v_b^2}$$

$$\therefore \tau_{bx} = K_\rho \rho |U_b| u_b \quad \text{and} \quad \tau_{by} = K_\rho \rho |U_b| v_b$$

So the bottom stress is assumed as : $\tau_b = K^* \rho H^{-2} |Q_y| Q_y$ …….(16)

Where H = (D + ζ) and D includes the undisturbed mean depth, the astronomical tide height and the height of water corresponding to the pressure effect of the storm. However, often D is considered as h by neglecting astronomical tide and the pressure

effect. While K* is bottom drag coefficient (Freeman et al 1957), Q is bottom transport. Freeman gave bottom drag coefficient as:

$$K^* = \gamma(D+\zeta)^{\frac{-1}{3}} \quad \text{.....(17)}$$

Where γ is Mannings frictional coefficient. Equation 16 can be written using 17 as:

$$\tau_b = \gamma(D+\zeta)^{-1/3}\rho(D+\zeta)^{-2}Q_y{}^2 = \rho\gamma(D+\zeta)^{-7/3}Q_y{}^2 \quad \text{.....(18)}$$

Using 15 and 18, equation (14b) can be written as :

$$\frac{\partial Q_y}{\partial t} = \frac{1}{\rho}(\tau_{Sy} - \tau_{by}) = \quad \frac{1}{\rho}\left[K_a\rho W^2 Sin\theta - \rho\gamma(D+\zeta)^{-7/3}Q_y{}^2\right]$$

$$\frac{dQ_y}{dt} = K_a W^2 Sin\theta - \gamma(D+\zeta)^{-7/3}Q_y{}^2$$

$$\therefore dQ_y = \{\, K_a W^2 Sin\theta - \gamma(D+\zeta)^{-7/3}Q_y{}^2 \,\}\text{dt} \quad \text{on integrating}$$

$$Q_y = [\, K_a W^2 Sin\theta - \gamma(D+\zeta)^{-7/3}Q_y{}^2 \,]\, t$$

Taking the initial condition $Q_y = 0$ at $t = 0$ we can write

$$K_a W^2 Sin\theta - \gamma(D+\zeta)^{-7/3}Q_y{}^2 = 0$$

$$\therefore Q_y{}^2 = \frac{K_a W^2 Sin\theta}{\gamma(D+\zeta)^{-7/3}} \quad ; \quad \text{or} \quad \therefore Q_y = \sqrt{\frac{K_a W^2 Sin\theta}{\gamma(D+\zeta)^{-7/3}}} \quad \text{.....(19)}$$

This is for steady state condition. Substituting eqn 19 in (14a), we get the Bretschneider's (1967) storm surge Bathystrophic equation as :

$$gH\frac{\partial\zeta}{\partial x} = fQ_y + \frac{1}{\rho}(\tau_{sx} - \tau_{bx})$$
$$\therefore \frac{\partial\zeta}{\partial x} = \frac{f}{gH}Q_y + \frac{1}{gH\rho}(\tau_{sx} - \tau_{bx}) \quad \text{.....(20)}$$

Substituting in (20) we can get

$$\frac{\partial \zeta}{\partial x} = \frac{f}{gH}\left[\frac{K_a W^2 Sin\theta}{\gamma(D+\zeta)^{-7/3}}\right]^{1/2} + \frac{1}{gH\rho}(\tau_{sx})$$ since τ_{bx} is assumed as zero in the beginning.

$$\frac{\partial \zeta}{\partial x} = \frac{f}{g(D+\zeta)}\left[\frac{K_a W^2 Sin\theta}{\gamma(D+\zeta)^{-7/3}}\right]^{1/2} + \frac{1}{gH\rho}(K_a \rho W^2 Cos\theta)$$

Since $\tau_{SX} = K_a \rho \left|\bar{W}\right| \bar{W}$ along x direction from Fig (2) we know $\bar{W} = W\cos\theta$

We can write $\frac{\partial \zeta}{\partial x} = \frac{f}{g}\left[\frac{K_a W^2 Sin\theta}{\gamma}\right]^{1/2}(D+\zeta)^{1/6} + \frac{K_a}{g(D+\zeta)}(W^2 Cos\theta)$ …(21)

Now the surge height due to the tangential wind stresses can be determined using numerical integration this equation assuming that the surge is zero at the seaward boundary that is at the shelf break.

The coefficients K_a and γ used for east coast of India are

$K_a = 1.1\times10^{-6} + 2.5\times10^{-6}$ and $\gamma = 0.009354(meters)^{1/3}$

Lecture Series of Berhampur University in Physical Oceanography

Lecture-13:

Oceanographic instrumentation

Prof. A.S.N.Murty

Physical oceanography is an experimental science and requires observation and exact measurement to achieve its aims. It can draw on the experience of the related science fields of physics and chemistry and make use of existing achievements in the areas of technology and engineering, but the oceanic environment places unique demands on instrumentation that are not easily met by standard laboratory equipment. As a consequence, the development and manufacturing of oceanographic instrumentation developed into a specialized activity. Manufacturers of oceanographic equipment serve a small market but aim at selling their products world-wide.

This lecture gives an overview of the range of instruments used at sea and the principles involved. It aims at covering standard classical instruments as well as modern developments. The following table summarizes its content.

research need	**available equipment / instrumentation**
provision of observing platform	• research vessels • moorings • satellites • submersibles • towed vehicles • floats and drifters
measurement of hydrographic properties (temperature, salinity, oxygen, nutrients, tracers)	• reversing thermometers • Nansen and Niskin bottles • CTDs • multiple water sample devices • thermosalinographs • remote sensors

measurement of dynamic properties (currents, waves,tides, sea level, mixing processes)	• current meters • wave gauges • tide gauges • remote sensors • shear probes

Platforms

All measurements at sea require a reasonably stable platform to carry the necessary instrumentation. The platform can be at the sea surface, at the sea floor, in the ocean interior or in space. The choice of platform depends on its capabilities to collect the required information in space and time.

Research vessels

Like any other ocean going ship, research vessels have to meet the requirement to be seaworthy and capable of riding out bad weather. The weather conditions in the investigation area thus define the minimum size for the vessel. Additional requirements, such as the handling of heavy equipment at sea or the need for a large scientific party during an interdisciplinary study, can increase the minimum size. Typical ocean going research vessels are 50 - 80 m long, have a total displacement of 1000 - 2000 tonnes and provide accommodation for 10 - 20 scientists (Figure 13.1).

Fig.13.1. ORV.Sagar Kanya of National Institute of Oceanography of India.

The shape of a research vessel is determined by the need for a reasonably large working deck, several powerful winches for lowering and retrieving instrumentation and at least one "A-frame", a structure which allows a wire to go from the ship's winch over the side of the ship or over the stern and vertically into the water (Figure 13.2).

Fig.13.2. Research vessel with 'A' frames with powerful winches

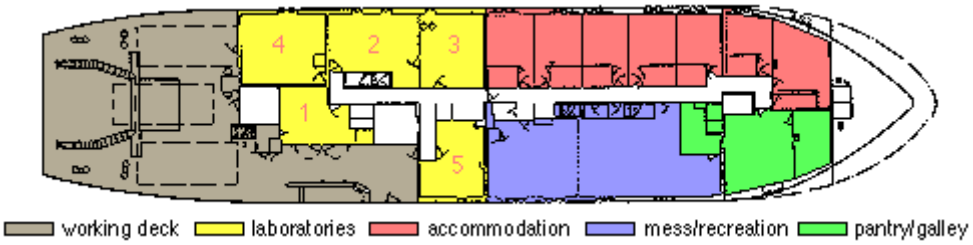

Fig.13.3. Plan of the main deck of the Australian research vessel *Franklin*, showing the main scientist accommodation and laboratory arrangement:

1. wet laboratory (CTD and multiple water sampler area)
2. operations room (echo sounder, ADCP, CTD, towed vehicle and thermosalinograph controls and displays)
3. computer room (terminals for data processing and analysis)
4. chemical laboratory (salinity, nutrient and oxygen analysis)
5. electronic workshop (instrument preparation)

An additional laboratory for chemical or biological work is located on a lower deck. One container laboratory can be placed on the work deck and connected with the chemical laboratory through a water-tight doorway.

Crew accommodation is on the lower and upper decks; the mess room and recreation area is a common area.

The requirement to be at sea for extensive periods of time, remain stationary while equipment is handled over the side and move at very slow speed when equipment is towed behind the vessel place additional demands on research vessel design. To increase endurance (the number of days a ship can remain at sea before running out ouf fuel), research vessels have only a moderate operating speed of 10 - 12 knots (18 - 28 km/hr). This compares with operating speeds of 15 - 20 knots for merchant ships. Most research vessels have an endurance of 20 - 25 days, which gives them a range of 6000 - 8000 nautical miles (11,000 - 14,800 km), sufficient to operate at the high seas within a few days of reach of land. Only the major oceanographic institutions of the world operate research vessels with global research capability.

All modern ships are powered by Diesel engines. Such engines are best operated at nearly constant speed. Merchant ships do not have to vary their speed much during their voyage; their propeller is diven directly from the engine. Various arrangements are used to allow research vessels to operate at very slow speeds. In diesel-electric systems the Diesel engine powers an electic motor which in turn drives the propeller shaft. Electric motors work efficiently at any speed, allowing the ship very accurate speed control. In another arrangement the Diesel engine drives a "variable pitch propeller". In such a propeller the pitch of the blades (the blade angle) can be controlled to give very low or zero propeller thrust even at full propeller rotation.

Lowering equipment over the side of a vessel requires more than zero thrust. Without active position control the ship will drift with the wind and across the instrument wire. To keep the wire vertical and free from the ship's hull the ship has to counteract the effects of wind and current. This is usually achieved through a pair of additional thrusters, one at the bow and one at the stern, which can push the ship sideways. The bow thruster is either a propeller set into a horizontal tunnel through the ship's hull or a propeller on a shaft that can be oriented in any direction and retracted when the ship is under way. The stern thruster is either a similar tunnel or a propeller built into the ship's rudder (an "active rudder"). The two thrusters together allow very accurate control over the ship's behaviour in wind, waves and current and enable it to turn itself around on the spot if neccessary.

The minimum laboratory requirements consist of a wet laboratory for the handling of water samples, a computer laboratory for data processing, an electronics laboratory for the preparation of instruments and a chemical laboratory for water sample analysis. Larger research vessels designed for multidisciplinary research have additional biological, geophysical and geological laboratories. Figure 13.3 shows a typical deck arrangement on a medium sized research vessel.

Research vessels are expensive to operate (US$15,000 - US$25,000 per day at sea). For many decades they were the only available type of platform for data collection on the high seas. The advent of deep-sea moorings, satellites and autonomous drifters has

reduced their importance, but research vessels still are an essential tool in oceanographic research. They are now used principally for large scale near-synoptic surveys of oceanic property fields and for targeted process studies (such as mixing across fronts, determination of the heat budget of small ocean regions etc).

Moorings

Moorings are appropriate platforms wherever measurements are required at one location over an extended time period. Their design depends on the water depth and on the type of instrumentation for which the mooring is deployed, but the basic elements of an oceanographic mooring are an anchor, a mooring line (wire or rope) and one or more buoyancy elements which hold the mooring upright and preferably as close to vertical as possible.

Subsurface moorings are used in deep water in situations where information about the surface layer is not essential to the experiment. The main buoyancy at the top of the mooring line is placed some 20 - 50 m below the ocean surface. This has the advantage that the mooring is not exposed to the action of surface waves and is not at risk of being damaged by ship traffic or being vandalised or stolen. Figure 13.4 shows a typical deep-sea mooring. The main buoyancy is at the top of the mooring line. To protect the mooring against fish bites, wire is used for the upper 1000 m or so of the mooring line, while rope is used below.

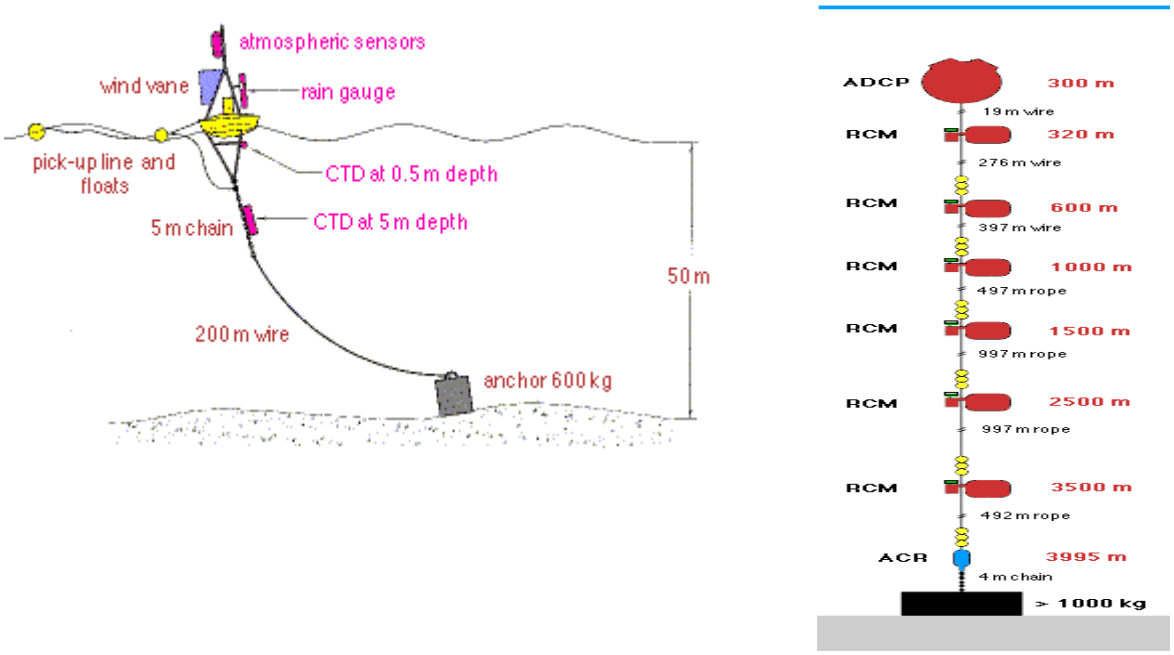

Fig.13.4 A typical example of a surface and subsurface mooring system

To keep the mooring close to the vertical it should have minimum drag, which can only be achieved by keeping the wire diameter small. This requires a small wire load from the instruments. Additional buoyancy is therefore distributed along the wire to compensate for the weight of the instrumentation. The buoyancy is arranged so that all sections of thew mooring are buoyant, enabling recovery of a damaged mooring which lost its upper part.

At the bottom of a deep sea mooring just above the anchor is a remotely controllable release. It can be activated through a coded acoustic signal from the ship when it is time to recover the mooring. Triggering the release brings the mooring to the surface. The anchor, usually a concrete block or a clump of disused railway wheels, is left at the ocean floor.

An experiment which includes the surface layer or the collection of meteorological data requires a surface mooring. The main buoyancy for such a mooring takes the shape of a substantial buoy that floats at the surface and can carry meteorological instrumentation (Figure 13.5). In the deep ocean surface moorings are mostly "taut moorings". They use only rope for the mooring line and make it a few per cent shorter than the water depth. This stretches the rope and keeps it under tension to keep the mooring close to vertical. The "inverse catenary" mooring is also used; this is an arrangement where a buoyant section of mooring line is included between two non-buoyant sections causing the profile of the line to form an S-shape. In this configuration the length of the mooring line is not critical and is about 25% greater than the water depth.

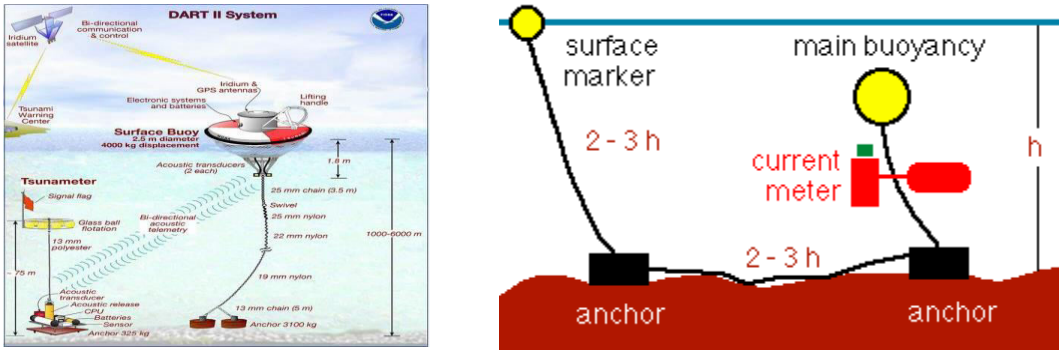

Fig.13.5 Surface mooring with a buoy

Moorings on the continental shelf, where the water depth does not exceed 200 m, do not require acoustic releases if a U-type mooring is used. A U-type mooring consists of a surface or subsurface mooring to carry the instrumentation, a ground line of roughly twice the water depth and a second mooring with a small marker buoy (Figure 13.6). When the time comes to bring the mooring in, the marker buoy is recovered first, followed by the two anchors and finally the mooring itself. U-type moorings are usually

"slack moorings"; the mooring line is longer than the water depth, and the mooring swings with the current.

Satellites

The advent of satellite technology opened the possibility of measuring some property fields and dynamic quantities from space. The advantage of this method is the nearly synoptic coverage of entire oceans and ease of access to remote ocean regions. Satellites have therefore become an indispensable tool for climate research. The major restriction of the method is that satellites can only see the surface of the ocean and therefore give only limited information about the ocean interior.

Most satellites are named for the sensors they carry. Strictly speaking, the satellite and its sensors are two separate things; the satellite is a platform, the sensors are instruments. An overview of the available satellite sensors is therefore given in the discussion of instruments below.

As platforms, satellites fall into three groups. Most satellites follow inclined orbits: Their elliptical orbits are inclined against the equator. The degree of inclination determines how far away from the equator the satellite can see the Earth. Typical inclinations are close to 60°, so the satellite covers the region from 60°N to 60°S. It covers this region frequently, completing one orbit around the Earth in about 50 minutes.

Some satellites have an inclination of nearly or exactly 90° and can therefore see both poles; they fly on polar orbits. A typical height of satellites on polar and on inclined orbits is 800 km.

The third and last group are the geostationary satellites. They orbit the Earth at the same speed with which the Earth rotates around its axis and are therefore stationary with respect to the Earth. This situation is only possible if the satellite is over the equator and orbits at a height of 35,800 km, much higher than all other satellites. Geostationary satellites therefore cannot see the poles.

The selection of a satellite as a platform logically includes the selection of a sensor and a suitable orbit. An ice sensor to monitor the polar ice caps does not achieve much on a geostationary satellite; a cloud imager for weather forecasting is not placed in a polar orbit.

Submersibles

Submersibles are not a frequently used platform in physical oceanography, but this is likely to change over the coming years. Three basic types can be distinguished, manned submersibles, remotely controlled submersibles and autonomous submersibles.

Manned submersibles are used in marine geology for the exploration of the sea floor and occasionally in marine biology to study sea floor ecosystems. They are not a tool for physical oceanography.

Remotely controlled submersibles are commonly used in the offshore oil and gas industry and for retrieving flight recorders from aircraft that fell into the ocean. In science they find similar uses to manned submersibles but are again not a tool for physical oceanography.

Autonomous submersibles are self-propelled vehicles that can be programmed to follow a predetermined diving path. Such vehicles have great potential for physical oceanography. Some major oceanographic research institutions are developing vehicles to carry instrumentation such as a CTD and survey an ocean area by regularly diving and surfacing along a track from one side of an ocean region to the other and transmitting the collected data via satellite when at the surface. Some time will pass, however, before these vehicles will come into regular use. Eventually, autonomous submersibles will greatly reduce the need for research vessels for ocean monitoring.

Towed vehicles

Towed vehicles are used from research vessels to study oceanic processes which require high spatial resolution such as mixing in fronts and processes in the highly variable upper ocean. Most systems consist of a hydrodynamically shaped underwater body, an electro-mechanical (often multi-conductor) towing cable and a winch. The underwater body is fitted with a pair of wing shaped fins which control its flight through the water. In addition to the sensor package (usually a CTD, sometimes additional sensors for chemical measurements) it carries sensors for pressure, pitch and roll to monitor its behaviour and control its flight. The data are sent to the ship's computer system via the cable. The same cable is used to send commands to the underwater body to alter its wing angle.

Fig.13.6 shows a towed vehicle during deployment. A typical flight path for this vehicle covers a depth range of about 250 - 500 m, which can be chosen to be anywhere between the surface and 800 m depth. The vehicle is towed at about 6 - 10 knots (10 - 18 km/h) and traverses the 250 m depth range about once every 5 minutes. When fitted with a CTD this results in a vertical section of temperature and salinity with a horizontal resolution of about 1 km.

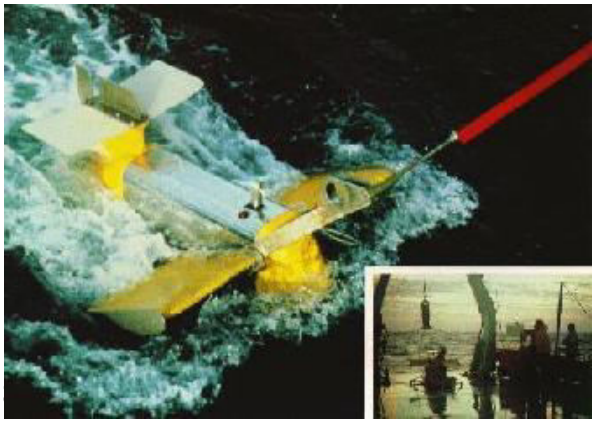

Fig.13.6 A towed vehicle during deployment and on towing

An alternative towed system does not employ an underwater body to carry the sensor package but has sensors (for example thermistors) built into the towed cable at fixed intervals. Because the distance between the sensors is fixed and the sensors remain at the same depth during the tow, these "thermistor chains" do not offer the same vertical data resolution as undulating towed systems and are only rarely used now.

Floats and drifters

The main characteristic of floats and drifters is that they move freely with the ocean current, so their position at any given time can only be controlled in a very limited way. Until a decade ago these platforms were mainly used in remote regions such as the Southern Ocean and in the central parts of the large ocean basins that are rarely reached by research vessels and where it is difficult and expensive to deploy a mooring. They have now become the backbone of a new observing system that covers the entire ocean.

Strictly speaking, a float is a generic term for anything that does not sink to the ocean floor. A drifter, on the other hand, is a platform designed to move with the ocean current. To achieve this it has to incorporate a floatation device or float, but it is usually more than that. But oceanographers use the terms very loosely and do not make a clear distinction between "floats" and "drifters".

Two basic types can be distinguished. Surface drifters have a float at the surface and can therefore transmit data via satellite. If they are designed to collect information about the ocean surface they carry meteorological instruments on top of the float and a temperature and occasionally a salinity sensor underneath the float. To prevent them from being blown out of the area of interest by strong winds they are fitted with a "sea anchor" at some depth (Fig.13.7). If they are designed to give information on subsurface ocean properties, additional sensors are placed between the surface float and the sea anchor. The depth range of surface drifters is usually limited to less than 100 m.

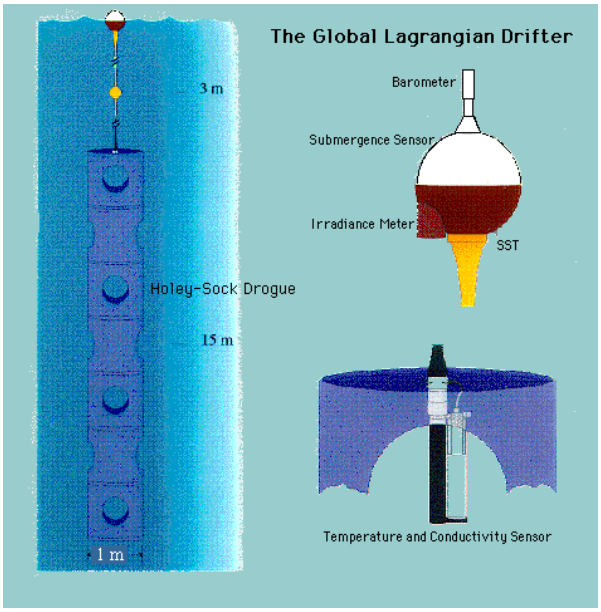

Fig.13.7. A Lagrangian drifter

Floats used for subsurface drifters are designed to be neutrally buoyant at a selected depth. These drifters have been used to follow ocean currents at various depths, from a few hundred metres to below 1000 m depth. The first such floats transmitted their data acoustically through the ocean to coastal receiving stations. Because sound travels well at the depth of the sound velocity minimum (the SOFAR Channel), these SOFAR floats can only be used at about 1000 m depth.

Modern subsurface floats remain at depth for a period of time, come to the surface briefly to transmit their data to a satellite and return to their allocated depth. These floats can therefore be programmed for any depth and can also obtain temperature and salinity (CTD) data during their ascent. The most comprehensive array of such floats, known as Argo, began in the year 2000. Argo floats measure the temperature and salinity of the upper 2000 m of the ocean (Fig.13.8a). This will allow continuous monitoring of the climate state of the ocean, with all data being relayed and made publicly available within hours after collection. When the Argo programme is fully operational it will have 3,000 floats in the world ocean at any one time.

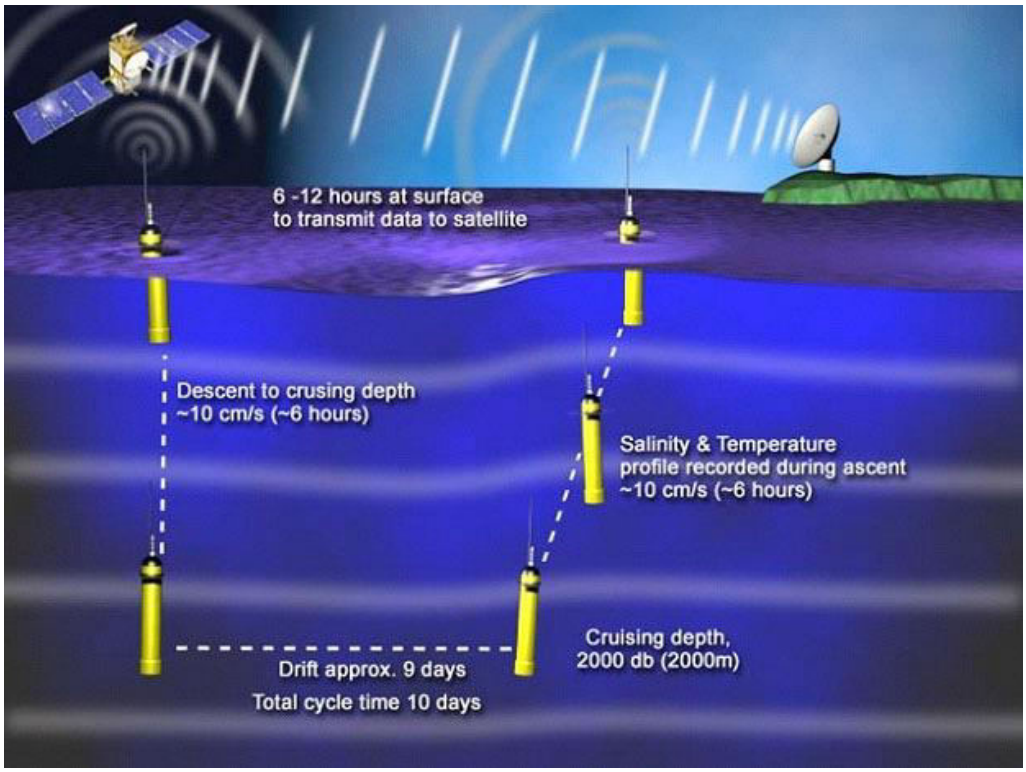

Fig.13.8a. Argo floats

Measurements of hydrographic properties

This section gives an overview of sensors and instrument packages for the measurement of temperature, salinity, oxygen, nutrients and tracers.

Reversing thermometers

There are two reversing thermometers as shown in Fig.13.9. One is Protected Reversing Thermometer (PRT) and the other is Unprotected Reversing Thermometer (UPRT). These two thermometers are attached to the Nansen Reversing Water Bottle. As these thermometers record temperature and depth of the water sample at the time of reversal, they are called reversing thermometers. While the PRT measures the *in situ* temperature, UPRT measures depth at which PRT measured the temperature. So both the thermometers are simultaneously used and attached to Nansen Reversing water bottle..

PROTECTED REVERSING THERMOMETER (PRT):

As shown in Fig.13.9, it contains a main reservoir through which the glass column runs through spiraling and branching with a graduated scale. Adjacent to this an auxiliary ordinary thermometer is fixed. Both these thermometers are enclosed with an outer glass

jacket for protection from sea pressure. Once the PRT is sent to the required depth, it records the temperature of the water at that depth and on reversal it cuts off from the main reservoir and extra mercury will not pass into the column due to spiraling and branching and so the meniscus is not disturbed while it is hauled up. After it is brought on to the deck when you see it in the set position, you can see the reading that it has recorded before the reversal.

UNPROTECTED REVERSING THERMOMETER (UPRT):

Its design is similar to that of protected reversing thermometer. But the only difference is the bulb is kept open without any protection by sea pressure. It has a main thermometer with looping and branching with a main reservoir at bottom and a secondary reservoir at the top in the set position. Adjacent to it an auxiliary thermometer is kept. Both the thermometers are enclosed in glass jacket which is open at the main reservoir. Because of the open end of UPRT when the thermometer is sent into the ocean at the desired depth, the value recorded by this thermometer is due to two effects. One is temperature effect and the other is sea pressure effect. As a result if we subtract the temperature effect we can get the effect of pressure. The sea pressure is nothing but the depth at which the sea water sample is collected. Both the protected and unprotected thermometers are enclosed to the Nansen reversing water bottle to know the temperature and depth of the water sample simultaneously.

By using both PRT and UPRT side by side we can get the *in situ* temperature at the depth it recorded.

By subtracting the value of PRT from UPRT, we get the depth of the sample at which it is collected.

To eliminate the effect of pressure, which compresses the pipe and causes more mercury to rise above the break point during the lowering of the instrument, the thermometer is enclosed in a pressure resistent glass housing.

Reversing thermometers require a research vessel as platform and are used in conjunction with Nansen or Niskin bottles or on multi-sample devices.

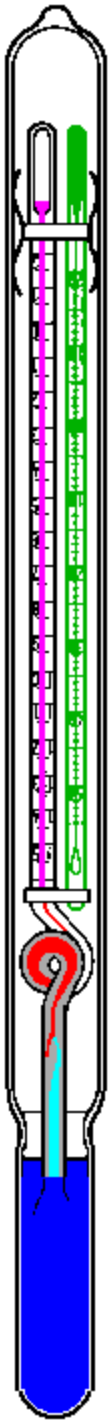

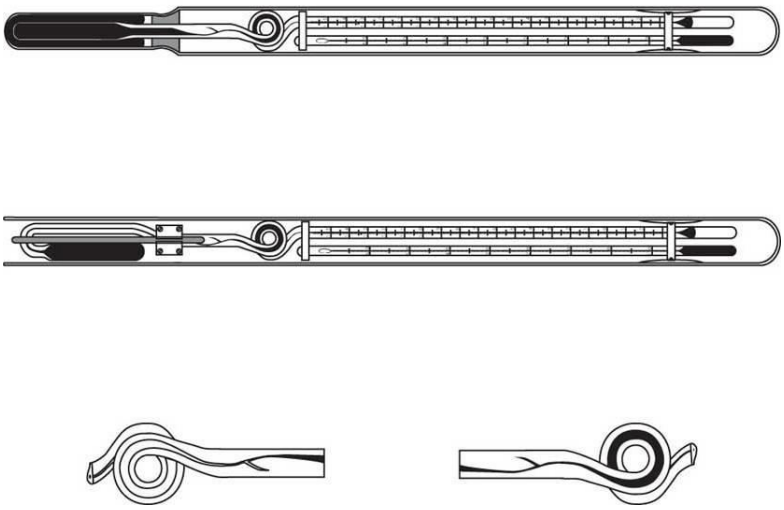

Fig.13.9. Protected and unprotected reversing thermometers with constriction and branching shown separately.

A reversing thermometer in the upright (not reversed) position. The mercury rises from the mercury reservoir (blue) through the capillary section (cyan and red) into the glass cylinder and upper reservoir (magenta).

When the thermometer is turned upside down (reversed), the mercury column ruptures at the appendix in the capillary section (between the red and blue). The red and magenta mercury settles into the upper reservoir, while the cyan mercury returns to the blue reservoir. The level of the magenta/red mercury can then be read against the scale and indicates the temperature.

The green thermometer is an auxiliary thermometer which gives the ambient temperature. It is used to check the temperature when the main thermometer is read on deck of the ship. Its reading allows to correct for the expansion of the glass tube that occurs due to the warmer ambient temperature on deck. The overall accuracy thus achieved is 0.02°C. If multiple reversing thermometers are used in parallel the accuracy can be increased to 0.01°C.

Nansen and Niskin Reversing bottles

For the measurement of salinity and oxygen, nutrients and tracer concentrations requires the collection of water samples from various depths. This essential task is achieved through the use of "water bottles". The first water bottle was developed by Fritjof Nansen and is thus known as the Nansen bottle. It consists of a metal cylinder with two rotating closing mechanisms at both ends. The bottle is attached to a wire (Fig.13.10). When the bottle is lowered to the desired depth it is open at both ends, so the water flows through it freely. At the depth where the water sample is to be taken the upper end of the bottle disconnects from the wire and the bottle is turned upside down. This closes the end valves and traps the sample, which can then be brought to the surface.

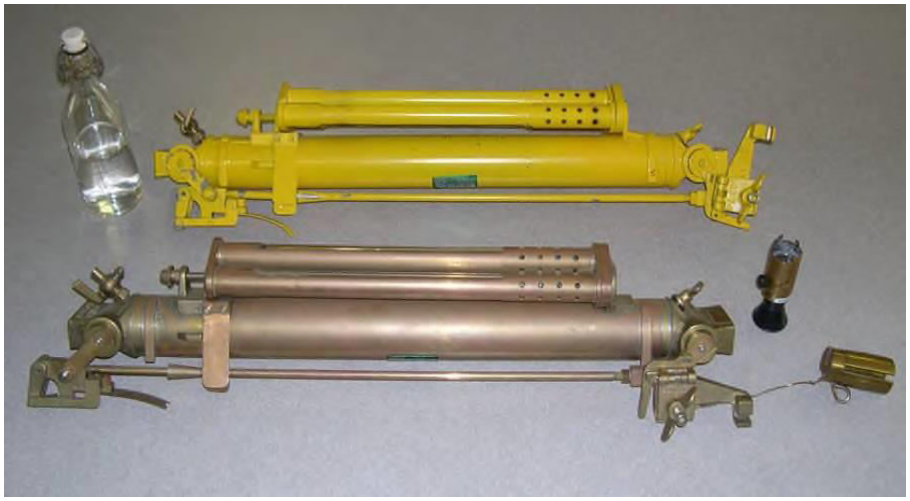

Fig.13.10. Attached Nansen bottles to the wire rope and the messenger hitting and releasing and reversed positions (top) Actual photographs (below).

In an "oceanographic cast" several bottles are attached at intervals on a thin wire and lowered into the sea. When the bottles have reached the desired depth, a metal weight ("messenger") is dropped down the wire to trigger the turning mechanism of the uppermost bottle. The same mechanism releases a new messenger from the bottle; that messenger now travels down the wire to release the second bottle, and so on until the last bottle is reached.

The Nansen bottle has now widely been displaced by the Niskin bottle (Fig.13.11). Based on Nansen's idea, it incorporates two major modifications. Its cylinder is made up of plastic, which eliminates chemical reaction between the bottle and the sample that may interfere with the measurement of tracers. Its closing mechanism no longer requires a turning over of the bottle; the top and bottom valves are held open by strings and closed by an elastic band. Because the Niskin bottle is fixed on the wire at two points instead of one (as is the case with the Nansen bottle) it makes it easier to increase its sample volume. Niskin bottles of different sizes are used for sample collection for various tracers. Niskin sampler also is very light compared to Nansen bottle

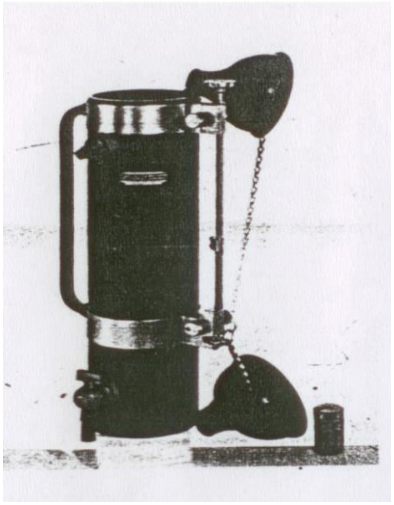

Fig.13.11. Niskin water samplers of different types

Nansen and Niskin bottles are used on conjunction with reversing thermometers. On the Nansen bottle the thermometers are mounted in a fixed frame, the reversal being achieved by the turning over of the bottle. On Niskin bottles thermometers are mounted on a rotating frame.

CTDs

Today's standard instrument for measuring temperature, salinity and often also oxygen content is the CTD, which stands for **c**onductivity, **t**emperature, **d**epth (Fig.13.12). It employs the principle of electrical measurement. A platinum thermometer changes its electrical resistance with temperature. If it is incorporated in an electrical oscillator, a change in its resistance produces a change of the oscillator frequency, which can be measured. The conductivity of seawater can be measured in a similar way as a frequency change of a second oscillator, and a pressure change produces a frequency change in a third oscillator. The combined signal is sent up through the single conductor cable on which the CTD is lowered. This produces a continuous reading of temperature and

conductivity as functions of depth at a rate of up to 30 samples per second, a vast improvement over the 12 data points produced by the 12 Nansen or Niskin bottles that could be used on a single cast.

Fig.13.12. CTD instrument and its recorder

Electrical circuits allow measurements in quick succession but suffer from "instrumental drift", which means that their calibration changes with time. CTD systems therefore have to be calibrated by comparing their readings regularly against more stable instruments. They are therefore always used in conjunction with reversing thermometers and a multi-sample device.

Multiple water sample devices

Multiple water sample devices allow the use of Niskin bottles on electrically conducting wire. Different manufacturers have different names for their products, such as *rosette* or *carousel*. In all products the Niskin bottles are arranged on a circular frame (Fig.13.13), with a CTD usually mounted underneath or in the centre.

Fig.13.13. a multiple Niskin samplers are arranged in a circular frame and being deployed

The advantage of multi-sample devices over the use of a hydrographic wire with messengers is that the water bottles can be closed by remote control. This means that the sample depths do not have to be set before the bottles are lowered. As the device is lowered and data are received fom the CTD, the operator can look for layers of particular interest and take water samples at the most interesting depth levels.

PETERSON GRAB:

The grab looks like the one that is shown in the Figure 13.14. It has two jaws which can easily be opened and closed with the help of two cross cissored rods. The grab will be lowered with the help of a rope tied to these rods. This grab is used to collect sediment and sedentary animals from the sea or estuarine bottom.

Fig.13.14 .Peterson Grab

Bathy thermographs (BTs):

There are two types of bathythermographs. One is Mechanical Bathythermograph (MBT) and the other one is Expendable Bathythermograph (X'BT).

MECHANICAL BATHY THERMOGRAPH (MBT): (Fig.6):

It looks like a torpedo with a nose in the front and fins at the rear end as shown in Fig.13.15. It consists of two elements. One is pressure element and the other is temperature element. Both are connected by a bourdon tube and stylus that marks on a smoked glass slide.

The pressure element consists of carpenter's bellows and the temperature element is a liquid in metal thermometer. The liquid used is xylene. Xylene is used here because it is sensitive for small changes of temperature and will not be solidified under subzero temperatures.

At the center of both the elements on either side a small sachet is available to keep the smoked glass slide on which the stylus will mark the graph that represents the temperature versus pressure (depth). After the instrument is recovered on board, the smoked glass slide is removed from the sachet and is kept in a viewer and the graph can be seen on the screen of the viewer that can be manually read off.

DISADVANTAGE:

The serious disadvantage of this instrument is that when it is being hauled-up, there is a chance of erasing of the graph on the smoked glass slide due to entering of water. Then the entire exercise becomes futile. Another problem is there is a chance of losing of the instrument due to its heavy weight.

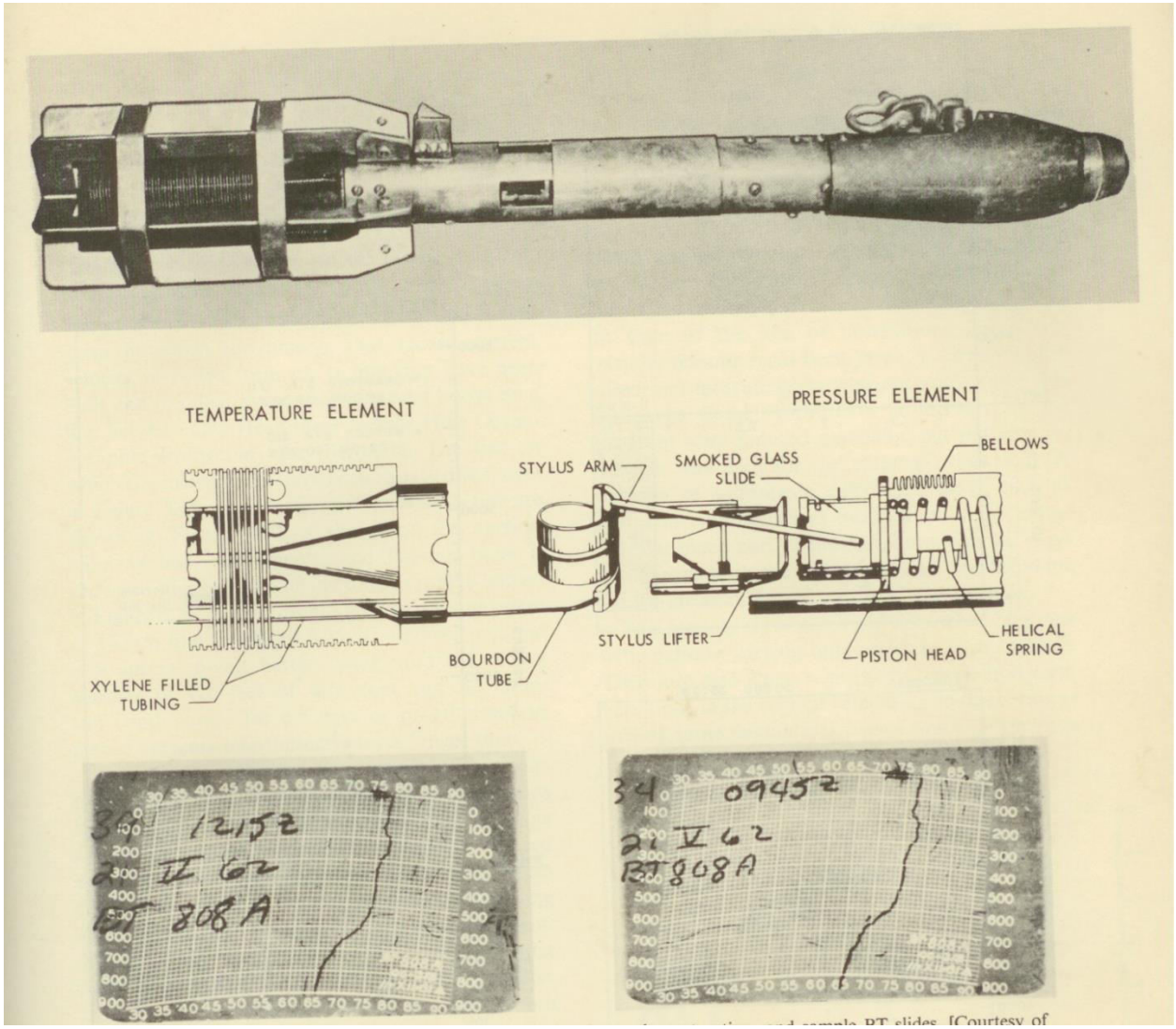

Fig.13.15. Mechanical Bathy thermograph. Middle: Temperature and pressure element. Bottom: the graph drawn by the metal stylus on the smoked glass slide.

8.2.5. EXPENDABLE BATHY THERMOGRAPH (X'BT) (Fig.7):

To overcome the serious disadvantage of erasing out of the graph on the smoked glass slide in the MBT, X'BT is designed as shown in Fig.13.16. As the name implies it is expended (spent) once it is used. It contains a thermistor probe wound around with a lean copper wire of 500 to 1000 meters. This wire is connected to a deck computer which has a soft ware fitted to the respective probes. The probe is released into the ocean through a launcher that looks like a plastic gun. Once the probe is fired through the launcher, the probe enters the water and goes to deep layers as per the length of the wire

(500 or 100 m). As it goes to different layers, the computer records temperature at different depths. Once the wire is finished, it is cut off from the computer and the probe is lost into the ocean. That is how it is expended. This instrument is preferred by everybody though it is expensive and lost every time of collection of data because we are sure to get the accurate data within a short span of time without much labor.

There was a world wide experiment in all the tropical oceans called Tropical Ocean Global Atmosphere (TOGA) program during 1980 – 85 to study the heat transport caused due to 1982/83 ElNino and other air-sea interaction problems. During this time X'BT has become popular and the data collected by this instrument simultaneously in all the three major oceans of Indian, Atlantic and Pacific has become invaluable.

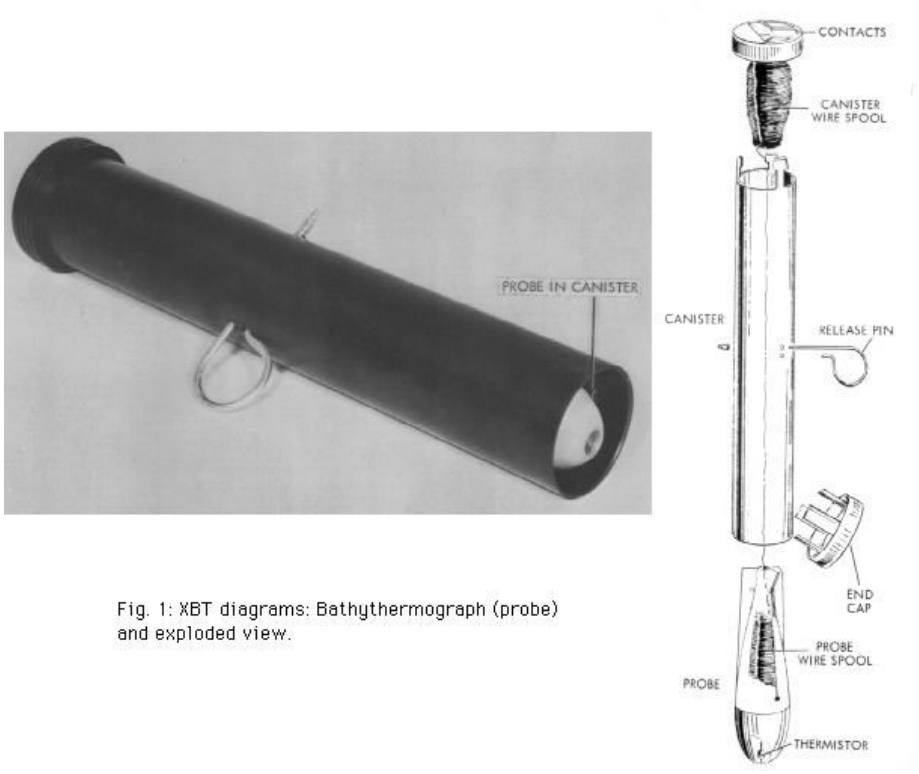

Fig. 1: XBT diagrams: Bathythermograph (probe) and exploded view.

Fig.13.16a. Expendable Bathy thermograph probe (left) ; The releasing of probe from the container along with its canister tail wire that is connected to the computer.

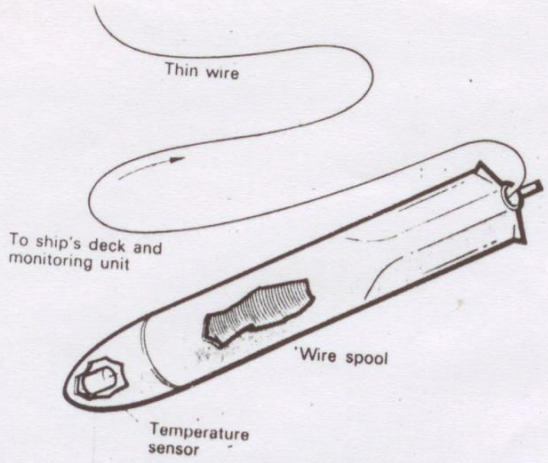

FIG. 4.8 *Diagrammatic representation of an expendable bathythermograph (XBT).*

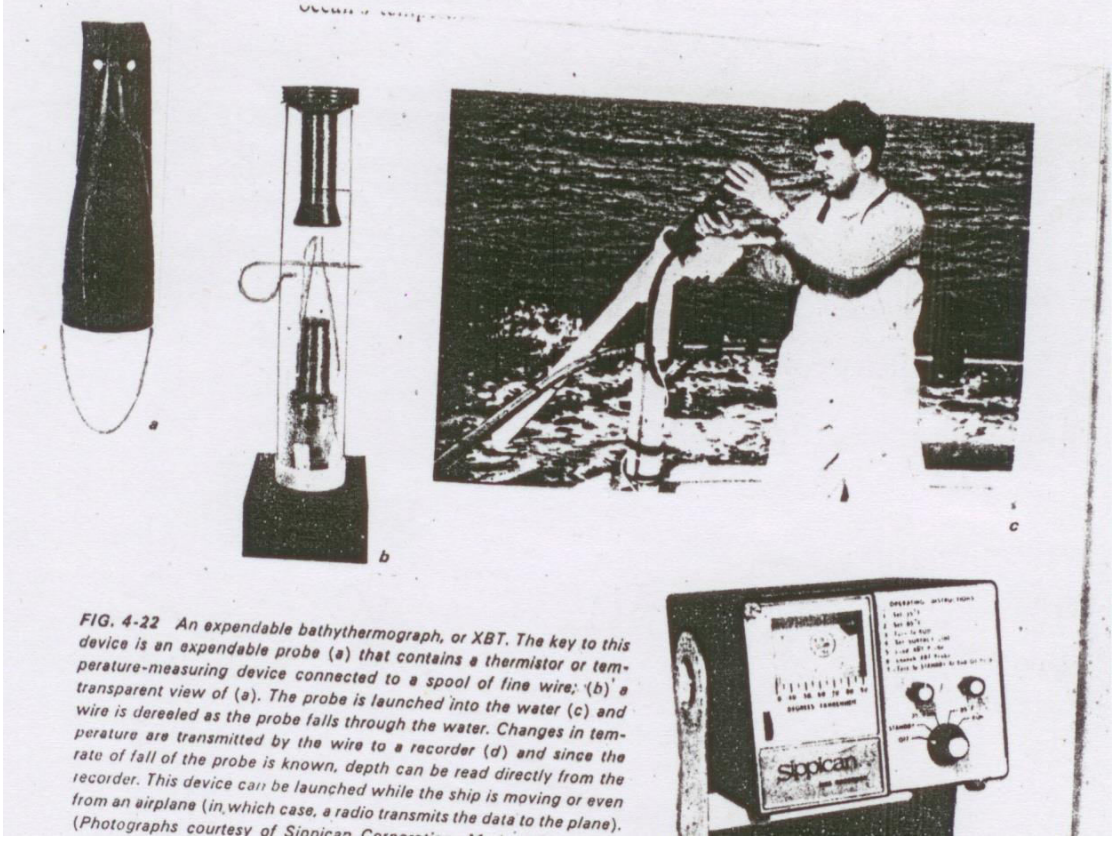

FIG. 4-22 An expendable bathythermograph, or XBT. The key to this device is an expendable probe (a) that contains a thermistor or temperature-measuring device connected to a spool of fine wire; (b) a transparent view of (a). The probe is launched into the water (c) and wire is dereeled as the probe falls through the water. Changes in temperature are transmitted by the wire to a recorder (d) and since the rate of fall of the probe is known, depth can be read directly from the recorder. This device can be launched while the ship is moving or even from an airplane (in which case, a radio transmits the data to the plane). (Photographs courtesy of Sippican Corporation.)

Fig.13.16b. X'BT probe, launcher from the deck of the ship and recording device

EXTINCTION AND TURBIDITY MEASUREMENT:

8.3.1. EXTINCTION COEFFICIENT:

The rate at which downward traveling light in the surface layer of the ocean diminishes is called extinction of radiation and is measured through a coefficient called extinction coefficient (K) which is computed with the help of the equation:

$$K = \frac{2.303}{L}\left(\log I_0 - \log I_z\right)$$

Where K is extinction coefficient, I_o is intensity of incident radiation, I_z is intensity of radiation at the required depth (z) and L is the distance between the two chambers of the hydrophotometer (usually fixed at one meter).

8.3.2. HYDROPHOTOMETER (FIG.8):

For measurement of extinction coefficient, the instrument used is called hydrophotometer as shown in Fig. 13.17. It consists of two chambers. One chamber consists of source light at 230 V (I_o) and the other chamber consists of photocell that measures the received light (I_z). Both chambers are fitted with a carrier frame of one meter length. The instrument works with a car battery and the source and received intensities are measured with a deck instrument that contains a volt meter and a micro ammeter.

Using the above equation, extinction coefficient can be computed with the data of hydrophotometer.

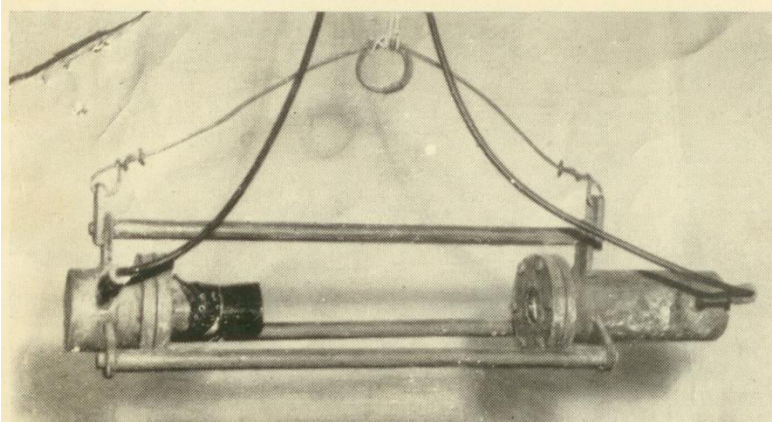

Fig. 13.17. Hydro photometer

8.3.3. SACCHI DISC (FIG.13.18):

This is a brass disc of 30 cm diameter alternatively painted black and white for clear visibility as shown in Fig.13.18. It is lowered into waters of usually shallow water bodies like estuaries, lakes, lagoons and back waters. When this disc is lowered into waters vertically down with the help of a plastic wire rope tied with a lead weight, the depth of

disappearance (d_1) and reappearance (d_2) is measured. The average depth ($D = \frac{d_1 + d_2}{2}$) is called the Sacchi depth and the turbidity is calculated using the extinction coefficient $K = \frac{1.7}{D}$. Here K is directly related to turbidity. As extinction coefficient is more turbidity is more and vice versa. Using a calibration graph between K and turbidity (T), a regression equation can be established for a particular lake and regularly can be used for understanding turbidity.

Fig.13.18. Saccchi disc

Thermosalinographs

The introduction of the CTD opened the possibility of taking continuous readings of temperature and salinity at the surface. Water from the cooling water intake of the ship's engines is pumped through a tank in which a temperature and a conductivity sensor are installed. Such a system is called a thermosalinograph.

Remote sensors

Most oceanographic measurements from space or aircraft are based on the use of radiometers, instruments that measure the electro-magnetic energy radiating from a surface. This radiation occurs over a wide range of wavelengths, including the emission of light in the visible range, of heat in the infrared range, and at shorter wavelengths such as Radar and X-rays. Most oceanographic radiometers operate in several wavelength bands. A detailed discussion of all applications goes beyond the scope of these lecture notes; so only the most basic systems are mentioned here.

Radiometers that operate in the infrared are used to measure sea surface temperature. Their resolution has steadily increased over the years; the AVHRR (**A**dvanced **V**ery **H**igh **R**esolution **R**adiometer) has a resolution that comes close to 0.2°C.

Multi-spectral radiometers measure in several wavelength bands. By comparing the radiation signal received at different wavelengths it is possible to measure ice coverage and ice age, chlorophyll content, sediment load, particulate matter and other quantities of interest to marine biology.

Measurements at radar wavelengths are made by an instrument known as SAR (**S**ynthetic **A**perture **R**adar). It can be used to detect surface expressions of internal waves, the effect of rainfall on surface waves, the effect of bottom topography on currents and waves, and

a range of other phenomena. Many of these phenomena belong into the category "dynamic properties" discussed below.

Measurements of dynamic properties

All instruments discussed so far produce information about oceanic property fields irrespective of the dynamic state of the ocean. The remainder of this lecture summarizes instrumentation designed to measure movement in the ocean.

An elementary way of observing oceanic movement is the use of drifters. As mentioned above, drifters are floats designed to carry instruments. But all measurements obtained from drifters are of little use unless they can be related to positions in space. A Global Positioning System (GPS) device which transmits the drifter location to a satellite link is therefore an essential instrument on any drifter, and this turns the drifter into an instrument for the measurement of ocean currents. Whether it does that job well or not depends on its design, and in particular the size and shape of its sea anchor.

Current meters

Ocean currents can be measured in two ways. An instrument can record the speed and direction of the current.

EKMAN CURRENT METER (FIG.13.19a):

It is an ingenious device prepared by a great oceanographer V.W.Ekman. It consists of a) propeller b) a compass and Receptacle c) a vane.

The vane helps to orient the propeller against the direction of the water current when it is lowered to the required depth at which we want to measure currents.

The propeller consists of a circular 10 cm diameter rim. The propeller is allowed to rotate at the desired depth by sending a metal weight called messenger along the wire rope which free the propeller from locking. A second messenger is dropped after few minutes to stop it. The number of revolutions made by the propeller is recorded by a dial box with a mechanical counter. The current speed is obviously proportional to the number of revolutions of the propeller per minute.

The current direction is recorded by the counting mechanism dropping lead balls (shots) at known intervals along a magnetic compass into a receptacle with 10^o sectors denoting eight directions. The numbers of lead shots that fall into each sector multiply by 10 and their addition will give the net direction of the current.

For example, the number of balls that fallen are as below:

Sector number	1	3	5	8
No.of balls	5	6	3	4

Then the resultant direction of the current is $(5 + 6 + 3 + 4) \times 10 = 180^0$.
Which means current is towards south.

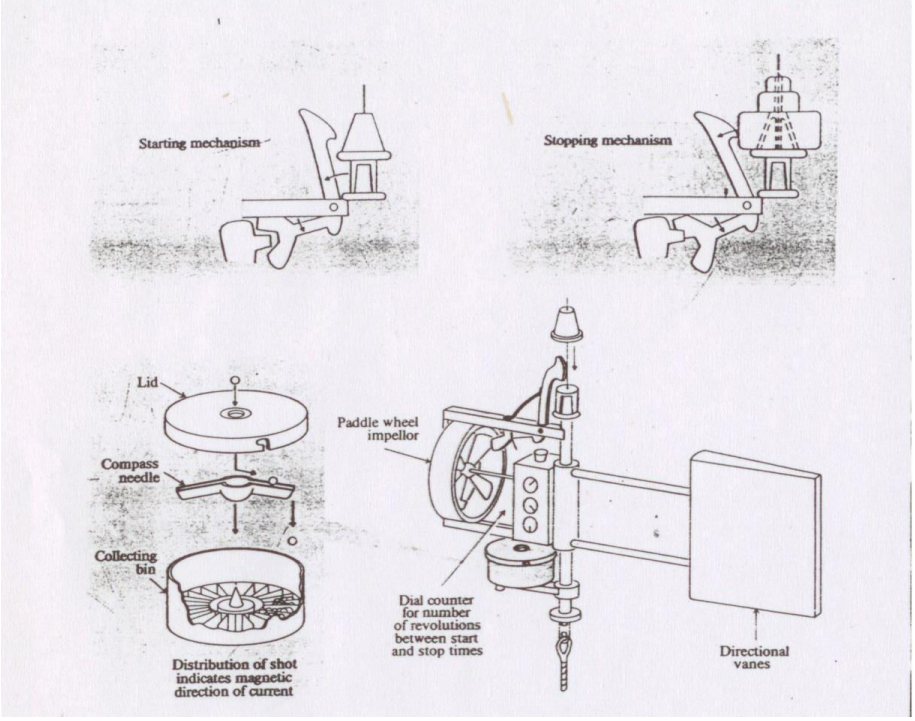

Fig.13.19a. Ekman current meter and its parts

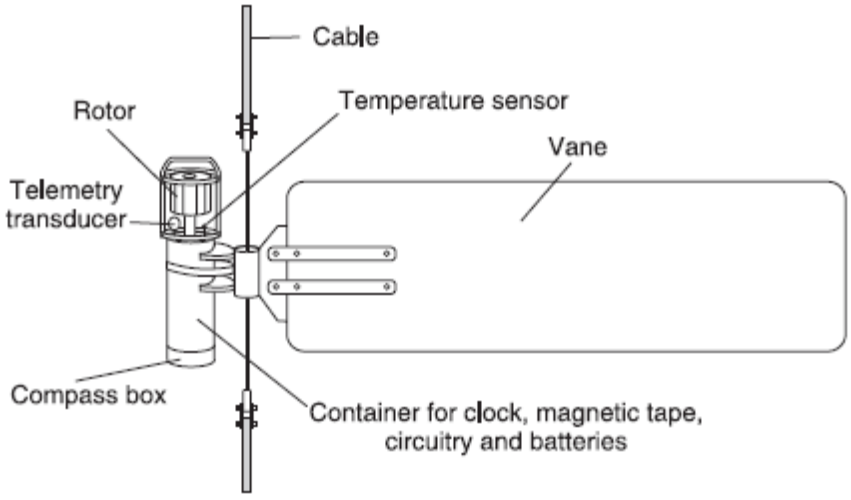

Fig.13.19b. Mechanical Savonius current meter

Mechanical or automatic current meters use a propeller-type device, a Savonius rotor or a paddle-wheel rotor (Fig. 13.19b & c) to measure the current speed, and a vane to determine current direction. Propeller sensors often measures speed correctly only if they

point into the current and have to be oriented to face the current all the time. Such instruments are therefore fitted with a large vane, which turns the entire instrument and with it the propeller into the current.

Propellers can be designed to have a cosine response with the angle of incidence of the flow. Two such propellers arranged at 90° will resolve current vectors and do not require an orienting vane.

Fig.13.19c. Aanderaa current meter & DCM-12 current meter

Mechanical current meters are robust, reliable and comparatively low in cost. They are therefore widely used where conditions are suitable, for example at depths out of reach of surface waves.

Electromagnetic current meters (Fig.13.19d) exploit the fact that an electrical conductor moving through a magnetic field induces an electrical current. Sea water is a very good conductor, and if it is moved between two electrodes the induced electrical current is proportional to the ocean current velocity between the electrodes. An electromagnetic current meter has a coil to produce a magnetic field and two sets of electrodes, set at right angle to each other, and determines the rate at which the water passes between both sets. By combining the two components the instrument determines speed and direction of the ocean current.

Acoustic current meters are based on the principle that sound is a compression wave that travels with the medium. Assume an arrangement with a sound transmitter between two receivers in an ocean current. Let receiver *A* be located upstream from the transmitter, and let receiver *B* located downstream. If a burst of sound is generated at the transmitter it will arrive at receiver *B* earlier than at receiver *A*, having been carried by the ocean current.

A typical acoustic current meter will have two orthogonal sound paths of approximately 100 mm length with a receiver/transmitter at each end. A high frequency sound pulse is transmitted simultaneously from each transducer and the difference in arrival time for the sound travelling in opposite directions gives the water velocity along the path.

Electromagnetic and acoustic current meters have no moving parts and can therefore take measurements at a very high sampling rate (up to tens of readings per second). This makes them useful not only for the measurement of ocean currents but also for wave current and turbulence measurements.

Fig. 13.19d. Electromagnetic current meter

Acoustic Doppler Current Profilers (ADCPs) (Fig. 13.20a) operate on the same principle as acoustic current meters but have transmitter and receiver in one unit and use reflections of the sound wave from drifting particles for the measurement. Seawater always contains a multitude of small suspended particles and other solid matter that may not all be visible to the naked eye but reflects sound. If sound is transmitted in four inclined beams at right angle to each other, the Doppler frequency shift of the reflected sound gives the reflecting particle velocity along the beam. With at least 3 beams inclined to the vertical the 3 components of flow velocity can be determined. Different arrival times indicate sound reflected at different distances from the transducers, so an ADCP provides information on current speed and direction not just at one point in the ocean but for a certain depth range; in other words, an ADCP produces a current profile over depth.

Different ADCP designs serve different purposes (Fig.13.20b). Deep ocean ADCPs have a vertical resolution of typically 8 metres (they produce one current measurement for every 8 metres of depth increase) and a typical range of up to 400 m. ADCPs designed for measurements in shallow water have a resolution of typically 0.5 m and a range of up to 30 m. ADCPs can be placed in moorings, installed in ships for underway measurements, or lowered with a CTD and multi-sample device to give a current profile over a large depth range.

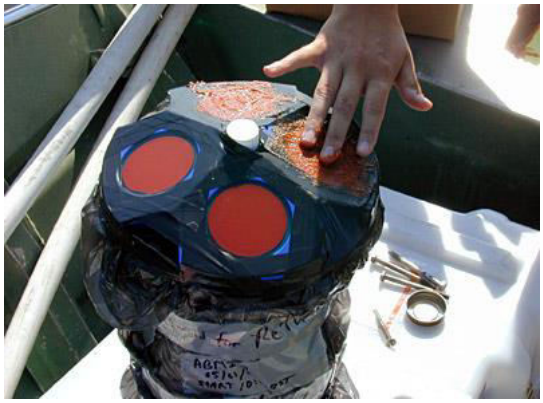

Fig.13.20a. Acoustic Doppler current Profiler (ADCP) & its hauling up

Two different varieties of ADCP (fig.13.20b) are shown below. The orange coloured parts are the sound transmitters/receivers; the white cylinder contains the electronics. The instrument on the left is designed for deep water applications; it has a resolution of 32 m and a range of 600 m. The instrument on the right is a typical shallow water design; its resolution can be varied between 1 m and 4 m, which gives it a range from 20 m to 110 m.

Fig.13.20b. Deep and shallow water ADCPs

Wave measurements

The parameters of interest in the measurement of surface waves are wave height, wave period and wave direction. At locations near the shore wave height and wave period can be measured by using the principle of the stilling well described for tide gauges below, with an opening wide enough to let pass surface waves unhindered. Wave measurements on the shelf but at some distance from the shore can be obtained from a pressure gauge.

An instrument suitable for all locations including the open ocean is the wave rider buoy (Fig.13.21, a small surface buoy on a mooring which follows the wave motion. A vertical

accelerometer built into the wave rider measures the buoy's acceleration generated by the waves. The data are either stored internally for later retrieval or transmitted to shore. Wave riders provide information on wave height and wave period. If they are fitted with a set of 3 orthogonal accelerometers they also record wave direction.

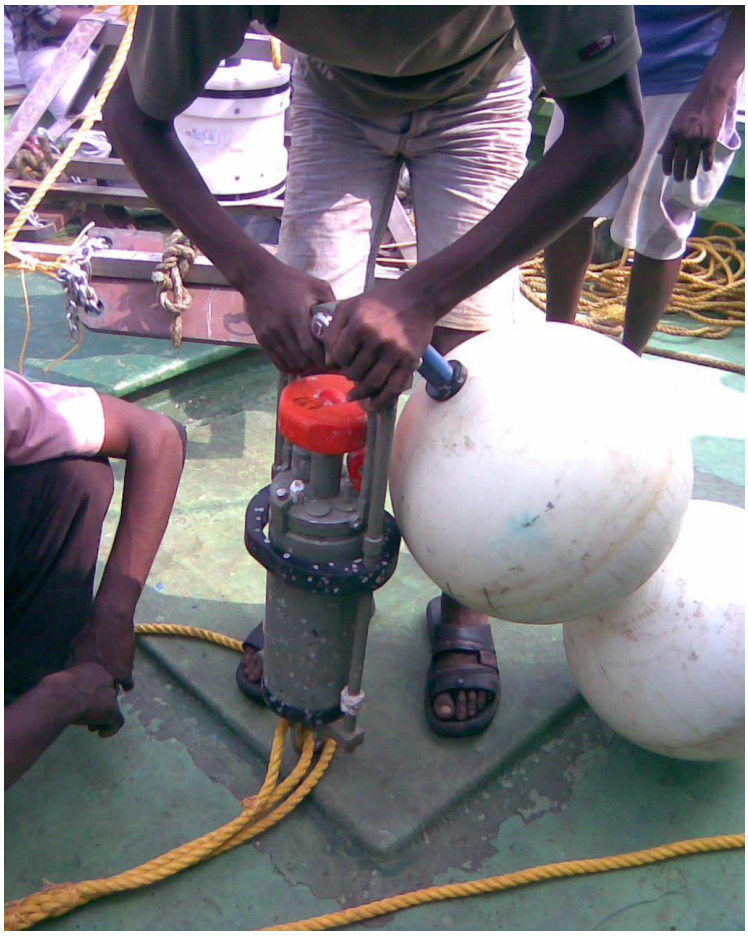

Fig. 13.21. A wave gauge before deployment

Tide gauges

Tides are waves of long wavelength and known period, so the major properties of interest for measurement are wave height, or tidal range, and wave induced current. The latter is measured with current meters; any type is suitable. Two types of tide gauges are used to measure the tidal range. The stilling-well gauge consists of a cylinder with a connection to the sea at the bottom. This connection acts as a low pass filter: It is so restricted that the backward and forward motion of the water associated with wind waves and other waves of short period cannot pass through; only the slow change of water level associated with the tide can enter the well. This change of water level is picked up by a float and recorded (Fig.13.22a).

The tide gauge shown in Fig.13.22a consists of a float (F), which operates in the float well (R), to which the slow moving tide has free access. The more rapid waves caused by winds are filtered out by means of the small size pipe (canal) (O) connecting the well to the ocean. The rising and falling of the float (F) turns a wheel on the gauge which moves the pen (P) to and fro across a wide strip of paper on a drum (D) which is moved forward by clockwork. The combined motion of pen and paper gives a continuous graph showing the rise and fall of the tide. Generally this entire assembly will be housed in a shelter as shown in Fig.13.18c. This shelter is built on a pier (a bridge on the ocean bank). The graph drawn by the tide gauge is monthly and so every month the chart is to be changed.

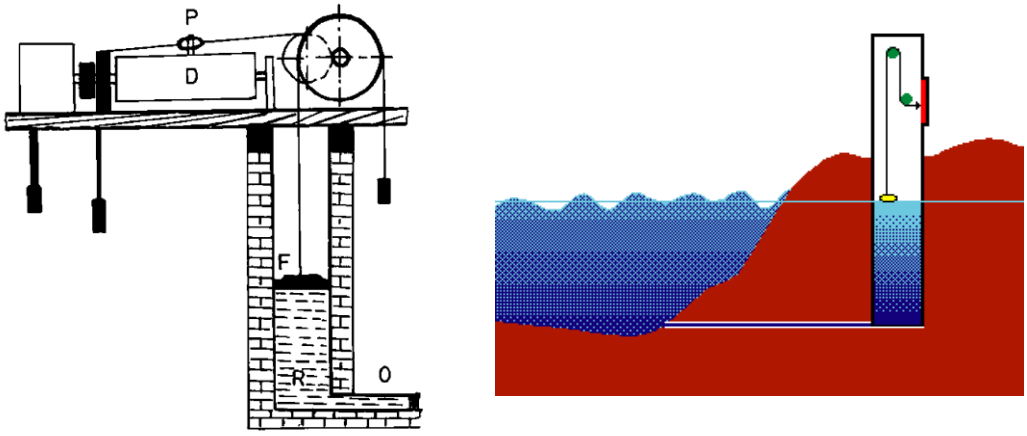

Fig.13.22a. A still well tide gauge connected to the sea with a narrow tube

Fig.13.22b. An automatic tide gauge recovered after recording

While stilling-well gauges record the water level at any time at the shore, the automatic electronic pressure gauges measure the data in offshore and remote locations. Such an instrument is placed on the sea floor and measures the pressure of the water column above it, which is proportional to the height of water above it as shown in Fig.13.18b. The data are recorded internally and not accessible until the gauge is recovered.

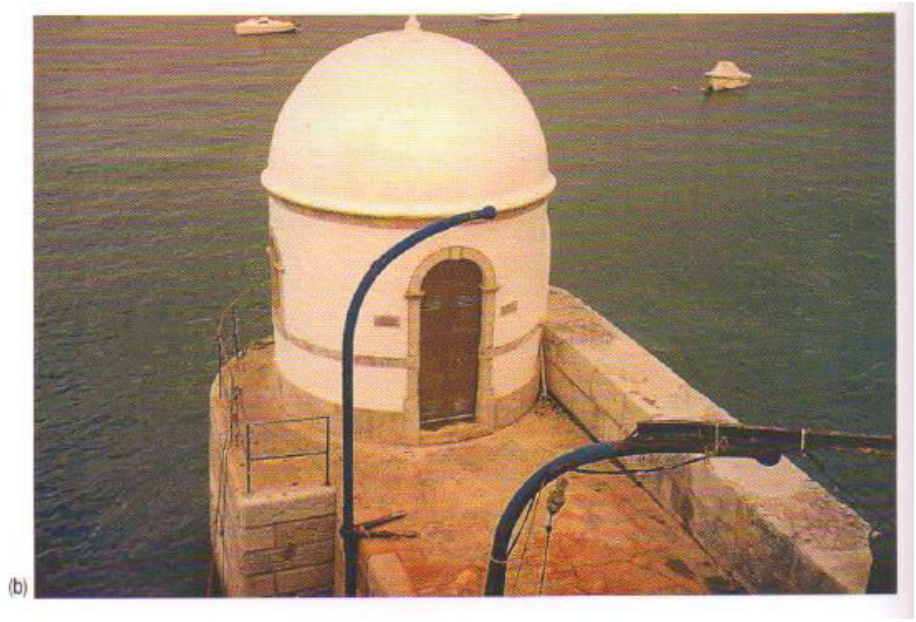

Fig.13..22c The pier (bridge) and the house where the still well tide-guage is kept in the back waters of the ocean.

Remote sensors

Sea level can also be measured from satellites. An altimeter measures the distance between the satellite and the sea surface. If the satellite position is accurately known this results in a sea level measurement. Modern altimeters have reached an accuracy of better than 5 cm. The global coverage provided by satellites allows the verification of global tide models. When the tides are subtracted, the measurements give information about the shape of the sea surface and, through application of the principle of geostrophy, the large scale oceanic circulation.

Lecture Series of Berhampur University in Physical Oceanography
By Prof.A.S.N.Murty

Chapter – 12

AIR- SEA INTERACTION

12.0. INTRODUCTION:

Turbulence is a type of fluid (gas or liquid) flow in which the fluid undergoes irregular fluctuations, or mixing, in contrast to laminar flow, in which the fluid moves in smooth paths or layers.

Turbulence is a very important phenomenon that affects all atmospheric & oceanic processes, but it is more important near the surface. Turbulence represents the irregularity or randomness of the flow. The existence of spectral gap in turbulence spectrum is essential for the separation of mean from turbulent part of the flow. For this purpose, a method of Reynolds averaging is used. Turbulence affects the mean (non-turbulent) part of the flow through a specific mechanism called eddy flux. The most unique measure for turbulence is kinetic energy of turbulent part of the flow.

12.1. SCALES OF OCEAN – ATMOSPHERE MOTIONS:

Atmospheric motion never ceases. Without atmospheric motion there is no weather system and without weather systems there is no life. Atmospheric systems embrace a wide range of time and space scales; from the tiniest turbulent eddies of not more than a second or two to the global climatic change of years.

Air and ocean are so closely linked for transport of energy, mass and momentum. In fact many of the systems originate because of the air – sea interaction. There are also links between the different scales of motion called 'scale interactions'. For example, the tropical component is a subsystem of global ocean-atmosphere interaction, the synoptic scale act as a subsystem of the tropical system and the mesoscale systems act as subsystems of synoptic scale motions.

A scale can be viewed as the distance between the inflow and the outflow of region of a system. It can be the time of start of a system to its maturity. The scale is therefore can be half wave length or half period. That is the reason why the interaction is carried up to half time in turbulent eddies.

a) ATMOSPHERIC SCALES:

S.No	Type of motion	Time dimension	Space dimension
1.	Microscale turbulent eddies in the boundary layer	Up to several minutes	< 100 m
2.	Cumulus and cumulonimbus clouds and other convective motions	Several minutes to an hour	100m-10 km
3.	Mesoscale fronts, lee waves and squall lines	Several hours to about 10 days	10 km-a few 100 km
4.	Synoptic scale systems, like tropical and extra tropical cyclones	About 2 days to a week	A few 100 km to 2000km
5.	Subtropical anticyclones and ITCZ	More than a week	Several 1000 km

b) OCEANIC SCALES

s.no	Type of motion	Time dimension	Space dimension
1.	Mid-ocean fronts	Half a day to a week	10 to 50 km
2.	Eddies and meanders	Several days to a few months	100 to 500 km
3.	Ocean gyres	Several weeks to several months	1000 to 3000 km

It is impossible to observe the three dimensional distributions of pressure, temperature and humidity in such fine detail to represent all the above scales. For a given net work of observations there is a smallest scale beyond which the scales can not be resolved by the available observation net work. Though they can not be resolved, these left out scales can not be ignored (neglected) because of the non linear nature of the equation of motion. This is called the closure problem because we have less number of equations and more variables. Therefore, we have to find a way to come out of this closure problem. The way is to use the technique of parameterization. Expressing the unknown parameter in terms of the known parameter is called parameterization. Thus these negligibly small scales can be parameterized by relating them with the observed ones.

12.2. REYNOLDS EQUATION AND REYNOLDS (EDDY) STRESSES:

The existence of shearing stresses is the phenomenon of viscosity or fluid friction. In moving air or water where the velocity varies in space frictional stresses are present as a result of momentum transfer between layers of different velocities. In the case of laminar motion, the exchange of momentum between the layers is the result of molecular motion.

If the velocity in x direction is u then the velocity shear in the z direction is $\frac{du}{dz}$. Then the frictional stress between the two layers according to Newton is

$$\tau = \mu \frac{du}{dz} \text{ dynes cm}^{-2}$$

The proportionality constant μ is called the molecular coefficient of viscosity. The frictional stress τ is force per unit area and so μ has the dimensions $\text{grcm}^{-1}\text{sec}^{-1}$. In some cases $\frac{\mu}{\rho}$ ($\text{cm}^2\text{sec}^{-1}$) is used. Then $\frac{\mu}{\rho}$ is called the kinematic coefficient of viscosity.

The term τ is also called the shearing stress as the force caused due to velocity shear. The term μ depends entirely on the random motion of the molecules as the laminar motion is in par with the kinetic theory of gases and the molecules follow the mean free paths. It is evident that μ is a physical property of the fluid which varies with temperature (t) for oceans as

$$\mu = \frac{0.01779}{1 + 0.03368t + 0.00022t^2}$$

μ for air depends on temperature of the gas as

Temperature ^{o}C	0	20	40
$10^{-4}\,\mu$ $\text{gcm}^{-1}\text{sec}^{-1}$	1.71	1.81	1.90

However, in the atmosphere and oceans the transfer of momentum is not by molecular random motion but by bulk mass transfer motion. This bulk mass transfer is known as eddy motion and instead of random motion turbulent motion prevails. So in place of molecular coefficient of viscosity (μ), eddy coefficient of viscosity (A) should be used.

Reynold's Equation of motion:

The analogy of turbulence and the associated eddy stresses were introduced by Osborne Reynolds (1894) and so these eddy stresses are often called as 'Reynolds stresses'. These eddy stresses were derived by Reynolds from equation of motion by averaging out the velocity variations due to eddies between the instantaneous and mean motions.

In a turbulent motion let u,v and w denote the instantaneous velocity components to be composed of an average flow on which random fluctuations are superimposed.

The analogy of turbulence consists in smoothing out (averaging out) the velocity variations due to the eddies and consider the gain or loss of momentum of the smoothed motion due to eddies. Then

$$u = U + u'$$
$$v = V + v'$$
$$w = W + w'$$

Where U, V and W are the average velocities and u', v', w' are the turbulent velocities around the average state such that $\overline{u'} = \overline{v'} = \overline{w'} = 0$ in the three coordinates.

One can derive the turbulent velocity equation from the equation of mean motion without friction and coriolis terms as

$$\frac{du}{dt} = \frac{\partial u}{\partial t} + u\frac{\partial u}{\partial x} + v\frac{\partial u}{\partial y} + w\frac{\partial u}{\partial z} = -\frac{1}{\rho}\frac{\partial p}{\partial x}$$

$$\rho\left[\frac{\partial u}{\partial t} + u\frac{\partial u}{\partial x} + v\frac{\partial u}{\partial y} + w\frac{\partial u}{\partial z}\right] = -\frac{\partial p}{\partial x} \quad \text{.....(1)}$$

Similarly taking the equation of continuity as

$$\frac{1}{\rho}\frac{d\rho}{dt} + \left(\frac{\partial u}{\partial x} + \frac{\partial v}{\partial y} + \frac{\partial w}{\partial z}\right) = 0$$

Or $\frac{\partial \rho}{\partial t} + u\frac{\partial \rho}{\partial x} + v\frac{\partial \rho}{\partial y} + w\frac{\partial \rho}{\partial z} + \rho\left(\frac{\partial u}{\partial x} + \frac{\partial v}{\partial y} + \frac{\partial w}{\partial z}\right) = 0$

Or $\frac{\partial \rho}{\partial t} + \frac{\partial}{\partial x}(\rho u) + \frac{\partial}{\partial y}(\rho v) + \frac{\partial}{\partial z}(\rho w) = 0$ .....(2)

Multiplying equation (2) both sides by 'u', we can write

$$u\frac{\partial \rho}{\partial t} + u\frac{\partial}{\partial x}(\rho u) + u\frac{\partial}{\partial y}(\rho v) + u\frac{\partial}{\partial z}(\rho w) = 0 \quad \text{.....(3)}$$

Adding equations (1) and (3) we can get

$$\left[\left(\rho\frac{\partial u}{\partial t} + u\frac{\partial \rho}{\partial t}\right) + \left(\rho u\frac{\partial u}{\partial x} + u\frac{\partial}{\partial x}(\rho u)\right) + \left(\rho v\frac{\partial u}{\partial y} + u\frac{\partial}{\partial y}(\rho v)\right) + \left(\rho w\frac{\partial u}{\partial z} + u\frac{\partial}{\partial z}(\rho w)\right)\right] = -\frac{\partial p}{\partial x}$$

Or $\frac{\partial}{\partial t}(\rho u)+\frac{\partial}{\partial x}(\rho uu)+\frac{\partial}{\partial y}(\rho uv)+\frac{\partial}{\partial z}(\rho uw)=-\frac{\partial p}{\partial x}$ ……(4)

Similarly for y and z directions we can write as

$\frac{\partial}{\partial t}(\rho v)+\frac{\partial}{\partial x}(\rho uv)+\frac{\partial}{\partial y}(\rho vv)+\frac{\partial}{\partial z}(\rho vw)=-\frac{\partial p}{\partial y}$ ……(5)

$\frac{\partial}{\partial t}(\rho w)+\frac{\partial}{\partial x}(\rho uw)+\frac{\partial}{\partial y}(\rho wv)+\frac{\partial}{\partial z}(\rho ww)=-\frac{\partial p}{\partial z}$ …….(6)

In analyzing the behaviour of turbulence, we consider the mean flow which is defined as time or ensemble average. The ensemble average is a statistical average of many realizations or experiments. So the mean motion can be obtained by taking the time average over a sufficiently long time interval 'T' as

$\frac{1}{T}\int_{-t/2}^{+t/2}\frac{\partial}{\partial t}(\rho u)dt=\frac{\partial}{\partial t}(\overline{\rho u})$ Such that $u=\bar{u}+u'$ ……(7)

The over bar denotes the average value.

Applying this time averaging (7) to equation (4), we can write

$\frac{\partial}{\partial t}(\overline{\rho u})+\frac{\partial}{\partial x}(\overline{\rho uu})+\frac{\partial}{\partial y}(\overline{\rho uv})+\frac{\partial}{\partial z}(\overline{\rho uw})=-\frac{\partial \bar{p}}{\partial x}$

Or $\bar{\rho}\left[\frac{\partial}{\partial t}(\bar{u})+\frac{\partial}{\partial x}(\overline{uu})+\frac{\partial}{\partial y}(\overline{uv})+\frac{\partial}{\partial z}(\overline{uw})\right]=-\frac{\partial \bar{p}}{\partial x}$ ……..(8)

Now to understand the terms under overbar expand each term as below:

$$\overline{uu}=\overline{(U+u')(U+u')}=\overline{UU}+2\overline{Uu'}+\overline{u'u'}$$

Similarly for $\overline{uv}$ and $\overline{uw}$ can be written

We can easily understand $\bar{u}'=\bar{v}'=\overline{w'}=0$ because average of all + and – values of fluctuations nullify each other but the average products of $\overline{u'u'}$, $\overline{u'v'}$, $\overline{u'w'}$ will not be zero and $\bar{U}$ = U. Using this analogy, equation (8) can be written as

$\frac{\partial}{\partial t}(U)+\frac{\partial}{\partial x}(UU+\overline{u'u'})+\frac{\partial}{\partial y}(UV+\overline{u'v'})+\frac{\partial}{\partial z}(UW+\overline{u'w'})=-\frac{1}{\rho}\frac{\partial P}{\partial x}$ ……(9)

Expanding LHS of equation (9) we can write

$\left[\frac{\partial U}{\partial t}+U\frac{\partial U}{\partial x}+V\frac{\partial U}{\partial y}+W\frac{\partial U}{\partial z}\right]+U\left[\frac{\partial U}{\partial x}+\frac{\partial V}{\partial y}+\frac{\partial W}{\partial z}\right]+\frac{\partial}{\partial x}(\overline{u'u'})+\frac{\partial}{\partial y}(\overline{u'v'})+\frac{\partial}{\partial z}(\overline{u'w'})=-\frac{1}{\rho}\frac{\partial P}{\partial x}$

$\left[\frac{dU}{dt}\right]+0=-\frac{1}{\rho}\frac{\partial P}{\partial x}-\left[\frac{\partial}{\partial x}(\overline{u'u'})+\frac{\partial}{\partial y}(\overline{u'v'})+\frac{\partial}{\partial z}(\overline{u'w'})\right]$

…….(10

Reynolds assumed $\overline{u'u'}=\frac{\tau_{xx}}{\rho}$, $\overline{u'v'}=\frac{\tau_{xy}}{\rho}$, $\overline{u'w'}=\frac{\tau_{xz}}{\rho}$ ……(11)

So equation (10) after applying equation 11, it becomes

$$\left[\frac{dU}{dt}\right] = -\frac{1}{\rho}\frac{\partial P}{\partial x} - \frac{1}{\rho}\left[\frac{\partial}{\partial x}(\tau_{xx}) + \frac{\partial}{\partial y}(\tau_{xy}) + \frac{\partial}{\partial z}(\tau_{xz})\right]$$

Similarly we can write for y and z directions as

$$\left[\frac{dV}{dt}\right] = -\frac{1}{\rho}\frac{\partial P}{\partial y} - \frac{1}{\rho}\left[\frac{\partial}{\partial x}(\tau_{yx}) + \frac{\partial}{\partial y}(\tau_{yy}) + \frac{\partial}{\partial z}(\tau_{yz})\right]$$

$$\left[\frac{dW}{dt}\right] = -\frac{1}{\rho}\frac{\partial P}{\partial z} - \frac{1}{\rho}\left[\frac{\partial}{\partial x}(\tau_{zx}) + \frac{\partial}{\partial y}(\tau_{zy}) + \frac{\partial}{\partial z}(\tau_{zz})\right]$$

……(12)

The equations (12) are called Reynold's equation of motion and all the terms for y and z directions also are written like equation (11) we get nine terms as below

$\Gamma_{xx} = \rho\overline{u'u'}$ $\Gamma_{yx} = \rho\overline{v'u'}$ $\Gamma_{zx} = \rho\overline{w'u'}$

$\Gamma_{xy} = \rho\overline{u'v'}$ $\Gamma_{yy} = \rho\overline{v'v'}$ $\Gamma_{zy} = \rho\overline{w'v'}$

$\Gamma_{xz} = \rho\overline{u'w'}$ $\Gamma_{yz} = \rho\overline{v'w'}$ $\Gamma_{zz} = \rho\overline{w'w'}$

……(13)

These are called Reynolds stresses. These nine stress terms are considered as tensor as shown in the figure 1 and are called Reynolds stresses. These terms have the dimensions $gcm^{-1}sec^2$ or dynes cm^2 and they can be shown that $\Gamma_{xy} = \Gamma_{yx}$, $\Gamma_{xz} = \Gamma_{zx}$ and $\Gamma_{yz} = \Gamma_{zy}$. So finally we are left with six stresses as: Γ_{xx} Γ_{yy}; Γ_{xy} Γ_{yz}; Γ_{xz} Γ_{zz}

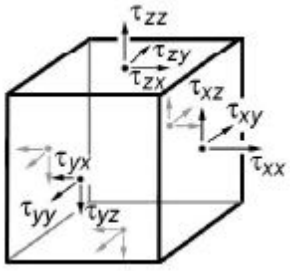

12.3. Richardson's criteria of turbulence:

The ratio of pressure force to inertial force is called the Richardson number: The Richardson number is a measure of the stability of the flow

$$Ri = \frac{\frac{g}{\rho}\frac{\partial \rho}{\partial z}}{(\partial v / \partial z)^2}$$

- If $Ri \ll 1$, stratification is weak and vulnerable to mixing;
- If $Ri \sim 1$, stratification is important and may be reduced by mixing;
- If $Ri \gg 1$, stratification is strong and resisting mixing.

Flux Richardson Number

But these quantities are difficult to measure, so Richardson assumed that the turbulent transport of Heat and Momentum could be modelled by diffusion equations:

$$H = -c_p \rho K_H \left(\partial \overline{T} / \partial z + \Gamma\right)$$

$$\tau / \rho \, \partial u / \partial z = K_M \left(\partial \overline{u} / \partial z\right)^2$$

From which:

$$R_f = \frac{g}{\overline{T}} \frac{K_H}{K_M} \frac{\left(\partial \overline{T} / \partial z + \Gamma\right)}{\left(\partial \overline{u} / \partial z\right)^2}$$

Often $K_H / K_M = 1$ and the temperature T can be written in terms of potential temperature Θ

Gradient Richardson Number

$$R_i = \frac{g}{\overline{\theta}} \frac{\partial \overline{\theta} / \partial z}{\left(\partial u / \partial z\right)^2}$$

where:

$R_i < 0.25$: slightly turbulent flow remains turbulent

$R_i > 0.25$: turbulence is suppressed

With regard to Turbulent Kinetic Energy also Richardson number can be defined as:

Richardson defined a stability criterion R_f as:

$$R_f = \frac{\text{negative buoyant production rate}}{\text{mechanical production rate}}$$

$$= \frac{-\hat{P}_B}{\hat{P}_M} = \frac{-g\,H}{\overline{T}\,\overline{\rho}\,c_p\,\tau\,du/dz}$$

12.4. PRANDTLE'S MIXING LENGTH THEORY:

To understand these turbulent stresses Prandtle (1925) has introduced the 'mixing length' concept by analogy to the 'free path' of the molecular motion that governed by kinetic theory of gases.

Consider for simplicity the average flow 'U' in the x direction such that the super imposed turbulent flows are u',v' and w'.

Let the eddy leaves its original position (x,y,z) with an average velocity $U_{(x,y,z)}$ and arrives the point ($x + l_x$, $y + l_y$, $z + l_z$) after traveling a distance $l_{(x,y,z)}$ where l_x, l_y, l_z are the x,y and z components of mixing length.

The velocity of the eddy at point 2 is given by

$$U_{x+lx,y+ly,z+lz} = U_{x,y,z} + l_x\frac{\partial u}{\partial x} + l_y\frac{\partial u}{\partial y} + l_z\frac{\partial u}{\partial z}$$

So the difference in velocity between 2 and 1 is

$$U_{(x,y,z)} - \{\, U_{x,y,z} + l_x\frac{\partial u}{\partial x} + l_y\frac{\partial u}{\partial y} + l_z\frac{\partial u}{\partial z}\,\} = -\{l_x\frac{\partial u}{\partial x} + l_y\frac{\partial u}{\partial y} + l_z\frac{\partial u}{\partial z}\,\}$$

Prandtle has shown that the magnitudes of each of these three terms are same as the magnitude of turbulent velocity in the respective direction.

i.e.

$$l_x\frac{\partial u}{\partial x} = u_x' = u'$$

$$l_y\frac{\partial u}{\partial y} = u_y' = v' \qquad (14)$$

$$l_z\frac{\partial u}{\partial z} = u_z' = w'$$

Substituting equations (14) in the Reynolds stresses (equation 13) we get

$$\Gamma_{xx} = \rho\overline{u'u'} = \rho\overline{u_x'u'} = -\rho\overline{l_x\frac{\partial u}{\partial x}.u'}$$

$$\Gamma_{xy} = \rho\overline{u'v'} = \rho\overline{u_y'u'} = -\rho\overline{l_y\frac{\partial u}{\partial y}.v'} \qquad \text{.....(15)}$$

$$\Gamma_{xz} = \rho\overline{u'w'} = \rho\overline{u_z'w'} = -\rho\overline{l_z \frac{\partial u}{\partial z}.w'}$$

Following the same analogy, Prandtle has shown that eqn.15 can be written as

$$\Gamma_{xx} = \rho\overline{u'u'} = -\rho l_x \frac{\partial U}{\partial x}\left(-l_x \frac{\partial U}{\partial x}\right) = \rho l_x^2 \frac{\partial U}{\partial x}\frac{\partial U}{\partial x} = A_{xx}\frac{\partial U}{\partial x}$$

$$\Gamma_{xy} = \rho\overline{u'v'} = -\rho l_y \frac{\partial U}{\partial y}\left(-l_y \frac{\partial U}{\partial y}\right) = \rho l_y^2 \frac{\partial U}{\partial y}\frac{\partial U}{\partial y} = A_{xy}\frac{\partial U}{\partial y} \quad \text{.....(16)}$$

$$\Gamma_{xz} = \rho\overline{u'w'} = -\rho l_z \frac{\partial U}{\partial z}\left(-l_z \frac{\partial U}{\partial z}\right) = \rho l_z^2 \frac{\partial U}{\partial z}\frac{\partial U}{\partial z} = A_{xz}\frac{\partial U}{\partial z}$$

Where

$$A_{xx} = \rho l_x^2 \frac{\partial U}{\partial x}, \quad A_{xy} = \rho l_y^2 \frac{\partial U}{\partial y}, \quad A_{xz} = \rho l_z^2 \frac{\partial U}{\partial z} \quad \text{.....(17)}$$

These are called eddy coefficients of viscosity. These are proportional to average velocity shear and the square of the mixing length.

12.5. Kolmogroff's similarity theory:

In the spectrum of turbulence, the energy cascades from larger to smaller eddies. This range is called inertial subrange. This line of reasoning led Kolmogorov in 1941 to a famous similarity argument.

Kolmogorov postulated that at sufficiently large Reynolds numbers, small scale motions in turbulent flows have similar universal characteristics.

For local isotropic small scale turbulence Kolmogrov proposed a local similarity theory or scaling based on his well known equilibrium range. This states that at sufficiently high Reynold's numbers there is range of small scales for which turbulence structure is in a statistical equilibrium and is uniquely determined by the rate of energy dissipation (ψ or ε) and kinematic viscosity (ν). Here the statistical equilibrium refers to the stationarity of small scale turbulence. The above two parameters led to the following Kolmogrov's microscales from dimensional considerations:

Length scale : $\eta = \nu^{3/4}\psi^{-1/4}$

Velocity scale: $\upsilon = \nu^{1/4}\psi^{1/4}$

Which are used to normalize any turbulence statistics and to examine their universal similarity forms.

If k_0 and k_d are the characteristic wave numbers of the energy containing eddies and the energy dissipating eddies respectively, then the inertial subrange for k is in between these two which is given by

$$k_0 < k < k_d$$

In this range the three dimensional variance spectrum E(k,ψ) of turbulence kinetic energy is entirely determined by the rate of dissipation (ψ) and the wave number (k). This leads to the spectrum

$$E(k, \psi) = C\, k^{-5/3}\, \psi^{2/3}$$ where C is called the Kolmogrov constant.

The spectrum is most easily determined from measurements. This means that once the constant 'C' is known, it is possible to determine ψ. The value of C is found to be about 0.5. Therefore, C_{min} depends on the energy level of the turbulence. The stronger the turbulence (the bigger ψ), the shorter the minimum length scale at which it is capable of stirring. The quantity $\nu^{3/4}\, \psi^{-1/4}$ is called the Kolmogorov scale and is typically of the order of a few millimeters or less.

12.5.1. Derivation:

The basic assumption of the Kolmogorov theory is the *Similarity Hypothesis*. Kolmogorov's hypothesis assumes that if the inertial range is large enough, the influence of the large scale forcing and the small scale viscous dissipation can be neglected.

In 1941 Andrei N. Kolmogorov derived a formula for the energy spectrum of turbulence. This spectrum gave the distribution of energy among turbulence vortices as function of vortex size.

Kolmogorov assumed that $K_3 = K_1 + K_2$ when energy is transformed from one wave number to the other. When the wave numbers of interacting vortices are equal then $K_1 = K_2$. Then it becomes $K_3 = 2\,K_1$. The other extreme is where one wave number is very small compared to the other, say $K = \delta = 0$, in which case energy is transferred to $K_3 = K_1 + \delta$, a nearby wave number.

Kolmogorov further assumed that mixing occurs from K_{min} to K_{max} such that energy is transferred from minimum to maximum wavenumbers. While in some range K_{max} to $K\nu$ the viscous dissipation of energy is not important, beyond $K\nu$ the spectrum is affected by the viscosity of the fluid. The range over which viscous effects are not important can be called the inertial range. Kolmogrov derived a formula for the energy spectrum over the inertial subrange.

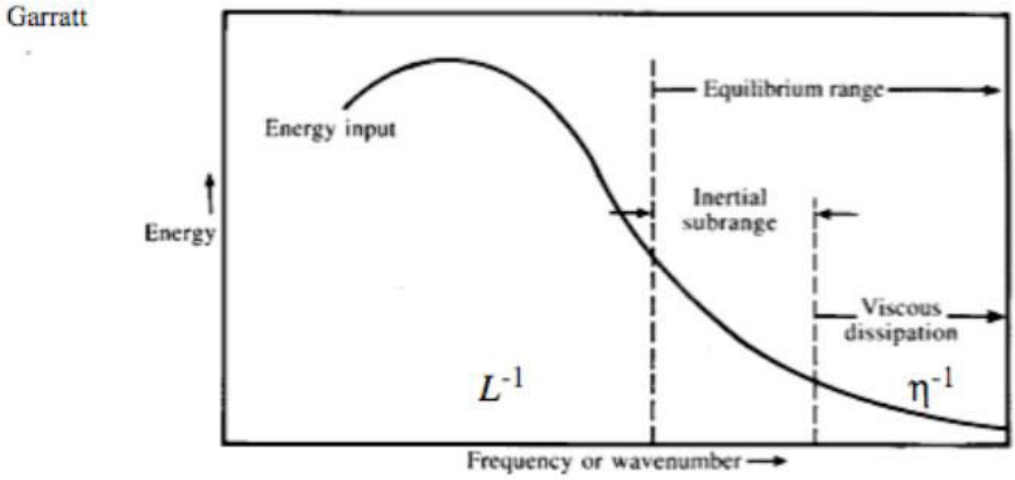

Fig.1. Schematic representation of the energy spectrum of turbulence

12.5.2. Kolmogrov's energy spectrum:

Kolmogrov's analysis deduced that E, the energy density per unit wave number should depend only upon the wave number K and rate of energy dissipation per unit volume ψ. The upper limit of the inertial range Kν should depend on the molecular viscosity ν and ψ.

The dimensions of these variables are

$K = L^{-1}$, $\psi = L^2T^{-3}$, $\nu = L^2T^{-1}$, $E = L^3T^{-2}$ .....(18)

The energy is given as $E(k, \psi) = C\, k^{\alpha}\, \psi^{\beta}$ …….(19)

where C is a constant.

To find α and β substitute the dimensional compatibility (eqn 18) into energy equation (19).

$$L^3T^{-2} = C\, L^{-1(\alpha)}\, L^{2\,\beta}\, T^{-3\,\beta}$$

Comparing the equal coefficients and finding α and β we get α = -5/3 and β = 2/3. This means the energy equation (19) becomes

$$E(k, \psi) = C\, k^{-5/3}\, \psi^{2/3} \quad \text{…….(20)}$$

Similarly the wave number at which molecular viscosity makes energy dissipation effects significant can be written as

$$K\nu = D\nu^{\gamma}\, \psi^{\delta} \text{ where D is constant } \text{……(21)}$$

Substituting eqn (18) dimensional compatibility in eqn (21) we get

$$L^{-1} = D\, L^{2\gamma}T^{-\gamma}\, L^{2\delta}T^{-3\delta}$$

Comparing the equal coefficients and finding γ and δ we get γ = -3/4 and δ=1/4 such that equation (21) becomes

$$K\nu = D\nu^{-3/4}\, \psi^{1/4} \quad \text{…….(22)}$$

The energy spectrum is the relation between E and K with ψ kept fixed. Below is shown an illustration of the relation between these two.

The energy spectrum in terms of the scale of the vortices is found by noting that if F(L) is the energy spectrum in terms of the scale L of a vortex then

$$\int E(k)dk = \int E(k)\frac{dk}{dL}dL = \int F(L)dL \text{ which means}$$

$$F(L) = E(k)\frac{dk}{dL} \quad \ldots\ldots\ldots\ldots\ldots\ldots\ldots\ldots\ldots(23)$$

Substituting the dimensional equality of eqn (18) into eqn (23) taking $k = 2\pi/L$, we get

$$F(L) = C\,k^{-5/3}dk/dL = C\,k^{-5/3}\,(2\pi/L)\,(1/L)$$

$$F(L) = C(2\pi)^{-5/3}L^{5/3}(2\pi).L^{-2}\ldots\ldots\ldots(24)$$

Comparing the coefficients in eqn (24)

$$\text{we get } F(L) = C'L^{-1/3} \qquad \{\text{ put } C(2\pi)^{-2/3} = C'\}$$

Thus the alternate version of Kolmogrov spectrum is $F(L) = C'L^{-1/3}$

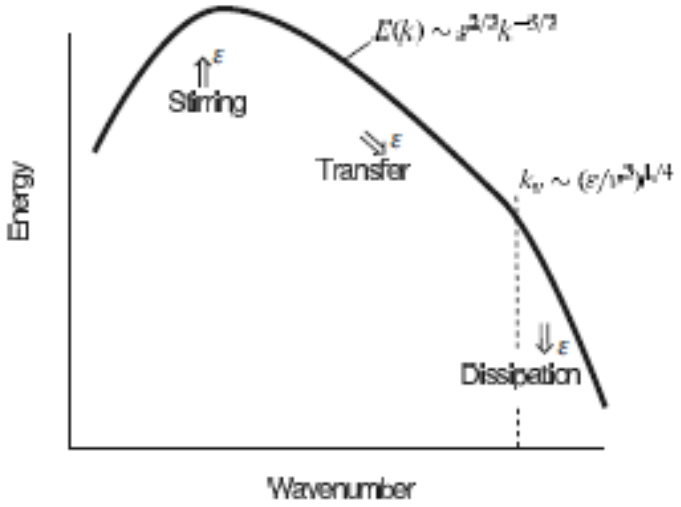

Fig.2. Schematic of Kolmogorov's energy spectrum.Energy is supplied at some rate ψ(or ε). It is cascaded to small scales, where it is ultimately dissipated by viscosity. There is no systematic energy transfer to scales larger than the forcing scale. So here the energy falls off

Thus the energy density is lower for the larger vortices and is concentrated in the smaller scale vortices.

12.6. TURBULENT KINETIC ENERGY EQUATION (TKE):

Turbulence is a very important phenomenon that affects all atmospheric processes, but it is more important near the surface. Turbulence represents the irregularity or randomness of the flow. The

existence of spectral gap in turbulence spectrum is essential for the separation of mean from turbulent part of the flow. For this purpose, a method of Reynolds averaging is used. Turbulence affects the mean (non-turbulent) part of the flow through a specific mechanism called eddy flux. The most unique measure for turbulence is kinetic energy of turbulent part of the flow.

12.6.1. Definition of K.E:

The kinetic energy in physics is $\frac{1}{2}\left(mv^2\right)$. So the KE of mean turbulent flow is similar to that. Let us say U is a velocity field. Then we can define $U = \bar{U} + U'$. Where U is instantaneous velocity, $\bar{U}$ is mean velocity and U' is turbulent velocity such that $\cup = iu + jv + kw$ in x,y and z directions respectively. We can define two kinds of kinetic energy:

i) Mean flow kinetic energy per unit mass (MKE/m) = $\frac{1}{2}\left(\bar{u}^2 + \bar{v}^2 + \bar{w}^2\right)$

ii) Turbulent kinetic energy per unit mass (TKE/m) = $\bar{e} = \frac{1}{2}\left(u'^2 + v'^2 + w'^2\right) = \frac{1}{2}\left(U'^2\right)$

The first equation represents kinetic energy of the mean flow and the second is turbulent part. Turbulent kinetic energy is one of the most important variables in micro meteorology. It is a measure of the intensity of turbulence. As the turbulence changes with time we are interested in TKE budget equation.

12.6.2. TKE equation:

Vortex stretching and twisting associated with turbulent eddies always tend to cause turbulent energy to flow toward the smallest scales, where it is dissipated by viscous diffusion. Thus there must be continuing production of turbulence if the TKE is to remain statically steady. The primary source of boundary layer turbulence depends critically on the structure of the wind and temperature profiles near the surface. If the lapse rate is unstable, boundary layer turbulence is convectively generated. If it is stable, then instability associated with wind shear must be responsible for generating turbulence in the boundary layer. The comparative roles of these processes can best be understood by examining the budget for TKE.

One can derive the turbulent velocity equation from the equation of motion without friction and coriolis terms as

$$\frac{du}{dt}=\frac{\partial u}{\partial t}+u\frac{\partial u}{\partial x}+v\frac{\partial u}{\partial y}+w\frac{\partial u}{\partial z}=-\frac{1}{\rho}\frac{\partial p}{\partial x} \quad \text{.....(1)}$$

In analyzing the behaviour of turbulence, we consider the mean flow which is defined as time or ensemble average. The ensemble average is a statistical average of many realizations or experiments. So for continuous observations we can write the time average as

$$\bar{u}=\frac{1}{T}\int_{t_1}^{t_2} u\,dt \qquad \text{Such that} \qquad u=\bar{u}+u' \quad \text{.....(2)}$$

$$\bar{u}=\bar{\bar{u}}+\bar{u'}=\bar{u}+\bar{u'},\quad \bar{u'}=\bar{u}-\bar{\bar{u}}=\bar{u}-\bar{u}=0 \quad \bar{uw}=\left(\bar{\bar{u}}+\bar{u'}\right)\left(\bar{\bar{w}}+\bar{w'}\right)=\bar{u}\bar{w}+\bar{u'w'} \quad \text{...(3)}$$

Applying equations (2) and (3) on equation (1) we can get

$$\frac{\partial u'}{\partial t}+\frac{\partial}{\partial x}(u'\bar{u})+\frac{\partial}{\partial y}(v'\bar{u})+w\frac{\partial u}{\partial z}(w'\bar{u})+\frac{\partial}{\partial x}(u'\bar{u})+\frac{\partial}{\partial y}(u'\bar{v})+\frac{\partial}{\partial z}(u'\bar{w})$$
$$=fv'-\frac{1}{\rho}\frac{\partial p'}{\partial x}+\frac{\partial}{\partial x}(u'\bar{u'})+\frac{\partial}{\partial y}(u'\bar{v'})+\frac{\partial}{\partial z}(u'\bar{w'}) \quad \text{.....(4)}$$

Similar equations for $\frac{\partial v'}{\partial t}$ and $\frac{\partial w'}{\partial t}$ can be obtained.

Multiplying equation (4) by u' and the other two equations ($\frac{\partial v'}{\partial t}$ and $\frac{\partial w'}{\partial t}$) by v' and w' respectively and averaging using (2) and (3) and removing the mean motion and applying the equation of continuity, we can get the Turbulent kinetic Equation (TKE) as

$$\frac{\partial E}{\partial t}=-\left[\bar{u'w'}\frac{\partial \bar{u}}{\partial z}+\bar{v'w'}\frac{\partial \bar{v}}{\partial z}\right]-\frac{\partial}{\partial z}\left(\bar{Ew'}\right)-\frac{1}{\rho}\frac{\partial}{\partial z}(\bar{p'w'})+\frac{g}{\theta}\left(\bar{w'\theta'}\right)-\varepsilon \quad \text{.....(5)}$$

MP TR BPL

Where E = $\frac{1}{2}\left(u'^2+v'^2+w'^2\right)$ and $\frac{\partial}{\partial z}(Ew')=\frac{1}{2}\frac{\partial}{\partial z}\left(u'^2w'+v'^2w'+w'^2w'\right)$ and ε = rate of dissipation. Out of these three 'MP' and 'BPL' are very important.

'MP' = Mechnaical Production, BPL = Buoyant Production Loss, TR = Redistribution of Transport and Pressure effects, ε = Frictional dissipation.

The Buoyancy Production term (BPL) represents a conversion of energy between mean flow potential energy and turbulent kinetic energy. It is positive for motions that lower the center of mass of the atmosphere and negative for motions that raise it.

The 'MP' (mechanical production) term tells about the generation of turbulence due to wind shear. So the term is proportional to the shear of the mean wind as from the first term of equation (5).

$$MP = -\left[\bar{u'w'} \frac{\partial \bar{u}}{\partial z} + \bar{v'w'} \frac{\partial \bar{v}}{\partial z} \right] \ldots\ldots\ldots\ldots\ldots(6)$$

The first term on the right hand side of equation (6) is zonal wind and the second term is meridional wind component. MP is positive when the momentum flux is directed down the gradient of the mean momentum ($\frac{\partial \bar{u}}{\partial z} > 0, \bar{u'w'} < 0$) .

12.6.3. Importance of Buoyant Production, Shear Production and dissipation terms:

The turbulence depends on a variety of mechanisms and the ABL depends on MP,TR and BPL as mentioned in equation 6. The most important are buoyant production or (consumption)(BPL) and shear production (MP) of TKE. Both of these vary significantly in time and space (especially with height). The third very important term is dissipation. This term provides the reduction of turbulence with time which is the primary purpose of turbulence. In meteorology TKE is very useful for parameterization of sub-grid processes.

In a statically stable layer turbulence can exist only if mechanical production (MP) is large enough to overcome the damping effects of stability and viscous dissipation.

This condition is measured by a quantity called the 'Flux Richardson Number'(R_f). It is defined as :

$$R_f = -\frac{BPL}{MP} \; ; \text{ If } R_f < 0 \text{ it is unstable ; and if } R_f > 0 \text{ it is stable}$$

If the boundary layer is statically unstable then $R_f < 0$ and turbulence is sustained by convection. For stable conditions $R_f > 0$.

One can assume stationary and zonal flow parallel to x coordinates in the surface boundary layer. Then in the equation (5), $\frac{\partial E}{\partial t} = 0$ and $\bar{v'w'} = 0$ then we can rewrite the equation (5) as:

$$-\left[\bar{u'w'} \frac{\partial \bar{u}}{\partial z} \right] - \frac{\partial}{\partial z}\left(\bar{Ew'} \right) - \frac{1}{\rho} \frac{\partial}{\partial z}\left(\bar{p'w'} \right) + \frac{g}{\theta}\left(\bar{w'\theta'} \right) - \varepsilon = 0 \quad \ldots\ldots\ldots\ldots\ldots..(6)$$

A B C D EE

Where 'A' is mechanical production term, B is turbulent transport, 'C' pressure effects, D Buoyant production loss and EE or (ε) is the dissipation term which is always positive reflecting the dissipation of smallest scales of turbulence by molecular viscosity.

The ratio of

$\frac{A}{D} = L = \frac{Mechanical\,production\,term}{Buoyant\,production\,term}$ is called Monin – Obukov length which is a dimensionless number and is considered as constant in the surface layer since the momentum and heat fluxes are assumed constant in the constant flux surface layer.

When the mechanical production term is expressed in terms of non dimensional form of friction velocity (u_*), L is given as

$$L = \frac{u_*^{\,3}}{kz\frac{g}{\theta}w'\theta'} \quad \text{since} \left[\because \overline{u'w'} = u_*^{\,2}\right] and \frac{\partial u}{\partial z} = \frac{u_*}{kz}$$ where k = 0.4 called Von Karman constant.

The Monin-Obukov length scale is thus the length upto which the generation of mechanical turbulence is equal to the fluctuation of turbulent kinetic energy produced by buoyancy.

The stability criteria with respect to L are as below:

If L > 0, stable
If L < 0, unstable
If L = 0, Neutral

The Figure 3 below shows the variation of each term of equation (6) during day time in the Atmospheric Boundary layer upto 1 kilometer. For example the shear term (A in eqn 6) starting at 10 reduces to zero at the tropopause. While the turbulent transport (B) is less than zero at the surface it increases to 0.5 at 1.0 km, the dissipation (EE) is maximum (-10 to 0.5) at the surface and it is least at 1 km. Note as dissipation is loss it is negative side. Transport also is least at the ground due to ground friction. The Buoyant production loss (red) is maximum (1.0) at ground and gradually reduces as it goes up to -0.5 at the tropopause.

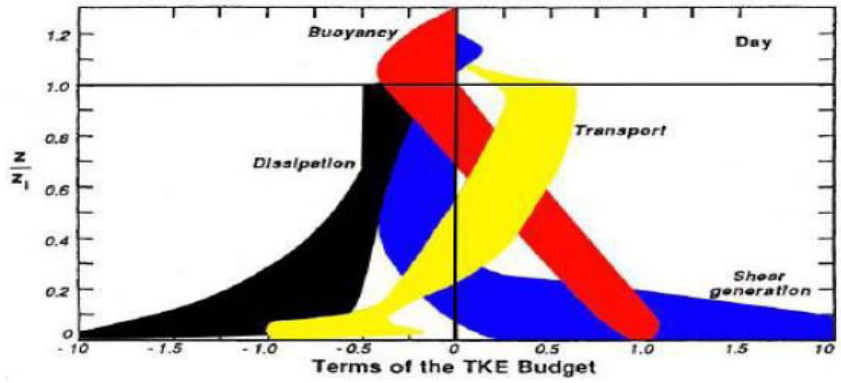

Fig.3. Variation of different terms in the TKE budget equation in the boundary layer. The shaded areas present variation of each term in day. Height variable is normalized (made unit less) with the depth of mixed layer (Z_1).

Lecture Series of Berhampur University in Physical Oceanography
By Prof.A.S.N.Murty

Chapter – 13

Determination of Air – Sea fluxes

In addition to the momentum flux, the upward turbulent fluxes of sensible heat, water vapor and latent heat can be written as

$$H_S = \rho C_p \overline{w'\theta'}$$

$$E_W = \rho \overline{w'q'}$$

$$H_L = \rho L \overline{w'q'}$$

Some of the methods available for determination of these eddy surface fluxes are i) the eddy correlation method, ii) the variance budget method or dissipation method and iii) the profile or gradient method.

There are also other methods like ageostrophic method, total energy budget method, the line integral method, the wind setup method and Remote Sensing methods. These methods are mostly applicable to the surface layer over the oceans.

Bulk Aerodynamic method:

An alternative method for computing the surface fluxes of sensible heat(H_S) and latent heat (evaporation) (H_L) is by bulk methods as shown below:

$$H_S = \rho C_p C_H V_S (T_S - T_a)$$

$$H_L = L C_E V_S (q_S - q_a)$$

Where C_H and C_E are empirical coefficients. Usually both are taken as equal to 1.7×10^{-3} L =2.5×10^6 J/kg; V_S the surface wind speed; T_S and T_a are the surface and air temperatures at anemometer level (10m); q_s and q_a are the saturation specific humidity at surface water and air over water.

Transfer of heat and water vapor: Heat budget :

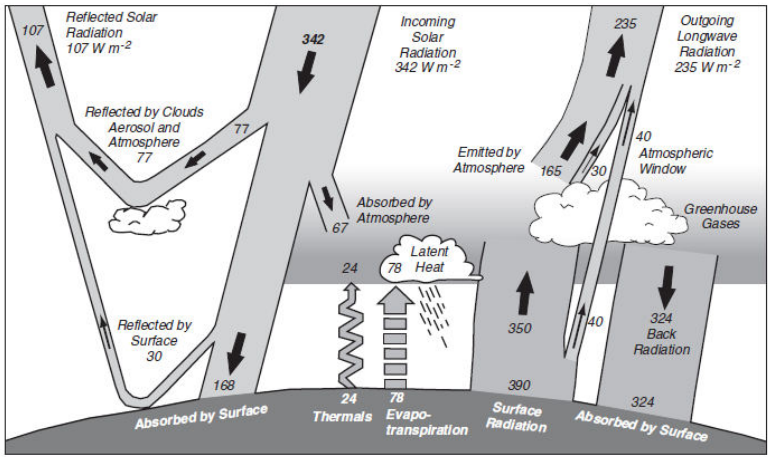

Fig.1 Estimate of the earth's annual and global mean energy balance.

The Fig.1 indicates, over a long term, the amount of incoming solar radiation absorbed by the earth and atmosphere (168+67=235 wm^{-2}) is balanced by the earth and atmosphere releasing the same amount of outgoing long wave radiation (165+30+40 wm^{-2}). About half of the incoming solar radiation (342÷2) is absorbed by the earth's surface (168 wm^{-2}). This energy is transferred to the atmosphere by warming the air in contact with the surface (thermals) (24) by evaporation(78) and by longwave radiation that is absorbed by clouds and green house gases (390-324). i.e. 24+78+390-324=168 The atmosphere in turn radiates longwave energy back to earth (324) as well as to space (165+30) out of its gain 67+24+78+350=519).

1. Balance at earth and atmosphere: Gain :168+67 =235 wm^{-2}, Loss: 165+30+40 wm^{-2} =235 wm^{-2}
2. Absorption at the earth's surface: 168 wm^{-2}, utility of this amount with interaction of air through thermals, evaporation and long wave radiation absorbed by clouds and atmosphere =. 24+78+(390-324)=168 wm^{-2}
3. Atmosphere Gain: 67+24+78+350=519 wm^{-2}; Loss of atmosphere due to radiation: 324+165+30 = 519 wm^{-2}

Explanation of the mean annual energy balance of the earth and atmosphere:

S.No	Radiation	W m^{-2}	W m^{-2}
1.	**Total insolation coming from the Sun**		**342**
Short wave component distribution to earth and atmosphere & balance			
	i) Directly reaching the earth & oceans	168	
	ii) Directly reaching the atmosphere	67	
2.	Total short wave absorption by earth & atmsophere		235
Albedo			
	iii)Reflected by clouds & atmosphere	77	
	iv) Reflected by earth & oceans	30	
3.	Total albedo of earth,ocean and atmosphere		107
4.	**Total shortwave gain (i+ii+iii+iv) or(2+3)**		**342**
So 1 = 4 balanced			
Long wave radiation Balance			
	i) Earth directly losing to space	40	
	ii) Emitted by atmosphere to space	165	
	iii) Emitted by clouds to space	30	
5.	Total loss of earth & atmosphere to space (i+ii+iii)		235
Short wave (2) = Long wave (5) balanced =235			

Water budget

The oceans dominate the hydrologic cycle (Fig.2), for they contain 97% of the global water inventory. Large changes in terrestrial parts of the water inventory (table 2) would be necessary to have any significant effect on the amount of water in the oceans. For example, it is estimated that during the glacial maxima of the past two million years, some 50000×10^{15} kg of water were added to the world's glaciers and ice caps, increasing their volume to about two and a half times what is today.

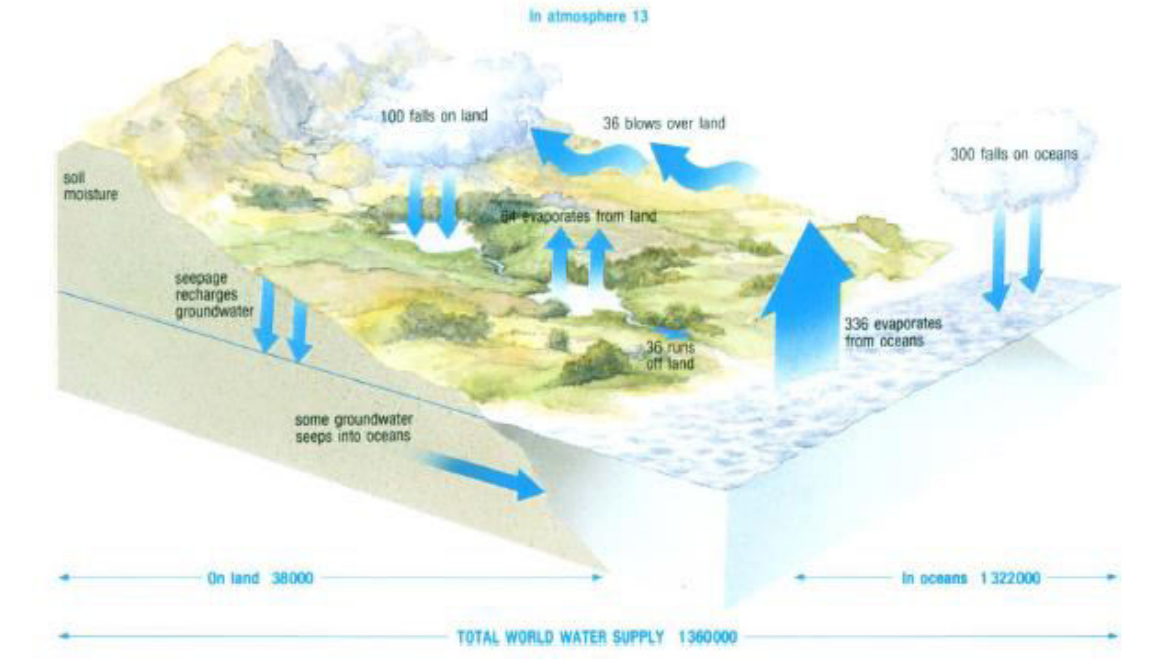

Fig.2 hydrologic cycle

Table .1

S.No	Stored in different stages		Annual movements(per annum)	
1.	In atmosphere	13×10^{15} kg	Precipitation on land	100×10^{15} kg
2.	On land	38000×10^{15} kg	Evaporation from land	64×10^{15} kg
3	In the Oceans	1322000×10^{15} kg	Blows over land	36×10^{15} kg
4	Total world water supply	1360000×10^{15} kg	Run off through streams	36×10^{15} kg
5			Evaporation from oceans	336×10^{15} kg
6			Precipitation in oceans	300×10^{15} kg

Rivers and streams	1
Freshwater lakes	125
Salt lakes and inland seas	104
Total surface water	230
Glaciers and ice-caps	29 300
Soil moisture and seepage	70
Groundwater	8 400
Total on land	38 000

Table 2. Water on land ($\times 10^{15}$ kg)

The concept of residence time can be defined with reference to Figure. It is the average length of time that a water molecule resides or is stored in any particular stage of the hydrologic cycle. It is calculated by dividing the amount of water in that part of the cycle by the amount that enters and leaves it in unit time.

Question:

1. Using the above figures calculate the heat lost from oceans per day in Joules.(take latent heat of evaporation as 2.25×10^6 J/kg)

An approximate value for the heat lost from the oceans by evaporation each day using the latent heat of evaporation as 2.25×10^6 J/kg and mass of water evaporates from oceans as 336×10^{15} kg per annum. This means mass of water evaporates per day is

336×10^{15} kg $\div$ 365 = 920×10^{12} kg
This means:
For 1 kg latent heat of evaporation = 2.25×10^6 J/kg
For 920×10^{12} kg = ? heat
= (2.25×10^6 J $\times$ 920×10^{12} kg =2.07×10^6 J/day .

What is the importance of evaporation of 2.07×10^6 J/day from the oceans if the earth receives about 9×10^{21} J/day from the sun?

It is very important because evaporation is more than a quarter time (25%) of the income and so is responsible for all the weather events and heat balance.

2. What is the residence time on land and atmosphere?

$$\text{Residence time on land} = \frac{100\times10^{15}}{36\times10^{15}} \approx 3\,years$$

Atmosphere contains : 13×10^{15} kg, Movement in atmosphere: 400×10^{15} kg

$$\text{Residence time in atmosphere} = \frac{13\times10^{15}}{400\times10^{15}} \approx 0.035\,years = 12.8\,days \approx 13\,days$$

Planetary Boundary Layer

The Planetary Boundary layer (PBL) is that part of the atmosphere which is directly influenced by the earth's surface, and responds to surface forcings as shown in Fig. 1.

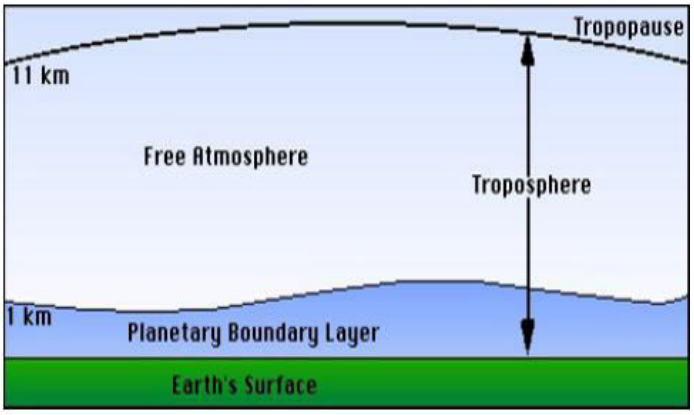

Fig.1. The troposphere is divided into two parts: a planetary boundary layer close to the earth's surface of about 1 km thicknes and the free atmosphere above it.

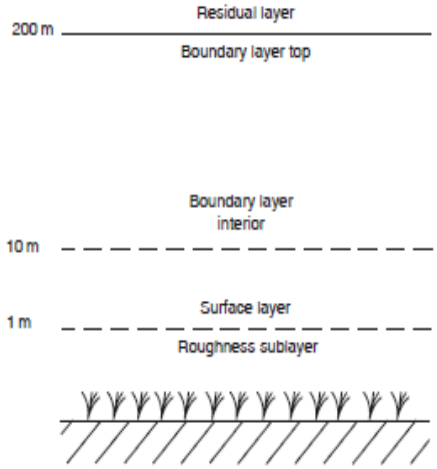

Fig.2. Idealized stable boundary layer

Atmospheric Boundary layer is defined as that part of the atmosphere extending from the surface of the earth to some height (usually 1 to 2 km) in the vertical upto which the effects of the surface (both ground and ocean) like roughness elements, heating and cooling, frictional drag, evaporation and transpiration, pollutant emission, terrain induced modification etc. are directly felt on time scales of a few hours to about a day.

The ABL studies gained importance because it is virtually controlling the human activity in the application of every branch of meteorology like air pollution, NWP, urban, agriculture, aviation and hydrometeorology. Particularly the stability of ABL decides the generation of weather systems like tornadoes, thunderstorms, cyclones and fronts.

The ABL can be broadly divided into two layers viz., Surface Boundary Layer (SBL) and the Ekman Layer(Boundary layer top) as in Fig.2. The surface layer or inner layer is

further subdivided into two more layers. They are interfacial (or roughness layer) and inertial sublayer as shown in Fig.3. In the roughness layer the turbulence is affected by roughness elements (squares in Fig.3). The inertial sublayer is the region with in which the velocity profile in neutrally buoyant conditions is logarithmic. The surface layer is thus mainly dependent on the ground characteristics.

The height of the ABL is not constant. It varies with temperature and turbulence over the day. When strong convection and thermal instability sets in, mass, momentum and energy are transported from the ground to upward. Then the Convective Boundary Layer develops which will influence the ABL height. In the night ground cools due to back radiation. So the turbulence reduces and hence an inversion in the surface layer develops for a brief period. Then the base of the height of inversion determines the height of the ABL.

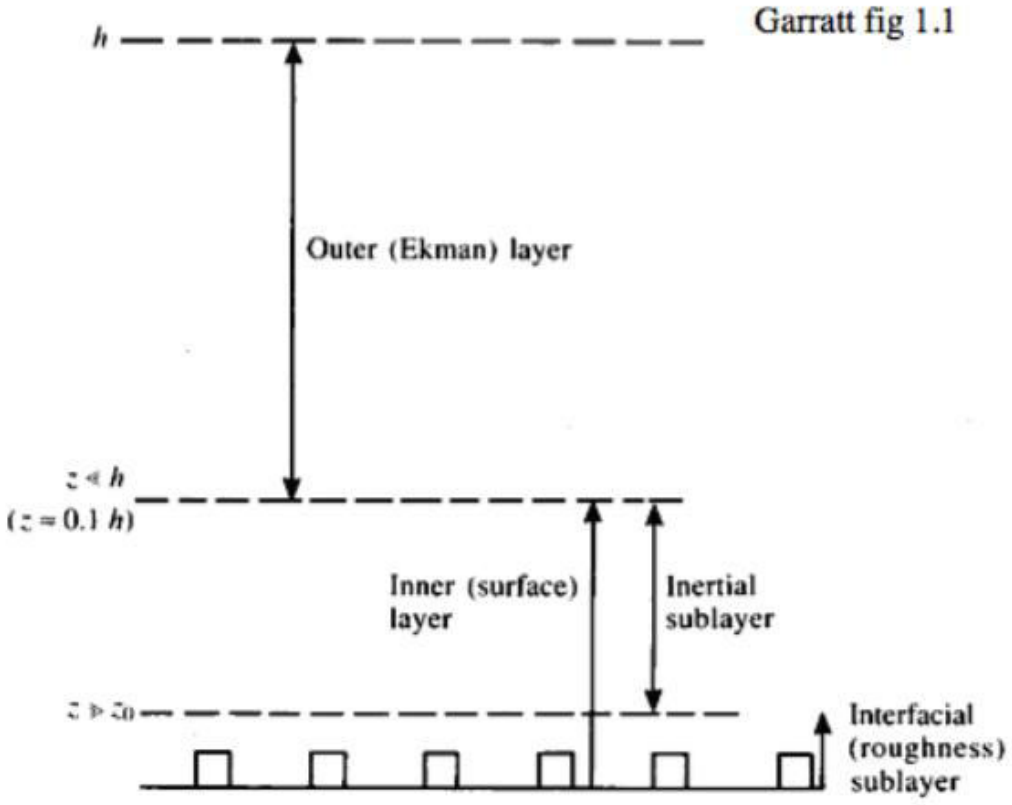

Fig.3.Fine structure of atmospheric boundary layer

Some of the most important features of PBL:

The atmospheric or Planetary boundary layer is the lowest part of the troposphere near the ground from where the friction stress decreases with height. The wind velocity decreases significantly from its geostrophic value above the boundary layer to the wind near the surface, and the wind direction changes counter-clockwise up to 30– 45° in the Northern hemisphere. In addition, thermal properties influence the boundary layer. Above the boundary layer, lays a statically-stable layer (inversion) with intermittent turbulence. The exchange processes between the atmospheric boundary layer and the troposphere take

place in the entrainment zone as shown in the Fig.4. The thickness of this layer is approximately 10% of the atmospheric boundary layer, which has a thickness of about 1–2 km over land and 0.5 km over the oceans. For strong stable stratification, its thickness can be about 10 m or less.

Daily variation of ABL with time:

The height of the ABL is not constant. It varies with temperature and turbulence over the day. When strong convection and thermal instability sets in, mass, momentum and energy are transported from the ground to upward. Then the Convective Boundary Layer develops which will influence the ABL height. In the night ground cools due to back radiation. So the turbulence reduces and hence an inversion in the surface layer develops for a brief period. Then the base of the height of inversion determines the height of the ABL.

Evolution of the atmospheric boundary layer.

The daily cycle is highly variable. After sunrise on the first day(x axis) (Fig.4), the atmosphere is warmed by the turbulent heat flux from the ground surface, and the inversion layer that was formed during the previous night starts dissipating. The new warm layer is very much turbulent and well mixed (mixed layer), and is bounded by an entrainment zone above. After wards in the evening from sunset time, the stable (night time) boundary layer develops near the ground. This stable layer has the character of a surface inversion and is about 100 m deep. Above this layer, the mixed layer of the day is much less turbulent and so it is called the residual-layer, and is capped by a free (capping) inversion which remains as the upper border of the boundary layer. After sunrise again on the second day, the developing mixed layer quickly destroys both the stable boundary layer and the residual layer. However, on cloudy days and in winter, when the solar radiation and the energy transport to the surface are weak, the mixed layer will not disturb the residual layer, and the boundary layer is generally stratified. On days with strong solar radiation, the boundary layer structure will be destroyed by convective cells, which develop some 10 m above the ground. These cells have relatively small upwind cells relatively high vertical wind speeds, and typically develop over large areas with uniform surface heating.

In the upper part of the atmospheric boundary layer (Ekman layer), the changes in the wind direction take place. The lowest 10% (upto 20 m) is called the surface or Prandtl layer (Table.1). Its height varies to about 20–50 m in the case of unstable stratification and a few meters for stable stratification. It is also called the *constant flux layer* because of the assumption of constant fluxes with height within the layer. This offers the possibility to estimate the fluxes of sensible and latent heat in this layer while in the upper layers flux divergences dominate. The atmospheric boundary layer is turbulent to a large degree, and only within a few millimeters above the surface the molecular exchange processes dominate. Because the turbulent processes are more effective than molecular processes and because of the assumption of a constant flux, the linear vertical gradients of properties very near the surface must be very large. Between this molecular boundary layer or laminar boundary layer and the turbulent layer, a viscous sublayer (buffer layer) exists with mixed exchange conditions and a thickness of about 1 cm. According to the similarity theory of Monin and Obukhov, a layer with a thickness of approximately 1 m (dynamical sublayer) is not influenced by the atmospheric stability – this layer is nearly neutral all of the time.

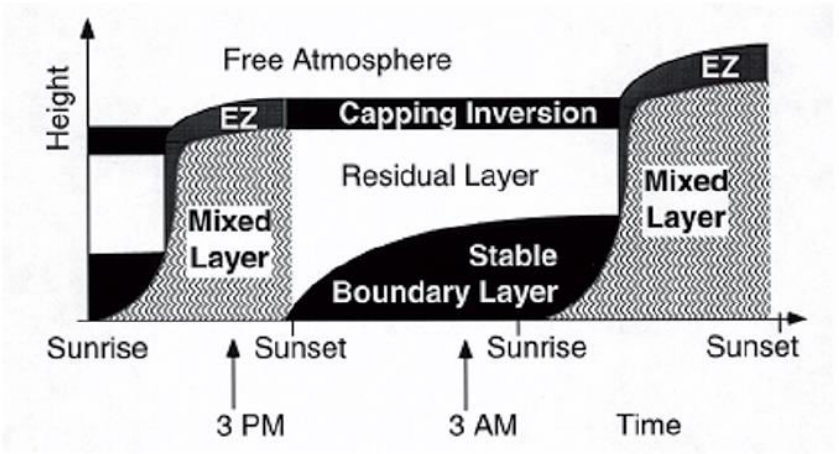

Fig.4. Daily cycle of the structure of the atmospheric boundary layer. EZ: Entrainment zone.

height in m	name		exchange		stability
1000	upper layer (Ekman-layer)		turbulent	no const. flux	influence of stability
20	turbulent layer	surface layer (Prandtl-layer)		flux constant with height	
1	dynamical sublayer				no influence of stability
0.01	viscous sublayer		molecular/ turbulent		
0.001	laminar boundary layer		molecular		

Table 1. Height of different layers in the atmospheric boundary layer

Lecture Series of Berhampur University in Physical Oceanography
By Prof.A.S.N.Murty

Chapter – 15

Wind field in the surface layer and Ekman layers

15. VERTICAL STRUCTURE OF WIND IN THE LOWEST TURBULENT LAYER (SURFACE LAYER):

The surface-air interaction occurs in two primary forms: mechanical and thermal. The mechanical contact arises from the friction exerted bythe wind against the ground. This friction causes the wind to be sheared and creates turbulence. In the absence of thermal processes, that is when the Atmospheric Boundary Layer is said to be neutral, the velocity profile is logarithmic characterized by friction velocity u_* and roughness height z_o. The friction velocity is intimately related to the level of turbulence in the lowest atmosphere.

If turbulent flow exists in the surface layer, the mixing length 'l' decreases linearly with decreasing height

$\therefore l = kz$ ……(3.6)

where k = 0.38 under neutral stability conditions and is called Von Karman's constant. Under equilibrium conditions, stress in the vertical would be constant. So from equation (3.4) we can write

$$\Gamma_{zx} = \rho l^2 \left[\frac{\partial \bar{u}}{\partial z}\right]^2$$

$$\text{Or} \quad \frac{\partial \bar{u}}{\partial z} = \sqrt{\frac{\tau_{zx}}{\rho l^2}} = \frac{1}{l}\sqrt{\frac{\tau_{zx}}{\rho}} = \frac{u_*}{l} \quad \text{……..(3.7)}$$

As $\sqrt{\frac{\tau_{zx}}{\rho}}$ has the dimensions of velocity it is represented as 'u_*' and is called frictional velocity.

Replacing 'l' from the equation (3.6) we can write Eqn(3.7) as

$$\frac{\partial \bar{u}}{\partial z} = \frac{u_*}{kz}$$

on integration this yields to

$$\bar{u} = \frac{u_*}{k} \ln z + c \quad \text{……..(3.8)}$$

To find the integration constant ' C ' very close to the ground, $\bar{u}$ = 0 at the roughness length $z = z_0$ .So Eqn (3.8) becomes

$$C = -\frac{u_*}{k} \ln z_0 \qquad \text{.....(3.9)}$$

substituting Eqn (3.9) in Eqn (3.8) gives rise to

$$\bar{u} = \frac{u_*}{k} \ln \frac{z}{z_0} \qquad \text{.....(3.10)}$$

where z_0 is called roughness parameter and is proportional to the average height of the obstacles. It is estimated that $z_0 = \frac{1}{30\varepsilon}$ where ε is the height of the obstacle.

In other words, equation (3.10) implies that the wind velocity varies logarithmically with height. This can be verified experimentally if we observe the wind at different heights and plot wind velocity (u) versus logarithmic height (lnz). The result is a straight line with an intercept Z_0. which means the wind varies logarithmically with a roughness length Z_0.which is shown in Fig.3.3. The roughness height for various surfaces is mentioned in table1.

.

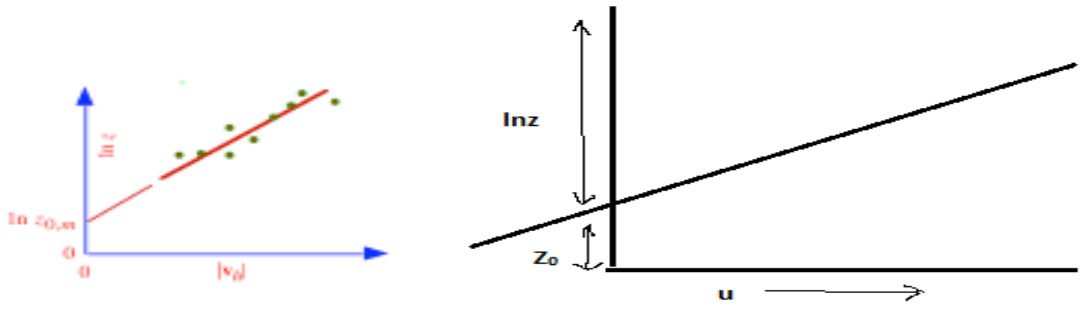

Fig.3.3. Variation of wind velocity in the surface layer.

surface	z_0 [m]
water	0.0001 - 0.001
bare soil	0.001 - 0.01
crops	0.005 - 0.05
forest	0.5

Table1. Approximate roungness heights for various surfaces

15.1. DRAG COEFFICIENT:

Stress can be computed from equations (3.7) and (3.10) as

$$\frac{1}{l}\sqrt{\frac{\tau_{zx}}{\rho}} = \frac{u_*}{l}$$

from (3.10) $$\therefore u_* = \frac{k\bar{u}}{\ln\left(\frac{z}{z_0}\right)}$$

$$\therefore \tau_{zx} = \rho\left[\frac{k}{\ln\frac{z}{z_0}}\right]^2\left(\bar{u}\right)^2 = \rho C_D\left(\bar{u}\right)^2 \quad \text{.....(3.11)}$$

where $C_D = \left[\frac{k}{\ln\frac{z}{z_0}}\right]^2$ is called the drag coefficient.

Thus the stress τ_{zx} is not directly measurable, but can be determined quantitatively if the dimension less quantity C_D, the drag coefficient is known. Several researchers estimated the drag coefficient through empirical methods and found that for wind speeds less than 6 ms^{-1} it is 1.3×10^{-3} and for wind speeds greater than 6 ms^{-1} it is about 2.4×10^{-3}.

15.2. VERTICAL STRUCTURE OF WIND IN THE EKMAN LAYER:

ASSUMPTIONS OF EKMAN:

1. At a level where turbulence is negligible the height is known as gradient level.
2. Flow is horizontal
3. Horizontal mean wind stress is small compared to the vertical mean wind stress
4. Uniform motion (nonaccelerated).
5. There is a balance between pressure gradient, coriolis at the top of the layer (gradient level) and so geostrophic balance exists there.
6. The eddy viscous coefficient is taken as independent of height.
7. The density does not vary appreciably.
8. Surface layer is considered very thin and for all practical purposes taken as equal to the ground (z = 0).

Above 50 or 100 m it is not realistic to assume that the turbulent stress is independent of height because the stress decreases with height and becomes negligibly small at gradient level (1000 m) where geostrophic balance occurs. Thus the layer of decreasing stress is 10 times thicker than that of the constant stress.

Taking the horizontal equation of motion as

$$\frac{du}{dt} = -\alpha \frac{\partial p}{\partial x} + fv + \alpha \frac{\partial \tau_{zx}}{\partial z}$$

$$\frac{dv}{dt} = -\alpha \frac{\partial p}{\partial y} - fu + \alpha \frac{\partial \tau_{zy}}{\partial z}$$

under the non accelerated conditions and taking the vertical shear stress and orienting the isobars in the x direction (east-west) , $\frac{\partial p}{\partial x} = 0$. After applying the above assumptions the above equations can be written as:

$$\rho fv + \frac{\partial \tau_{zx}}{\partial z} = 0 \quad \text{.....(3.12)}$$

$$-\frac{\partial p}{\partial y} - \rho fu + \frac{\partial \tau_{zy}}{\partial z} = 0 \quad \text{.....(3.13)}$$

To solve these equations, multiply (3.13) by i and add to (3.12) then take $\tau_{zx} = \mu \frac{\partial u}{\partial z} = \rho k \frac{\partial u}{\partial z}$ and $\tau_{zy} = \mu \frac{\partial v}{\partial z} = \rho k \frac{\partial v}{\partial z}$ then we can write the equations(3.12) and (3.13) combined as

$$-i\frac{\partial p}{\partial y} - \rho fi(u + iv) + \rho k\left[\frac{\partial u}{\partial z} + i\frac{\partial v}{\partial z}\right] = 0 \quad \text{.....(3.15)}$$

According to geostrophic approximation we know, $-\frac{\partial p}{\partial y} = \rho f u_g$. Substituting this in (3.15) and rewriting

$$-if(u + iv - u_g) + k\frac{\partial^2}{\partial z^2}(u + iv) = 0 \quad \text{.....(3.16)}$$

At gradient level the wind is constant and it is geostrophic. So even if we add u_g in the second part no change in (3.16).

$$\therefore -if(u + iv - u_g) + k\frac{\partial^2}{\partial z^2}(u + iv - u_g) = 0 \qquad (\because u_g = cons\tan t)$$

or $$\frac{\partial^2}{\partial z^2}(u + iv - u_g) - \frac{if}{k}(u + iv - u_g) = 0 \quad \text{.....(3.17)}$$

The solution of this differential equation is

$$u + iv - u_g = Ae^{z\sqrt{\frac{if}{k}}} + Be^{-z\sqrt{\frac{if}{k}}} \quad \text{.....(3.18)}$$

Substituting $\frac{1+i}{\sqrt{2}}$ *for* $\sqrt{i}$ and putting $a = \sqrt{\frac{f}{2k}}$ and re writing

$$u + iv - u_g = Ae^{a(1+i)z} + Be^{-a(1+i)z} \quad \text{.....(3.19)}$$

The two boundary conditions we know are

i) at the surface z = 0 , u+iv = 0 and

ii) at the gradient level (upper limit), z = ∞ , u + iv = u_g

According to the second boundary condition at z = ∞, the constant 'A' in equation (3.19) vanishes. Substituting the first boundary condition equation (3.19) becomes

$u + iv - u_g = -u_g e^{-a(1+i)z}$ or $u + iv = u_g[1 - e^{-a(1+i)z}]$

we know $e^{-iaz} = \cos az - i\sin az$ substituting this and separating the real and imaginary parts we finally get

$u = u_g[1 - e^{-az}\cos az]$ .....(3.21)

$v = u_g[e^{-az}\sin az]$ .....(3.22)

These are called Ekman Spiral equations in the atmosphere. These show the variation of wind in the turbulent layer.

15.2.1. INTERPRETATION OF EKMAN EQUATIONS:

i) to get the angle of deflection $\frac{dv}{du} = \tan\theta$ differentiate (3.21) and (3.22) with respect to 'z' and taking the ratio at z = 0 (at the surface) we get

$\frac{du}{dz} = a\, u_g e^{-az}[\cos az + \sin az]$, $\therefore$ at the surface z =0 , $\frac{du}{dz} = a\, u_g$

similarly we get $\frac{dv}{dz} = a\, u_g e^{-az}[\cos az - \sin az]$ and at z = 0, $\frac{dv}{dz} = a\, u_g$

$$\therefore \tan\theta = \frac{dv}{du} = \frac{dv/dz}{du/dz} = \frac{au_g}{au_g} = 1$$

$$\therefore \theta = \frac{\pi}{4}$$

This means that the wind direction close to the surface layer makes an angle of 45^o with respect to the isobars and points towards the low pressure.

ii) At z = $\frac{\pi}{a}$, the equations (3.21) and (3.22) becomes

$u = u_g[1 - e^{-\pi}\cos\pi] = u_g[1 + e^{-\pi}]$ .....(3.23)

similarly $v = u_g[e^{-\pi}\sin\pi] = 0$

that is equation (3.23) says u is greater than u_g. This means that wind increases with height and turns clockwise (veers).

iii) At z = $\frac{2\pi}{a}$, equations (3.21) and (3.22) turns as

$u = u_g[1 - e^{-\pi}]$ .....(3.24)

and $v = u_g[e^{-2\pi}\sin 2\pi] = 0$

Which means equation (3.24) says u < u_g. This is the gradient level where the wind speed is less than the geostrophic. Equations (3.23) and (3.24) also say that the wind variation is exponential.

In middle latitudes, the gradient level occurs at nearly 1 km height. i.e. z = $\frac{\pi}{a} = \pi$

$$\therefore e^{-az} = e^{-\pi} = \frac{1}{23}$$

15.2.2. HODOGRAPH:

If we plot the ratios of $\frac{u}{u_g}$ and $\frac{v}{v_g}$ on x and y axis the graph looks as shown in Fig.3.4. This graph is called hodograph and it shows the veering of the wind is like a spiral. This derivation was first made by W.F.Ekman to describe the effect of wind in the generation of currents in the upper layers. The same analogy is applied in the atmosphere also and so this is called the Atmospheric Ekman Spiral. So this layers above the surface layer up to the gradient level where the wind veers clockwise turning with an angle of 45° at the surface layer is also called spiral layer.

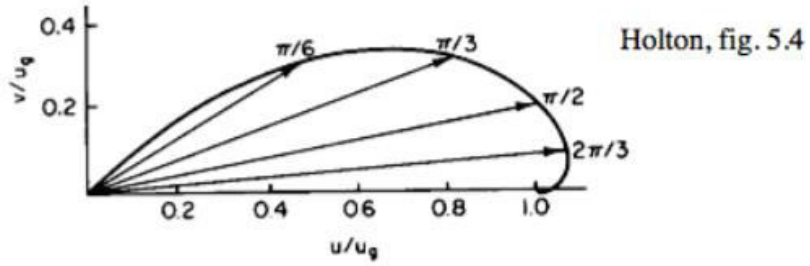

Fig.3.4. Hodograph of the wind components in the Ekman spiral solution. The arrows show the velocity vectors for several levels in the Ekman layer, while the spiral curve traces out the velocity variation as a function of height. Points labeled on the spiral show the values of az. Thus $\frac{\pi}{6}$ etc are az values.

15.2.3. ESTIMATION OF EDDY COEFFICIENT OF VISCOSITY:

We took $a = \sqrt{\frac{f}{2k}}$,

we understood the gradient level $\frac{\pi}{a}$ = 1.0 km =10^5cm, $\therefore a = \frac{\pi}{10^5}$

$$\therefore a = \sqrt{\frac{f}{2k}} = \frac{\pi}{10^5}, \quad \frac{f}{2k} = \frac{\pi^2}{10^{10}}, \text{ taking } f = 10^{-4}$$

we get $k = 5 \times 10^4 \, cm^2 s^{-1}$.

This is one way of estimation of eddy coefficient of viscosity.

TRY THIS PROBLEM:

If the geostrophic wind is westerly at 15 m s^{-1}. Compute the net cross isobaric transport in the Ekman layer. Take k = 5 m^2/s, f = 10^{-4} s^{-1}, $\rho = 1 kgm^{-3}$ and D = 1 km. (Hint: take only 'v' component of velocity for cross isobaric transport and substitute Ekman velocity equation in the mass transport M = $\int_0^D \rho v dz$). Integrate up to Ekman depth 'D'.

Answer:

The net cross isobaric Ekman mass transport in the Ekman layer 0 to D is:

$$M_y = \int_0^D \rho v dz = \int_0^D \rho u_g [e^{-az} Sin\, az] dz$$

Put I = $\int_0^D [Sin\, az\, e^{-az}]\, dz = Sin\, az \frac{e^{-az}}{-a} - \int \frac{e^{-az}}{-a} (-a) Sin\, az\, dz$

$$\therefore 2I = -\frac{1}{a} e^{-az} [Sin\, az + Cos\, az]$$

Or $I = -\frac{1}{2a} e^{-az} [Sin\, az + Cos\, az]$

$$\therefore M_y = -\frac{\rho u_g}{2a} e^{-az} [Sin\, az + Cos\, az]_{z=0}^{z=D}$$
$$= -\frac{\rho u_g}{2a} \{e^{-aD} (Sin\, aD + Cos\, aD) - e^0 (0 + 1)\}$$

Given D = 1 km = 1000 meters, $a = \frac{f}{2k} = \frac{10^{-4}}{2 \times 5} = 3.16 \times 10^{-3}$

Substituting all the given values:

$M_y = \frac{-1 \times 15}{2 \times 3.16 \times 10^{-3}} \left[e^{-1000 \times 3.16 \times 10^{-3}} (Sin\, 1000 \times 3.16 \times 10^{-3} + Cos\, 1000 \times 3.16 \times 10^{-3})\right] = 59.06 \times 10^3$